PERFORMANCE MONITORING OF ROTARY BLASTHOLE DRILLS

Jonathan P. Peck
Department of Mining and Metallurgical Engineering
McGill University, Montreal.
February 1989.

A Thesis submitted to the Faculty of Graduate Studies and Research in partial fulfillment of the requirements for the degree of Doctorate of Engineering.

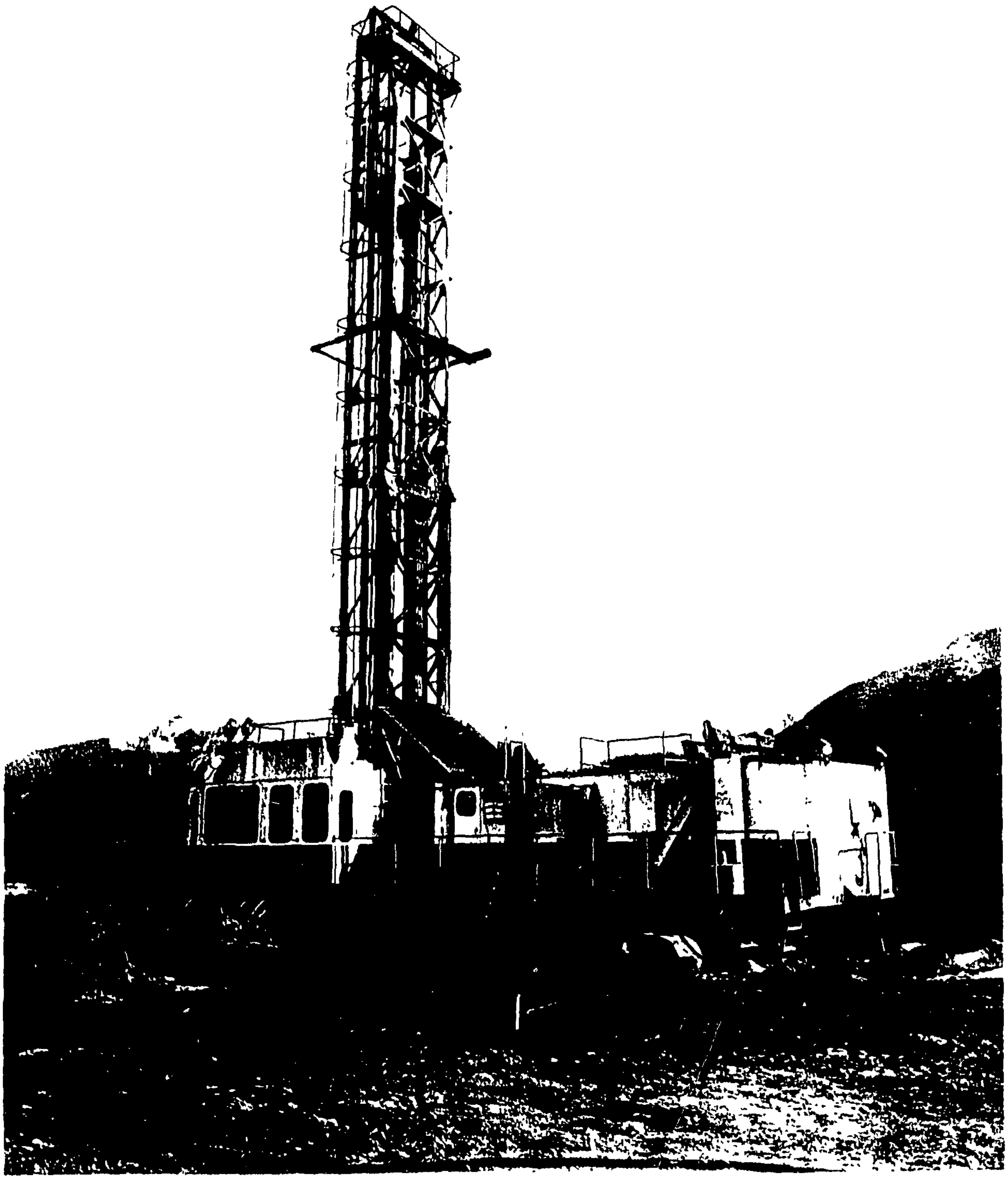

ABSTRACT:

Rotary blasthole drills operating in a western Canadian surface coal mine were instrumented with microprocessor-based monitoring equipment. During routine production drilling, the performance parameters of penetration rate, torque, rotary speed, pulldown and bailing air pressure were monitored at sampling intervals of 10 centimeters (4 inches). The acquired digital data were subsequently correlated with both geological and geomechanical rock properties permitting a detailed examination of machine-rock interaction. The results from a statistical analysis of the drill data identified unique ranges of performance parameters for the sandstone, siltstone, mudstone and coal units encountered at the mine. Correlation of these ranges with geophysical logs in the monitored boreholes, enabled a further calibration of drilling parameter variation to rock type. A relationship between drill performance parameter responses and rock compressive and shear strength was established. This correlation demonstrated the possibility of estimating rock strength properties based on drill performance data. Trend analysis techniques applied to the monitored drill data permitted a further understanding of the nature of tricone bit wear for the particular study environment. The applications of drill monitoring techniques are illustrated in terms of geological exploration, mine planning, tricone bit selection and wear evaluation, and drill automation and control.

RESUME

L'objet de cette recherche concerne l'instrumentation par un dispositif de microprocesseurs, d'enregistrement et de traitement de donnees sur des foreuses rotatives de très grande puissance. Ces foreuses sont utilisées pour les trous de pré-clivage et dynamitage dans une mine de charbon à ciel ouvert, de l'ouest Canadien. Au cours des forages de routine, l'efficacité des foreuses fut contrôlee par des transducteurs mesurant la vitesse de pénétration du foret, la vitesse de rotation et le couple force du train du tige, la pression de la poussée de la tête hydraulique et enfin la pression de l'air de refroidissement injecte. L'intervalle de l'échantillonage des donnees en utilisant au trepan tricône de 311 cm (12 1/4 po.) etait de 10 cm (4 po.). Les données recueillies ont éte par la suite comparées aux donnees geologiques et géoméchaniques pour fins de correlation foreuse-roc. Le résultat des analyses statistiques des donnees de forage a permis d'identifier des plages de performance uniques, spécifiques aux grès, aux differents schistes sedimentaires (siltstone et mudstone) et aux depôts de charbon presents dans la mine. Les correlations effectuees entre ces enregistrements de forage et les logs géophysiques post-forage ont permis de préciser encore la calibration des parametres de forage en fonction de la variation lithographique de la roche. D'autres etudes ont egalement permis d'etablir des correlations entre les parametres de forage et les résistances en compression et en cisaillement du roc. Grâce a ces corrélations, il est demontre qu'il est possible d'evaluer les proprietes mechaniques du roc a partir des paramètres de forage. Enfin, l'analyse des tendances des donnees des parametres de forage a permis de mieux comprendre le processus d'usure des trepans tricône dans l'environnement particulier de cette recherche. Les applications des techniques d'enregistrement de paramètre de forage dans les domaines d'exploration geologique, de planification de l'extraction minière, de sélection et d'usure des trepans tricône, et de l'automatisation et du contrôle des operations de forage sont abondamment illustrees.

LIST OF SYMBOLS AND ABBREVIATIONS:

g - acceleration due to gravity

ϕ - angle of internal friction

ϵ_f - axial strain at failure

σ_f - axial stress at failure

I - bailing air pressure

BCY - bank cubic yard

C_3 - bit constant

C_4 - bit constant

G - bit constant

k_{cs} - bit constant

D - bit diameter

μ - coefficient of friction

COV - coefficient of variation

C - cohesion

r - correlation coefficient

A - cross-sectional area

D_x - d exponent

K - drillability constant

S_d - drilling strength

a - drilling strength exponent

W - downpressure (hydraulic)

E_c - total energy imparted to the rock during crater formation

α - experimental constant

β - experimental constant

δ - experimental constant

ft/h - feet per hour

ft - foot

ft-lb - foot pound

Hp - horsepower

h - hour

KE_t - kinetic energy; translational component

KE_r - kinetic energy; rotational component

KE_{tl} - kinetic energy; total

m - mass

MPa - mega pascals

mV - millivolt

min - minute

σ_n - normal stress

R - penetration rate

π - pi

lbs - pounds

psi - pounds per square inch

α - proportionality

k - dimensionless shape factor for a non-linear stress-strain curve

τ - shear strength

τ_a - shear strength; measured

τ_b - shear strength; estimated/calculated

τ_n - shear stress

SE(R) - specific energy, Rabia (1982, 1987)

SE(T) - specific energy, Teale (1965)

W_s - specific energy, Mellor (1972)

X - time index

σ_c - unconfined compressive strength

σ_c(calc) - unconfined compressive strength; calculated/estimated

σ_c(meas) - unconfined compressive strength; measured

r_0 - outside radius

r_i - inside radius

rpm - revolutions per minute

Q - rock abrasiveness

RQI - rock quality index

N - rotary speed

T - torque

v - velocity; linear

w - velocity; angular

V_c - volume of impact crater

V_r - volume of rock excavated in 1 second

E_t - Young's Modulus (tangent)

E_s - Young's Modulus (secant)

TABLE OF CONTENTS:

1.0 INTRODUCTION:

2.0 ROTARY DRILLING:

3.0 DRILL MONITORING INSTRUMENTATION:

LIST OF FIGURES:

Appendix I:

Appendix III:

LIST OF TABLES:

1.0 INTRODUCTION:

1.1 Overview of the Project:

This thesis is based upon studies into rotary blasthole drill performance monitoring, conducted at the Fording River Mine of Fording Coal Ltd. in Elkford, British Columbia. The studies and observations were made over a period from June 1987 to September 1988, during which time 4600 feet of 10 5/8 inch diameter and 12,500 feet of 12 1/4 inch diameter blastholes using Bucyrus-Erie 45R and 60R rotary drills respectively, were monitored. Hole depths ranged from 50 feet to 140 feet and penetrated multiple coal seams and Coal Measure rocks, individually less than 3 feet to greater than 30 feet in thickness. Monitoring established that distinctively characteristic responses to drill penetration were associated with each of the rock units at the mine.

The continuous monitoring of 5 drill performance parameters for both routine production blastholes and selected exploration testholes, enabled the inter-relationships between these to be identified. In addition, the correlation of drill parameter and borehole gamma logs allowed the characteristic patterns and performance data ranges to be classified on the basis of rock type. A statistical analysis of the specific drilling parameter ranges for coal, mudstone and sandstone/siltstone, permitted an examination of the dominant mechanisms of rock breakage by a roller-cone bit in each of these rock types.

Once the unique drill parameter patterns were identified, then a correlation to measured rock properties was undertaken. Unconfined compressive strength, σ_c, and Young's modulus, E, were determined from laboratory testing of core taken from holes located at distances less than 1 foot from 5 drill monitored and gamma logged blastholes.

Based on these results, it was determined which particular drilling parameters were most sensitive and reliable to profile changing rock mass characteristics. Using these capabilities, the lateral and vertical variations of both coal seams and waste rock units were traced across a structurally complex bench area at the mine. Interpretation of the drill log data enabled the construction of detailed cross-sections which illustıated coal seam thickness, dip and offsets, due to the presence of numerous normal and reverse faults and related folds. These were inferred from the monitored data but were also mapped on exposed bench faces.

During the monitoring period, records of the bits used on the particular drills were maintained in terms of cumulative footage drilled and wear condition. The combination of these manual records with the data using trend analysis techniques, then enabled the influence of bit wear on characteristic drilling parameter responses to be evaluated.

This work has been an important component of Fording's comprehensive program of integrated studies on drilling, blast practice, fragmentation, loading systems, transport, coal recovery and mine planning. The ability to recognize rock mass characteristics while drilling has immediate significance to the optimum operation of the drill, and also upon the next operation of appropriate explosives loading and firing to produce optimum fragmentation. The results of these studies may eventually form the basis for integrating drill performance data into both short and long range planning modules within the mine's mainframe based Mine Engineering Applications system. The criteria established for recognizing different rock types and particular situations from the monitored data, will also form the basis for the development of a functional control strategy towards eventual drill automation.

This study was unique in that such a detailed investigation of the interaction between the rock and the drill had never been attempted under field conditions. In addition, the volume and resolution of both the drill and geological data that was acquired during the monitoring period went beyond any previous efforts to examine this relationship. As a result of these factors, the study defined appropriate techniques and methodologies to evaluate the effects of geological properties on drilling performance. These can be used as a guideline for any subsequent investigations in different mining environments.

1.2 Proposed Hypothesis:

The drill is a machine used in mining to excavate holes as part of the overall rock breakage process. The central issue of this thesis is whether the performance of this machine can be related to the geological environment so that a firm basis for the understanding of the machine-rock interaction can be established. The hypothesis evaluated is that the performance parameters of the machine reflect the nature of the medium ie. rock mass, being penetrated. If the relationship between the machine performance and the physical and mechanical properties of the rock mass can be clearly established, then the machine becomes a diagnostic tool, besides simply an excavator in the process of rock fragmentation. This hypothesis has been evaluated by accounting for the effects of the operator and the degree of wear on the bit. These were isolated and accounted for in an effort to create a controlled field experiment. Under these circumstances, any changes in the drilling performance can therefore only be the result of variation in the rock properties.

The incentives to develop and validate this hypothesis are significant;

1 - the definition of the geology by the drill can be used for mine planning, scheduling, and reserve estimation.,

2 - the state of health of the drill and bit can be evaluated effectively at any stage during their operational lives,

3 - the results would have a significant impact on future machine design, arising from the definitive understanding of the machine-rock interaction,

4 - the increased depth of understanding of drill performance in relation to the rock should improve the logic which will be incorporated into a control strategy for drill automation.

The work was undertaken in a surface coal mine. This was an ideal environment to examine the influence of the rock on machine performance due to the layered nature of the geology and pronounced property contrasts between the different rock units. The performance of the drill was determined from the monitoring of 5 important parameters ie. penetration rate, applied downpressure, torque, rotary speed and bailing air pressure. These were examined, singly and in combination, in order to determine their relevance to the characterization of the machine-rock interaction.

The data acquisition mode appropriate to these field conditions and type of drill required the design, development and implementation of a drill monitoring instrumentation system. From preliminary studies at the mine, certain data requirements were established in terms of sampling resolution, accuracy and quantities on a borehole by borehole basis. In addition, since the monitoring was being undertaken during routine blasthole drilling in a producing mine, the design and utilization of the system had to be integrated with existing mining procedures. This phase involved the selection of suitable microprocessor-based data loggers and transducers as well as the development of a monitoring strategy which permitted effective data collection with minimal impact to drill productivity.

The inter-relationships between the drilling parameters for the particular site conditions were examined. These were determined under controlled geological conditions, where their variation due to changing rock properties was restricted as much as possible. Under this constraint, the relationships established reflected the true associations between the parameters for the type of drilling being used. In subsequent phases therefore, when the geology was not constant, the behaviour of the drilling parameters in this circumstance could be compared to those relationships established under ideal conditions. The deviations existing between the two sets of data would thus be related to the changing nature of the rock.

In order to provide a full evaluation of the drill-rock interaction, then appropriate, detailed and accurate geological and geomechanical data was required. This involved the use of borehole gamma logs, diamond drill coring and mapping of exposed bench faces to clearly identify the nature of the geological variations influencing the monitored drill performance. This phase of the investigation was conducted at both a macro and micro scale in order to evaluate the extent to which the geology affected machine-rock interaction. The large database of monitored drill data (>17000 feet) and the geological and geomechanical data enabled the correlation of the performance parameters to the geological environment. The depth and range of this work has not been approached before in any mining or civil excavating environment, and aims to provide a sound foundation for future studies into machine-rock interaction.

1.3 Structure of the Thesis:

Initial steps to validate the central hypothesis comprised an examination of the various drilling parameters and how they are developed by the drill. This is discussed in section 2.2.1, followed by a review of tricone bits and past drillability investigations in sections 2.2.2 and 2.3 respectively.

Drill monitoring systems are addressed in section 3.0, including a review in section 3.2 of past instrumentation studies. Section 3.3 investigates the design, development and implementation of an appropriate drill monitoring system in the current research project. This section examines the phases followed in instrumenting a 60R drill rig using existing data logger and transducer technology. Section 3.3 also discusses the implementation and utilization of sensors to monitor torque and rotary speed, designed specifically for the project.

Preliminary drill monitoring studies were conducted at the Fording River Mine, in order to establish the criteria for the design of a more comprehensive field study program. The results from this preliminary work examined the correlation of the parameter responses of a 45R drill with gamma logging data and thus rock type characteristics. An initial identification of which drill parameters were most responsive to the changing nature of the rock mass was also made. The results of this work are considered in section 4.3, preceded by a review of the Fording River Mine in terms of its geology and mining practice in section 4.2.

It was concluded from the results of the monitoring of a 45R drill that the geology was a significant factor affecting the overall drilling process. Therefore, extensive geological and geomechanical investigations were conducted in the second phase of the thesis study to determine precisely the extent to which the properties of the rocks affected drilling performance. Core logs were obtained in close proximity to drill monitored boreholes, together with gamma logging of these same holes, see section 5.1. Core samples were selected to determine the range of unconfined compressive strengths within the particular types of rocks. Thin sections of representative specimens were analyzed to enable a validation of variations observed in the strength data with rock composition. These results are reviewed in sections 5.2 and 5.3, which in turn defined more clearly the influence of microcomposition on rock strength and thus drilling performance. The rock properties at all scales were considered to require clear definition prior to attempting any correlation with performance parameters.

Once the instrumentation was installed on the drill, then the accuracy of the data was required to be determined. The limitations and the capabilities of the data, and the inter-relationships between parameters were required to also be resolved conclusively. This was accomplished by the monitoring of the drill under controlled geological and operational constraints in a selected test borehole. This phase was an important component since it had been demonstrated in past investigations that the drilling models and parameter relationships established were site-specific and could not necessarily be applied to any other set of circumstances. It was of paramount importance, therefore, that if the proposed hypothesis was to be validated then the site-specific conditions had to be clearly established for this particular experiment. The results of controlled drilling trials are reviewed in section 6.2.

It was also evident from the investigations of section 2.3, that there has been some hesitancy on the part of past researchers to correlate drill parameter variations with rock type. This appeared to be mainly as a result of insufficient conclusive evidence to validate this claim. The instrumentation used in the past was also less effective in terms of resolution, accuracy and processing power than the present monitoring system. No prior work had attempted to examine in detail how in fact the rock affects drill performance having assumed that the bulk properties of the formations being drilled were homogeneous. The relationship, however, between drilling performance and geological properties at a smaller scale was never evaluated.

An initial aim in this thesis study, was to clearly establish the relationships between the drill parameters and the bulk properties of the rock types. In section 6.3, well defined limits in the various drilling parameters were determined for the rock types encountered in the mine. In addition, the reproducibility of the defined ranges of drilling performance for the different rock types from borehole to borehole indicated that the proposed study hypothesis was valid at this scale, section 6.3.

The parameters whose responses were most effective in identifying one rock type over another were also isolated. These results were validated with reference to proposed rock breakage mechanisms for rotary drills in hard versus soft rocks in sections 6.3 to 6.5.

Through the use of selected representative drilling models, the responses of the parameters, both individually and combined, were evaluated in relation to the measured strength properties of rock. A correlation of the drilling performance parameters to measured rock compressive strength is provided in section 6.4.1. Section 6.4.2 evaluates the relationships defined between calculated drilling indices and shear and compressive rock strength. In addition, the correlation of the observed results with rock breakage mechanisms is attempted. Based on these results, a method for the estimation of Young's modulus is presented with a comparison to measured values in section 6.4.3.

Several areas of application of drill monitoring technology, incorporating the capability of the drill to identify changing rock properties, are discussed in chapters 7.0, 8.0 and 9.0.

In chapter 7.0 the drilling responses are related to the complex geology along a working bench at the Fording River Mine. The effect of bit wear on the drilling performance parameters is examined in section 8.3. This phase was important in order to determine which particular parameters were indicative of the wear process, and relationships between wear and footage drilled. Section 8.3 also examines the possibility of predicting the degree of bit wear, based on recognized trends and observed deviations from the norm in one or more parameters over time. This would offer the ability to change bits in advance of excessive wear or total failure. The period leading up to failure is generally associated with high levels of machine vibration which promote structural wear.

Chapter 9.0 addresses the established influences of both the geology and the bit on the drilling performance. This discussion is aimed at isolating those factors which are considered important as part of any future control strategy for both partial and full automation of a rotary blasthole drill.

1.4 Units of Measurement:

Throughout this thesis, only **imperial** units of measurement are used. These were adopted for this work for the following reasons:

1 - at the Fording River Mine, all drilling instructions and staked depths (which include coal and borehole depths) are given in imperial units (feet) and,

2 - depth gauges on the operator's panel of the monitored drills were in imperial units. Some of the other gauges (pulldown and bailing air pressure) were in both imperial and metric, and,

3 - all past rotary drilling investigations and developed models were reported in imperial units.

4 - Drilling equipment manufacturers (Bucyrus-Erie, Dresser-Security etc.) are only recently using metric units. Most past guides and manuals are in imperial units.

Therefore, on the basis of these points, it was decided at the beginning of the project to maintain only imperial units for all subsequent data presentation and calculations.

Appendix II provides a Table of Conversions for imperial units to their metric equivalents.

2.0 ROTARY DRILLING:

2.1 Introduction:

The following sections will focus only on the types of rotary blasthole drills that were monitored in this investigation. Therefore, discussion will be referenced primarily to electric rotary blastholes drills of a similar design to the Bucyrus-Erie 45R and 60R drills operating at the Fording River Mine.

A brief introduction to rotary drilling is provided in section 2.2, followed by a detailed review of drilling performance parameters in section 2.2.1. This latter discussion will focus mainly on those parameters which were considered to be important for the current thesis study.

Since the monitored drills at the mine used tricone bits, a review of the criteria for the design and selection of these is provided in section 2.2.2.

A subsequent section (2.3) will review the extensive past theoretical and empirically based drilling studies which have examined the inter-relationships between the different parameters and how they are influenced by changing rock properties. Since the drilling that was monitored at the mine involved tricone (roller-cone) bits only, most of the past investigations reviewed will be those that involved these types of bits.

2.2 Rotary Drilling:

Many of the techniques and principles of rotary drilling were developed by the petroleum industry as a direct result of the need to explore and exploit oil reserves from depths in excess of 20,000 feet. In the mining industry prior to World War II, some rotary drills were being used in soft rock deposits such as coal, porphyry copper and weathered iron ore formations. The additional need for iron during the war years prompted the exploitation of lower grade, hard iron ore deposits due to the depletion of much of the softer, higher grade iron ore mines. At this point however, the only available type of drill capable of operating in these harder materials were small diameter percussion rigs and churn drills. The move to larger volume iron ore mining clearly indicated the mechanical and economic limitations of these drills in terms of depth and diameter of the holes. As a result, more effort was concentrated on designing and developing machinery capable of drilling large diameter, deeper blastholes in hard rock. In parallel with the technology improvements in oil drilling, was the evolution of rotary blasthole drills using tricone bits (first using steel milled-teeth then tungsten-carbide inserts) and compressed air, specifically developed for surface mining applications.

In response to the rapidly changing needs of the mining industry in the post war years, drill and drill bit manufacturers invested heavily in extensive research and development programs. These drillability studies sought to better understand the complexities of drilling mechanisms in order to optimize the processes of selecting, operating and maintaining this equipment. The importance of these efforts being prompted by drilling's influence upon overall mine productivity and unit costs. In addition, improvements in blasting design and explosives type prompted the need for increasing diameters of blastholes towards increased fragmentation tonnage and therefore larger, more powerful drills. Paralleling these developments, was the introduction of larger loading and haulage equipment, to handle the increased size and volumes of broken material thus created (Bucyrus-Erie, 1979).

2.2.1 Drill Performance Parameters:

The primary operating variables associated with rotary drilling can be classified as *Independent*, ie. those parameters controlled by the drill operator and *Dependent* parameters or those which are related to changes made in the former. These will be described in the following section in terms of: 1 - what their units of measurement are, 2 - how they are developed, and 3 - how they are manipulated by the drill operator. These points will be discussed with reference to electric rotary blasthole drills only, of a similar design to those monitored at the research site.

The name given in the heading for each parameter is the common name used for this thesis. The upper-case letter in parentheses for each parameter name, is the symbol for the variable, which will be used in the text throughout this document interchangeably with the common name. Other commonly used names for particular parameters will be mentioned when necessary.

A -Independent Variables:

Hydraulic downpressure; pulldown (W): This parameter is applied axially to the tricone bit at levels necessary to exceed the compressive strength of the rock, σ_c, thus fracturing it into chips and thereby achieve penetration, see Figure 2.1. Each drill rig type has a characteristic optimum value of W in order to achieve maximum penetration rates without exceeding the machine and bit specifications. This optimum value corresponds to the best contact at the bit-rock interface with optimum indexing. For a certain drill, there is an optimum value of W based on particular combinations of hydraulic pressure, drill (maximum load capacity, rotation speeds etc.) type, bit type and formation, at which the maximum amount of rock is

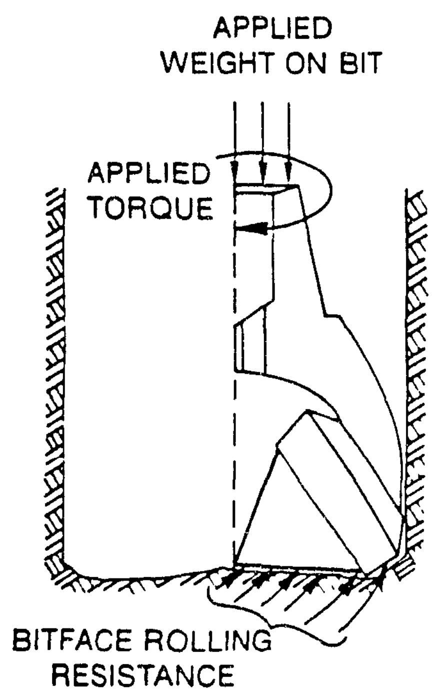

Figure 2.1 - Applied W and T on the Bit (Warren, 1984).

drilled per unit of energy. Under these conditions the maximum penetration rate can be realized. At levels below this critical value, ineffective penetration by the bit in the rock will occur together with accelerated bit wear. As wear of the bit occurs over time, greater W will be required to be applied in order to maintain a similar penetration rate.

For large blasthole drills, this parameter must be applied constantly with little or no backlash or the bit will bounce causing reduced bit life, lower penetration rates and higher maintenance costs due to excessive drill vibration. A portion of the overall machine weight is applied by the pulldown motor via the pulldown chains, rotary head and drill stems to the drill bit. In addition, the weight of the drill stem (steel, bit and stabilizer etc.) also contribute to the total weight acting on the bit, see Figure 2.2 (Bucyrus-Erie, 1979).

The amount of pulldown required for proper drill penetration is low compared to rotary power. The rate at which W is applied must be varied by the operator to correspond to changes in the compressive strength of the material being drilled. However, W should remain as constant as possible throughout the drilling in order to maintain optimum drilling rates and bit life. For the drills at the mine site, pulldown was controlled by a valve on the operators panel, which by turning it clock-wise would increase the hydraulic pressure to the pulldown motor. An analog gauge mounted on the panel, allows the operator to see what level of downpressure is set. The force thus created by the hydraulic motors is applied through the system described above and shown in Figure 2.1 and 2.2, to the drill bit as an axial force component. Pulldown force applied to the bit in this manner, depends on the size of the hole (pounds per inch bit diameter; lbs/inch) and values of σ_c for the particular rocks being drilled. For the 60R drill monitored at the study site, see Figure 2.3, pulldown was seen to range from 4600 lbs/inch in soft rocks to 8300 lbs/inch in harder units. Equivalent hydraulic downpressure gauge readings

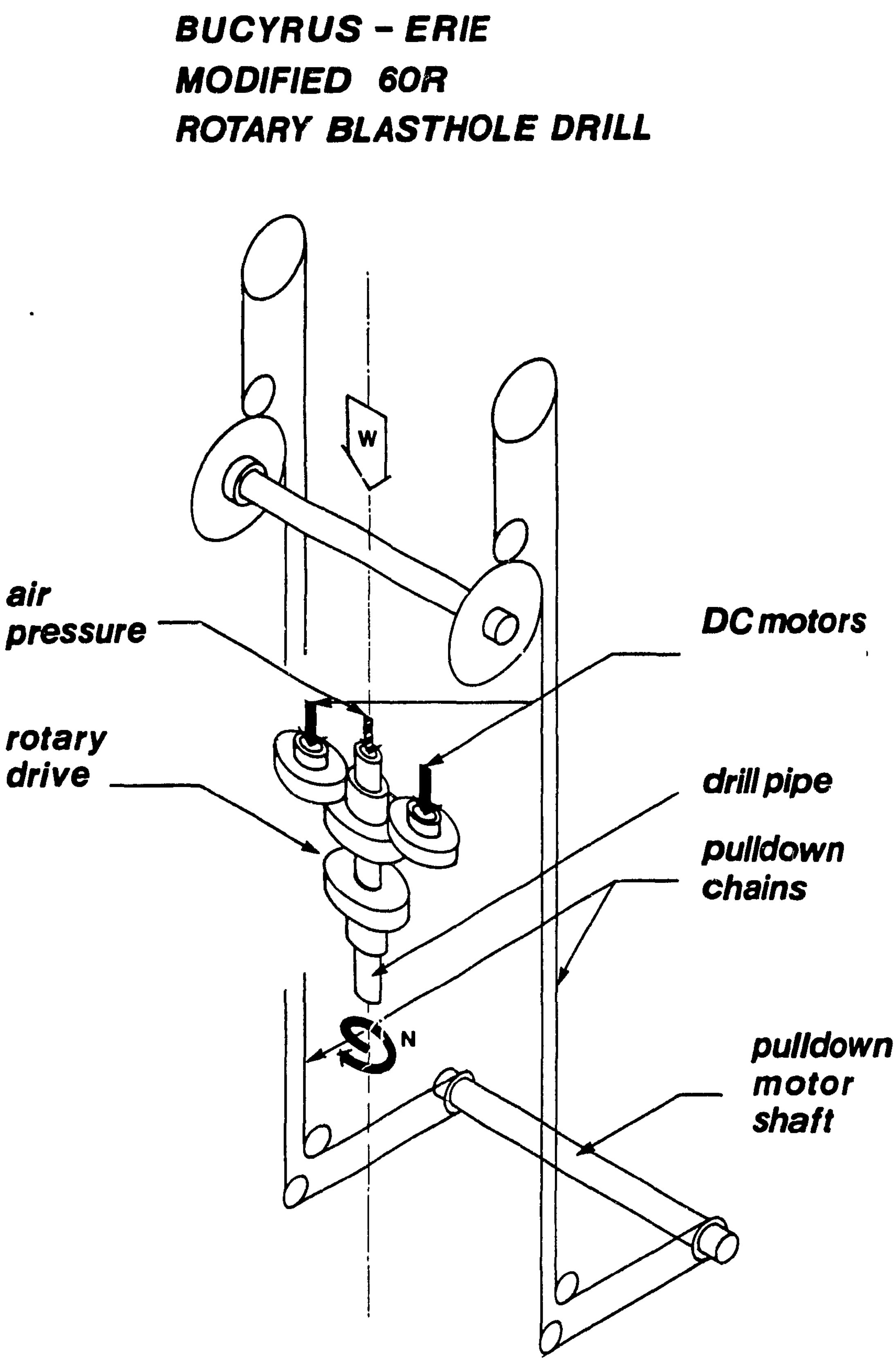

Figure 2.2 - Schematic of the Pulldown System of a Bucyrus-Erie 60R Drill (Mottola, 1988).

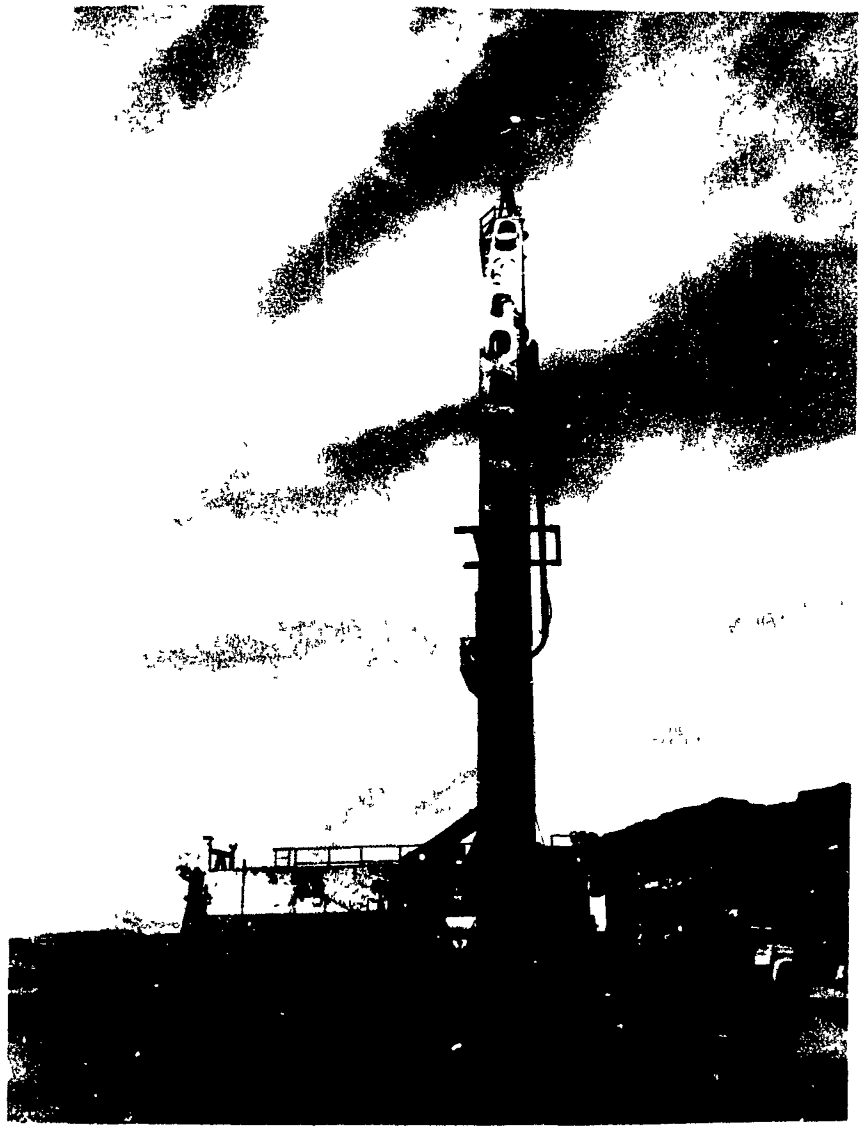

Figure 2.3 - Bucyrus-Erie 60R Series III Rotary Blasthole Drill at the Fording River Mine, Eagle Mountain, EX Bench.

would be 540 pounds per square inch (psi) in soft rocks and 1100 psi in hard rocks. The complete specifications for the 60R drill are provided in Table 2.1. This parameter is also referred to as weight on bit or applied weight, which are considered to be the total weight acting on the bit in pounds (lbs). These can be derived from pulldown (lbs/inch) by multiplying by the diameter of the bit (inches) being used and is related to the downpressure by an empirical equation discussed in section 3.0.

Rotary Speed (N): For rotary blasthole drills sufficient rotary power must be supplied to the bit for all drilling situations. Required rotary power for a given material and hole size is proportional to bit speed and W. Theoretically, doubling the rotation speed will double the penetration rate, however, the pulldown also has an influence (Nelmark, 1980).

The most common power sources for rotation of the bit on blasthole drills are electric, hydraulic or pneumatic. For the 60R drill, N is developed by 2 x 130 Hp electric motors. These motors turn the drill steel at the rotary head thus turning the drill bit at the bottom of the hole, see Figure 2.2. Limits to N are hot bearings in the bit and motor load specifications as influenced by W. The value of N is controlled by a rheostat and monitored by an analog gauge with both instruments mounted on the operators panel. Typical rotary speeds range from 60 revolutions per minute (rpm) in hard ground to 70 rpm or greater in softer materials, see Table 2.1.

B - Dependent Variables:

Penetration Rate (R): The rate of advance of the bit through the rock is a function of all the independent variables as well as the nature of rock being drilled and the bit design.

This parameter is generally regarded as the one factor which determines overall productivity of the equipment ie. the drillability. However, a balance must be achieved whereby good penetration is obtained for minimal bit and machine damage through proper operation within the machine capabilities ie. maintenance of proper levels of N and W. In many surface mining operations, however, high R values are maintained through the use of excessive W and N resulting in increased downtime through overloaded rotary motors and accelerated bit wear.

Torque (T): The torque T is the rotary force component applied to the rotating bit at sufficient levels to overcome the interaction between forces (rolling resistance) resisting the cutting and grinding action generated at the bit-rock interface (Figure 2.1). The amount of T required to rotate the bit is dependent upon the level of W, bit design and rock type. The maximum levels of

Table 2.1 - Bucyrus-Erie 60R Series III Rotary Blasthole Drill.

<u>Bucyrus-Erie 60R Series III Rotary Blasthole - Fording River Mine:</u>

Weight (approximate operating weight): 260,000 lbs
Mast Height: 107 ft (extended mast)
Length of Drill Steel: 50 ft
Number of Drill Steel: 3 @ 50 ft (+15 ft)
Weight of Drill Steel (50 feet): ≈ 7000 lbs
Weight of Stabilizer: ≈ 600 lbs
Weight of Bit (12 1/4 inch diam.) ≈ 220 lbs
Average Penetration Rate: 200-220 ft/h
(for 12 1/4 inch bit)
Average Rotary Speed: 55 to 70 rpm
(2 x electric rotary motors @ 130 Hp)
Maximum Pulldown: 125,000 lbs (10204 lbs/inch)
(≈ 1100 psi downpressure)
Maximum Drill Torque: ≈ 15000 ft-lb

(Bucyrus-Erie Co., 1978)

applied T which can be developed by a typical blasthole drill, is also limited by the maximum power capacity of its hydraulic or electric rotary motors. Additional torque can develop in deep boreholes as a result of the frictional forces developed between the drill steel and the hole wall when slight hole deviation or eccentric rotation is present. High torque is prominent especially in angled holes. For shallow vertical holes, as in routine production blasthole drilling, the resistance to cutting (and therefore T) would increase with an increase in W and/or N and be reduced with increasing bailing velocity and/or pressure. T will also vary, at constant N and W, as a result of the nature of the rocks being drilled, and is generally higher in abrasive rocks such as sandstones (Eronini et.al., 1981).

Bailing Air Pressure (I): Drill cuttings in blasthole drilling are usually removed by compressed air. The air is transported to the bit-rock interface via a hollow stem drill string. Air passages or jets in the bit allow most of the compressed air to pass through it, to lift the chippings back up the outside of the drill steel to surface. About 10 percent of the air is diverted through bit bearings for cooling (Nelmark, 1980). The 60R drill at the mine site relied upon air as a bailing medium. Alternatives for production blasthole drilling are water or water mixed with air.

A pressure difference exists between the air descending within the drill steel and that rising in the annulus outside the rods. This pressure difference is required to both counteract the difference in air densities due to suspended rock particles and to overcome the frictional resistance to airflow. An increase in R due to an increase in W, increases the weight (greater volume) of the suspended rock particles and therefore the differential fluid pressure. Increased W causes increased insert penetration with a reduction in flow area at the bit-rock interface, and therefore the flow air pressure will increase - the pressure difference also increases if the bailing air velocity (ie. greater volume of drilling fluid present) is increased. Jamming, clogging and balling of the bit can occur if the excavated material is not efficiently removed from the bit-rock interface (Maurer, 1962).

Bailing Air Velocity/Volume: The required flow rate necessary for efficient drilling is a function of the volume of material removed by the bit and the maximum size of rock particles developed. This parameter is governed by the rated capacity of the air compressor on-board the drill, which is related to the dimensions of the drill steel and bit diameter. As penetration rates increase, greater amounts of drilling fluid are necessary to bail the increased heat developed at the bit-rock interface and the increased volume of rock fragments to the surface. Too low a bailing velocity causes "regrind" where the rotating bit inserts come in contact with previously fragmented rock and secondary crushing of the chips into smaller pieces occurs. Alternatively, too high a bailing velocity causes sandblasting of the bit and drill steel causing excessive wear. These phenomena result in reduced overall bit life and performance (Nelmark, 1980).

The efficiency of the flushing mechanism therefore influences R, eg. in poor bailing situations (ie. rate of chip development exceeds that of chipping removal) this parameter will be reduced and balling (clogging) and jamming of the bit can result. A "perfect cleaning" situation would be one in which each chip would be removed from the face as rapidly as it is developed (Maurer, 1962, see section 2.3).

Increases in R can generally be realized by increasing W and N, provided there is sufficient bailing air volumes developed by the flushing system for cleaning the hole bottom and cooling the bit bearings. However, increases in these two operational parameters beyond the design specifications of the bit will result in accelerated bit cutting and bearing structure wear, and drill stem vibration.

Bailing velocity is also an important factor to consider in the application of rotary drilling equipment. The return velocity of hole-cleaning air will vary according to drilling conditions, i.e. weight of cuttings, hole depth, amount of moisture encountered, etc. The consensus of most equipment manufacturers is that 5000 feet per minute represents the minimum value, and when heavy cuttings result from the drilling operation, excessive depth or moisture, higher velocities are necessary (Reed, 1986).

For soft formations, doubling N and W will double R if the bailing volumes and velocities are sufficient (Benston, 1956).

Two additional independent variables affecting drilling performance are:

- **Bit Design:** The bit is operator selected and governs the type of response from drilling ie. influences the value for R, N, W and resulting level of T. The details of bit design are covered in section 2.2.2.

Rock Mass Characteristics: Variations in the textural, compositional and structural nature of the rock, will be indicated by corresponding changes in the drilling performance parameters. The extent to which one or several parameters will respond to changing rock mass characteristics is dependent upon all the conditions surrounding the drilling. These criteria have to be defined on a site specific basis in terms of drill, bit and rock types present. Each of these categories will be examined both independently and in terms of their inter-relationships with drilling performance in sections 6.2 to 6.5.

2.2.2 Tricone Rock Bits:

The present study at the Fording River mine involved the monitoring of rotary blasthole drills using tricone bits with tungsten-carbide inserts, of diameter 10 5/8 inch and 12 1/4 inch.

Tricone bits are the oil industry standard and therefore numerous, well documented investigations are found throughout the literature. In order to understand rotary drilling rock breakage mechanisms, it is necessary to first examine the design of tricone bits. The mechanisms of rock breakage using this type of bit is examined in sections 6.2 to 6.5.

A tricone bit is comprised of 3 conic shaped rollers having arrays of tungsten-carbide inserts, which rotate across the surface of the rock under an applied W normal to the bit axis. Figure 2.4 shows a 10 5/8 inch diameter tricone bit installed on

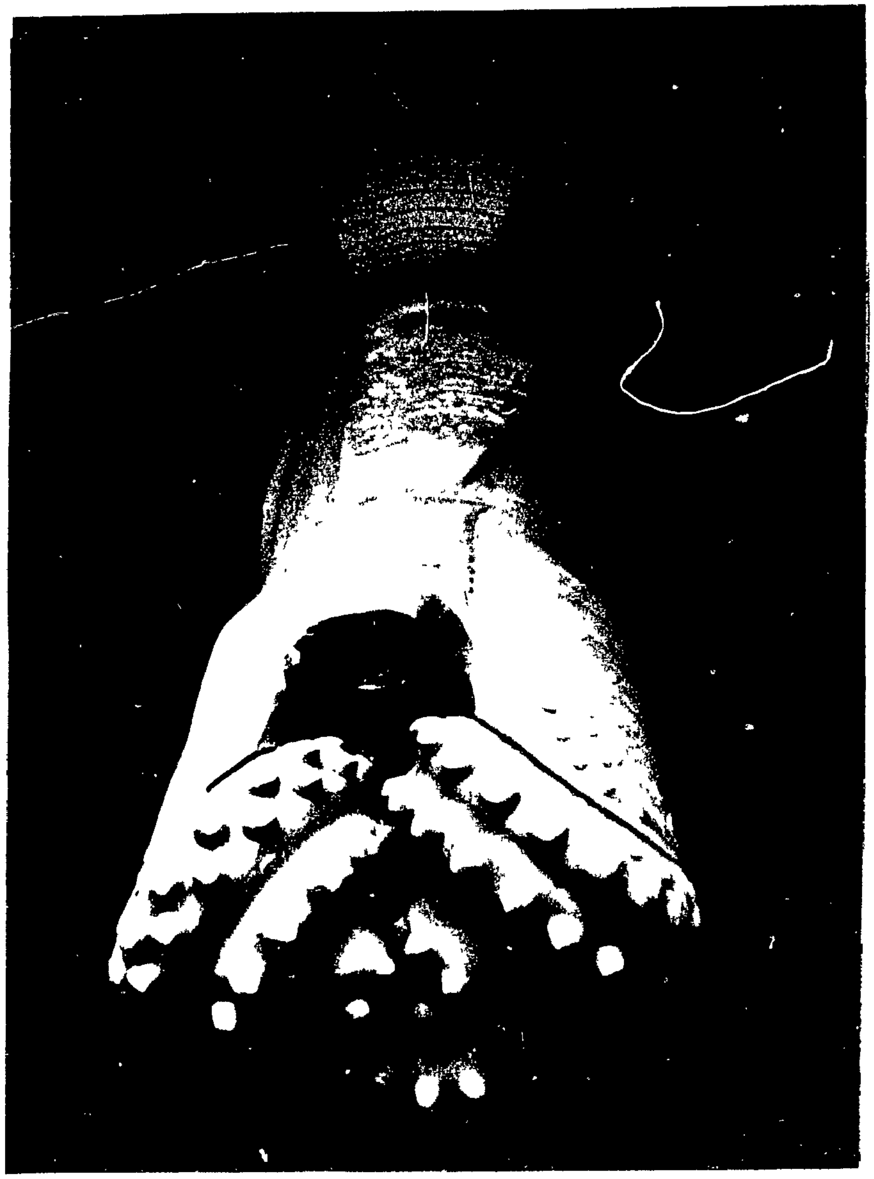

Figure 2.4 - Smith-Gruner Q7J, 10 5/8 inch diameter tricone bit installed on a 45R Drill, Fording River Mine.

a 45R drill to illustrate the geometry of the cones.
These bits may have a slight scuffing or shearing action mainly in soft rock formations, but primarily operate to break rock into chips through a process of repeated indentation of the teeth

under static conditions of W with rotation (Teale, 1965). Indexing (or distance relationship between adjacent teeth indentations) is important in creating a second free surface to which the fractures can propagate. This phenomenum results in the removal of a larger volume of rock than can be expected from a single crater. The depth and volume of broken rock created per bit teeth indentation and rotation (for a particular bit load) determines the value for R ie. the drilling rate (Hartman, 1966; Cobbs and Reader, 1973). A more detailed discussion of rock breakage mechanisms related to tricone bits is provided in Chapter 6.0.

The particular indexing design is a function of rock type and is accounted for when selecting a particular bit for drilling in a certain formation. The rock chips, are "bailed" to the surface via air, mud or water under pressure, which also serves the purpose of lubricating and cooling the bit bearings and cutting structures (teeth). For most surface mine operations, the drill fluid is usually compressed air, for this keeps the hole dry, assisting blasting, and air does not freeze and thus block the hole, as would water in very cold climates (Nelmark, 1980). In addition, the use of air has eliminated the need for water to be delivered, several times a day to the operating drills. However, water as a medium does reduce dust problems considerably, particularly for Coal Measures rocks.

Based on results from field trials using tricone bits and both air and water flushing, it was concluded that both R and bit life could be improved using water as a medium. This was due to the fact that a larger removal force is available when using a liquid as opposed to air, implying a greater potential drilling rate from more efficient hole cleaning. In addition, the water serves to cool and lubricate the bit more effectively (Bingham 1964).

A - Design and Selection Criteria for Tricone Bits:

The selection of the proper tricone bit design will be dependent upon several different criteria;

1 - the type (lithology and strength characteristics) of rock units to be drilled;
2 - flushing media being used and depth of holes;
3 - blast design (depth/diameter/inclination of blastholes);
4 - and operational specifications of the drill (ie. W, N, horsepower, length/diameter of steel etc.).

All of these factors indirectly or directly influence R, which governs the overall economics of the drilling operation.

The actual design and therefore selection of a tricone bit is heavily dependent upon the nature of the formation to be drilled. The action of the cones on the formation is of great importance when determining the ability of the bit to drill with a desired value of R. This parameter is generally seen as being inversely proportional to σ_C. However, other rock properties such as shear strength, τ, hardness, abrasiveness, porosity, permeability, pore pressure, stickiness (ie. shale) and elasticity of the formation also govern the rates to be achieved (Allen, 1977). These factors are accounted for within the design of a particular tricone bit.

For a soft formation, the bit requires a gouging-scraping action, in contrast to a hard rock bit whereby a crushing-chipping action is necessary for penetration. The desired actions are governed by the degree to which the cones approach that of a true roll. A maximum gouging-scraping action results from a rolling mechanism furthest from a true roll. Maximum chipping-crushing is developed by cones closely approaching a true roll. Factors in bit design which account for these mechanisms are:

(1) degree of journal angle (see Figure 2.5)
(2) amount of offset (see Figure 2.6)
(3) profile of the cone.

A combination of the smallest journal angle, largest offset angle, and greatest variation in the cone profile angles will result in an action deviating the most from that of a true roll (soft formation bit). In contrast, a true rolling action will be developed for a bit design incorporating the largest journal angle, no offset and least variation in cone profile (hard formation bit) (Allen, 1973).

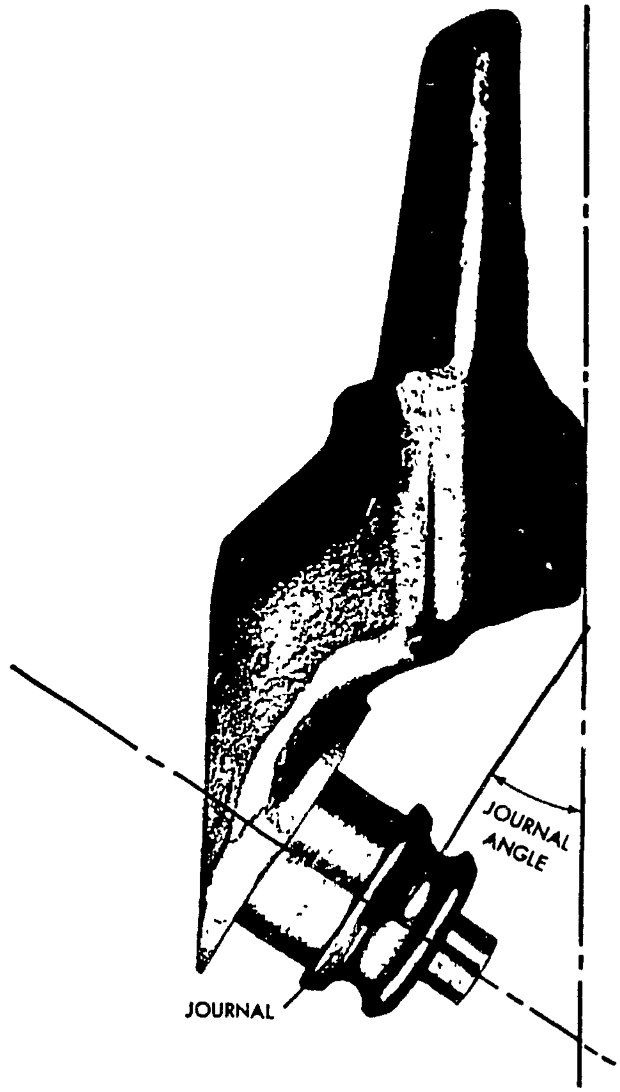

Figure 2.5 - Tricone Bit Leg Journal Angle (Benston, 1956).

B - Tooth Design: Limitations in tooth design are the result of a combination of formation characteristics as well as bit structural requirements. For low strength rocks (soft), deep, slender and widely spaced teeth are necessary to achieve the best value of R. However, the use of larger teeth imposes structural constraints upon the bit design, primarily a reduction in the size of the bearing structures. This factor in turn limits the maximum allowable load which can be applied to the bit. Therefore tooth angles are designed to enable complete tooth penetration at minimum weight. Additionally in soft rock, teeth spacing must be sufficiently large to enable easy removal of crushed 'ine) material from between the teeth and to prevent balling of the bit.

For rocks of higher compressive strength, the tooth depth requirements are not as crucial and therefore bearing sizes are larger, enabling greater bit weights to be imposed. The hard formation bits have short, small, well seated and closely spaced teeth due mainly to the nature of the rocks being drilled producing smaller chips. The particular tooth arrangement is due to the generally high abrasiveness of these rocks and the reduced chipping action of the bit, resulting in teeth that are closely spaced to counteract rapid tooth wear and excessive lateral loading. Tooth angles are kept large to withstand the high loads necessary to overcome the high σ_c for these rocks. The factors of close spacing and heavy setting of teeth generally determines the tooth depth for these bits (Benston, 1956, Estes, 1971).

C - Shape of Tungsten-Carbide Inserts: For tungsten-carbide insert bits, the shape of the insert affects the performance of the bit in a particular rock type. In a medium hard formation, spherical, double conical or projectile inserts would be required as their geometry enables the least amount of insert area to be put on the rock. This in turn results in the application of the maximum pressure point loading on the formation per insert and therefore the best situation with which to fracture the rock and produce chips. In softer formations, long, sharp chisel inserts would be more appropriate to enhance the gouging-scraping action necessary to penetrate the formation

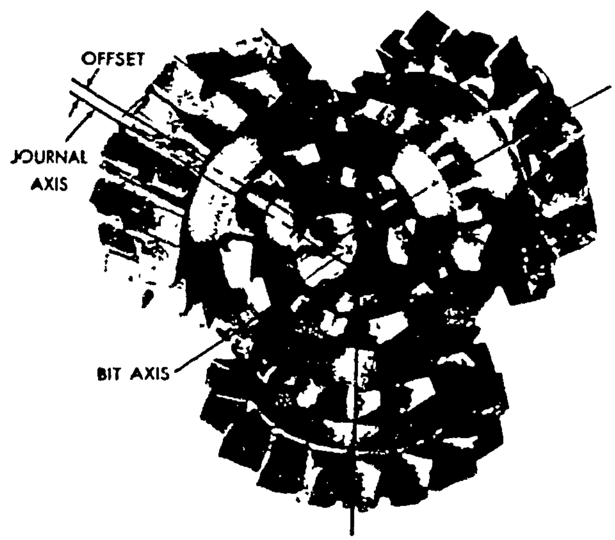

Figure 2.6 - Tricone Bit Offset (Benston, 1956).

FORMATION	BIT TYPE	INSERT SHAPE	APPLICATIONS	ROCK HARDNESS RANGE
Soft	SS6M/S8M 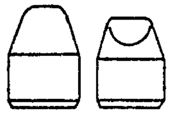	Long Tooth-Shaped Carbide Insert	Economically drills most soft formations which can be drilled with steel tooth bits Maximum penetration rates with minimum down pressures	0-20,000 psi (0-138 MPa)
Medium	M8M/M8M3 	Tooth-Shaped Carbide Insert	For medium-hard and slightly more abrasive formations than those requiring the S8M Faster penetration with lower drilling weights than those usually required for harder formation steel tooth bits	10,000-35,000 psi (69-241 MPa)
Medium-Hard	H8M 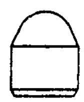	Conical Shaped Carbide Insert	For hard abrasive formations requiring higher drilling weights Bit is designed for higher penetration rates in high strength formations	30,000-55,000 psi (207-379 MPa)
Hard	H10M/H10M3 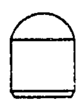	Conical or Ovoid Shaped Carbide Insert	For hardest and/or most abrasive formations requiring maximum drilling weights Durable cutting structure provides long life	45,000-100,000 psi (310-689 MPa)

Figure 2.7 - Shape of Tungsten-Carbide Inserts (Dresser-Security, 1987).

most rapidly, see Figure 2.7.

In order to improve the performance of rock bits, partial or complete tooth deletions are necessary. The nature of soft to medium hard formations generally result in the packing of broken material within the spaces between teeth. This phenomenum results in a reduction in the penetration of the teeth giving rise to a decrease in the drilling rate or balling of the bit. Therefore to avoid this situation, sufficient space between teeth must be provided in addition to a method of removing the collected material. A design which reduces packing is to have at least one cone out of the three having more closely spaced teeth. This overlapping tooth arrangement assists in removing the material between the teeth on the remaining cones. Also a variety of tooth deletion arrangements are required in order to develop adequate spacings while achieving the desired cutting performance (Benston, 1956).

D - Tooth Deletions: When selecting a rock bit, the amount of variation in the drillability of the formation being drilled is also a factor to be considered. For example in an area of predominantly medium strength limestones, a bit having particular characteristics for this class (strength) of rock will be required. However, if the formation is also interbedded with thick, higher strength dikes and/or sills, then a bit should be selected to also drill these rocks effectively in addition to the limestones, with as little reduction as possible in overall performance.

E - Classification and Use of Insert Bits: Journal bearing insert bits have bearing capacities in excess of the cutting structure capacity and are therefore classified (and selected) according to levels of W (lbs or lbs per inch bit diameter) and N required to give acceptable values of R at minimum cutting structure damage (Figure 2.8). This is of course provided that the bit was properly selected initially according to the formation strength (Allen, 1977).

Tungsten-carbide inserts are extremely resistant to abrasive wear and breakage, and will give consistent performance during the bit's life if used properly. The compressive strength of individual tungsten-carbide inserts is in the range of 450,000 to 650,000 psi (3100 MPa to 4480 MPa), depending upon the service requirements (Cobbs and Reader, 1973). Continuous development of new grades and shapes of carbide inserts, improved methods of setting inserts in the cones and better knowledge of cone metallurgy to hold inserts in place are reasons for utilizing insert bits. Additionally, greater seal, bearing and body durability result in improved bit life and therefore cost savings through more footage per bit versus milled tooth bits (Neilson, 1969; Garner, 1972; Allen, 1977).

Bit size, in.	High rpm-low wt. range, rpm	1,000 lb	Low rpm-high wt. range, rpm	1,000 lb
BIT TYPE-F2				
Formation: Softest shales, clays, and salts				
7⅞	90	12	55	28
8½-8¾	90	13	55	31-32
9⅞	90	15	55	37
12¼	85	19	55	44
Formations: Unconsolidated soft shale with sand streaks				
7⅞	60	20	40	37
8½-8¾	60	21-22	40	41-42
9⅞	60	25	40	47
12¼	60	31	40	55
BIT TYPE-F3				
Formations. Medium soft shale				
6¼-6½	70	15-16	55	20-21
7⅞	70	23	55	32
8⅜-8¾	70	27-28	55	34-36
9½-9⅞	70	30-32	55	39-40
11	70	33	55	44
12¼	70	34	55	47
Formations. Soft and medium soft limestone and dolomite				
6¼-6½	65	20-21	45	27-28
7⅞	65	31	45	39
8⅜-8¾	65	34-35	45	42-44
9½-9⅞	65	38-40	45	48-49
11	65	43	45	50
12¼	65	47	45	53
Formations: Unconsolidated medium soft shales, limestones, and sands				
6¼-6½	55	20-21	40	25-26
7⅞	55	31	40	35
8⅜-8¾	55	34-35	40	39-40
9½-9⅞	55	38-40	40	44-45
11	55	43	40	50
12¼	55	47	40	54

Figure 2.8 - Recommended W and N for Journal Bearing Bits (Allen, 1977).

2.3 Drillability Investigations:

Once the effects of bit design upon overall drill performance had been assessed, researchers turned to studies of the individual drilling parameters to evaluate their influence upon penetration rates. The effects of bit loads, rotation speeds, rotary torque/horsepower, flushing hydraulics and rock mass properties on drilling rates were investigated in detail. Theoretical approaches, based upon the stress and failure mechanisms of rock under the load of individual rock bit inserts were attempted (Outmans, 1960; Maurer, 1962; Eronini et.al., 1981). From such studies it was hoped that a prediction of rock failure could be made with subsequent derivation of a drilling rate. This appeared to be the logical path of investigation whereby all the drilling parameters could be incorporated into one unifying analysis. However, areas such as fracture mechanics, bit geometry, rock mass variation, flushing media properties, bit hydraulics, bit loads and speeds and additional operating influences that were known or unknown, prevented numerous investigators from succeeding in their tasks. Therefore it was clear from these drilling complexities that a less scientific basis but more practical approach be followed, in order to determine the relationship(s) between the parameters (Cunningham, 1978).

These drillability[1] investigations were broadly based upon the following concepts:

1 - the hardness and toughness of the rocks,
2 - the power input to the drill compared with total volume of the hole and,
3 - the penetration of the bit related to the resistive forces of rocks on the applied penetrative forces (Paone et.al., 1969).

Three main approaches were followed by researchers investigating drilling performance which primarily involved the development of a relationship between rate of penetration and the other parameters ie. point 3 above. These studies involved,

1 - laboratory studies of full size and scaled down drilling equipment under controlled conditions;
2 - empirical investigations combining both laboratory and field trials;
3 - theoretical studies with respect to machine-rock interaction, and total drilling system numerical simulations.

---

1 - drillability is a measure of the susceptibility of rock to be penetrated by a drill (Paone et.al.,1969)

Since the overall objective in most drilling applications is the minimum cost/foot, this factor was seen as being related to the value for R. Therefore the majority of drilling studies examined the relationships between this parameter and all the other drilling variables it depended upon. Choquin (in Girard,1985) defined an equation which describes the general relationships determined in past investigations relating the interaction of the drilling parameters with the ground, as:

$$R = K\ [N^{\alpha} \cdot W^{\beta} / A^{\delta}] \quad ...2.1$$

where K = drillability constant

A = variable dependent on condition of the bit

and α, β and δ are exponents based on the conditions surrounding the particular study.

2.3.1. The Influence of Different Parameters on the Rate of Penetration, R:

A - Weight on the Bit (W): Most studies indicate that an increase in W generally gives rise to a corresponding increase in R. This relationship is represented by an equation of the form,

$$R = K \cdot W^{\beta} \quad ...2.2$$

The exponent β has been shown by many investigators to vary between 0.5 and 2.4, with the variation attributed to the type of drill used and the characteristics of the rocks drilled in the experiment. These studies were both laboratory and field based using diamond and rotary tricone bits. Choquin (in Girard, 1985) obtained from various laboratory and field studies by several authors that $\beta = 1.5$ for hard ground, $\beta = 0.6$ for soft ground and $\beta = 1.0$ for ground of medium hardness. Laboratory studies by Tsoutrelis (1969) using a scaled down drill at constant $N = 270$ rpm and W ranging between 375 to 1260 pounds derived a value for $\beta = 1$.

Warren (1981), however, noted the considerable differences between experimental results and those calculated from a form of equation 2.2 for different values of ß. He proposed a new equation (see equation 2.26) which accounted for the N and the strength of the formation. This new equation allowed him to explain more clearly a more gradual reduction in R for higher values of W.

Eronini et.al.(1981) and Maurer (1962) both developed, based on actual drilling studies on roller-cone bits, curves for R = f(W). These authors noted that up to a certain W, R follows a trend similar as to the earlier studies, but drops off after reaching a critical value for W. Eronini et.al.(1981) noted that this phenomenum was due to some interaction between the different drilling parameters, whereby for further increases in W, T increased rapidly, while N decreased, as did R. Maurer (1962) also indicated that after a certain value of R is reached, the cleaning at the bit becomes insufficient, with this condition worsening as R continues to increase. With increasing W, the cuttings are not being removed as quickly as they are created and therefore R will decrease due to balling and jamming at the bit.

Brooks et.al.(1963) during actual field monitoring trials, found the value for ß = 1.0 in equation 2.1. They also noted that the values of ß derived by other authors were based upon different conditions and modes of measurement and as a result are difficult to compare. The variation in the values of ß were thus considered the result of different weight ranges being used, and/or the tests not completely covering the entire possible range for the relation R = f(W). Additionally, the levels of N and types and strengths of the materials used in these studie. were also different.

Girard (1985) indicated that the values of ß determined appear to be more a machine than a material dependent parameter. He cautioned that the application of any of these experimentally derived relations to actual field trials may result in considerable errors. This is due to the fact that (1) these equations assume conditions of perfect bit cleaning which may not be realized in actual drilling, and (2) the measurement on surface of drilling parameters, may be very different from the actual mechanisms occurring at the bit-rock interface.

B - Influence of Rotary Speed: The general equation for this relationship is given as,

$$R = K^2 \cdot N^{\alpha} \qquad \ldots \; 2.3$$

Here Choquin (in Girard, 1985) found that α ranged from 0.4 to 1.0, with $\alpha = 0.8$ for soft ground and $\alpha = 0.4$ for hard ground. Maurer (1962) noted that for a "perfect cleaning" situation ie. a condition where all rock debris is removed between rock impacts, R N. Where this is not seen in actual drilling studies, the slope of the R vs N curve decreases for increasing N thereby indicating a poor cleaning condition at the bit, see Figure 2.9.

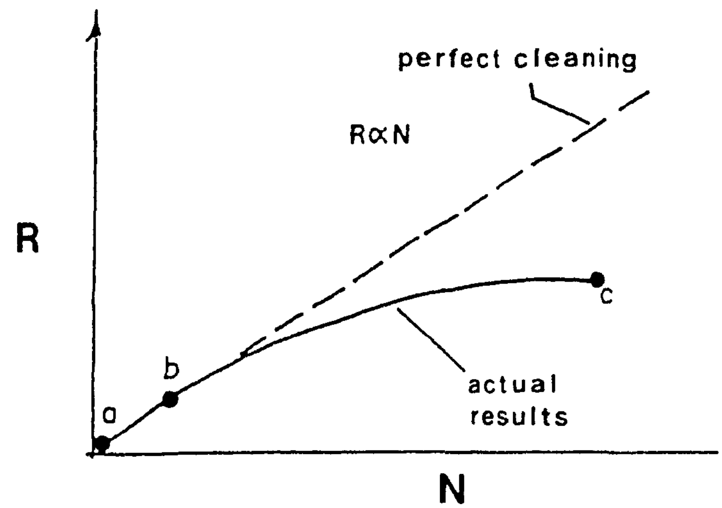

Figure 2.9 - R versus N (Maurer, 1962).

Warren (1981) indicated a similar variation which he explains as being due to a loss of drilling efficiency at higher values of N. This loss according to other researchers, was attributed to a reduction in the time fractures have to propagate and develop chips (Hartman, 1966).

C - Influence of Bit Wear: Most of the studies undertaken account for some form of bit wear within their drillability equations as constants or exponents on one or more of the primary parameters. Bit wear is generally seen to result in a reduction in R provided that all other drilling parameters remain constant. Choquin (in Girard, 1985) noted that for a half-used, worn roller cone bit, a reduction of 50 to 75 percent in R can occur depending upon the type of tooth wear.

Somerton (1959) concluded from laboratory studies on tricone bits, that a 60 percent worn bit will result in a halving of R. This fact was also seen by Cunningham (1960).

Fish (1961) in his studies on drillability using drag bits, noted that rock properties which might have an influence on the drilling process were: (1) the strength properties that determine drilling forces, (2) the abrasive properties that determine the rate of bit wear and (3) the structural properties which determine the nature of the drill cuttings. He concluded that an acceptable drillability index for rotary drills, would have to clearly indicate the value of R for a given bit life and level of W as seen by his equation,

$$R = f(N, \tau, \text{bit hardness}, Q)\ W / \sigma_c \quad \ldots\ 2.4$$

where τ = shear strength

σ_c = compressive rock strength

Q = rock abrasiveness

Simon (1959) noted for roller cone bits (milled steel) that the rate of penetration was at a maximum for a bit with sharp tooth edges but so is the torque required to rotate the bit. As the bit breaks in or wears, the relative decreases in power to the bit is greater than the relative decrease in the rate of penetration at constant weight on the bit.

Warren (1984), based on field studies using an instrumented drill, indicated that the possibility of detecting downhole bit failure was promising.

The effect of bit wear on the performance of rotary drilling is examined in more detail in relation to the results of the current thesis study in section 8.0.

thesis study in section 8.0.

D - Influence of Bit Diameter: Based on laboratory studies using roller cone bits, Maurer (1962) indicated that for tests at constant N and W, R was proportional to the inverse of the diameter, D, squared ie.

$$R \alpha 1 / D^2 \quad \ldots 2.5$$

Other studies indicated however, that the exponent on D could range from 1 to 3, depending on the conditions surrounding the particular study.

2.3.2. Relationships Between Other Drilling Parameters:

A - Torque (T) and Weight (W): Maurer (1962) indicated from laboratory data, that for conditions of perfect cleaning, T varied with the square of W,

$$T = K \quad W^2 \quad \ldots 2.6$$

This relationship is shown in Figure 2.10 for N = 60rpm. He also noted that in the field where imperfect conditions of cleaning exist, this equation becomes,

$$T = K \quad W^{1.5} \quad \ldots 2.7$$

Additional studies showed that T varied directly with W and that the relation is highly dependent upon the diameter of the bit. It was noted by Girard (1985) that T was independent of the strength of the rock. However, in the present monitored drilling research in Coal Measures rock by the author, T appeared to be highly dependent upon rock strength. This fact was also demonstrated from the results of field studies by Hagan and Reid (1983).

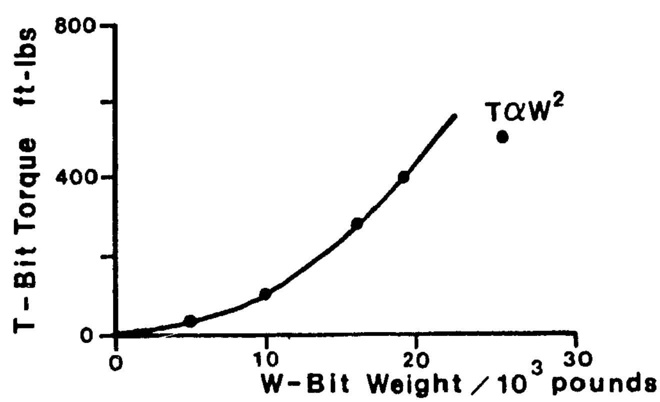

Figure 2.10 - T versus W (Maurer, 1962).

B - Rate of Penetration (R), Weight (W) and Rotary Speed (N): Young (1969) from field tests, showed that the relationship between two parameters is not independent of other parameters. He states that the α in equation 2.3, is not due mainly to the nature of the rock, but is a result of the weight on the bit. This fact was also indicated by Galle and Woods (1960) with their equation,

$$R = K \cdot W^{1.2} \cdot N^{0.5} \qquad \ldots 2.8$$

where W is the weight in lbs/inch bit diameter. This equation is used extensively in the oil industry for drilling rate prediction, primarily for soft formation roller bits.

C - Equations Relating Torque: A limited number of studies have examined the relationship between T and R when all other parameters are held constant. Girard (1985) indicated that very few authors were interested in the contributions of T, that apparently appears to be a very important parameter to determine drillability. Several authors he noted were able to develop a drilling model using T, which produced reasonable results for actual drilling conditions (T being related to N and W). Somerton (1959) defined an equation for the drillability constant K, from laboratory studies using bicone bits, for controlled W and N as,

$$K = R \quad A / T \cdot W \qquad \ldots 2.9$$

where A = cross-sectional are of the hole. In this equation it can be seen that T, considered to be the torque at the bottom of the hole required to turn the bit, was proportional to R.

He also noted that rotary drilling was a very inefficient process. He proposed that the loss of energy in transmission from the surface to the bit may be large thus limiting the total amount of energy directly available for rock breakage. These energy losses due to drill steel vibration, frictional forces between steel, borehole walls and drilling fluids are not between steel, borehole walls and drilling fluids are not accounted for in this equation, and therefore the calculated T may be very different from true T. This is a valid statement for deep boreholes, like those drilled in the oil industry.

Teale (1965) proposed the notion of specific energy, SE(T), which accounted for bit torque, as

$$SE(T) = (2 \pi N \cdot T / A \cdot R) + (W/A) \quad ...2.10$$

where A = cross sectional area of the hole. The concept of specific energy will be examined in more detail below.

Maurer (1962) derived a power to rate relationship based on laboratory cratering experiments as,

$$R = (4 V_c \cdot P) / (\pi \cdot E_c \cdot D^2) \quad ...2.11$$

where P = rotary power on the bit and

E_c/V_c = the energy per unit volume applied by the bit

V_c = volume of impact crater

E_c = total energy imparted to the rock during formation of the crater.

Since P = 2 π N T, equation 2.11 becomes,

$$R = (8 V_c \cdot N \cdot T) / (E_c \cdot D^2) \quad ...2.12$$

This equation indicates that the drilling rate R, is proportional to T under perfect cleaning conditions. This equation was seen to be valid up to 20,000 pounds weight on bit, W, for T α W^2 under perfect conditions. For field conditions, T α $W^{1.5}$. At higher values of W, it is presumed that cuttings begin to accumulate under the bit teeth, thus reducing the friction between teeth and the rock and producing a decrease in T.

For perfect conditions, Maurer (1962) noted that T, should be independent of N.

Morlan (1962), developed an equation for the estimation of T, based upon the formation drillability K, the required load on bit W, and the bit diameter D. This equation was developed from laboratory studies using roller bits of up to 12 1/4 inch diameter.

$$T = 5252\ K \cdot D^{2.5} \cdot W^{1.5} \qquad ...2.13$$

For $K = R / N \cdot W$, substitution into equation 2.13 gives,

$$R = T \cdot N / 5252 \cdot D^{2.5} \cdot W^{0.5} \qquad ...2.14$$

Warren (1984) proposed a torque relationship based on a force balance concept. This equation indicated that for a given tricone roller bit, T was largely determined by the applied value of W (lbs), tooth geometry, and depth of tooth penetration. The equation thus derived was,

$$T = [C_3 + C_4 \sqrt{R/(N \cdot D)}]\ W \cdot D \qquad ...2.15$$

However, this equation required the determination of bit constants C_3 and C_4 which were dependent upon the ratios of T/W and R/N. Laboratory studies indicated that a comparison of actual T versus predicted values using this equation showed very high correlation. Subsequent field trials using commercial measurement-while-drilling instrumentation, enabled both T and downhole W data to be acquired for every foot drilled. During these trials N was maintained constant at 90 rpm. Comparison of actual with predicted data, yielded a modified equation for T which matched the observed with estimated T data with a mean error of 10 percent and a correlation coefficient of 0.991.

A portion of the difference between actual and estimated T values could not be correlated with the properties of the rocks penetrated, as the results of subsequent downhole gamma and sonic logs were inconclusive. However, these studies were seen to indicate that lithology and rock properties may influence T, yet the effect of these factors were determined to be accounted for by the value for R in equation 2.15. Since the formation characteristics did not appear to affect T independently of R, it was concluded that T alone was not an effective indicator of rock mass properties.

2.3.3. Evaluations of the Strength of the Material being Drilled:

The strengths of the formations being drilled appear to be difficult to evaluate and integrate into one equation relating this property with all the other drilling parameters. Several researchers have used the term "drilling resistance" or "drilling strength" in order to avoid confusion with the compressive strength of rock (Somerton, 1959; Warren, 1981). Some investigations have indicated close to a one to one agreement between drilling strength and compressive strength, while others have shown a wide discrepancy between the two. Somerton (1959) introduced the term "drillability" as a means of relating the nature of the ground into an equation for drilling performance. Others have indicated that the intersection of the curve R/N=f(W/D) (where D = diameter of the bit) with the X axis (Bingham, 1965) or the slope to this curve (Tsoutrelis, 1969) define a parameter which relates in a relative sense to the compressive strength of rock.

This section is aimed at providing an overview of what work has been conducted in the past in this area. Sections 6.4 and 6.5 will re-examine this topic in relation to the drill performance data acquired during the current thesis study.

Somerton (1959) on the basis of laboratory tests using air flushed bicone microbits, derived the equation,

$$R / (N \cdot D) = f\ (W / S_d \cdot D^2) \quad \ldots 2.16$$

where S_d was considered to be a parameter related to the drilling resistance. Rearranging this equation gave,

$$R = G \cdot N \cdot D \cdot (W / S_d \cdot D^2)^2 \quad \ldots 2.17$$

where G = 1.5, and was derived from a plot of R/DN vs. W/D^2S_d. He was unable however, to determine if any relationship existed between S_d and the compressive strength of rock. He did indicate that for rocks containing 2 or more mineral constituents of different strengths, a greater amount of rock breakage occurred in the weaker grains. Additionally, that the smaller the amount of bit tooth in contact with the rock, the greater would be the stress concentration imposed upon the rock for a given bit weight. He also noted that rock strength was a difficult parameter to evaluate and one needed to understand the actual mechanics of rock breakage more fully to derive its relationship with drilling performance.

Equation 2.17 was also dependent upon the geometry of the bit being used, accounted for by the term G, which was shown to vary between 0.7 and 3.8. This term was related to bit design and the nature of rock breakage ie. true rolling hard rock bits which involved impact-compressive failure while non-true rolling soft rock bits with their scraping-gouging action, involved torsional-shear failure. However, he found that the bit geometry was too complex a factor, thus preventing it from being properly analyzed and integrated into a drilling rate model.

Based on these results, Somerton (1959) concluded that the compressive strength of rock was not a reliable rock strength parameter for determining the drillability of general rotary drilling applications.

Simon (1959) in response to the work by Somerton (1959) noted that the term G, in equation 2.17 is not a constant. It may instead be a function of one or several additional dimensionless groupings of the many variables associated with the rotary drilling mechanisms, for example some measure of bit wear.

Maurer's (1962) "perfect cleaning" model of drilling works under conditions of drilling where all rock debris is removed between rock impacts. Under these conditions, R is equal to,

$$R = k\ (N \quad W^2 / D^2 \cdot S^2) \qquad ...2.18$$

where k = drilling constant and S = drilling strength.

For imperfect conditions, as is usually the case in field drilling, regrinding of the cuttings usually gives rise to lower R values than predicted from equation 2.18.

Simon (1959) examined the dimensionless drilling parameter k, and concluded that it was equivalent to the average distance between the tips of successive bit teeth. This constant was also dependent upon several other parameters eg. rock properties, mud properties, pressure conditions, bit dullness and bit design. Although dependent on these factors, k is constant for a given bit at a given depth.

Further studies by Fish (1961), see equation 2.4, found that in laboratory drilling tests using drag bits, R for constant N was related to σ_c. He also determined that variations of both W and T were a linear function of R, but at extremes of W and T, a departure from linearity occurred.

At higher levels of W and T, clogging of the bit occurred and the value for R was not a representative value. For lower levels of W and T, with the occurrence of bit wear, a greater level of W was required to maintain the same level of R. A linear relationship was obtained by him between W/R and σ_c.

According to Bingham (1964) there were two main reasons to relate drill performance to rock properties: (1) the mining and petroleum industries were unlikely to find a means to predict drillability without a means of relating it to some rock property and, (2) such a correlation might indicate how good drilling really is, rather than what it might ideally be.

Bingham (1964) indicated that the best physical basis is to relate power input from the drill to the resistance offered by the material being drilled. In the best situation, drilling was limited by the resistance of the rock to failure and therefore some strength property was considered by him to be involved. According to him, not only the mechanism of failure must be assumed, but also the means must be found to relate some rock property. The concern in drilling should be with a macroscopic failure mode and not a microscopic one. His proposed approach makes use of the Mohr-Coulomb failure criteria, which states that "... yielding or fracturing should occur when the shearing stress exceeds the sum of the cohesive resistance of the material, C, and the frictional resistance on the slip planes or shear fracture planes..." This statement in the form of an equation is,

$$\tau_n = (C + \sigma_n \tan \phi) \quad ...2.19$$

where τ_n = shear stress

C = cohesion

σ_n = normal stress

ϕ = angle of internal friction

and is represented graphically in Figure 2.11.

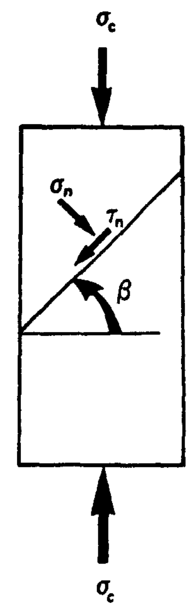

Figure 2.11 - Rock Specimen under Axial Load (Brady and Brown, 1985).

Since from Figure 2.11, $\tau_n = (0.5 \cdot \sigma_c \sin 2\beta)$, and for the critical plane $\sin 2\beta = \cos \phi$, this becomes,

$$\tau_n = (0.5 \cdot \sigma_c \cos \phi) \quad ...2.20$$

where σ_c = compressive stress

This equation is for drilling at atmospheric pressures, where τ_n represents the shear failure strength of the rock.

Bingham (1964) also found that the shear strength of rocks was related to bit weight and diameter based on both laboratory and field studies by the equation,

$$\tau \cdot k_{cs} = (W/D)^{0.5} \quad ...2.21$$

where τ = shear strength (psi)

k_{cs} = a bit constant for degree of wear $((ft^3/lb)^{0.5})$

W = bit weight (lbs)

D = bit diameter (ft)

For a sharp bit $k_{cs} = 0.85 \times 10^{-4}$ $(ft^3/lb)^{0.5}$. He also noted that the intercept of this equation (where the inverse of k_{cs} = slope) i.e. $(W/D)^{0.5}$ was a more consistent indicator of macroscopic rock strength than unconfined compression test data. Therefore, determination of this intercept value enabled an estimation of the shear strength to be derived through equation 2.21, and provided the value of ϕ was known, the compressive strength could be calculated using equation 2.20. Strengths estimated in this manner were seen to agree within 10 percent of the measured compressive strengths.

The ratio of penetration rate over rotary speed to weight on bit over bit diameter was seen by Bingham (1964) to relate to the known variation in rock strength encountered while drilling. This relative strength index, referred to as the D exponent is expressed by the equation,

$$D_x = [\log (R/(60 \cdot N))] / [\log ((12 \cdot W)/(D \cdot 10^6))] \quad ...2.22$$

where D_x = relative strength index ($ft^2/rev \cdot lb$)

The ability of this calculated parameter to reflect known differences in rock properties is demonstrated in sections 6.4 and 6.5.

Cunningham (1978) based on micro-bit and full scale roller-cone bit laboratory studies, derived an equation for R as,

$$R = K \cdot W^a \cdot N \quad ...2.23$$

where K and a were determined through drilling tests in a given formation at two different values for W and equal N. Substitution of the values of R, W and N from these tests into equation 2.23 gave two equations and two unknowns which could be solved for K and a. By plotting a graph of log R to log W, he was able to develop a plot having lines of equal drilling strength, see Figure 2.12.

According to these results, drilling strength, S_d, could be treated as a single physical property of the formations drilled unique only to roller cutter bits. For any value of S_d, K and a were functions of S_d as shown by,

$$R = N \cdot W^a / 0.424 \cdot S_d^{1.5} \quad ...2.24$$

The variable a is calculated from first determining R for a certain N, determining S_d from a plot of R versus W and then calculating a from,

$$a = 0.178254 \ln S_d + 1.09793 \quad ...2.25$$

Cunningham did not believe that a close correlation between compressive strength and drilling rate existed. However, he noted that by using S_d a better correlation with drilling parameter response was apparent.

Warren (1981), based on true scale laboratory and field trials using soft formation rotary tricone bits, also used the term "S" to indicate a relative term for the strength of rock. He noted that S showed good correlation with the shear strength of rock, τ, and reasonable correlation with σ_c.

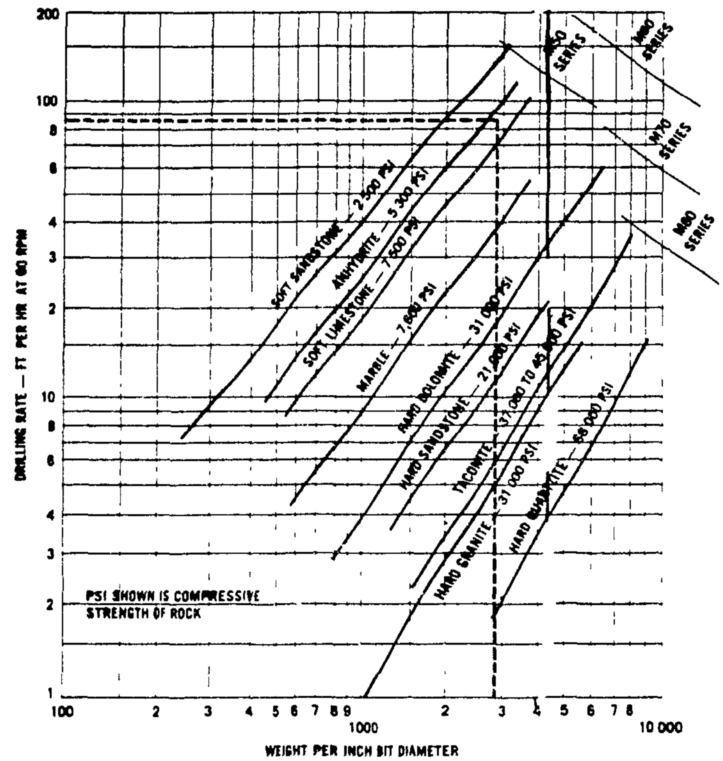

Figure 2.12 - R versus W (lbs/inch) (Reed Mining Tools Inc., 1983).

A basic drilling model was thus developed by him, using dimensional analysis and generalized response curves as,

$$R = (a\ S^2 \cdot D^3 \ / \ N^b \cdot W^2)^{-1} + (c \ / \ N \cdot D) \quad \ldots 2.26$$

The bit constants were calculated from a plot of ND/R versus $(NS^2D^4/N^{0.6}W^2) \times 10^4$, where c = y intercept and a = slope of the best fit line.

This model was based on tests undertaken using 6 to 12 1/4 inch tricone bits, on a laboratory drill rig having adequate W, N, T and hydraulic capacity to test the bits under realistic conditions. Limestone blocks were used with water as a flushing medium, with the hydraulic conditions maintained essentially constant. A total of 9 drilling parameters were monitored at 7 second intervals. Both W and N were servo-controlled to ensure they remained constant throughout each test.

Using the recorded drilling parameters, he applied them to existing drilling models to examine how closely the calculated R data correlated with experimental values, see Figure 2.13.

Equation 2.8 from Galle and Woods (1960) for example, could not be applied in a practical situation without the assumptions from which it was developed being specified. Additionally, as noted by Warren (1981), the equation did not properly reflect the effect on R with changing W and N when all other conditions remained constant. Additionally, Maurer's (1962) "perfect cleaning" theory based on studies of single tooth impacts was not applicable to most soft formation drilling. The deviation in R versus W noted by Maurer (1962) as being the result of imperfect cleaning, is indicated by Warren (1981) that such a situation will occur under all reasonable hydraulic conditions for soft rocks. The model by Cunningham (1978) also failed to follow the experimental data of Warren (1981).

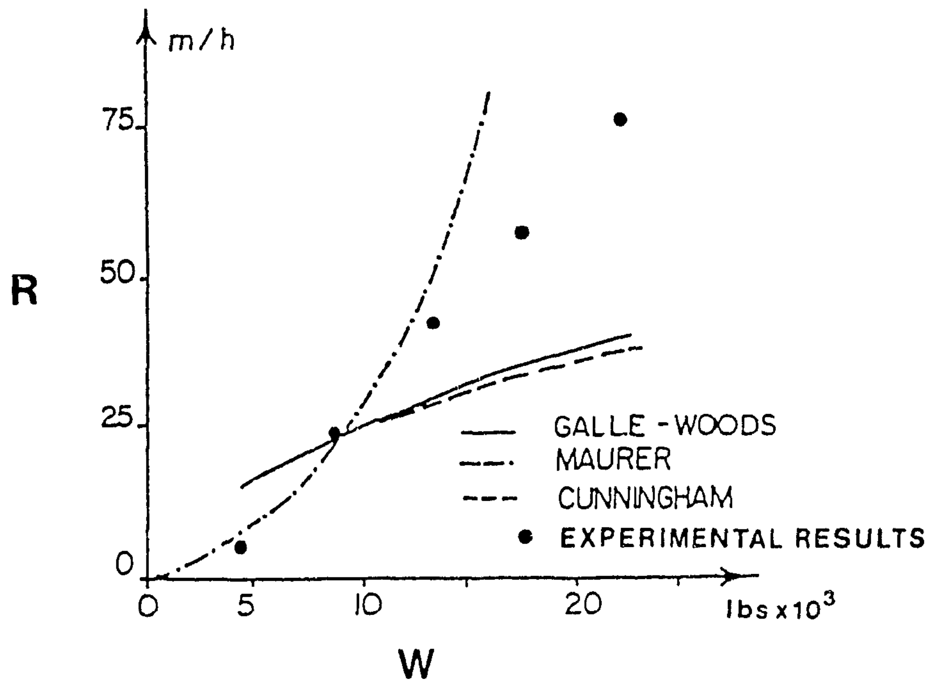

Figure 2.13 - R versus W (Warren, 1981).

Warren (1981) noted that his drilling model was not as elegant as others, but produced results which are more consistent with both field and laboratory observations.

Based on shear strengths determined from laboratory testing of core, he found an excellent correlation between these values and S calculated from equation 2.26. Correlation between these drilling strengths and compressive strengths was almost as good.

Specific energy, SE(T), was initially defined by Teale (1965) as the energy required to remove a unit volume of rock during drilling. Its basis was Kick's Law of grinding, an empirical concept relating energy input to rock particle size reduction. The model was developed from laboratory and field studies using roller cone bits of 12 1/4 inch diameter. According to Teale (1965), the value of SE(T) was an intrinsic property of the rock, independent of the size, shape and type of drill bit and flushing method employed. SE(T) is therefore expressed as in equation 2.10,

$$SE(T) = (2 \pi N \cdot T / A \cdot R) + (W/A) \qquad \ldots 2.10$$

where A = cross-sectional area of the bit (in^2)

The first term of equation 2.10 relates to the component of energy due to the rotation of the bit, while the second term is due to the axial component of W. For ideal conditions ie. the properties of the rock remain essentially constant (ie. σ_c and τ), and no bit wear, clogging and no losses as a result of vibration or friction of the rods on the side of the hole occur, it has been found that SE(T) is constant for a given W. Additionally, for the same conditions, T was seen to be proportional to W implying a constant coefficient of friction, μ, at the bit-rock interface. Under such conditions, the following would hold true,

$T \alpha W$ if μ, σ_c and τ are constant

$R \alpha T$ if N, W, μ, σ_c and τ are constant

$R \alpha W$ if N and μ, σ_c and τ are constant

$R \alpha N$ if W is constant

This would appear to imply that the variations of SE(T) would be related to changes in μ, σ_c and τ, based on the responses of the other parameters. It was determined by Teale (1965) that the minimum value of specific energy, obtained from drill data using two different roller cone bits, appeared to correlate with the value for σ_c of the medium being drilled. (Note that the units for SE(T) in equation 2.10 are the same as units for σ_c ie. pounds per square inch or psi). He pointed out, however, that σ_c is in no sense an absolute measure of rock strength, yet was dependent on the method of testing used for its determination. Additionally, it was concluded that the minimum value of SE(T) equalled the maximum mechanical efficiency of the roller bit, sometimes occurring at low values of W and N.

A correlation of calculated SE(T) data versus measured σ_c was examined in the current thesis study to determine whether this parameter is a suitable predictor or index of rock strength variation. The results from this comparison are discussed in sections 6.4 and 6.5.

Mellor (1972) attempted to determine a means of normalizing specific energy values for all types of rock cutting and breakage processes. Since it was clear that specific energy is very dependent upon the bit type, degree of wear and the mode of breakage, it would be convenient to standardize these values from different processes such that they could be compared to reference values of specific energy. He noted that unconfined compressive strength was not equivalent to the specific energy, but that it had the same physical dimensions and therefore could be proportionally related. In order to establish the unconfined compressive strength as a valid normalizing factor for specific energy, it was considered necessary to demonstrate that, (1) compressive strength was a reasonably consistent and reliable indicator of ease of rock breaking for a wide range of rock types and, (2) compressive strength was actually proportional to the specific energy for breakage mechanisms similar to those operating in standard compressive strength testing. The equation relating these two parameters is given as,

$$W_s = k/2\ (\sigma_f \cdot \epsilon_f) \qquad \ldots 2.27$$

where W_s = specific energy

k = dimensionless shape factor for a non-linear stress-strain curve.

σ_f = axial stress at failure

ϵ_f = axial strain at failure

For linearly elastic rocks, k=1.0 and if the Young's modulus is equal to σ/ϵ, equation 2.27 becomes,

$$W_s = \sigma_c^2\ /\ 2\ E_s \qquad \ldots 2.28$$

where E_s = secant modulus from zero load to failure. Assuming that secant modulus is equivalent to tangent modulus, E_t, times some constant C, then the equation,

$$W_s = \sigma_c^2\ /\ 2\ C\ E_t \qquad \ldots 2.29$$

is possible, where C is a constant greater than 1, and generally equal to 1.5. For rocks that are not strongly anisotropic, the ratio of σ to E_t is in the range of 2×10^{-3} to 5×10^{-3} and therefore,

$$W_s \approx \sigma_c \times 10^{-3} \qquad \ldots 2.30$$

The normalizat n of specific energy to unconfined compressive strength gives a dimensionless index ie. (W_s/σ_c). This index in turn was considered by Mellor (1972) to be a suitable indicator of the effectiveness of the drilling process when effects of variable material properties have been removed.

Rabia (1982) indicated that the specific energies calculated using equations 2.29 and 2.30 were too small in comparison to values calculated using equations 2.10 and 2.31, and therefore could not be compared. This was also apparent in the current study, yet here the value of W_s was considered as an index independent from the traditional specific energies. The use of this equation using the results of the present study will be demonstrated in section 6.5.

Rabia (1982,1987) modified the original definition of specific energy to, (1) - the energy required to remove a unit volume of rock or SE(R) and, (2) - the energy required to create a new surface area or SE_a.

Based on field data obtained using rotary drills with tricone bits, very large values for specific energy were calculated in soft rocks. His equation for specific energy, SE(R),

$$SE(R) = 20\ W \cdot N \ /\ D \cdot R \qquad ...2.31$$

gives SE(R) in in-lbs/inch^3.

Rabia (1982) concluded that drill performance prediction on the basis of SE(R) data only is not reliable since it is not an intrinsic property of rock. Large variations in lab and field specific energy values were observed by him, since rock breakage parameters appeared to control the numerical value of the results. Rabia (1982) attempts to relate derived data to Teale's implication of $\sigma_c \approx$ minimum SE(R), indicated that SE(R) was highly dependent on drill type and bit design. He also pointed out that the SE(R) concept breaks down further with bit wear and clogging due to inefficient flushing.

By pure definition of specific energy, Rabia(1987) stated that no relationship with rock properties can exist. He indicated that specific energy was not a fundamental intrinsic property of rock and therefore the prediction of drill performance is not accurate using only this parameter. However, it was later demonstrated that for a given bit type the specific energy can be useful to distinguish between different lithologies, where any sudden increases or decreases in this parameter reflect changes in the rock type or problems with the bit.

The specific energy given in equation 2.31 is considered constant for any combination of W and N. This is because changes in W • N usually result in increases in penetration rate R, and thus the balance of the equation is maintained. Rabia (1987) noted that the specific energy was a direct measure of bit performance in a known rock type and related to the interaction mechanisms operating at the bit-rock interface. Therefore for a homogeneous rock, specific energy should remain essentially constant over the length of that unit. Thus, specific energy defined by equation 2.31 was considered dependent upon the bit type, bit wear, cuttings removal, rock type and rock properties. The losses in transmitted energy from the bit to the rock indicated earlier, are considered by Rabia (1987) to be a function of the cutting efficiency (bit performance) and are accounted for in equation 2.31. In this regard, low specific energy values indicate efficient cutting with high values reflecting inefficient drilling. Examples of inefficient drilling are in plastic, clayey rocks such as shales and mudstones, or very hard rocks.

Laboratory simulation studies by Eronini et.al. (1981) sought to define a dynamic drilling model for rotary drills. From the results of their study it was shown that bit forces and torques were substantially inter-related. Additionally, the influence of certain rock properties on variables measured at the bit or on surface clearly supported the idea that changes in these could assist in characterizing the formation being drilled. Initial assumptions were that the effect of the changing nature of the rock on the drilling performance would be reflected by variation in both R and calculated specific energy. However, no consistent trend was apparent for the specific energy log, indicating that this parameter may not be an adequate indicator of drilling performance. The observation was made that the specific energy does not take into account the rate at which work is done on the rock. However, the ratio of the specific power (power input per unit rock face area) and the specific energy has the same units as for the R, and may provide a better correlation with rock properties.

Bauer and Calder (1967, 1971) developed an empirical equation for estimating values of R using tricone bits, based upon a knowledge of the value for σ_c of the rocks being drilled.

$$R = N \cdot [W \cdot (61 - 28 \log \sigma_c)/(D \cdot 300)] \quad ...2.32$$

It was noted that the equation gave reliable results provided that sufficient tests were conducted to obtain a meaningful value for σ_c. This equation is used presently by a major rotary drill manufacturer as a means of assessing the required type of drilling equipment for a customer in a particular mining environment (Bucyrus-Erie Co.,1979).

Mathis (in Leighton et.al., 1982) during blasthole drilling investigations, defined the RQI or rock quality index. This value was based upon the ratio of W to R and was considered by him to be reflective of variations in rock quality.

The majority of the equations to estimate R reported in the literature required the use of experimental constants to account for bit wear and design, flushing conditions and rock properties. This aspect made them somewhat impractical for immediate use. Mathis derived from these a generalized equation for R equal to,

$$R = N\ W\ f(\sigma_c)\ K \quad ...2.33$$

where $f(\sigma_c)$ decreased as σ_c increased and K was a constant dependent upon the experimental conditions and drilling equipment used. Using this equation and keeping both drilling procedure and N constant, the only other variables were R and W. Therefore, according to Mathis, the ratio of these last two parameters should reflect variations in rock quality. Thus he defined the Rock Quality Index (RQI) as,

$$RQI = W/R \quad ...2.34$$

It is to be noted that W in eqn.2.34 is equal to the hydraulic downpressure in psi. Leighton et.al. (1982) and Leighton (1986) stated that both these parameters were easily measured during drilling of individual blastholes. They also found from field trials that a reasonable determination of rock mass quality could be obtained from this index.

A simple relation to calculate the kinetic energies of the axial and rotary components applied (in theory) to the bit while drilling, was developed by the author and Mottola (1988). It was assumed that if the energies required to achieve penetration of the rock could be determined, this value in turn would reflect the strength of the material. As a result, such an index could effectively profile the changes in rock properties based on the drilling parameter responses. As for the equation of Rabia (1982), it was considered that all the energy losses surrounding the drilling process would be accounted for in the equation, as it was based on the monitored responses of the drill.

This equation is based upon the standard equations for determining the kinetic energies of rigid bodies in translation, KE_t and rotation, KE_r, or,

$$KE_t = 0.5\ m\ v^2 \qquad \text{...2.35}$$

$$KE_r = 0.5\ I_0\ w^2 \qquad \text{...2.36}$$

where m = mass of the body (lbs)

v = linear velocity of the body (in/sec)

I_0 = mass moment of inertia of the entire body about the axis of rotation (ft-lb)

w = angular velocity of the body (revs/sec;rads/sec)

The units for kinetic energy are ft-lb. Assuming that the effect of the bit is negligible, the moment of inertia for the drill pipe (hollow cylinder) is,

$$I_0 = 0.5\ m\ (r_0^2 + r_i^2) \qquad \text{...2.37}$$

where m = total mass of the drill pipe plus assembly including applied load

r_0 = outside radius of drill steel

r_i = inside radius of drill steel

Therefore the sum of the two equations 2.36 and 2.37 gives,

$$KE_t + KE_r = 0.5\ m\ v^2 + 0.25\ [m\ (r_0^2 + r_i^2)\ w^2] \qquad \text{...2.38}$$

Substituting the appropriate drilling parameter for the variables represented in this equation as,

$m = W$ = applied weight (lbs)

$v = R$ = penetration rate (in/sec)

$w = N$ = rotary speed (revs/sec)

and therefore equation 2.38 becomes (for 60R drill $r_0 = 5.376$ inch and $r_i = 3.877$ inch),

$$KE_{t1} = 0.5\ W\ R^2 + 10.98\ W\ N^2) \quad ...2.39$$

Note that W includes the total weight of the drill steel and bit, and the head assembly (= 14142 lbs) plus the applied load from W.

Equation 2.39 in theory thus gives the total kinetic energy, KE_{t1}, in in-lbs. Dividing this equation by the volume of rock excavated in 1 sec V_r or,

$$V_r = (R\ A) \quad (in^3) \quad ...2.40$$

A = cross-sectional area of the borehole ($\pi\ r^2; in^2$)

calculates the *effective* applied load per cross-sectional area i.e. the total pressure applied to the rock to produce penetration, having units in psi. These units are equal to those usually reported for rock compressive strengths.

This application of equation 2.39 and 2.40 to the monitored drill data of the current research investigation is examined in sections 6.4 and 6.5.

2.4 Conclusion:

Girard (1985) noted that most of the drilling equations reviewed are of a form,

$$R = f(\text{all other drill parameters})$$

where the differences in the equations are in the coefficients and exponents for the various parameters. The coefficients are usually attributed to either the machine or the formation but no one has yet determined which part of the drillability equation is specific to each component.

The different forms of the models presented above are testimony to the inherent difficulties involved in unravelling drilling mechanisms. The particular form of an equation is a result of their empirical derivation being based on very different conditions of testing. These would include drill and bit type and diameter, laboratory versus field conditions, full scale or reduced scale drills, ranges of N and W used, rock types and monitoring equipment used, if at all. The exclusion of T in some of these models for example, is possibly due to the difficulty in accurately monitoring this parameter.

Similar difficulties were also seen to be responsible for the many problems associated with successfully relating σ_c to drilling performance.

3.0 DRILL MONITORING INSTRUMENTATION:

3.1 Introduction:

In order to monitor the true drilling parameters with sufficient accuracy and reliability, suitable recording systems were developed. The initial systems were analog based chart strip recorders using mechanical and hydraulically operated transducers linked to various drill mechanisms on surface. In the mid 1960's, the oil industry began to utilize digital computers in the monitoring and development of control logic for drilling rigs. As the electronic industries began to miniaturize components, further advancement was made in the implementation of down-hole measurement devices, providing a means of monitoring more precisely the actual bit-rock interaction without interference from drill string and mud column influences (Cunningham, 1968; Deily et.al.,1968; Miller and Rollins, 1968)

The results from drillability investigations in the oil industry are equally valid for the types of drilling and equipment commonly used in mining. As the transfer of technology between the oil industry and mining increased, so did the number of private, governmental and educational groups which were actively pursuing research in mining related fields. Over the past decade, however, there has been relatively little innovation in the drilling technology sector, except for possible improvements in both bit design and materials. This trend is in the process of reversing itself, whereby new drilling machinery and accessories designed for the mining community are being made available. In parallel with this direction, is the importance of understanding and then utilizing monitored drilling performance parameters to ensure successful implementation of new technology in mining applications.

For the current research project the uses of recorded drilling parameters were to be evaluated in several ways:

1 - to identify the inter-relationships between drilling parameters for the monitored 60R blasthole drill using a

particular bit type,

2 - to characterize the performance of the monitored drill with respect to rock mass properties by relating the responses of the individual parameters to unique rock breakage mechanisms,

3 - to precisely correlate the drill parameter patterns to lithology and rock strength for site characterization applications,

4 - to assess the capabilities of performance monitoring techniques towards using the blasthole drill as a diagnostic tool in a variety of applications including automation and control.

The actual measurement and recording of drilling performance parameters requires the use of appropriate instrumentation to successfully acquire meaningful data. A discussion is provided in the following section 3.3 outlining the phases involved in the design and construction of the drill monitoring system used throughout these investigations. Prior to this, several studies which involved the development of drill instrumentation and/or field performance monitoring will be reviewed. These investigations were aimed at monitoring the performance of rotary drills in both underground and surface mining environments for various applications.

Research into drill performance monitoring in underground coal mining was primarily to develop a means to diagnose roof conditions during roofbolting operations, (Luisigna and Felleman, 1983). In surface coal mining, this technology was investigated in order to assist in blast design to optimize both digging productivity and recovery through control over fragmentation, (Scheck et.al., 1982; Leighton et.al. 1982,1986; Hagan and Reid 1983; Lebel, 1984; Mol et.al., 1987).

3.2 Past Development of Drill Monitoring Instrumentation:

Underground studies by the United States Bureau of Mines (USBM) in the late 1970's involved monitoring the performance of small rotary drill/roof-bolter rigs. These investigations were aimed at assessing those drilling parameters capable of accurately reflecting ground conditions around underground openings,(i.e. estimate relative strengths and detect fractures and interfaces between different rock types), towards improving rockbolt placement. It was seen that the variation in the calculated SE(T) provided the best correlation with changing rock properties. This parameter was seen to compensate for changes in machine operation. However, the ability of this parameter to detect variations in the rock mass was seen to be dependent upon the degree of difference between rock textural, compositional and structural domains. It was also determined that the instantaneous value for R on its own was useful for the detection of abrupt changes in ground conditions, e.g. large voids (Luisigna and Felleman, 1983; Howie, 1988).

Monitoring the performance of rotary blasthole drills in western Canadian coal (Greenhills Mine) and hard rock (Afton and Equity Mines) surface mines was undertaken in the past by several workers. Work by Leighton et.al. (1982) and Lebel (1984) using an analog chart strip recorder, illustrated the potential of correlating measured drill performance variation of Bucyrus-Erie 40R and 45R, and Reed SK-60II rigs with changing rock mass properties. The RQI (Rock Quality Index) derived from these investigations (eqn.2.34) related W to R. This index was reported to enable a more precise determination of ground "blastability" by indicating weak and strong rock zones. A correlation between the RQI and a powder factor was also derived, permitting improved explosives loading, thereby optimizing fragmentation . This approach, however, introduced some bias into the results due to drill operator involvement and manual extraction of the data from chart strip records.

In subsequent Australian investigations, Hagan and Reid (1983) evaluated the potential of performance monitoring of production rotary blasthole drills as a means of improving the efficiency of blasting in surface coal mining. They proposed that a continuous readout of either R or T obtained while drilling, would provide an immediate indication of the variability of the rock mass. Based upon such results, charging could be carried out in those zones of high strength as indicated by a low R value (high T), whilst weak zones of high R (low T) were stemmed. The blast energy would thus only be concentrated in those areas requiring breakage, thereby preventing or reducing venting of the energy within weaker zones.

Since the rock mass properties are of primary consideration in optimizing blasting, then their characterization is critical to effective blast design. It is to be emphasized that monitored drilling techniques are most successfully implemented in geological areas where there is a clear contrast between rock types in terms of strength and lithology. Additionally, the geology of the area defined from core or surface mapping, has to be known in advance of the drill performance parameter interpretation.

As was recognized by Leighton et.al. (1982) and Leighton (1986), proper interpretation of the drilling performance records of a mine would enable the detection of zones of weak rock. This information in turn could be applied towards an improved blasting design to enable selection of the type of explosive, charge distribution, stemming length and primer position, as well as the burden, spacing, and effective sub-drilling or stand-off drilling in a blasthole or group of blastholes.

Work undertaken by Scheck et.al. (1982) to instrument a rotary blasthole drill was motivated by the need to improve blasting practices in certain Appalachian surface coal mines. Hard bands within the geological sequence of rocks were required to be accurately detected to ensure proper fragmentation. At this mine, experienced drill operators could detect the hard bands from the action of the blasthole drill. If the driller maintained a careful log of the overburden, then the blasting design could be modified to match the rock characteristics. If the driller was inexperienced or unconscientious, the manual log was generally inaccurate and of little assistance to blast design. In order to overcome operator-dependence, a microprocessor-based monitoring system was designed and implemented. A Bucyrus-Erie 60R blasthole drill was instrumented to record drilling operating parameters such as depth, T, N, W, R and vibrations that might be related to the rock characteristics. These recorded parameters were then correlated to the site geology through algorithms developed to identify hard bands based on the drilling response of T x N, in turn being used to generate an appropriate blasthole design.

Recent work by Mol et.al. (1987) discussed the results obtained from combined drilling and shovel performance monitoring in an Australian surface coal mine. A microprocessor-based monitoring unit was installed on a Bucyrus-Erie 55R blasthole drill, with the capability of recording depth, R, W, and T and N. Based upon published drilling models for SE(T) and σ_c, relative strength indices were calculated from these drill parameters. Variations in these strength indices with depth showed good correlation with the known positions of hard waste rocks and softer coal units. Such data acquisition while drilling, permitted timely blast design modifications, aimed to optimize fragmentation and reduce geophysical logging of production blastholes. It was therefore the conclusion of this study, that cost savings through improved productivity could be realized from monitored drilling.

These studies involved the use of a microprocessor-based mine equipment logger (MEL), a 12-bit, eight channel system with keyboard and display for monitoring drill performance. This unit was developed by Broken Hill Pty. Co. Ltd. with the feature that the monitored data could be downloaded to magnetic tape for subsequent processing and analysis by a computer in the mine office.

Several monitoring systems are commercially available as a retrofit on rotary blasthole drills. Bucyrus-Erie developed and manufactured the Holepro I system for use on large rotary diesel/electric rigs. This microprocessor-based system had the capability of measuring, recording and printing out the following parameters: R, W, as well as T and N, all with respect to depth. The minimum sampling interval of this system was 17 inches. It provided hardcopy output on shift and production drilling in terms of number of holes drilled, depth drilled, operational time etc. It did not analyze this data, however, to derive any relative indication of hard or soft ground. The division of Bucyrus-Erie Co. offering these systems is presently closed, and very few HolePro systems were sold due to its unreliability and poor overall design.

Another system from Thunderbird Pacific Corp., is the Drilling Efficiency Indicator (DEI) and optional Stratalogger. The DEI provides information via a digital indicator on the depth drilled, R, distance from hole bottom and accumulated depth drilled. This system claims to be able to distinguish hard or soft zones on the recorded variations in R alone. It also provides hardcopy output of summary shift reports and penetration rate vs depth logs.

The Model 245 Drill Monitor from Interactive Sciences (U.S.), was designed to acquire, record and process drill parameters. The unit provides a readout of depth drilled and R, and generates a hardcopy output of the parameters with depth. Propel time, idle time and total meters drilled in the shift are also recorded and displayed. As for the other systems, no interpretation of the drilling performance is provided to correlate directly with changes in geology. The system was installed and utilized on drills in an Indiana surface coal mine over the past few years, although little published data is readily available (Sessoms, personal communication).

3.3 Drill Monitoring Equipment Development:

In this present study, a drill monitoring system was developed using off the shelf components for installation on rotary blasthole drills. The aim was to develop a system to successfully and accurately monitor and record the critical parameters required to give a complete assessment of drilling performance. This research was partly directed towards answering the question as to which performance parameter(s) alone or in combination best provides an indication of changing ground conditions in terms of variations in: rock type, rock strength and fracturation. Other issues were the accuracy, precision and reliability with which lithological units and their interfaces could be located using such a device. Subsequent chapters deal with these latter points, with the following discussion pertaining to the design of drill monitoring instrumentation for the present project.

3.3.1. Description of the Basic ADM System:

The development of the ADM (Automated Drill Monitor) system was based upon experience gained by the author using analog chart-strip instrumentation (Lutz Co., PL-3) for the monitoring of percussive drills in the Montreal area. The results of these studies are discussed in detail in Peck (1986).

From these investigations, conducted as part of the author's MEng thesis work, the numerous problems and delays associated with the handling and analysis of analog data prompted the need for the design and construction of the current ADM system. This new device was to have the capability of monitoring and recording drill performance data digitally, thus providing considerable flexibility in terms of data collection and handling. The author was personally involved with the conceptual design, component selection and construction of this digitally-based drill monitor system. A prototype unit was ready for field trials, in which the author was also an active participant, within six months. This original system was subsequently modified and improved over the next 12 months, based on field work in both surface and underground environments using a variety of drill types.

In preparation for the Fording Coal project, the system underwent further modification conducted in part by the author over an intensive period of 4 months, from February 1987 to May 1987. The changes were mainly to ensure the successful adaptation of the ADM to the large rotary blasthole drills operating at the minesite. These drills are described in more detail in section 2.2.

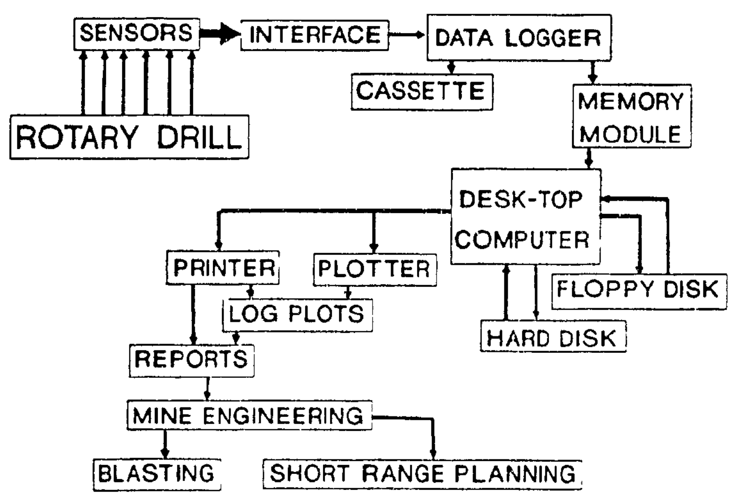

Figure 3.1 - Layout of ADM System.

Figure 3.1 tracks the paths for data acquisition, conversion and storage for the ADM. The capture of the performance data was achieved using electromechanical sensors, installed on the drill, which generated electrical (voltage) signals proportional to the actual parameter being monitored. These voltages would be scaled by the transducers selected to generate from 0 to 10 volts for the full range of parameter monitoring, with this signal subsequently converted from an analog to digital format. Figure 3.2 shows the ADM system used in the present investigations.

Transducers used for measuring pressures are manufactured by Omega Engineering, and were purchased for their ruggedness and accuracy. These sensors were purchased for two ranges of pressure, 0 to 1000 psi (gage) and 0 to 5000 psi (gage), both having the following specifications:

Excitation: 9 to 20 Volts D.C.

Output: 0 to 6 Volts D.C.

Performance:

Accuracy: ± 0.5 % of full scale

Operable Temperature Range: -55° to +127°C

Proof Pressure: 1.5 x full scale

Burst Pressure: 5 x full scale

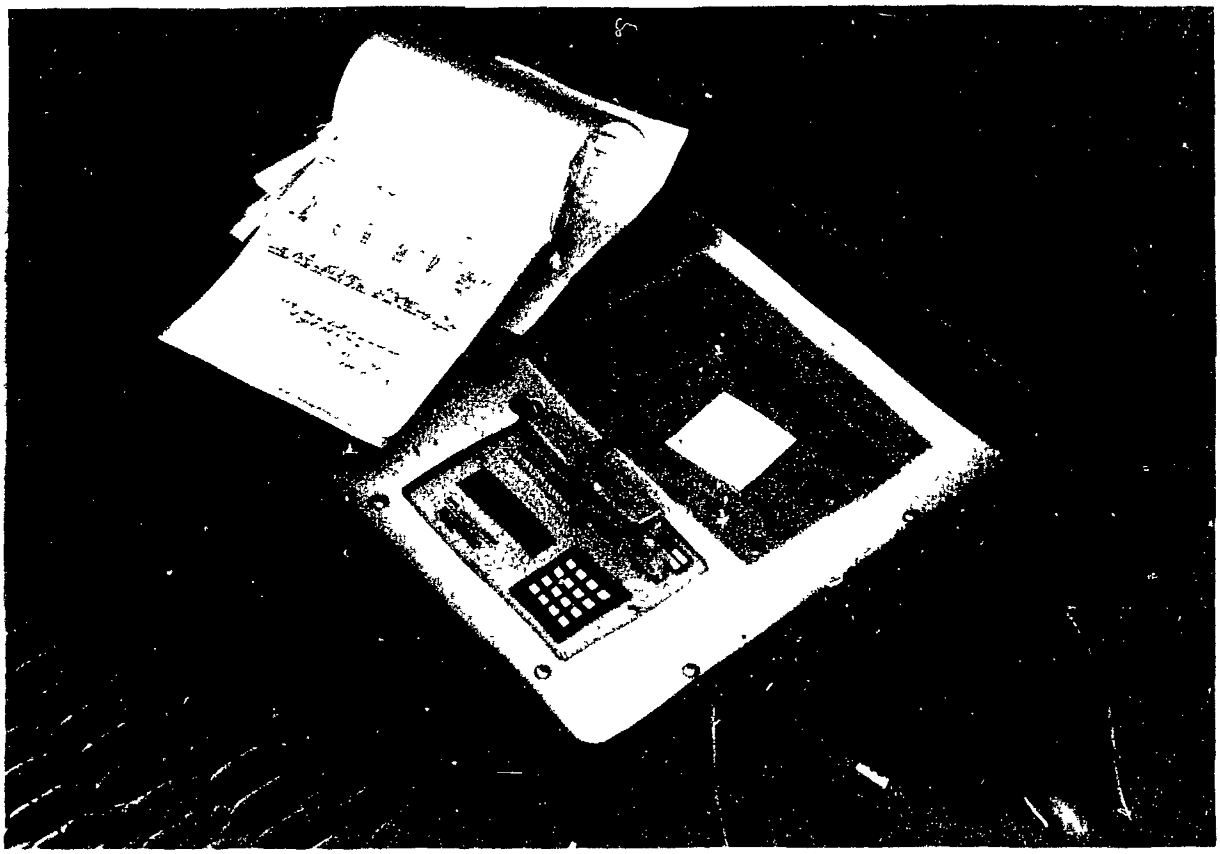

Figure 3.2 - Modified Version of the ADM System.

The transducer to measure displacement was a Celesco position sensor, model DV-301. This transducer was simply a potentiometer driven by a series of pulleys connected to a stainless steel cable. The unit was enclosed in a NEMA (environmentally sealed) steel enclosure and installed at the top of the drill mast with the steel cable fixed to the moving drill head assembly. As the head assembly moved downward during drilling, the cable through the pulleys, turned the potentiometer generating a voltage proportional to the actual linear displacement of the drill. As the drill head moved up upon completion of drilling, a spring with a tension of 18 ounces wound the cable back into the transducer casing. The conversion factor for voltage to displacement (in inches) was based upon the transducer manufacturer, and therefore, for this particular unit, at maximum extension of the cable ie. 200 inches, a voltage of approximately 5 volts would be generated. The accuracy of this sensor was rated at 0.01 % distributed over the maximum displacement, or 2 inches at 200 inches. The transducer was also rated for sustained vibrations of up to 10g's, and bursts of 200g maximum, levels which were expected due to the high vibration environment surrounding drilling.

Penetration rates were subsequently calculated from the recorded displacements by differentiating the sampling interval chosen at beginning of recording, over the time taken to travel this distance. As noted earlier, this phase is performed in real-time within the memory of the CR21XL, prior to the data being dumped into final storage memory.

Power for the transducers was provided through the same cables transmitting the response of the sensors to the ADM. Clean and constant excitation voltages of 5 volts for the pressure transducers and 25 volts for the displacement sensor are required to ensure maximum resolution and accuracy. Therefore a power supply card was developed to operate in tandem with the data logger, to provide continuously regulated voltages to the transducers, for external power input to the card of 12 to 36 volts. The external power was generally derived from car or drill compressor 12 to 24 volt batteries.

The analog to digital conversion is performed within a powerful data logger, a Campbell Scientific CR21XL. This logger can also be programmed to convert some of the voltage signals received from the transducers to their appropriate engineering units. A minimum amount of conversion is done in real-time while monitoring the variables of depth and drill penetration rate. This permits an immediate cursory assessment of the drilling being done, in addition to providing a check on the proper operation of the complete system. However, it was part of the system design to minimize such functions performed by the logger during acquisition of the data, in order to maintain the fastest sampling rate possible. This converted data can be accessed and reviewed via a 16 character LCD display within the logger. This particular data logger was selected after examining a total of 10 commercially available units for the following reasons;

1 - wide operating temperature range; -25° to +50°C;
2 - the system is programmable and comes available with user-friendly software for customized applications;
3 - has the capability of preliminary treatment of the acquired data i.e. math functions of averaging, maximums and minimums;
4 - is powered by rechargeable batteries - at full charge the system can operate for approximately one month;
5 - compatibility with IBM-PC based computer systems;
6 - provides several possibilities for data storage and transmission;
7- allows real-time display of data during acquisition.

In addition, the initial cost of the logger was substantially lower than the closest competitor.

The digitally converted data can be subsequently stored, either within the logger memory (maximum 48K binary format) or transferred externally to either a cassette tape (maximum 192K binary per 20 minute tape) or a solid state memory module (maximum 756K binary). Once the data is stored in any of the described manners, it can be transferred again to a micro-computer for conversion to ASCII format. The software to accomplish this stage were programs provided by the manufacturer of the data logger. These programs could also be customized by the user for entry of factors to convert the remaining acquired voltages to engineering units. Figure 3.3 summarizes the functions of the CR21XL data logger.

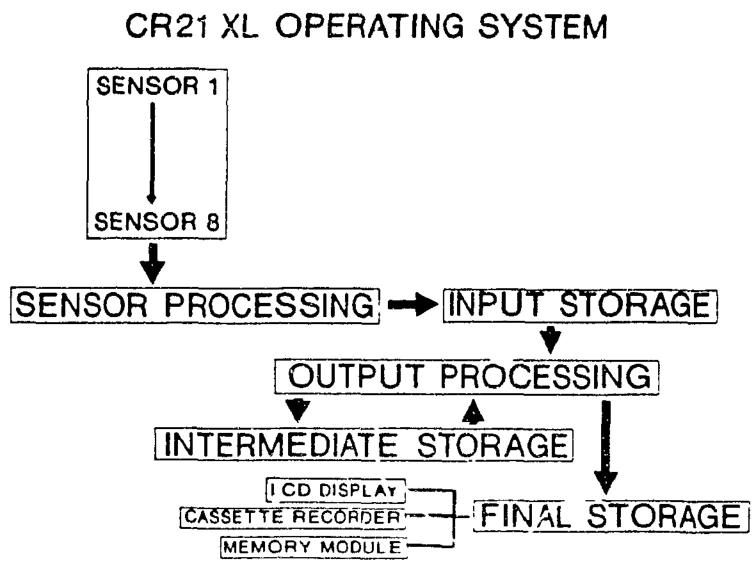

Figure 3.3 - Schematic of the Operation of the CR21XL Data Logger (Campbell Scientific, 1986).

At this point, a series of software routines designed by the author and programmed by a computer programmer, enable the further processing of the data (in ASCII format) in order to display the individual parameters with respect to depth in the borehole. A choice of measurement units can be made to display the processed parameters in either Imperial units (feet/hour, ft-lbs, psi etc.) or Metric equivalents (meter/hour, Nm, bar etc.). Linking programs to commercial software packages such as LOTUS 1-2-3 and AUTOCAD were also developed to accept the processed drill data, in order to have greater flexibility in the display and further manipulation of the drill parameter data. The drill data logs generated using these procedures will be discussed in later sections, with reference to field studies conducted using the ADM.

3.3.2. Design Criteria of the Current ADM System:

In order to protect the acquired signals from the transducers from electrical noise disturbance, several measures were taken during the design of the system. As a first step, the entire box (fibreglass, neoprene sealed, with an interior aluminum and steel frame) was grounded to ensure electrical screening from any outside source. Secondly, shielded cables to link the transducers to the ADM were purchased (comprising an interior jacket of metallic mesh which surround the conducting wires). This type of cable generates (via the shield) a metallic gain around the wires transmitting the signals from the sensors. Theoretically, if any electrical disturbance is introduced to the system, it will be concentrated at the same gain as that of the shielding. As a result, the noise will propagate in the direction of least resistance i.e. along the shielding to be dissipated via the ground of the box. Thus the signal generated by the transducer should not, if the shielding is effective, be interfered by any outside electrical noise. The cables were also covered by a thick layer of polypropylene rubber and the interior injected with a rubber gel to both insulate (temperature and electrically) and waterproof the wires.

The analog to digital (A/D) convertors within the CR21XL, operate by integrating the analog signals over a predefined time period to derive a digital signal. The conversion is performed using 14 bit A/D convertors giving a stated resolution of 1/7500 for a measurement in single-ended mode, e.g. 0.67 millivolts (mV) for 5 volt range. For differential mode measurement, this resolution increases to 1/15000.

The choice of utilizing single vs. differential mode measurement is based upon the advantages and disadvantages of each for the application of monitoring drill performance. Differential mode measurement would be selected in order to increase the signal to noise ratio, ie. reduce the level of noise within the monitored signal. In this mode, two separate wires connect the transducer to the data logger input channel, i.e. both positive and negative polarity inputs. The first measurement is achieved by first taking a data point from one side (negative or positive terminal) followed by a data point from the other and calculating the difference (1st intermediate point). This value is subsequently integrated and converted (A/D). A second value is then taken, yet the data entry points are inverted (ie. if a point from the positive input was taken for the first data point above, then here the first point is taken from negative terminal) and the difference again determined, integrated and converted (2nd intermediate point). The final data point is obtained by the average of the absolute values of the two intermediate points. By integrating the signal in both directions, the input offset voltage, or noise due to thermal effects in the amplifier section of the datalogger are reduced. A further advantage of the type of measurement, is that if the incoming signals have a ground potential different from that of the ADM system (grounded), the difference in ground between the transducer and the logger will be eliminated (Campbell Scientific, 1986).

Single-ended measurements rely upon a transducer signal from only one input referenced to ground. A single integration is performed for each measurement, rather than two for differential measurement. Since in this case the ground reference level is that of the ADM, all differences between the ground of the transducer and the ADM will be added to the signal as noise. However, advantages of single-ended measurement are:

1 - within the limitations of the selected data logger, 16 inputs of data from different transducers are possible versus 8 for differential mode;

2 - the time required to perform single-ended measurements is approximately one half the time necessary for differential mode measurement.

As a result of the faster measurement time, the greater is the number of samples per time interval possible. Therefore, the higher sampling rates imply greater amounts of data can be collected and thus improved resolution. It was for this reason that the ADM was configured for single-ended measurement. However, this phase could have resulted in a noisier overall signal, but as was seen in the present field study, this was not the case.

In addition, a choice can be made for this data logger of the integration time for A/D conversion. Two speeds are possible; a slow integration time of 16.67 milliseconds , and a fast integration time of 250 microseconds. Since A/D conversion involves integration, it functions in part as a filter thereby reducing further the noise levels in the acquired signal. When the integration speed is slow, the narrower is the band passing from the conversion, resulting in a reduction in noise. On the other hand, the reaction time of the system is greater in this mode, as is the risk of filtering out portions of the desirable frequency ranges of the signal. The slow integration time provides a more noise free reading than the fast integration time. One of the most common sources of noise is 60Hz from AC power lines. The slow integration time of 16.67 milliseconds is equal to one 60Hz cycle. During the integration time, the AC noise will integrate to 0.

The fast integration time of 250 microseconds is useful for several reasons. In fast mode, the time skew between measurements is minimized in addition to increasing the throughput rate. The current drain on the batteries of the datalogger is also lower.

Therefore selection of fast versus slow A/D integration depends on the following criteria:

1 - the desired throughput rate of data acquisition (depends on resolution required, number of parameters to be monitored etc.);

2 - the speed of acquired signal variation;

3 - the influence of AC power sources.

Based upon the requirements desired by the drill monitoring system i.e. a minimum of 0.4 inches resolution, maximum 3 parameters, for drill rates of up to 400 ft/h, and logger specifications of maximum execution time of the acquisition programme (as configured for the present project) of 0.1 seconds, the fast integration mode was selected. In addition, tests were conducted on-site using an ADM system configured first for fast integration and then slow integration. Comparison of the acquired signals indicated that noise due to AC power influence was not present, and therefore the fast mode was utilized for the remaining field period.

As for choosing single-ended over differential mode measurement, it was seen in a series of laboratory and field tests that protection against electrical noise was less important than attempting to maximize the sampling rate of the system. The effect of electrical noise was seen to be minimal, if not non-existent during recent field monitoring studies. If the recorded signals were interfered by random noise disturbances, then the drill logs from two parallel boreholes (in which the geology was identical) would be different from each other. However, this was not the case, and it will be demonstrated in subsequent sections that the variations in recorded parameter logs for two adjacent boreholes are highly reproducible. It was apparent, that the primary reason for most differences in drill signals in such a situation, was the result of operator variation of the primary parameters of downpressure and rotary speed.

As a backup to these methods for filtering the incoming signals, a moving average filter was developed to treat the drill data outside of the acquisition mode, if it was felt that a low signal to noise ratio was present. The filter could average all the drill parameter values over a selected window, of width from 0.4 to 16 feet. The computed average of the data within this window is then allocated to the middle of the interval as the filtered point.

3.3.3. Modified Version of the ADM for the Field Studies:

There were several major changes made to the original system in order to install the instrumentation on the blasthole drills at the minesite. The bulk of the modifications were related to the hardware, primarily the transducers installed on the drills. The ADM system in its original configuration was capable of monitoring only 3 parameters, namely, depth, penetration rate and thrust. However, for the present field study, the drills were rotary (electric) machines having several additional parameters to be monitored.

The parameters of rotary speed and torque were considered very important to fully understand the performance characteristics of the drills, and therefore appropriate techniques to reliably acquire these needed to be developed. The air pressure used for flushing and cooling the drill bit was also to be monitored and therefore an additional input on the ADM was necessary.

Since these particular drills were five times the size (mast height, length and width) of drills monitored in the past with the ADM, a modified transducer for depth and penetration rate was required. A Rayelco brand P-1000A transducer was thus employed for the project, capable of monitoring up to 1000 inches of displacement (83.34 feet). The transducer was rated for operation for up to 10g continuous vibration and a burst maximum of 200g. It was seen during field trials, that for continued high vibration drilling, the signal generated by the potentiometer would saturate, producing flat line responses when plotted with respect to depth. The steel cable attached to the potentiometer is a seven strand woven cable, having a tensile strength of 4000 lbs, yet was considerable weaker in shear. This component was seen as the weak point in the system due to its susceptibility to breakage from vibration, fraying and sabotage. This sensor generated a voltage equivalent to 1.00 mVolt/Volt/inch, thereby producing a maximum of 10 volts for an accuracy of 0.03%, or 30 inches for full cable extension, which for these drills was 768 inches (64 feet). In addition, lengths of cables from transducers to the ADM of up to 164 feet were necessary.

The nature of the project required that the drill monitoring be capable of minimum 4 inches resolution for a maximum of 6 parameters. Therefore expected maximum drill rates which could be monitored (based on system execution time of 0.1 seconds) were around 1970 ft/h. It was also possible with this configuration to monitor, if necessary, at 2 inches resolution, for drill rates up to 984 ft/h. During tests conducted at the beginning of the field study, it was seen that the 4 inch sampling interval produced the least error over the full length of transducer extension, see Table 3.1. The reported 0.03% accuracy for the Rayelco is dependent upon many factors, including length of cable (for excessive lengths, loss of signal can occur due to resistive properties of the wire), vibration levels, ADM processing speed and temperature. As a result of any or a combination of these factors, the measurement error (between selected sampling interval and max, average and min values) was in excess of the specification value. However, this data was still within an acceptable range of accuracy for the project. In order to ensure as fast a processing time as possible, yet introducing some error, the fast integration mode for A/D conversion was also selected.

Table 3.1: Data from Test Hole # 1, June 2, 1988.

Sampling Interval:	Recorded Value:		Error %:
0.4 inches	Average: 0.3939 in	± 0.0129	1.53
	Maximum: 0.6025 in	± 0.0198	50.63
	Minimum: 0.1441 in	± 0.0047	63.83
2 inches	Average: 1.9740 in	± 0.0647	1.30
	Maximum: 2.1737 in	± 0.0713	8.69
	Minimum: 1.7285 in	± 0.0567	13.58
4 inches	Average: 3.8964 in	± 0.1278	2.59
	Maximum: 4.1732 in	± 0.1369	4.33
	Minimum: 3.6009 in	± 0.1181	9.98

3.3.4. Instrumentation of a Bucyrus-Erie 60R Electric Rotary Blasthole Drill:

As a result of the additional required parameters, a new ADM unit was constructed to permit a maximum of eight parameters to be acquired at any one time. The transducers for the modified system were installed over a period of 3 weeks in May 1988, by both the author and maintenance personnel at the mine.

The Bucyrus-Erie 60R drill that was instrumented used both hydraulic and electric motors. The hydraulic motor produced the pulldown pressure through a series of gears, sprockets and drive chains, and therefore the pressure in the feed line to this motor was monitored. An Omega 0 to 5000 psi pressure transducer was connected to the hydraulic feed line, where normal operating pressures of up to 1500 psi could be expected. Burst pressures were not a problem to consider, due to 2000 psi relief valves being present on the feed lines. Calibration of the measured (gauge) pressure with operator panel gauge reading (analog needle gauge - range 0 to 3000 psi) and with actual weight on the bit (pounds) was achieved through a series of 1 day tests conducted at the field site. A bit load measurement unit was obtained from the drill bit manufacturer, Dresser-Security, which comprised a load cell and analog readout unit. The load cell was placed under the drill steel with the bit removed, and the hydraulic pulldown pressure incrementally increased (as controlled from the operator's panel) by 100 psi up to 1500 psi. At each new pulldown setting, the readings on the load cell and the operator's panel were manually recorded. These readings, over a complete range of pressure settings were later compared to the digitally acquired readings from the pressure transducer by the ADM. From these results a curve of psi to pounds was developed to calibrate the ADM readings with gage pressure and thus to actual bit load in pounds. This relationship was established as,

$$\text{Bit Load (lbs)} = 80 \times \text{gage pressure (psi)} + 14142 \text{ lbs} \quad ...3.1$$

The factor of 14142 lbs, is the load at 0 psi hydraulic pressure, and accounts for the weight of the drill steel, stabilizer and drill head assembly (includes two rotary motors).

Air pressure was also monitored using an Omega 0 to 200 psi pressure transducer attached to the air line leading from the compressor to the drill head. The gauge range of this parameter was 0 to 120 psi, yet pressure was extremely stable at 23 to 25 psi for normal operating conditions. In a situation of caving or excessive drill rates in soft ground causing bit jamming, the air pressure rises in excess of 35 psi, at which point the cperator would reduce the pulldown pressure and raise the steel to clear the cuttings in the hole. Therefore, air pressure was monitored to identify such situations when they occurred. The relationship between voltage developed by the transducer and psi (gage) is established by the sensor manufacturer, yet any offsets (due to atmospheric pressure etc.) to this calibration were established by comparing the operator gauge readings to those acquired by the ADM. A similar approach was followed for calibration of the transducers monitoring hydraulic pulldown pressure.

The 60R drill utilizes two D.C. electric rotary motors, which through a mechanism of gears, clutches and a transmission, produces the rotation of the drill steel. The clutch allows the motors to operate in tandem, in order to eliminate the possibility of one motor overworking the other. The motors are generally matched for similar horsepowers of 130 Hp at 600 volts, producing motor rotary speeds of 1125 rpm. The combined power of the motors enable the drill to obtain drill bit rotary speeds of up to approximately 90 rpm, for torques in excess of 14000 ft-lbs (Bucyrus-Erie, 1978). The speed of the motors is controlled through a rheostat in the operator's cabin, and a gauge showing rotary speed in rpm (0 to 120 rpm) is also provided.

The monitoring of bit rotary speed was initially attempted using a D.C. tachometer generator. This unit was to be attached to the shaft of one of the rotary motors of the drill, which for speeds of 1000 rpm would generate a voltage of 40 volts. Since this generated voltage was in excess of the maximum permissable input voltage to the ADM, a series of electronic circuits reduced the signal to provide a maximum value of 5 volts for 1000 rpm. The relationship between motor speed and drill steel/bit speed was determined from examination of the gear ratios at the drill rotary transmission. This correlation was in turn corrected and refined based on comparison with operator panel gauge readings (not reliable due to the damping of the gauge) and digital hand-held tachometer measurements of the actual drill steel. However, no suitable method was found to properly secure and couple the tachometer generator to the motor without considerable modifications to the motor housing. Thus vibration levels were very high, resulting in very low signal to noise ratios.

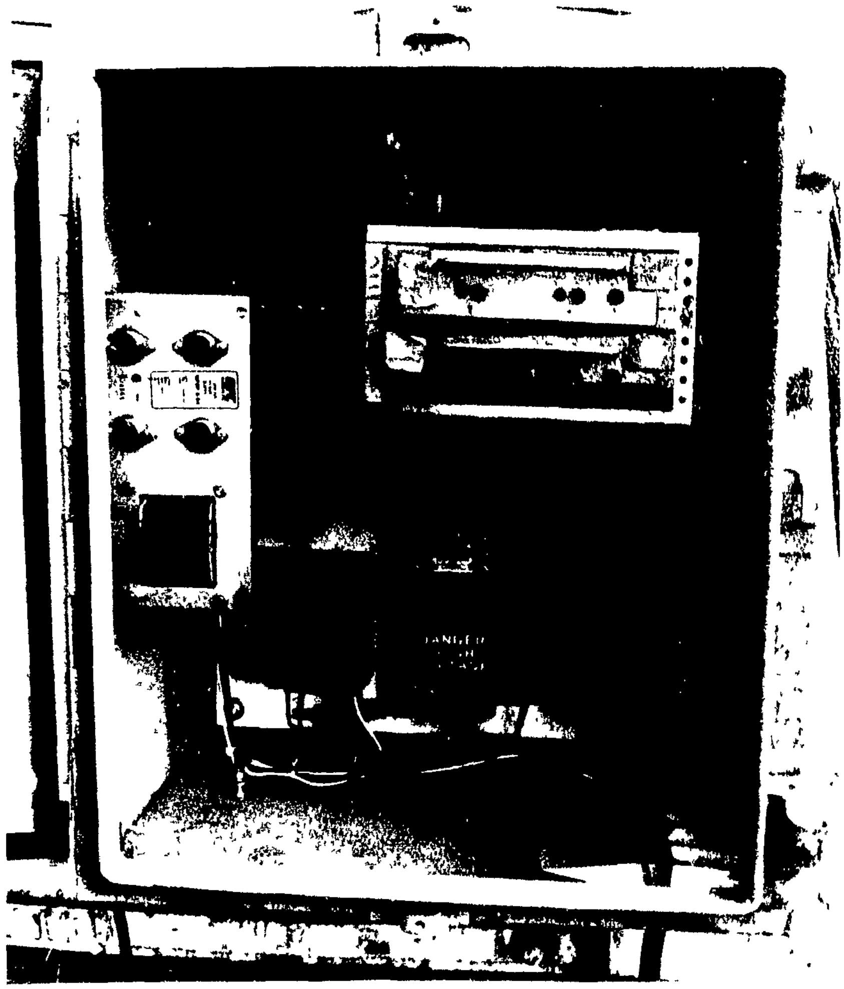

Figure 3.4 - Interface panel for electric rotary blasthole drills.

Therefore an alternative method of monitoring drill bit rotary speed was examined.

For D.C. motors, the amount of voltage into the motor is (linearly) proportional to the rotary speed output. On this basis it was possible to monitor the changing voltage to the motor, as controlled by the operator, and derive an indirect measurement of the rotary speed. It is noted, however, that this relationship is most accurate for when the motor is (1) unloaded, and (2) constantly excited.

Using this approach, an electronic panel was partially designed yet completely constructed by the Electrical Group of the mine, incorporating voltage and current isolation amplifier cards with adjustable gains, to step down the maximum 600 volts input to the motor to a maximum of 4780 mV output to the ADM. This interface panel was connected to the armature of one of the rotary motors, with cables transmitting the scaled voltages to the ADM. Only one voltage polarity (positive) could be measured, due to a diode installed on the input terminal to the panel. This reduced the chances of monitoring negative voltages, not accounted for within the ADM acquisition programming. Figure 3.4 is a photograph of the panel, enclosed within a steel NEMA enclosure and installed inside the drill housing. Based upon a comparison of these acquired voltages with rpm measurements from the operator's panel and the hand-held tachometer, a relationship between voltage and rotary speed in rpm was established as,

ADM reading(mV) x 0.02 (rpm/mV) + 15 = Bit speed (rpm) ...3.2

The multiplier of 0.02 is the factor based on scaling by the panel of the input motor voltage, to derive an output voltage in mV. The correction factor of 15 rpm is added to this product, based on correlation with actual drill steel speed measurements made with the tachometer.

Rotary torque, in a manner similar to rotary speed, can be measured directly from the electric motors. For shunt type D.C. motors, as is the case for the 60R drill, the torque depends only upon the armature current. The relationship between armature current (load) in amperes and torque in ft-lbs is a straight line, if the field current is constant. Field current is relatively stable for the site and therefore we could assume that this type of relationship would be valid. Based on the specifications of the individual 130 Hp motors, it was indicated that full load (stall) was 320 amperes at 14762.7 ft-lbs torque, i.e. 1 ampere = 46.13 ft-lbs.

The panel used for rotary speed measurement was expanded to include a current isolation amplifier and a voltage amplifier. This first component enables the isolation of the signal from the motor shunt current from the ADM system (to eliminate or reduce possibility for noise in the signal). In addition, this card was gained so that the shunt voltage of 60 mV (for 320 amperes) was amplified to 600 mV at the output i.e. a gain of 10. This voltage was then passed through the voltage amplifier with a gain of approximately 7.8, to bring the signal to a maximum of 4680 mV for input to the ADM (where 1 ampere = 14.625 mV i.e. 4680/320). A potentiometer was installed on the voltage isolation amplifier to adjust the null offset voltage to 0 mV for an input of 0 mV. This type of circuit was connected across the shunts for both motors, with the signals directed through a summing circuit to provide one reading of torque based on the combined responses of the two motors. This is due to the fact that since both motors are responsible for the rotary power input to the drill bit, both responses should be monitored. Also if only one motor was monitored, it can occasionally occur that one motor will work harder than the other. The summing circuit will therefore account for this possibility of unbalanced motor load. The calibration relationship thus developed relating recorded mV readings to torque in ft-lbs, for 1 mV = 3.1544 ft-lbs (46.13 /14.625), is,

$$\text{ADM Readings (mV)} * 3.1544 \text{ (ft-lbs/mV)} = \text{Readings (ft-lbs)} \qquad \ldots 3.3$$

As for the calibration equation for rotary speed, this relationship is included in the processing software of the ADM to derive torque values in ft-lbs for plotting with respect to depth.

The electrical panel housing the equipment for rotary speed and torque also included a regulated power supply unit (see Figure 3.4). This power supply took the noisy 120 volt source available on the drill to produce a clean, regulated voltage of 27 volts. This power source, as indicated earlier, was subsequently channelled through the ADM regulated power card, to provide excitation voltages to both the pressure transducers and the Rayelco displacement sensor.

3.3.5. Summary of the Fording drill instrumentation and monitoring period:

The operation of the ADM system during the continuous 2 month period of May 15 to July 12, 1988 was essentially without major equipment failures. A particular delay of 5 days during this period was suffered as a result of a broken steel cable on the Rayelco position transducer. However, the bulk of the downtime was the result of having to forward the broken sensor to California to be repaired. This required a turn-around period of 3 to 4 days, which due to the remote location of the mine, an additional delay of up to 2 days was usual. In order to prevent any further problems, a second Rayelco transducer was purchased as a back-up. The removal/installation of the unit at the top of the drill mast required a maximum of 20 to 30 minutes, and could be completed during the lunch break when the drill was not operating. Inspections of the cable attached to the drill head, as well as the housing containing the Rayelco and bolts fixing it to the mast, were conducted on a daily basis by the author to minimize the chances of any damage to the unit. No further problems occurred.

Due to the susceptibility of the cable drawn transducer to damage, it was proposed that an alternative method of position measurement be devised. Preliminary discussions with mine maintenance personnel concluded that an optical incremental encoder could be installed at an appropriate location on a shaft of the drive train sprockets to obtain a precise reading of bit displacement. It was originally planned to do this modification before the end of the planned field period of 1988, but was eventually considered to be outside the scope of the project. In addition, the Rayelco transducer provided accurate displacement measurement if care was taken to ensure the integrity of the cable.

It can also be indicated that high frequency noise generated by the drilling process may not be effectively eliminated by the filtering techniques discussed previously. However, despite this possibility, analysis of the large drill performance database recorded in this study does demonstrate patterns which are representative of the machine-rock interaction. Examples of the monitored data correlated to the site geology are shown in subsequent sections. This aspect of proper filtering of the acquired data is an important component of drill and equipment performance monitoring in general. In other drill monitoring situations where the geological control is not as strong as in the present investigation, the role of filtering should be properly addressed. This would be undertaken prior to any interpretations being made between performance parameter variation and geology.

4.0 PRELIMINARY DRILL MONITORING STUDIES AT THE FORDING RIVER MINE:

4.1 Introduction:

The following discussion briefly describes the Fording River Mine operation where monitored drilling studies were conducted by the author over the past few years. Section 4.2 provides an introduction to the mine in terms of its general geology and mining practice. Section 4.3 presents the results of initial investigations monitoring the performance of a 45R drill, which served as a base for more detailed studies with a 60R drill.

4.2 Fording Coal Limited/Fording River Operations:

Fording Coal Limited is one of Canada's largest producers of metallurgical coal. With head office in Calgary, and operations in Alberta and British Columbia, the Company is a wholly owned subsidiary of CP Limited.

The Fording River Operation is located 19 miles northeast of Elkford, in the Fording River Valley of British Columbia (Figure 4.1). The mine's reserve consists of over 660 million tons clean coal in 15 seams ranging in thickness from 3 to 100 feet. Production commenced in 1972 at 6.6 million tons per year. Current annual capacity is 65 million bank cubic yards (BCY) waste, producing in excess of 11 million tons clean coal to varied domestic and foreign markets. The coals range in rank from medium to high volatile bituminous and are utilized as both metallurgical and thermal products (Gold et.al., 1987).

4.2.1. Geology:

The majority of rock in the mining areas is comprised of a 1800 to 1900 feet thick sub-unit of the Kootenay Group known as the Mist Mountain Formation with dips ranging from 0° to 25°. The depositional environments of this formation have a marked influence on the mineability of the coal in this area, in that the seam thicknesses and lateral continuity appear to be modified

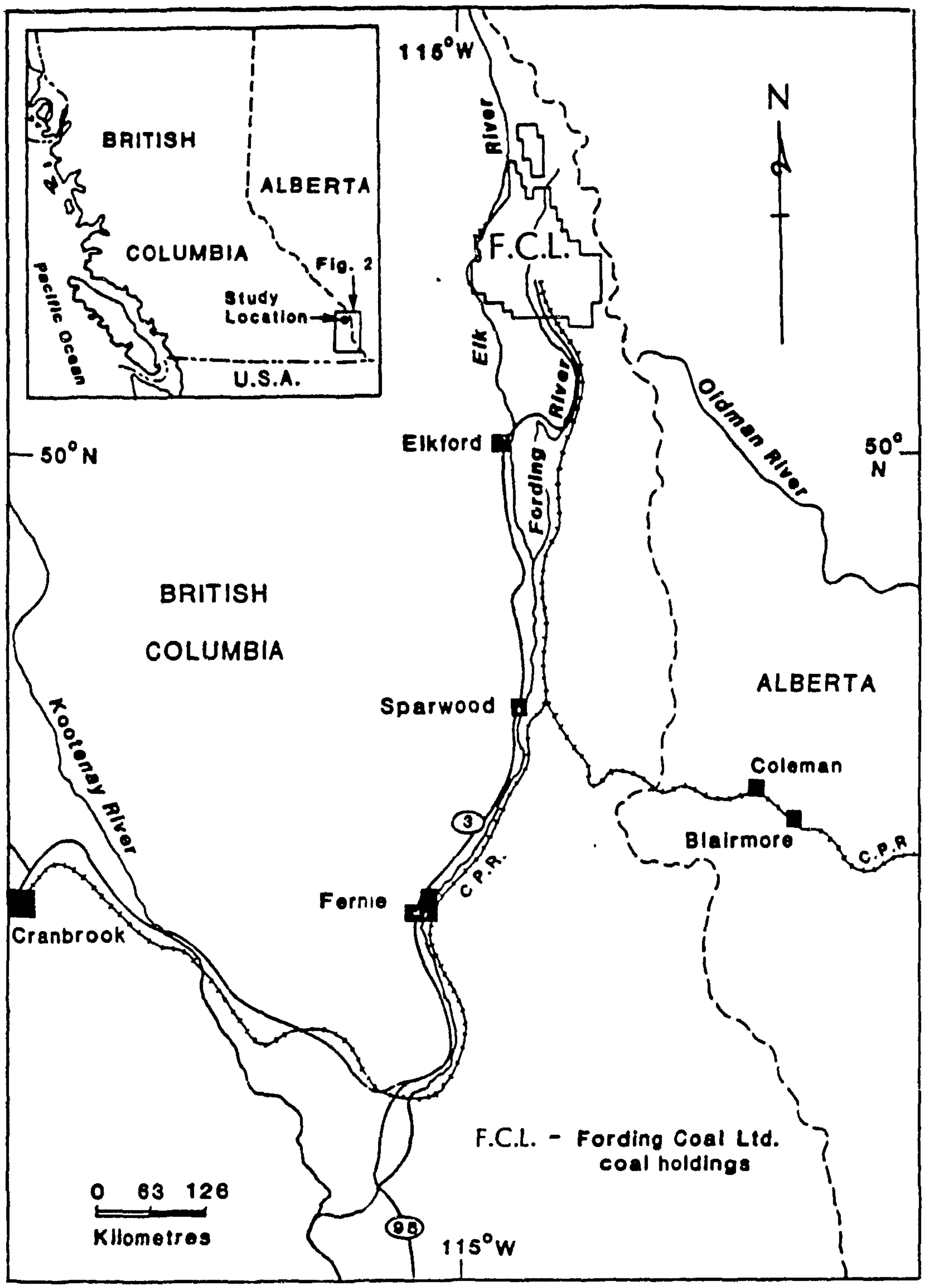

Figure 4.1 - Location map of the Fording River Mine (Donald, 1984).

by sandstone units. One example is the draping of coal seams over channel sandstones and washouts, which have resulted in considerable variations in observed interburden thickness. The term interburden is used here to describe any rock type which occurs between 2 coal seams.

The general stratigraphic sequence is a non-marine succession composed of interbedded siltstone, sandstone, silty shale, mudstone and coal and is shown in Figure 4.2. Siltstone is the predominant rock type in this formation, comprising up to 40 to 50% of the sequence. These rocks are generally thin to medium bedded, weathering a medium to dark gray, and interbedded with fine grained sandstones. Where the siltstones are interbedded and interlaminated with mudstone, shale and coal they appear considerably darker due to a higher content of organic material. Where these rocks are highly siliceous and ferruginous they appear orange-brown when weathered. The siltstones are also characteristically highly calcareous and well indurated.

Sandstones are the second most common rock type encountered at the minesite, accounting for up to 15% of the sequence. These commonly weather light to medium gray and are coarse to very fine grained. They occur either as channel deposits in which their grain size becomes finer with increased height in the stratigraphic sequence, or as interbedded sandstone, siltstone and mudstone sequences in which the grain size either coarsens or fines with depth; ie. either sandstone → siltstone → mudstone or mudstone → siltstone → sandstone sequences would be possible with depth. Thin coal seams generally cap these latter sequences. The sandstones also commonly grade laterally into interbedded sequences of sandstone and siltstone.

Mudstone and shale comprise 20 to 25% of the formation. These units are argillaceous and carbonaceous, weathering dark gray to black with an orange brown color where limonitic or pyrite rich laminations are present. Clay minerals in the mudstones are mainly illite and kaolinite, which are the primary minerals

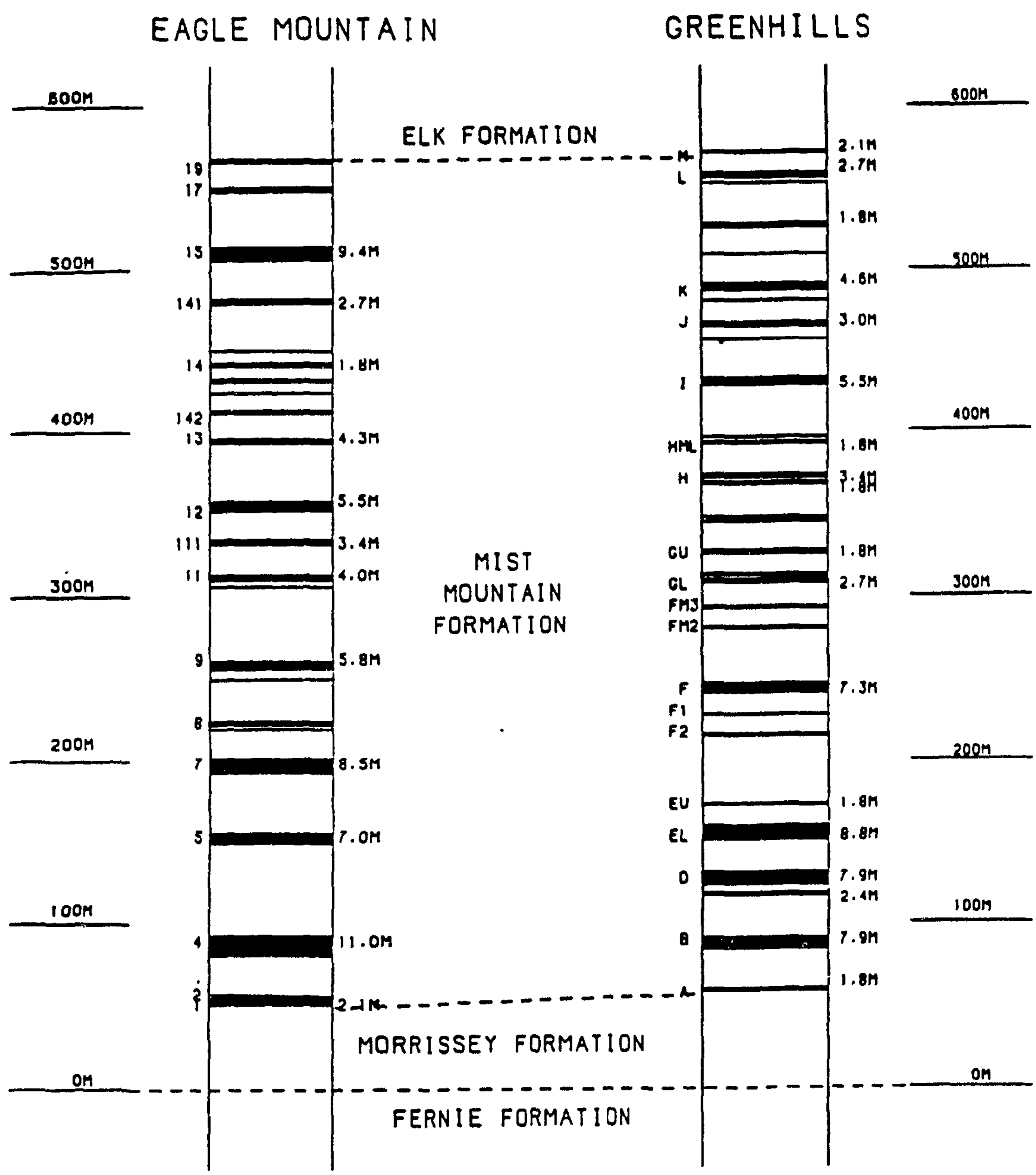

Figure 4.2 - General Stratigraphic Section, Fording River Mine (Gold <u>et.al.</u>, 1987).

(slightly radioactive) which result in the high gamma log response in the presence of these rocks.

Coal makes up the remaining 15 to 20% of the sequence, with thicknesses ranging from 1 to 100 feet including partings of waste rocks (Donald, 1984). Coal seams are also seen to be stratigraphically bounded, on their upper and lower bedding contacts by mudstones (Golder Associates, 1977).

The structural geology of the area consists of two north-south trending synclines with one on each side of the Fording River. These synclines are separated by the Ericson Fault, a normal fault with a vertical displacement of 1000 feet up to the east. The Fording River Valley has resulted from the erosion of the intervening anticline along the locus of the Ericson Fault (Figure 4.3). Several unnamed thrust faults are also indicated on Eagle Mountain. Splays related to these larger faults are responsible for localized seam and waste rock disturbances in terms of drag folds and smaller normal and reverse faults observed on Eagle Mountain. The presence of these minor structures tend to sometimes complicate the mining of the coal.

The syncline seen to the east of the Fording River in Figure 4.3 roughly bisects Eagle Mountain, with a plunge to the NW. The east limb of this fold dips at 35° to 45°, whereas the west limb shows dips of 20° to 25°.

Joint sets are approximately orthogonal to bedding with spacing ranging from 4 inches to >6 feet. Two major joint sets were determined from mapping by the author in the Eagle Mountain as;

S_1: 84°/270° and S_2: 81°/190° (dip/dip direction)

Based on mapping surveys conducted in the past at the mine, joint set S_1 is considered to be normal to the main direction of stress responsible for the folding and subsequent creation of the Rocky Mountains, while S_2 is related to the regional plunging fold structures ie. the anticlines and synclines. These two joint

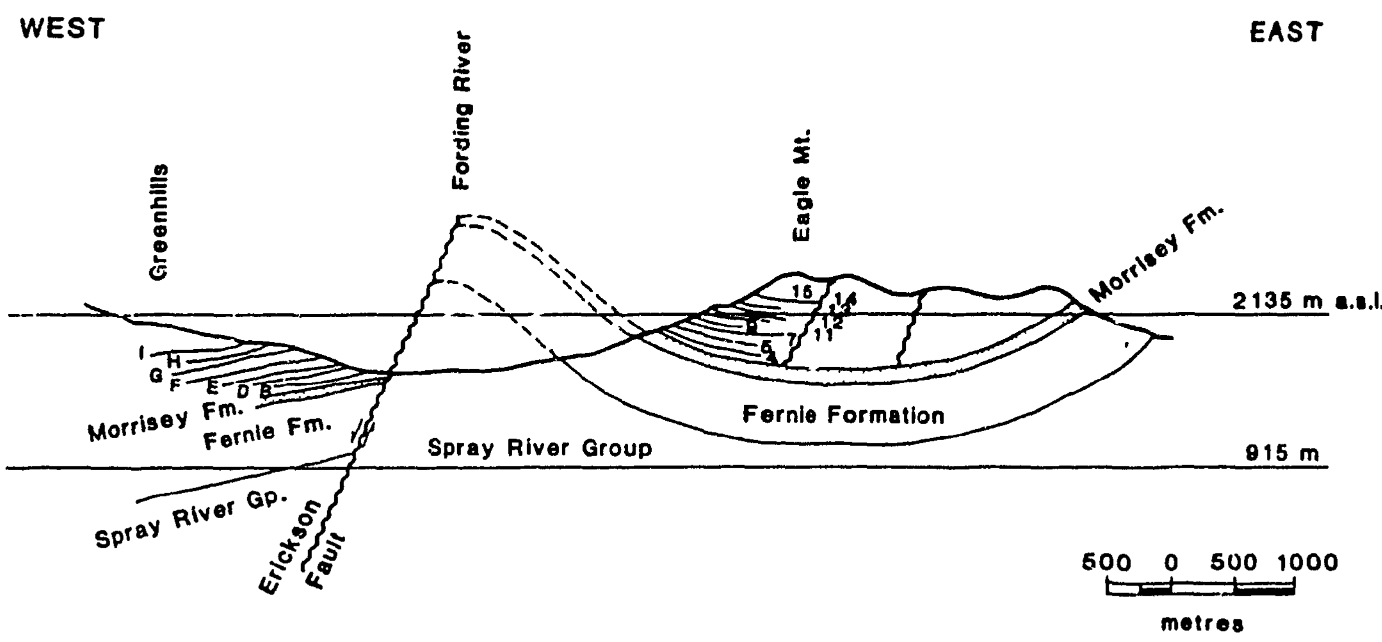

Figure 4.3 - East-West cross-section, Fording River Mine (Donald, 1984).

sets are nearly orthogonal (80° between them), which is typical of most Rocky Mountain area coal-bearing sequences (Golder Associates, 1977).

4.2.2. Mining:

Production at the minesite is achieved with a combined truck/shovel and dragline operation from several separate mining areas. Mining topography varies from valley bottom, to contour (hillside), to ridge/mountain top. Generally, development and benching is carried out with five 30 cubic yard and three 15 cubic yard shovels combined with fifty-nine 120 and 170 ton haul trucks. The truck/shovel fleets are presently being consolidated in the Eagle Mountain area. Lower level subcrops and pit bottoms are frequently mined with a 60 cubic yard dragline. Fording currently operates a fleet of three Bucyrus-Erie 45-R and four Bucyrus-Erie 60-R drills.

4.3 Preliminary Drill Monitoring Studies - Lake Pit:

Early investigations involved the monitoring of a Bucyrus-Erie 45R drill at the Fording River mine. These studies clearly illustrated the capabilities of interpreted drill performance data acquired by a microprocessor-based monitoring system. It was demonstrated from these results, that depth locations, thicknesses, relative strengths of both coal and associated inter- and overburden waste rock units could all be identified based on the responses in the recorded drilling parameters. This work also served an important role in both the debugging and decisions associated with design modifications of the drill monitoring system in preparation for the more comprehensive study carried out from May to September 1988. Prior to discussing the results of this more recent work, a brief review of the data obtained from the initial investigation will follow.

This initial study of September to November 1987, involved the monitoring of 5 drill parameters using the drill monitoring system previously described in section 3.3:

- displacement of the bit (ft)
- instantaneous penetration rate (ft/h)
- downpressure (psi)
- rotary torque (ft-lbs)
- rotary speed (rpm)
- bailing air pressure (psi)

For this study, a sampling interval of 4 inches was selected during acquisition of these drill performance parameters.

A total of 74 blastholes were monitored for a displacement of 4425 feet. These 10 5/8 inch diameter blastholes were of varying depth and were monitored during routine production drilling. Spacings between blastholes were generally around 29.5 feet, with actual spacings based upon relative rock unit strength, presently defined by geophysical logging, see Figure 4.4.

In addition, 9 of the drill monitored holes were gamma logged, with 50 earlier gamma and 4 neutron logged exploration holes present within the study area. These geophysical logs permitted the identification of the rock types in the test area, with these results subsequently correlated to the responses of the drilling parameters.

Figure 4.4 shows the study area, on the west side of the mine (Greenhills), for the period of September to November 1987. This diagram also identifies the locations of holes monitored by drill, gamma and neutron logging.

Mineable coal seams in this particular area of the mine varied in thickness from 3 feet to 20 feet with dips averaging 17° to the east or west. Coal seams (average unconfined compressive strength, σ_c = 2465 psi) were separated by variable thicknesses of sandstone (σ_c = 19720 psi), siltstone (σ_c = 18995 psi) and mudstone (σ_c = 8120 psi) waste rock units. Based upon the horizontal, well-bedded nature, as well as the clear strength

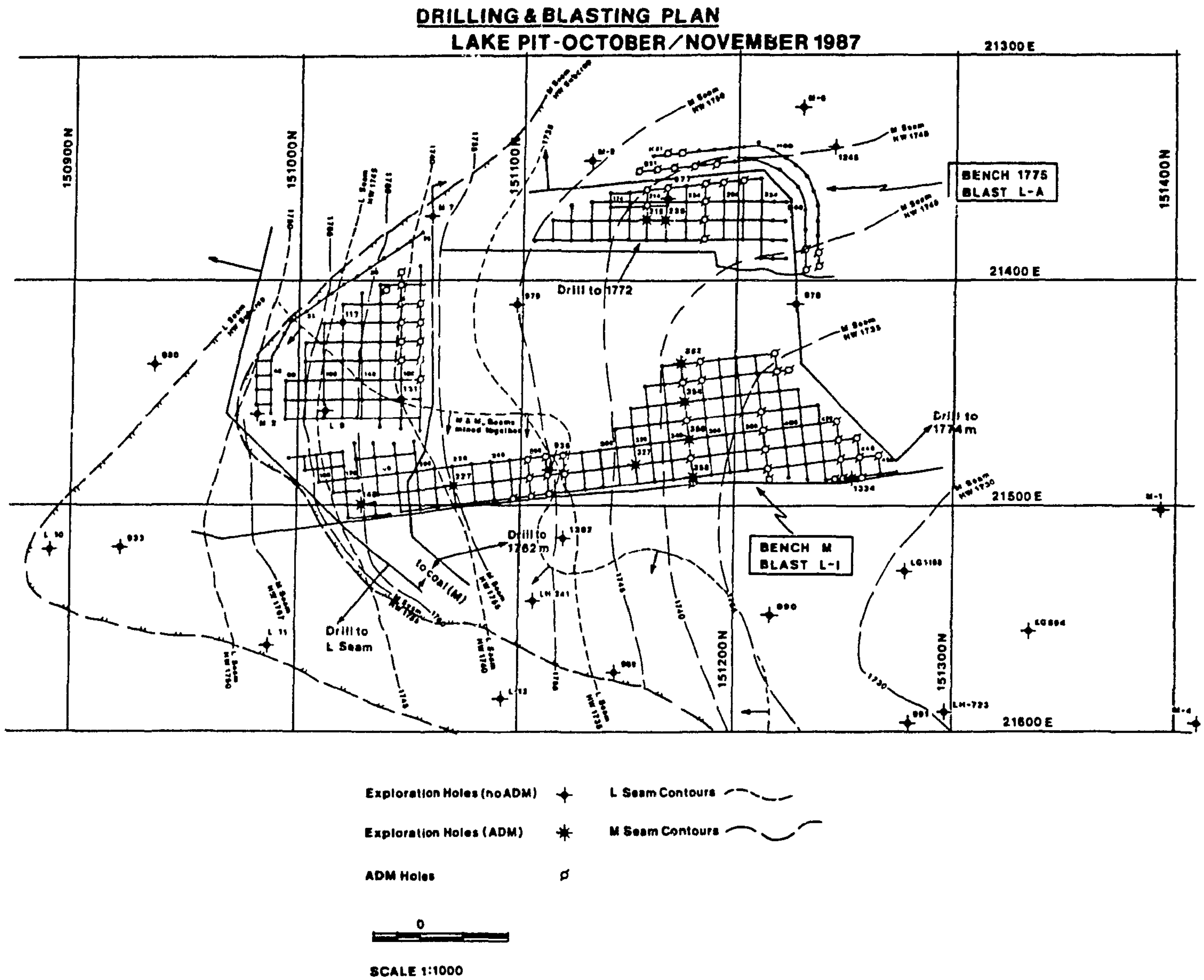

Figure 4.4 - Lake Pit Bench Plan.

contrasts between the different rock units, the area was well suited for drill monitoring trials.

4.3.1. Geophysical Logging:

Present practice at the mine to identify coal versus waste rocks, is to use gamma logs to provide an indirect means of determining formation densities (gives an indication of bulk strength) based on the response of the probe to changing concentrations of radioactive elements present in the rock units. The log response would be lower in more consolidated and dense formations because the gamma ray absorption increases with the density of the medium through which it passes. Clean sandstones and siltstones, for example, would normally exhibit a low level of natural radioactivity and combined with their high density, produce a low gamma response. The clay minerals and fine particles in shales and mudstones show higher levels due to the adsorption of the heavy radioactive elements of uranium, thorium and potassium. In addition, these units generally have lower densities than the siltstones and sandstones. Coal beds, due to their low content of radioactive components, show very low gamma responses (Dresser Atlas, 1982).

Gamma ray logs, however, are sensitive to variations in the borehole diameter such as through caved zones, resulting in potentially inaccurate definition of coal/waste rock interfaces. The resolution of gamma logs under ideal conditions has been reported to be ± 0.7 feet, with the precision of locating coal bands diminishing with the presence of sandstone-mudstone units in the coal seams (Schwaetzer, 1965). The gamma logging unit presently in use at the minesite is a WIDCO Model 1200, where an analog chart-strip trace is generated for the logged borehole. Gamma logging is carried out only when production drilling is in an area where geological information is considered insufficient or inconsistent with driller's manual logs.

Gamma logs are interpreted by examining the relative responses with respect to a scale established for the particular logging tool and the rocks present at the site. Less than two scale units (each unit is represented by a square on which the log trace is superimposed) is regarded as mudstone, 2 to 4 units equals siltstone, 4 to 10 units is sandstone and greater than 10 units is coal. This is to say that the lowest gamma log responses are in coals and clean sandstones. When coal stringers are interbedded with sandstone, however, the fact that both their gamma responses are very low, can sometimes prevent their discrimination from one another. The highest gamma responses are for the mudstones and shales, yet as the clay contents of a sandstone or siltstone increases, higher responses will be seen. Interbedded siltstones and sandstones generally produce jagged gamma log traces (Donald, 1984).

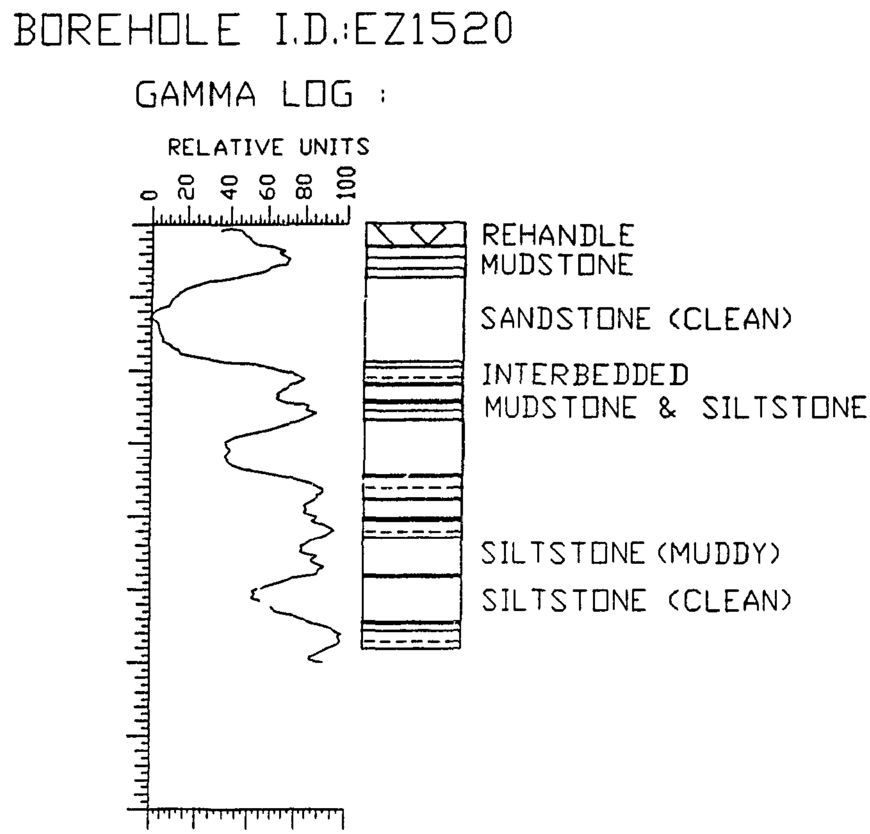

Figure 4.5 - Interpreted Gamma Log, Borehole EZ1520, Eagle Mountain.

Figure 4.5 shows a gamma log and interpreted geological log based on this approach. No coal was present in the sequence shown, which consisted mainly of massive sandstones and interbedded siltstones and mudstones. Note the very low gamma response for the upper massive sandstone unit, compared to the intermediate response for the lower sandstone horizon. This lower unit therefore has a higher argillaceous content than the upper clean sandstone. The interbedded siltstones and mudstones give a high and jagged response. Also indicated are the responses for rehandle (low) and a muddy compared to a clean siltstone. Depth increments are in feet.

Limited neutron logging is done, mainly in areas where little or no exploration holes exist or when the available data from other sources is inconclusive or contradictory. Neutron log data measurement, as for gamma logs, is also affected by several factors namely: changes in hole size, fluid saturation, porosity and lithology. Normally when neutron log responses are properly interpreted, a clear distinction of the various units of Coal Measure rocks is obtained. However, the resolution of the logs can be reduced when certain conditions in the borehole exist. The combined analysis of neutron and gamma logs provide a better and more reliable interpretation of the geology (Matuszak, 1972).

Drill performance monitoring, however, was hoped to provide a direct indication of "ease of rock breakage" or drillability, governed by drill rig and bit type and the strength characteristics of the rock. It was speculated that the recorded variations in drilling parameters could thus reflect variation in the strengths of rock formations more precisely than gamma and neutron logs. In addition, this data could be acquired <u>while</u> drilling, without the need for subsequent logging of the borehole. As well, this data would be recorded and stored digitally, enabling it to be manipulated with greater ease and flexibility than analog traces.

4.3.2. Preliminary Drill Monitoring Results:

From examination of the recorded drill data, penetration rates appeared dependent upon such factors as the downpressure and rotary speed (both operator dependent) and bit condition. With variation of these first two parameters by the operator over the depth of hole drilled, the range of penetration rates (and torque) in a particular rock unit may not be the same as in an adjacent borehole, where different levels of downpressure and rotary speed were used.

From observation of the operation of the drill, it was apparent that any increase of the downpressure by the operator would result in a corresponding increase in both penetration rate and torque. It was generally seen, however, that after drilling an initial 3 feet to 10 feet at very low downpressure, when collaring the hole in rehandle, maximum levels of downpressure were set by the operator for the remainder of the hole. Therefore, the drill parameter responses could be readily compared from one borehole to the next under these conditions. Any subsequent decreases in downpressure were generally related to the intersection by the drill of soft rock zones, ie. coal and mudstone.

It was consistently observed that a correlation of all the parameter logs in each monitored hole was required to confirm the actual control over performance variation, ie. whether operator or rock related. Therefore, during these field trials, the gauges on drill operating panels were manually monitored. Readings of all the gauges (including depth) were recorded to evaluate any adjustments made to the drilling process by the operator. This data provided a coarse means of distinguishing anomalies in the drilling parameter responses which were due to the operation of the drill and not related to the rock itself.

Figure 4.6 illustrates a borehole from this investigation, showing all the monitored drill parameters except for the bailing air pressure. This parameter generally remained constant over the length of hole, with increases resulting from a blocked or damaged bit or caved borehole.

Based on the geology interpreted from the gamma log in this figure, the drill penetration rate logs alone appear to clearly illustrate characteristic data traces for the different rock types present. High penetration rates were recorded when drilling in the coal seams, with lower values in the waste rock units. Monitored torque is low in the coal while high in the harder waste rocks, with similar trends shown for the pulldown pressure (downpressure). Note that the changes in these three parameters have sufficient sensitivity to identify the 2.5 feet thick mudstone parting located at a depth of 85.5 feet between coal seams. This parting is also clearly indicated on the gamma log trace. The log for rotary speed did not appear to demonstrate any pronounced difference in response whether in hard or soft rocks.

Several interesting trends were therefore evident from the comparison of drill parameter logs to gamma logs for all the boreholes monitored in this study, using as an example Figure 4.6:

- The observed patterns in penetration rate were due to the changing nature of the rock being drilled, where lower values are recorded in hard rocks and higher rates in softer materials. These responses may also reflect increased/decreased downpressure and/or rotary speed made by the operator due to problems related to the equipment or ground being drilled.

- The variations in rotary torque indicate very clearly the presence of soft/hard rock units. Variations could also arise from adjustments by the operator to the downpressure and/or rotary speed (verified by examination of the respective log), where an increase in these parameters produces higher torque and vice versa. When downpressure and rotary speed are at constant

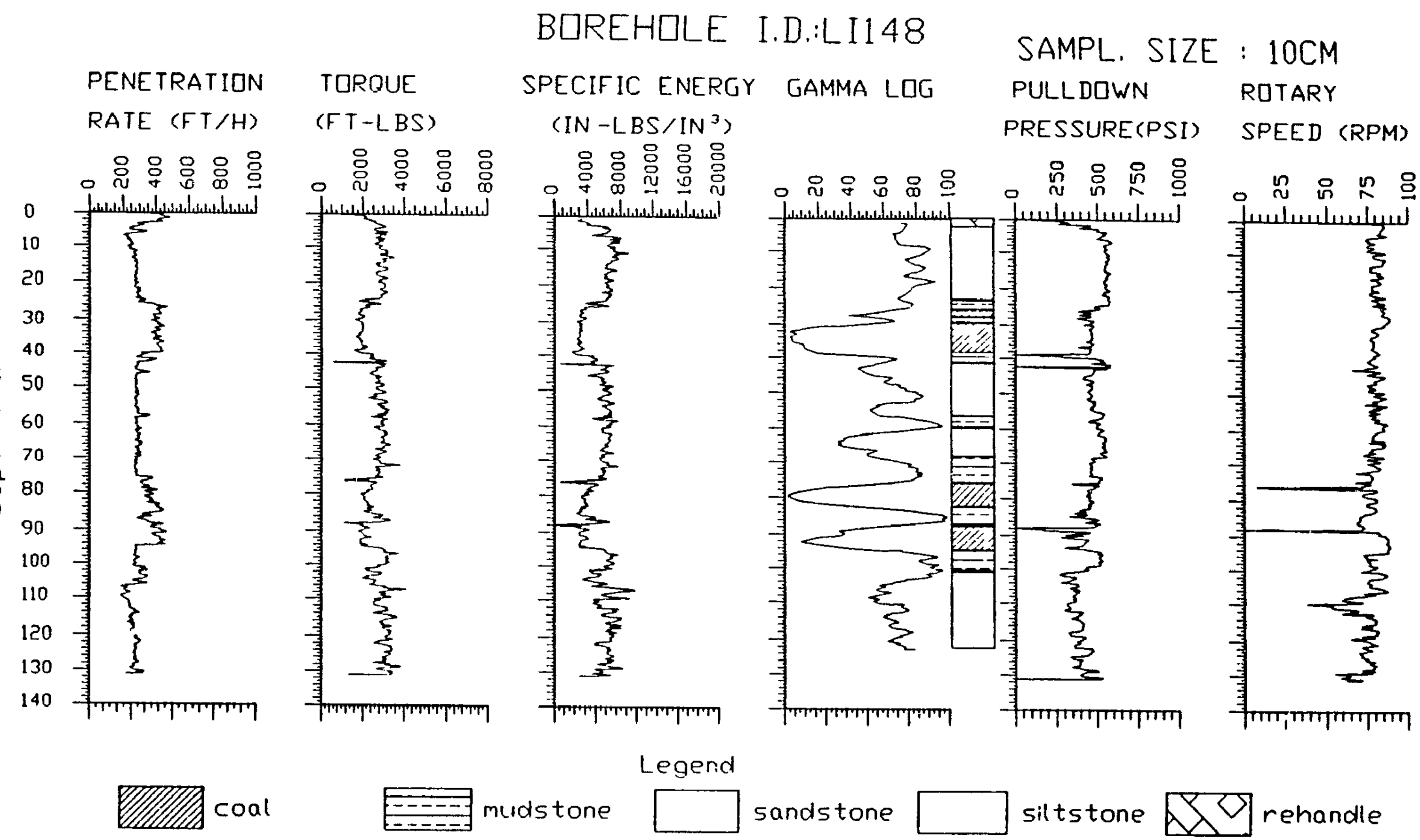

Figure 4.6 - Drill, Gamma and Geological Logs for Borehole LI148.

settings, high torque was observed when drilling harder rocks, ie. siltstones/sandstones, with substantial decreases recorded upon encountering soft rocks ie. coal, weathered units etc. These response patterns agree with those proposed conceptually by Hagan and Reid (1983). Higher torque than expected was observed for drilling in some mudstone units, possibly due to the clayey (and/or silty?) nature of these rocks binding the bit. This as a possible cause was also indicated by associated low penetration rates in these intervals.

High torque was also observed when drilling with a worn bit; associated with this situation were below normal levels of downpressure.

- The monitored patterns in downpressure, at constant rotary speed, were observed to reflect variation in rock characteristics with decreases in hard to soft rock transitions and increases for soft to hard rock transitions. These responses only occurred when the downpressure was set at maximum by the operator from the beginning of the borehole. The variations were therefore not due to an operator adjustment to compensate for the changing ground, yet was an automatic response of the hydraulic system of the drill. This is discussed in more detail in a subsequent chapter.

Downpressure was only decreased by the operator when torque levels began to exceed the recommended panel gauge range eg. in the case of binding due to wet, hard or caved ground or a failed bit.

In rehandle, the weight of the drill string with rotation was enough to begin penetration, resulting in less damage to the bit and drill structure. In this situation, an initial interval of very low downpressure and torque, together with fluctuation in penetration rate can be observed.

- The rotary speed was observed to remain essentially constant throughout drilling at 70-80 rpm. Most variations were related to operator adjustment of both rotary speed and downpressure in order to reduce drilling vibration or to overcome binding ground.

Minor increases were apparent when drilling in coal seams, yet the overall sensitivity of rotary speed to vary in hard or soft rocks, when compared to the other performance parameters, was poor.

- A specific energy parameter was calculated based on equation 2.10 of Teale (1965), which incorporates all the drill parameters and compensates for any changes made in one parameter by changes in another. In this study, the correlation between the relative response in specific energy and the location of rock units as identified from geophysical logs was good. Figure 4.6 shows that the calculated specific energies are lowest in the softer coal units and highest in the harder sandstones and siltstones. Further analysis in a subsequent section is aimed at examining the inter-relationships between drill performance and rock characteristics, in particular the correlation between specific energy and rock properties.

Figure 4.7 illustrates the locations of coal units identified on the basis of specific energy and the other drill parameter log responses in boreholes monitored along the bench of the study area. The seams M_u, M seam, L_l and L_u shown are considered exploitable ie. ≥ than the 3 foot cutoff thickness designated by the mine. The smaller seams MM_1 and MM_2 are considered stringers and are therefore treated as waste. Note the location of borehole LI 148 shown in Figure 4.6, in this diagram.

Evaluation of the data from the September-November 1987 study clearly indicated that drill performance parameter variations are related to changes in rock mass characteristics. More detailed investigations which were carried out in May to September 1988, enabled the detailed distinction of the geology based on the instantaneous changes detected in the drilling process, such that coal vs. mudstone vs. siltstone etc. could be easily identified without extensive use of additional investigation methods. This

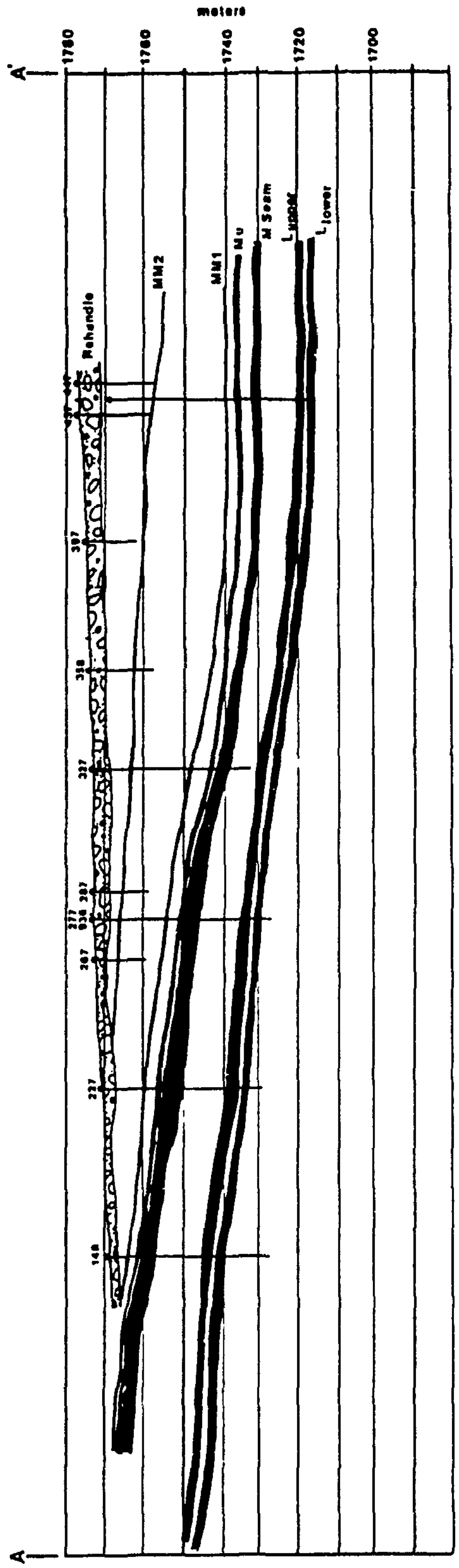

Figure 4.7 - Cross-Section, LI Bench, Lake Pit.

data is discussed in detail in the following sections.

4.4 Mine Engineering Application Systems:

Several systems currently in use at Fording River will benefit from the drill monitoring research currently underway. These include the Drilling and Blasting and Short Range Planning (SRP) systems.

The Drilling and Blasting system currently utilizes manual data collection and interpretation techniques. Apart from database requirements such as operating hours, drilled meters, bit usage, etc., a key element is the operator reported coal intersections. Gamma ray logging is used to confirm coal intersections and provide an indication of rock type. This information is critical in issuing hole-by-hole loading instructions to account for the complex stratigraphy and structure.

The drilling and blasting function could be greatly enhanced with a drill monitor capable of characterizing and reporting rock and coal strata depths and thicknesses. Savings relate to optimised explosive loads in waste and reduced coal dilution due to blasting above and below seams.

The Short Range Planning (SRP) System is a complex system based on the MEDSYSTEM planning package. A strong inter-relationship exists with other engineering systems. The effectiveness of the system is to a large part determined by the frequency of the updates and quality of input data. An important input to the system is a geological gridded seam model. The model is built using manually interpreted and input production drillholes in addition to the exploration holes. Drill monitoring could be utilized to automatically provide timely updates to seam structure within the model.

The SRP system is currently utilized to produce sections, bench maps, and volumes for planning, scheduling, and reconciliation.

Future development relates to the drilling and blasting functions including automated blast pattern design and loading instructions.

Monitoring the performance of drills provides the types of data necessary to successfully maximize the benefits to be derived from all these systems.

4.4.1. Applications of Monitored Drilling:

As described earlier, the capabilities of the Mine Engineering Application systems presently in use or planned at the minesite could be greatly enhanced through the use of the equipment performance data. The monitored drill data as demonstrated, can be used to precisely identify coal seam location and thicknesses across a particular bench level. In addition, the depths and thicknesses of overburden, interburden and rehandle could also be pinpointed. Once this type of data has been acquired then it can be used in a variety of applications.

Based on the interpreted drill performance, and data from traditional sources such as geophysical and driller logs, a revised geological interpretation could be generated for each monitored bench level. Here the percentages of waste to coal could be easily determined from rock unit depths and thicknesses as obtained from drill intersections. These revised models would be of assistance during the pattern design and reserve calculation of adjacent blocks of ground. The monitoring of rotary exploration holes would also permit updates in reserve estimation and mine models on a larger scale. This data would be further refined and upgraded when combined with the smaller scale bench models as this information becomes available.

Improved coal and rock-rehandle contours defined through monitored drilling enable more precise bench plans to be generated and thus better blast designs. These in turn lead to reduced dilution, in addition to improved scheduling of equipment based on more accurate estimates of muckpile volumes. Monitoring also allows for the collection of information on overdrilling, bit usage, drill productivity (ie. downtime vs. actual drilling time) and overall drill costs.

By identifying particular "problem" environments using drill monitoring in advance of the shovel eg. hard bands of sandstone, blasts can be designed to reflect the foreknowledge of the problematic ground. The goal of the drill and blast phases then becomes to prepare the ground in such a way as to improve overall productivity through efficient and economical usage of the shovel. This is made possible by minimizing the effort required by the shovel when excavating (ie. diggability), through prior creation of an optimum muckpile.

The geological applications of the drill data are presented in chapter 7.0 in reference to more recent drill monitoring investigations at the Fording River Mine.

5.0 GEOLOGICAL AND GEOTECHNICAL INVESTIGATIONS ON EAGLE MOUNTAIN:

5.1 Introduction:

From June to July 1988, a total of 186 blastholes were monitored during routine production drilling on Eagle Mountain (Figure 4.3). Using an instrumented 60R drill, the parameters of penetration rate, rotary speed, torque, downpressure and bailing air pressure were recorded in all holes at a sampling interval of 4 inches. In addition, 45 of the drill monitored boreholes were subsequently gamma logged.

Core was obtained for the current studies to enable, along with the gamma and drill log data, a detailed and accurate geological model of the study bench area to be developed. In addition, core specimens from selected depths, were used to obtain values for unconfined compressive and point load strengths and Young's Moduli.

Thin section analysis of tested specimens enabled the identification of microgeological factors which influenced the laboratory derived rock strengths. These results are discussed in section 5.4.

Subsequent correlation of the monitored drill parameter responses from boreholes around the cored holes with this data, permitted an understanding of the control these geological and geomechanical properties have on drilling performance. This latter component is discussed in section 6.5.

5.2 Geology of EZ/EM bench:

Two cored holes of 67 feet were drilled by SDS Drilling of Calgary, between June 27 and June 30, 1988, in an area surrounded by drill monitored boreholes, see Figure 5.1. In addition, the cored and monitored holes were subsequently gamma logged to confirm the results of core logging and thus provide an accurate identification of the various rock types present. The geologic logs for both CHEM 1 and CHEM 2, based on gamma and core logging, are presented in Figures 5.2 and 5.3. Figure 5.4 is the legend

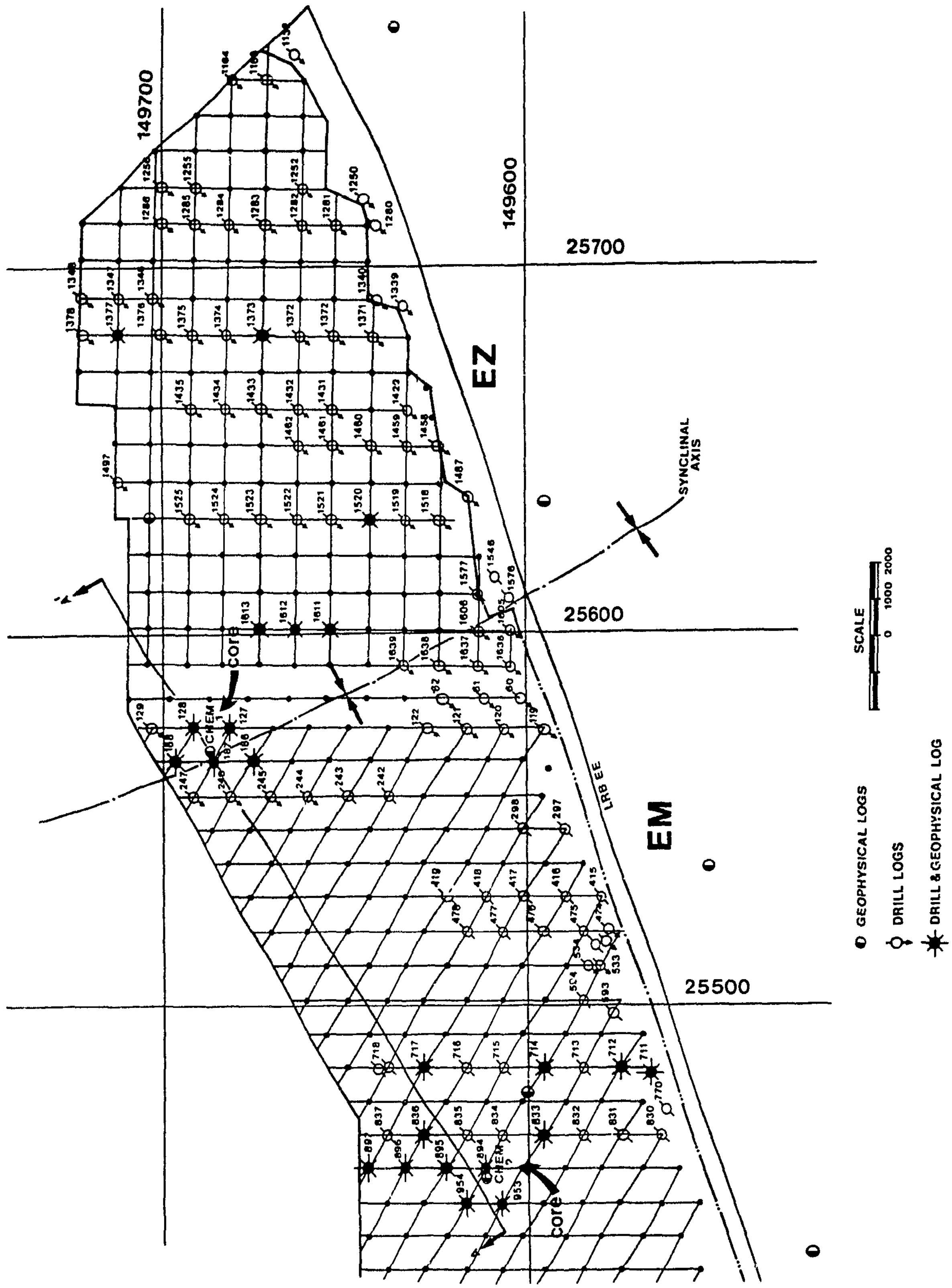

Figure 5.1 - Drill, gamma and cored hole locations on EZ/EM Bench, Eagle Mountain.

for the rock types illustrated by patterns in their geologic logs. The geology for the monitored bench height was predominantly siltstones and sandstones (straight waste) with several thin (less than 3 feet) partings of mudstone and/or coal dividing these more massive units.

The gamma logs in Figures 5.2 and 5.3 indicate clearly the typical fining up (↑) or down (↓) sequences in these rocks, as shown by the direction of the arrows plotted on the traces. These trends are recognized in gamma logs by the sense of the slope of a line drawn through the midpoints of the peaks. Negative slopes correspond to fining down, while positive slopes relate to fining up sequences (Donald, 1984). Here, siltstones primarily, are observed to be interbedded with sandstone units (very low gamma responses), thin mudstone (ragged high gamma response) and coal bands (low response). The location of the sandstones are highlighted in these diagrams (SDST), as these are important for subsequent discussions.

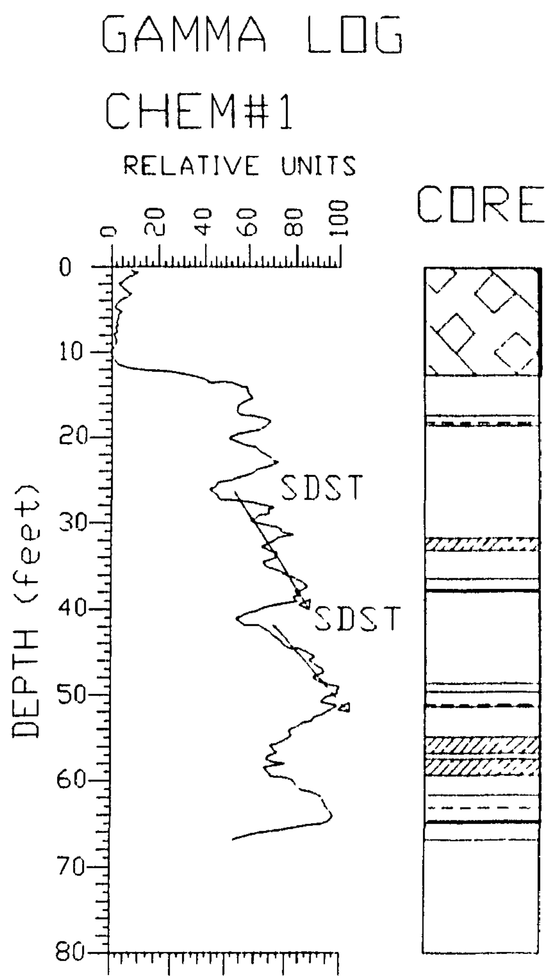

Figure 5.2 - CHEM1 Cored Hole.

Core recovery for both holes was greater than 90 percent overall and generally exceeded 95 percent in most intervals. No core was obtained for the first 9.84 feet of the holes, as this upper zone was in rehandle. As a result, this upper interval was drilled using a 6.25 inch tricone bit and lined with steel casing. A Stratapax bit was subsequently used for coring to the final depth of 67.2 feet.

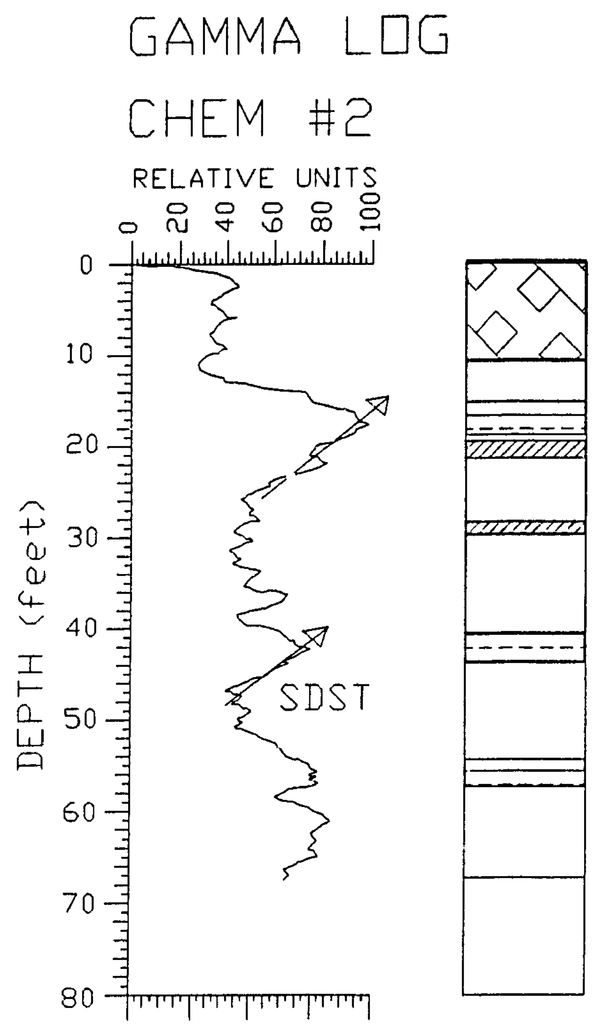

Figure 5.3 - CHEM2 Cored Hole.

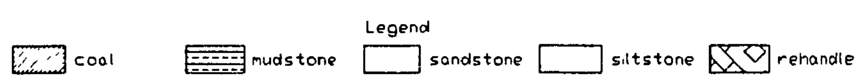

Figure 5.4 - Legend for the Rock Types in Figures 5.2 and 5.3.

5.3 Laboratory Testing of Core:

A - Compressive strength: The 3 inch NX diameter core was logged for rock type and fractures and then cut into specimens of length not less than two times the diameter i.e. a minimum of 6 inches, for subsequent compression testing. Methods for determining the unconfined compressive strength of the rocks were carried out according to the recommendations outlined by the ISRM (Brown, 1981).

A total of 34 core specimens were tested to obtain unconfined compressive strengths. Prior to testing of any of the specimens they were weighed and measured to calculate the density.

Most of the core test samples obtained were siltstone and sandstone, due mainly to the difficulty associated with preparing suitable specimens for the weak, friable rocks such as mudstone. Thin sections were also prepared on the broken remains of some of the tested core specimens, and analyzed to determine the precise composition and the extent to which any variability could influence the compressive strength. The results of these analyses are discussed in section 5.4. All these data, except density, are shown in Table 5.1. This data is also presented in Table 5.2 in comparison to data from other core testing investigations in the same suite of rocks.

A total of 28 of the determined compressive strengths were considered to be valid according to the mode and reason of failure. Reasons for the types of sample failure are examined in more detail in the following discussions. This was an important phase to determine the nature and extent of variation in the measured strengths of the rocks. Since in subsequent sections of the thesis, correlations were to be made between these measured values and the monitored drilling parameters, the validity of the strengths had to be ensured. In addition, it was an important phase to examine the degree of influence microcompositional heterogeneities had on compressive strengths and thus on drilling performance.

Table 5.1 - Compressive and point Load strengths and Young's Modulus data for Fording Coal Rocks.

SAMPLE:	TEST:	SIGMA:(psi)	MODULUS:(psi)	ROCK:	DEPTH(ft)	DEPTH(m):	COMMENTS:
CHEM 1:							
5	P	5454.90	N.A.	MD SLST	15.17	4.62	SAMPLE FAILED ON CALCITE HEALED FRACTURE
6	U	13699.60	1653874.35	MD SLST	15.89	4.84	THIN SECTION
7	U	19952.00	2646039.75	MD SLST	16.61	5.06	THIN SECTION
8	P	19640.25	N.A.	MD SLST	17.19	5.24	
11	U	2688.30	658465.30	SLST	20.16	6.15	NON-VALID TEST DUE TO FAILURE MODE
12	U	14547.85	2158474.35	SLST	20.66	6.30	THIN SECTION
14	U	5814.50	1939769.40	SLST	23.55	7.18	NON-VALID TEST DUE TO FAILURE MODE
16	U	8955.20	1418872.85	MD SLST	29.31	8.94	
17	P	2182.25	N.A.	MDST	30.31	9.24	NON-VALID TEST DUE TO FAILURE MODE
19	U	11136.00	1730683.75	MDST	33.21	10.12	
20	P	17821.95	N.A.	MD SLST	33.73	10.28	
21	U	13273.30	1996345.50	MD SLST	34.28	10.45	
24	U	21538.30	2670067.70	SDST	39.13	11.93	THIN SECTION
25	U	24945.80	3680169.60	SDST	39.77	12.12	THIN SECTION
26	U	19245.85	2644543.35	SDST	40.49	12.34	THIN SECTION
27	U	27084.55	3405678.80	SDST	41.05	12.52	FINE-GRAINED AND MASSIVE; THIN SECTION
28	P	7637.15	N.A.	SDST	41.52	12.66	NON-VPLID TEST DUE TO FAILURE MODE
29	U	14536.25	2147473.20	SDST/SLST	42.31	12.90	THIN SECTION
31	P	4728.45	N.A.	SDST	43.57	13.28	NON-VALID TEST DUE TO FAILURE MODE
36	U	13686.55	1702181.10	MD SLST	46.61	14.21	
40	U	10792.35	1791214.00	MDST	51.48	15.70	
43	P	3055.15	N.A.	SDST	54.32	16.56	NON-VALID TEST DUE TO FAILURE MODE
45	U	21861.65	3019095.75	SDST	56.40	17.20	THIN SECTION
46	U	22963.65	2661915.80	SDST	56.91	17.35	THIN SECTION
51	U	14250.60	2934208.40	SLST	65.76	20.05	
CHEM #2:							
54	U	16226.95	1902165.10	MD SLST	22.81	6.95	
55	U	15857.20	2331675.40	MD SLST	23.32	7.11	
56	U	4331.15	849125.80	SDST	28.19	8.59	SAMPLE FAILED ON INCLINED COAL STR.
57	U	8225.85	1367405.10	SDST	28.54	8.70	SAMPLE FAILED ALONG CALCITE HEALED FRACTURE
58	P	13966.40	N.A.	SDST	30.34	9.25	
59	P	9819.40	N.A.	SDST	31.32	9.55	NON-VALID TEST DUE TO FAILURE MODE
60	U	10453.05	2508123.00	SDST	38.11	11.62	
61	U	23511.75	3064775.10	SDST	38.77	11.82	THIN SECTION
63	P	6327.80	N.A.	MDST	41.03	12.51	
65	P	2910.15	N.A.	MDST	42.49	12.95	
66	U	19667.80	2927316.55	SDST	43.23	13.18	
67	U	11070.75	1736878.15	SDST	45.40	13.84	THIN SECTION
68	U	11427.45	2635897.00	SDST	45.90	13.99	
69	U	11586.95	2713741.70	SDST	46.43	14.16	
70	P	16003.65	N.A.	SDST	46.90	14.30	
72	U	10073.15	2243116.65	SDST	49.15	14.98	NON-VALID TEST DUE TO FAILURE MODE
73	U	4799.50	865494.85	SDST	50.97	15.54	NON-VALID TEST DUE TO FAILURE MODE
74	U	7590.75	2085865.60	SDST	51.67	15.75	NON-VALID TEST DUE TO FAILURE MODE
75	P	4000.55	N.A.	SDST	52.33	15.95	NON-VALID TEST DUE TO FAILURE MODE
76	U	14014.25	2352571.35	SDST	53.00	16.16	
79	U	6477.15	1267764.00	SL MDST	56.33	17.17	THIN SECTION
81	P	13457.45	N.A.	SLST	58.25	17.76	
82	P	2546.20	N.A.	SLST	59.12	18.02	NON-VALID TEST DUE TO FAILURE MODE
86	P	13821.40	N.A.	MD SLST	63.09	19.23	
86A	P	2182.25	N.A.	MD SLST	63.59	19.39	NON-VALID TEST DUE TO FAILURE MODE
87	P	2910.15	N.A.	MD SLST	64.24	19.59	NON-VALID TEST DUE TO FAILURE MODE
88	U	23214.50	3078051.30	SLST	66.09	20.15	
90	P	13311.00	N.A.	SLST	68.01	20.73	

Table 5.2 - Comparison of Rock Property Data.

PROPERTY:	ROCK:	McGILL:	GOLDEP (1983):	DRESSER(1971-1983):	LEHEL(1984):
UNCONFINED COMP. STRENGTH (psi)	SDST	18136.60 (14) (10453 05 - 27084 55)	21654) (8) (14355.00 - 29580.00)	21296 15 (9) (14555 10 - 33909 70)	(16675 0 - 22475 0)
	SLST	16820.00 (11) (8955.20 - 23214 50)	16965 00 (5) (12035 00 - 22620.00)	- -	(5800 0 - 22040 0)
	MDST	9468.50 (3) (2910.15 - 11136 00)	8544 45 (7) (3770.00 - 14355.00)	- -	(8700 0 - 14355.0)
	COAL	-	1348 50 (3) (500.25 - 3016.00)	- -	(-)
MODULUS (psi)	SDST	2726303.05 (14) (1736882.5-3680172 5)	4629850 00 (3) (4292000.0 - 4495000 0)	- -	- -
	SLST	2179032.45(11) (1418868.5-3078045 5)	5698500 00 (2) (5292500.0 - 7293500 0)	- -	- -
	MDST	1596554.4(3) (1267764.0-1730691.0)	5698500 0 (1) (-)	- -	- -
	COAL	-	449500 00 (1) (275500 0 - 1798000.0)	- -	- -
		(Tangent Modulus)	(Secant Modulus)		
DENSITY (gm/cm3)	SDST	2.65 (14) (2.58-2.81)	2.59 (3) (2.44 - 2.67)	2.70 (9) (2.55 - 2.88)	2.70 -
	SLST	2.63 (11) (2.59-2.70)	2 62 (3) (2.53 - 2.71)	- -	2.70 -
	MDST	2.54 (3) (2.51-2.58)	2 77 (3) (2.60 - 3.01)	- -	2 70 -
	COAL	-	1 32 (3) (1.19 - 1.39)	- -	- -
BASIC FRIC.ANG. (degrees)	SDST	-	28 6 (7) (26 - 30)	- -	28.00 -
	SLST	-	31 5 (8) (23 5 - 39)	- -	33 50 -
	MDST	-	29 6 (5) (26 - 33)	- -	31 00 -
	COAL	-	22 9 (5) (16 - 32)	- -	- -
POINT LOAD STR. (psi)	SDST	14985.8 (2) (13966.4 - 16003.7)	20305.8 (5) (9004.5 - 33422.5)	- -	- -
	SLST	16438.7 (4) (13311.0 - 19662 0)	15784 7 (5) (5800.0 - 25665.0)	- -	- -
	MDST	4619.7 (2) (2910.2 - 6327.8)	9229 3 (4) (1450 0 - 27985.0)	- -	- -
	COAL	-	3045 0 (1) (1595.0 - 9715 0)	- -	- -

B - Point Load Strength: Samples whose lengths were less than the length to diameter ratio of 2 were point loaded. Of 23 samples tested, only 8 were considered valid, based on consideration of the mode of failure as for the unconfined compression tests. Point load testing and compressive strength calculations were conducted according to ISRM standards (Brown, 1981). This test is one in which fracture of the specimen occurs as a result of induced tension. Since these rocks were considered highly anisotropic ie. greater strength perpendicular to rather than parallel to bedding, and to enable a correlation to the measured unconfined compressive strength data, all the samples were loaded axially (ie. perpendicular to the bedding). However, it is clear from Tables 5.1 and 5.2 that regardless of this approach, the weakness planes and effects developed at the contacts between loader points and core, produced considerable scatter in the measured data. Data for some of the more isotropic core samples gave results which were comparable to those obtained from uniaxial tests.

C - Young's Modulus: The results from both compression and point load testing in the present study, including calculated modulus and rock type are provided in Tables 5.1 and 5.2. The modulus data reported is the tangent modulus, which is the slope of the axial stress-axial strain curves from compression tests at 50 percent of the peak strength.

D - Comparison of Measured Rock Property Data with Known Ranges: Table 5.2 outlines rock property data generated by the present investigation (shown under the heading "McGill") in comparison to data from other studies conducted on samples from the same formation of rocks.

The Golder Associates data indicated in this table were derived from core testing programmes undertaken as part of a blasting study commissioned by Fording Coal Ltd. in 1981-1983. Additional data for this study was obtained from testing of core from the same rock formation (Mist Mountain) from other operating coal mines in the Elk Valley (Golder Associates, 1983).

The data from Dresser-Security (1971, 1979,1983) was based on the results from core testing undertaken between 1971 and 1983 as part of a drillability assessment. Only the test results for core from the same area of the mine as the present study are displayed.

The rock property data from Lebel (1984), are values from core testing of samples from the Greenhills mine, located to the south of the Fording property. As for the other reported results, these tests were carried out on rock specimens from the same stratigraphic horizon as in the current investigation and are therefore useful for comparison purposes. However, it is assumed that the strength data determined in the present work are the most reliable as all aspects regarding the testing procedure and the precise locations of the core both in the bench and stratigraphically are known.

As is seen in Table 5.2 the results from the current core testing show that the sandstones in the research area have overall average strengths of 18137 psi, siltstones 16820 psi and mudstones 9425 psi. Average coal strengths of 1349 psi[1] are reported by Golder Associates (1983).

5.3.1.Validation of Compressive Strengths:

A detailed rock testing study on drillability conducted by Bingham (1964) noted that considerable variation in compressive strengths was derived from core cut from the same block of rock. The difference seen in those studies between the maximum and minimum compressive strengths was approximately 2 to 1. This ratio was considered by him to be particularly valid for unconfined compressive tests as compared to triaxial tests

---

1 - see Appendix II for metric equivalent.

conducted over a range of confining pressure. However, it was noted that the maximum value of compressive strength better indicated macroscopic strength than did the minimum values. These latter values were considered to be related to microscopic features in the core which reduced the measured strength to anything less than the true value.

Several reasons proposed for premature sample failure (and thus dispersion in the data) during compression testing in the present study were:

a - eccentric loading (ends not perpendicular to specimen axis) of the sample resulting in tensile failure at platen-sample interface. This can have a significant effect on the shape of the stress-strain curve, the peak strength and the reproducibility of results. Secondly,

b - end effects, resulting from friction between the specimen ends and the platens and differences between the elastic properties of the rocks and the steel. This results in the creation of shear stresses at the specimen-platen contact and overall disruption of uniaxial stress gradients throughout the sample (Brady and Brown, 1985). This also implies that the axial stress is not a principal stress and that stresses within the specimen are not always uniaxial;

c - premature failure along pre-existing weakness planes, at the ends (due to mechanisms given in (b) above) and within the specimen.

The first and second case was clearly evidenced by examination of the crushed core, where neither a conical type (shear fracture) or tensile type failure, typical of these types of rocks, was developed. (Note that the predominance of one of these two types of failure depends on the strength, anisotropy, brittleness and grain size of the particular specimen, see section 5.4). Rather a localized failure at either end of the core occurred resulting in rotation and slippage of the sample between the platens and thus a low recorded strength value.

The third type of failure mode appeared to be more common and in line with the observations made by Bingham (1964). In such cases, it was generally seen that failure was induced prematurely by the presence of microgeological features inherent in these types of sedimentary rocks.

During the initial selection of samples for testing in this thesis study, attempts were made to choose only representative specimens which were compositionally and structurally homogeneous. However, the characteristic nature of sedimentary rocks is the presence of stratification or layering of materials at scales ranging from meters down to millimeters. For the rocks of the present study, microlaminations (thickness 1 millimeter and less) of platy, weak clay minerals and/or coal were commonly identified in core and in thin section. However, these zones were difficult to identify in hand sample in rocks having a dark color (due to the high percentage of clay minerals and organic matter) and so were unknowingly present in some of the selected test specimens. In addition, there was considerable variation in the composition of the matrix. Varying percentages of microcalcite to microquartz cements were observed, with an occasional chlorite-rich sample. The ratios of these in the cement were seen to exert some influence over the sample strength in compression. Therefore the compressive strength values taken as valid data were those samples which did not fail prematurely as a result of end effects or related phenomena. Only those samples which exhibited the expected failure geometries were used in subsequent analyses.

5.4 The Influence of Microgeological Features on Compressive Strength:

5.4.1 Past Studies:

Numerous investigations were conducted in the past to examine the effects of microgeological variations on the compressive strength of rock. The more appropriate of these, in relation to the testing results obtained in this thesis study, will be briefly reviewed.

Results obtained by Al-Jassar and Hawkins (1977), from testing limestone core specimens, indicated that premature failure occurred in compression in zones where thin shale seams criss-crossed the sample. The preferred orientation of platy clay minerals in these bands were seen to result in a reduction in the internal friction and thus failure at lower applied loads. It was also demonstrated in this study that higher compressive strengths were obtained in rocks having a finer-grained calcite matrix, where the influence of the two good cleavage directions of calcite would be minimized.

Hoek and Bieniawski (1965) suggested that for fine-grained, well-cemented and dense rocks, high loading stress is required to propagate grain boundary cracks. The highly interlocked fabric of these tightly packed, dense rocks, in addition to the composition of the matrix and component grains, would be responsible for a high rock strength.

Similar conclusions were noted by Rowlands (1977) that grain size was an important control upon rock strength. Reasoning for this was seen by him to be due to the greater surface area of abrasion and greater amount of interlocking grains boundaries resulting from a smaller grain size. The resistance to shear would therefore be higher and if all other influences were maintained constant, then a greater rock strength would result. Howarth (1987) indicated that fracture patterns were straight with very few crack interactions for loading of fine-grained, dense rock specimens. However, testing of medium-grained, weakly cemented samples, showed that fractures created from loading, split and coalesced by following the weak grain boundaries of both framework and matrix components. Therefore, the actual micro-strength properties of the component grains and cements were factors which affected the overall strength of the sample in compression.

The shape of the grains were considered by Price (1963) to also affect the compressive strength. It was indicated from testing of sandstones, that the presence of angular, brittle quartz grains served as a stiffening component, opposing the internal fracture mechanisms operating during deformation. Therefore, a higher internal friction develops along potential failure surfaces resulting in higher observed rock strength. This effect was considered to result from the increasing influence of angular grains interlocking with increasing load.

Price (1963) and Smart et.al.(1982) noted, that a positive, curvilinear relationship existed between the compressive strength and the percentage of quartz in the samples.

Petrographic and compression testing studies undertaken by the author on samples of sandy limestone, also indicated a curvilinear trend relating quartz percent and strength. However, in the rocks that were examined, it was determined that it was not only the percentage of quartz present but more importantly their spatial relationship to one another and the nature of the matrix. Detrital quartz grains in contact with one another (grain supported) were seen to form a supporting framework. Therefore the strength of the material was considered highly dependent upon the resistance of this framework to the applied load. In matrix supported rocks, however, it was observed that the overall strength was dependent upon the strength properties of the cement. For rocks of the same investigation, the quartz grains were generally seen to be supported by the calcite-shaly matrix and were not in contact. The "floating" quartz grains appeared therefore, to have little effect as a supportive framework to increase rock strength. What was apparent, was that as the percentage of quartz grains increased, a point was reached at which the grain to grain contacts also increased. In these particular quartz rich rocks, failure occurred across the quartz grains in contact, which were more resistant to the applied load than the surrounding calcite matrix resulting in higher measured compressive strengths.

At lower percentages of quartz grains, the matrix was the factor governing the strength of the samples ie. intergranular failure predominated. For this type of failure, it was indicated that the presence of fine versus coarser grained calcite cement resulted in higher values of compressive strength (Peck, 1986).

Similar results were also reported by Sangha et.al. (1974) from microfracturing studies of sandstone under compression. These results indicated that failure occurred across the clay-calcite matrix and not the sandstone's quartz grains for matrix supported samples. It was concluded that intragranular failure of quartz grains became more prominent and that rock strength increased, as the percentage of quartz (increased grain support) and/or loading increased.

A study by Fahy and Guccione (1979) showed that for matrix supported, quartz-rich rocks, a decrease in strength occurred for an increase in the amount of quartz grains in the samples. This factor was attributed to intergranular fracturing which occurred in the calcite matrix around the quartz grains. Rock strength in such a case was considered controlled by both the percentage and the grain to grain interactions of the quartz, similar conclusions as those in Peck (1986).

Howarth and Rowlands (1987) indicated that the observed increase in strength with increasing quartz percentage was primarily a result of the increased interlocking of grains.

Brown and Phillips (1977) noted that compressive strengths generally increase with bulk density for most rocks, but this relationship was not well defined for rocks in the range of 2.50 to 2.80 gm/cm^3. This range corresponds to the densities determined in the present thesis study, and therefore poor correlation with measured compressive strengths was obtained. In sedimentary rocks all strength properties generally decrease with an increase in porosity (Howarth et.al., 1986).

Compressive strengths also appeared to increase as a result of increased packing densities or the space in a given area occupied by grains (Howarth and Rowlands, 1987). Rocks, especially sandstones having more than one range of grain size were seen to demonstrate higher compressive strengths. As the intergranular spaces between the larger quartz grains became packed with smaller grains the overall strength of the sample increased. Similar results were observed by Peck (1986).

In summary, **textural** features affecting rock strength are the size, shape and degree of interlocking, porosity, grain orientation and the nature of grain boundaries. **Compositional** features are the strength properties and percentages of framework grains and cementing materials (Howarth and Rowlands, 1987). These features will be examined in the next section in relation to the rocks of the thesis study area.

5.4.2. Current investigations:

Figure 5.5 is a thin section photograph taken on siltstone compressive strength sample #29, indicating the presence of an argillaceous/coaly lamination trending parallel to bedding (parallel to the lower edge of the photograph) and

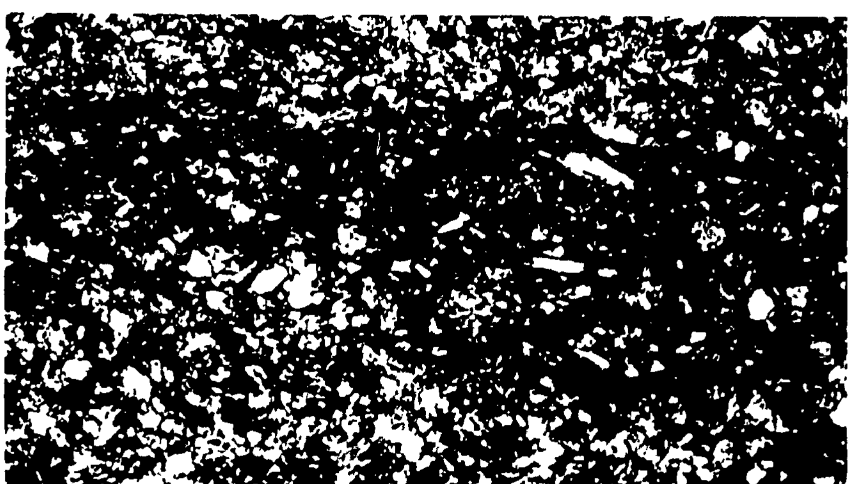

Figure 5.5 - Thin Section of Sample #29, Siltstone (Crossed Nichols, 100x).

perpendicular to the core axis. Results from past research and confirmed by the present tests, indicated that for these types of layered rocks, deformation and failure occurred along these thin weakness planes for loads considerably less than expected, independent of their orientation with respect to the applied load.

Further evidence for reduced compressive strengths was demonstrated from the detailed thin section analysis, mainly for the siltstone/sandstone samples.

A - Composition of the Matrix:

The matrix (cement) serves to bind the constituent or framework particles of the rock together and therefore contributes towards its overall strength. It was observed in thin section, that two main cement types were present ie. calcite and quartz, with the former predominant as a fine grained component, comprising up to 58.7 percent of the matrix content. Quartz was seen to constitute up to 41 percent of the overall composition of the rock as a cement component. In addition to these constituents, chlorite was occasionally present in amounts up to 10 percent.

It would be reasonable to predict therefore, based on a knowledge of the mineralogical strength properties of the cement types (i.e. quartz > calcite > chlorite), that lower strengths would be seen in those rocks with calcite and chlorite rich cements and little quartz. Higher strengths would be obtained in those specimens with a higher quartz to calcite ratio and little or no chlorite. This assumes that no other factors are contributing to a reduction in compressive strength ie. the presence of coaly/mudstone laminations shown in Figure 5.5. Thin section analysis of samples such as siltstone sample #25 appeared to corroborate these statements. Here, the cement is composed of 12.9 percent quartz and 35 percent calcite (9.2 percent organic content), as compared to siltstone sample #12/13, having 32.3 percent calcite and no quartz as cement (9.0 percent organic content). Their respective unconfined compressive strengths are 24940 psi and 14544 psi.

It was also clearly seen that the higher the amount of organic material present in the test samples, then the lower was the strength. This fact was evidenced in the siltstones, where in some cases organic contents were as high as 17 percent i.e. muddy siltstones; see Sample #29, Figure 5.6. This particular variety of rocks generally accounted for the lower end of the ranges of strength for siltstones shown in Table 5.2.

The percentages of quartz grains (Qz(G)), quartz cement (Qz(M)), calcite cement (Ca), chlorite cement (Ch) and organic material (Or), either as cement or detrital constituents are shown with respect to increasing compressive strength for the particular core specimens in Figure 5.6. The compositional controls on rock compressive strength discussed above, are better illustrated for the samples of this investigation by this bar graph. It is seen in this figure that higher compressive strengths are **generally** determined on samples having high quartz percentages as both matrix and framework components, in addition to a low calcite (cement) percent. The effect on strength due to the amount of chlorite and organic material are not as clear. However, a comparison of samples #25 and #26 which have very similar compositions, indicate that a possibility for the lower strength in the latter specimen may be due in part to its higher percentage of both chlorite and organic material. The high percentage of chlorite in sample 45/46 may also be responsible for the lower strength in a rock having a high quartz cement percent and very little calcite.

Samples in which calcite cement is in higher proportions than quartz generally demonstrate a reduced strength, see samples 6, 29 and 67.

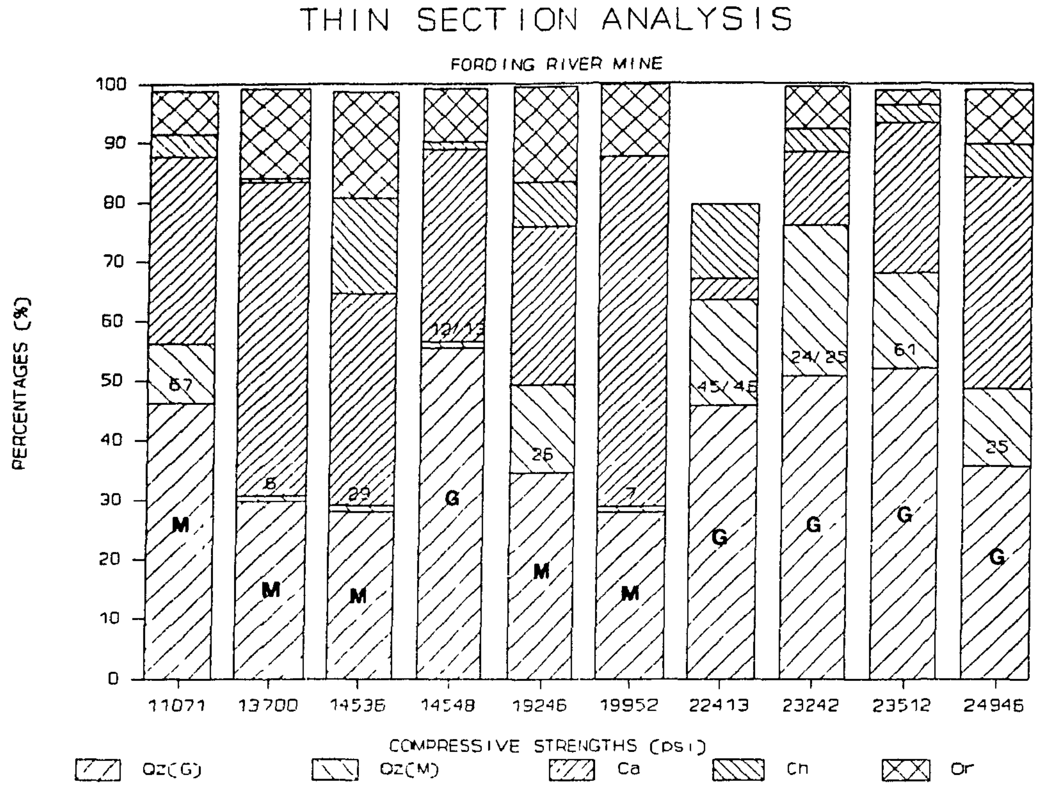

Figure 5.6 - Mineral Constituent Percentages vs. Compressive Strength.

B - Grain Supported vs. Matrix Supported:

Figure 5.6 also indicates that the grain supported (G) samples compared to the matrix supported (M) specimens exhibit higher compressive strengths. This may account for the low compressive strength of sample #67, which has a high percentage of quartz as grains and cement, in addition to 31 percent calcite as a cement constituent. However, the presence of the more brittle quartz does not appear to influence the compressive strength. The rock strength therefore, is most likely wholly dependent upon the properties of the calcite cement in which these grains are suspended. This trend would be in line with past studies testing similar detrital rocks as reviewed in section 5.4.1.

C - Detrital Grain Size:

Further assumptions which could be made to validate the rock strengths determined, is in terms of the sizes of the mineral grains (framework) present in the samples. Figure 5.7 shows a plot of measured compressive strength against grain size. The two curves illustrated are for the siltstones (slst) and sandstones (sdst) identified on the basis of grain size (>0.062 mm = sandstone; 0.004 mm to 0.062 mm = siltstone; modified Wentworth Scale; Lane, 1947).

Regression analysis of the siltstone data gives a coefficient of correlation equal to 0.694, while for sandstone it was slightly higher at 0.731. Based on this data, it could be stated that the compressive strength appears to increase for an increase in grain size. This trend is opposite to what was generally observed in past investigations (Price,1963; Smart <u>et.al.</u>,1982). This could be due to the fact that with increasing grain size, grain to grain contacts increase, resulting in an overall higher strength (Peck, 1986). It is apparent from the thin section analysis that the sandstones not only are grain supported, but also have from 10 to 25 percent microquartz as a cement constituent (remainder is calcite). The siltstones

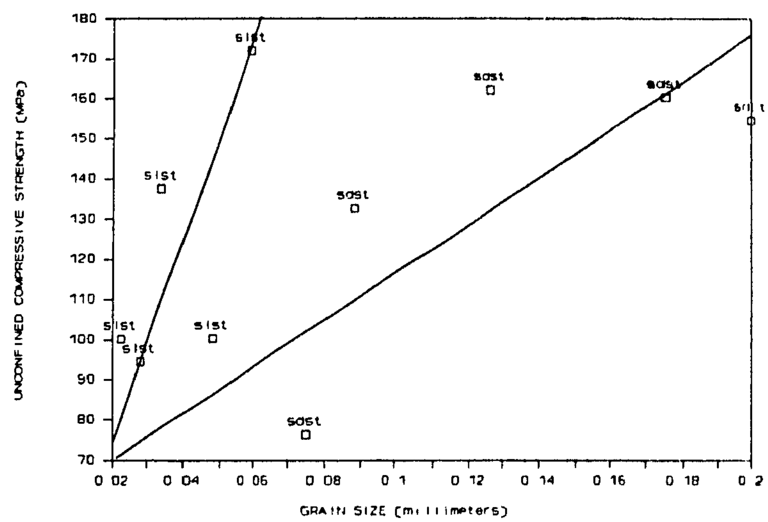

Figure 5.7 - Plot of Compressive Strength vs. Grain Size. (slst=siltstone;sdst=sandstone)

however, consist of predominantly calcite cements, with no microquartz. These would appear to be the main reasons for the differences in the slopes of the lines illustrated in Figure 5.7. Another related possibility, is that the smaller the grain size the greater is the percentage of weaker constituent minerals, ie. calcite, chlorite and organic material. These factors together would account for the trends seen in Figure 5.7.

Figure 5.8 is a bar graph similar to Figure 5.6, where the percentages of the constituent minerals in the rock samples are displayed with respect to increasing grain size. This diagram supports the hypotheses above, in that it is clear that with increasing grain size the percentage of calcite decreases, with

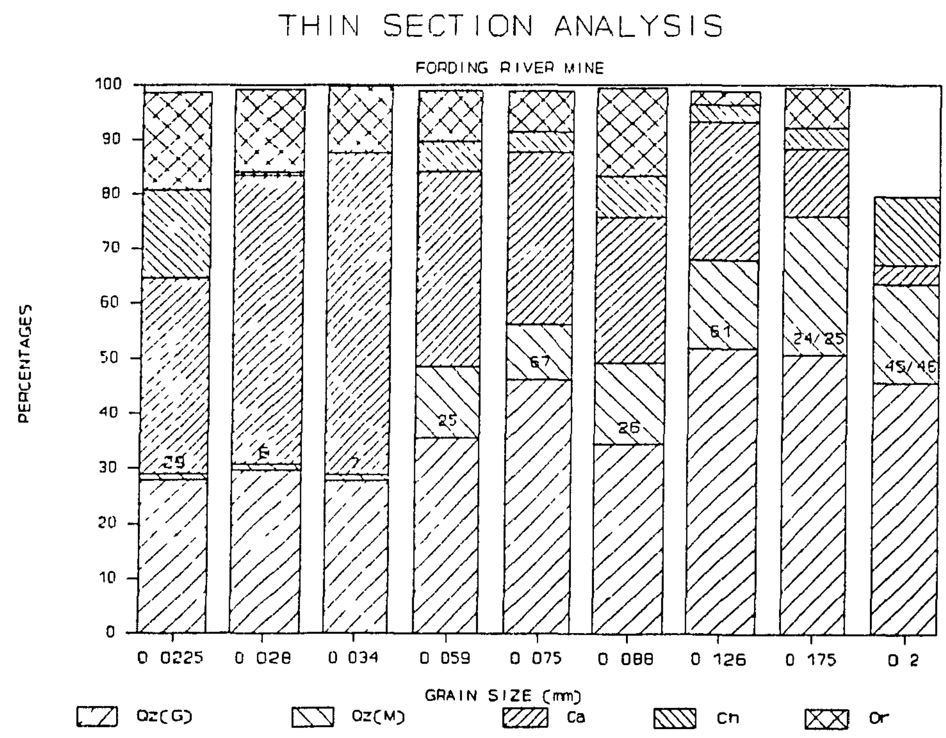

Figure 5.8 - Mineral Constituent Percentages vs. Grain Size.

related increases in both the amounts of quartz grains and quartz cement. In addition, there is also a general decrease in the overall amounts of organic content with increasing grain size. These factors therefore contribute to the higher compressive strengths thus obtained for coarser grained samples.

However, a greater number of both strength tests and detailed petrographic analyses would have to be conducted to confirm the hypotheses presented above.

5.5 Conclusions:

The ranges of compressive strength obtained for the test samples of cored holes CHEM1 and CHEM2 correspond to those determined from previous investigations. These data also clearly indicate the well-defined strength contrasts between the different units.

It was also apparent that within the sandstone/siltstones of the study area there is considerable compositional variability. These variations have been demonstrated through thin section analysis to be the reason for the exhibited dispersion in the laboratory derived compressive strengths.

These are important results for subsequent phases of the thesis where the drilling parameters are to be correlated to the rock properties. The potential variations in rock strength due to composition, should therefore assist in validating the dispersion in the drilling data. This approach will be demonstrated more clearly in sections 6.2 to 6.5.

6.0 CORRELATION OF DRILLING PERFORMANCE PARAMETERS TO GEOLOGY:

6.1 Drilling performance relationships to rock mass properties:

Once the effects of bit design upon overall drill performance had been assessed and partially understood, researchers turned to studies of the individual drilling parameters to evaluate their influence upon penetration rates. The effects of bit loads, rotation speeds, rotary torque/horsepower, flushing hydraulics and rock mass properties on drilling rates were investigated in detail. Theoretical approaches, based upon the stress and failure mechanisms of rock under the load of individual rock bit inserts were attempted (Fish,1959; Maurer,1962; Hartman,1966; Eronini et.al.,1981; Lebel,1984). From such studies it was hoped that a prediction of rock failure could be made with subsequent derivation of a drilling rate. This appeared to be the logical path of investigation whereby all the drilling parameters could be incorporated into one unifying analysis. However, areas such as fracture mechanics, bit geometry, rock mass variation, flushing media properties, bit hydraulics, bit loads and speeds and additional operating influences that were known or unknown, prevented numerous investigators from succeeding in their tasks. Therefore it was clear from these drilling complexities that a less scientific basis but more practical approach be followed, in order to determine the relationship(s) between the parameters (Cunningham, 1978).

In the present study, the concern was not with predicting or estimating penetration rates, as was the aim of past investigations. Here the goal was to enable an estimation of the properties of the rocks being drilled based on a detailed monitoring of all the important drilling parameters. The drilling models developed in the past were capable of providing reasonable estimates of drill rates on the basis of input rock strengths. Therefore, it was considered possible to obtain reliable estimates of rock strength based on the input to an appropriate drilling model, of accurate drill performance data.

In order to achieve this end, several preliminary stages were necessary. Firstly, an examination of the inter-relationships between the drilling parameters for the particular conditions surrounding the field experiment was undertaken based on data from a monitored test drillhole. Certain conditions were controlled during this test phase, within the limitations imposed by a field based study. This was an important phase to determine the nature of the responses between the drilling parameters for the particular drill, bit type and diameter and geological environment, see section 6.2.

Secondly, the capability of the individual parameters to identify changing rock properties was evaluated based on a correlation of these responses to those from gamma logs. This phase also included the definition of the optimal conditions under which the reliability and sensitivity of the particular parameter would be at a maximum. This was related to the rock breakage mechanisms and the role of the parameters in these processes, and required the identification of the range of the monitored drill data for these particular conditions (section 6.3).

Following this, in section 6.4 the parameters were incorporated into selected drilling models to evaluate their individual contributions to the overall response when combined with all the other parameters. It was also necessary to determine which model(s) had the best arrangement of the individual parameters such that their combined response would be one that demonstrated the greatest sensitivity to changing rock properties (section 6.4 and 6.5). Finally, a "calibration" of the drilling responses to the actual rock properties determined from laboratory testing of core specimens was accomplished (section 6.5).

6.1.1. Relating Drilling Performance to Rock Properties:

If the assumption is made that rock breakage is a result of the combined influence of both rotary and axial forces generated by drilling, then it should follow that the strength of the material should relate in part to the magnitudes of these applied energies.

The stresses developed through bit-rock interaction are dynamic in nature, yet past studies have indicated that the rate at which they are applied is slow enough for them to be modelled using a static approach. In this regard, rotary tricone drilling can be represented by an indentation process, with the factors affecting rock penetration related to the applied load, the rock properties and the geometry of the indentor. (Details of these studies are given in Lebel (1984) and will not be reviewed further). For the purposes of the present study, since applied load is continuously monitored along with other related performance parameters, a correlation between variations in these and the properties of the rocks is attempted. The geometry of the indentors did not change throughout the monitoring period as the same type of bit was used for all boreholes.

It should be recognized that there are inherent differences, however, between the intact rock strengths determined in the laboratory versus the strength of the rock mass being drilled. The rock mass strength would be dependent upon:

a - the intact strength under the dynamic conditions of loading associated with a tricone bit,

b - the confinement by the surrounding rock,

c - the fracturation condition, and possibly

d - the moisture content of the rock.

Therefore any approach which attempts to utilize drill performance parameters as a means of estimating bulk rock strength has to account for the influence of each of these factors on the observed variations in the former. The effect of each of these rock mass characteristics on drill performance is discussed in the following sections.

A - Relationship Between Tricone Bit Rock Breakage Mechanisms and Intact Rock Strength Testing:

It has been demonstrated in the past that the test procedure for determining unconfined compressive strength is very similar to indentation of rock by a bit insert (Lebel, 1984). However, it can also be stated that compression strength testing is a static process with continuous applied load (increasing at a constant rate) acting on the same area of influence on the core specimen for the duration of the test. This is in contrast to the more dynamic nature associated with rock drilling.

Teale (1965), in laboratory investigations involving the static loading of roller bits confirmed that the depth and volume of insert penetration are proportional to the applied load. This criteria would also be related to the particular compressive strength of the rock being tested. Maurer (1962) found a good correlation between the crater depth and the reciprocal of both the shear and compressive strength of rock. Combining these statements with the results of Teale, indicates the connection between the applied weight and the rock strength. Simply stated, that for a rock of given strength, the depth of insert penetration (ie. penetration rate) will increase for an increase in applied load. In addition, for constant applied load, the depth of penetration in a higher strength rock will be less than that for a rock of lower strength. Therefore on this basis the variations in the applied (constant) load and penetration rates appear to offer some chance of providing an indication of changing rock strength.

Some similarity exists between axial loading of the rock in both compression testing and drilling. The transmission of axial load to the indentors in rotary tricone drilling, can be speculated to be evenly distributed across the whole rock face rather than examining the stress concentration at a single indentor. In this regard, the applied stress acting on the rock at any instant in time is equivalent to the applied load over the area of influence of the bit (Warren, 1984). This is similar to the process for determining the stress at failure in strength testing, which is equal to the applied load at this point over the area of influence of core sample and platen. Additional processes are also involved in drilling, however, in combination with the applied load towards rock breakage and therefore this parameter alone is not representative of the actual compressive strength of the material. In actual drilling, the role of the applied weight is not so simple. Here, the rock is subjected to numerous repeated impacts, some possibly at the same point, in addition to the lateral forces applied by torque to initiate failure and create chips. Therefore, not all of the applied energy is used towards fracturing the rock. Some of the energy is dissipated into the unbroken rock surrounding the borehole, in addition to mechanical losses in the drill string. For improper cleaning, some additional energy is expended in the regrinding of the broken rock. At the same time as these losses occur, the remaining energy is promoting rock failure and chip formation (Warren, 1984).

Conversely, the compressive strength of rock on its own is not a suitable indicator of drillability. Other properties such as shear strength, lithology and structure have to be considered in order to provide a more detailed and accurate understanding of the drilling parameter responses.

Similar conclusions were also indicated by Somerton (1959) who had found it a difficult task to evaluate rock strength based on only the drilling performance parameters. He noted that in order to estimate this rock property, knowledge of the rock breakage mechanism was required. This was dependent on the bit type being used ie. whether true-rolling, hard rock bits involving impact-compressive failure or non-rolling soft rock bits with scraping-gouging action promoting torsional-shear failure were involved. He made the initial assumption that all other strength properties bear a consistent relationship to the unconfined compressive strength and therefore, he proposed that it was of use in comparing with the drillability of rock. However, he added that this latter property was not to be based solely on the penetration rate, but should also incorporate the responses of the other drilling parameters as well. In subsequent laboratory investigations using this approach, he found that a comparison of the maximums of unconfined compressive strength to the combined drillability index did not give very good results on an absolute value basis. He therefore concluded the compressive strength was not a reliable property for general rock drilling correlations. He determined a "drilling strength" index which were simply corrected values of compressive strength to improve the correlation with the combined responses of the drilling parameters. No relationship was ever established nor understood between this parameter and the compressive strength of rock, yet it was used extensively in the past (and in the present - Cunningham, 1978, eqn.2.24) as a means of estimating drillability.

Warren (1981) developed an equation (2.26) which combined the responses of penetration rate, rotary speed, bit diameter and weight on the bit to determine a relative strength index. Subsequent correlation of this data, calculated from laboratory drill monitoring studies, with measured rock properties indicated excellent agreement with both compressive and shear strengths. It was noted by him that the good correlation obtained was due to the controlled laboratory conditions surrounding the drilling. However, the drilling model was subsequently used in field trials with good results.

It is important to note that these drilling models only yield meaningful results when used for situations where conditions are similar to those under which they were originally developed. Therefore, their application and subsequent results must be used with these potential limitations in mind.

B - The Effect of Geological Structure on Drilling Performance:

The influence of the fractures within the rock mass on drilling performance was not directly evaluated in the present thesis study. Fractures were logged from the core in the laboratory, but there was a delay of 3 weeks between this stage and the time that the core was originally recovered at the test bench site. In addition, the core was transported the 3000 miles from the minesite to the university by truck, and as such it was difficult to determine which were natural and which were mechanically induced fractures.

Two predominant joint sets were, however, identified from mapping studies conducted by the author in the test area. These near vertical structures were determined to be essentially orthogonal to one another and to bedding. These are discussed in section 4.2.1. Joint spacings had been mapped in the past at another area close to the study bench, where the same joint orientations were identified. In this study, it was found that the spacing of the S_1 joints in sandstone were from 8 to 12 inches, while in siltstones and mudstones, distances of 4 to 8 inches were common. For the S_2 joints, sandstone had fracture spacings of 1 to 2 feet, and 8 to 12 inches in siltstones and mudstones (Golder Associates, 1977).

Hagan and Reid (1983) indicated that the effect of fractures on drilling performance is dependent upon their mean spacing. They noted that drill parameters variations will usually not reflect the difference in bulk rock strength of two units which exhibit similar intact rock strengths but dissimilar mean spacings between discontinuities. Higher absolute penetration rates and lower torques would be observed in rocks of identical intact strength only when the mean discontinuity spacing decreases below the diameter of the blasthole. Therefore, using this observation, the mean fracture spacings given earlier and the diameter of the bit used during these thesis studies, drill parameters would only be affected by the discontinuities, when their mean spacing was less than 12.25 inches. However, due to the orthogonality of both the S_1 and S_2 surfaces and the blastholes (generally) with respect to bedding these structures would appear to have little or no effect on the monitored drill performance in the present investigation.

C - Influence of Confining Pressures on In-situ Intact Rock Strength: It also has to be recognized that the compressive and shear strength of rock are higher due to the influence of confining pressures imposed by the rock surrounding the borehole. Therefore, the magnitude of energy input, axially and from rotation, to break the rock under confinement is in excess of the unconfined strength of the material.

On this basis, comparisons between the unconfined rock compressive strengths and drill energies may not be realistic nor valid (Simon, 1959). For purposes of the present study, it can be stated that the applied energy from drilling required to achieve bit penetration is proportional to the in-situ rock strength. Assuming that influencing factors such as confining pressures, are constant over the length of blasthole monitored, the in-situ rock strength could be seen as being proportional to the unconfined strength. Therefore, it follows that the drill energy would also be a reflection of this latter rock property.

D - Relationship Between Laboratory Derived Strength Data and In-Situ Rock Strength: An important question can be asked; is the strength value obtained from compression tests representative of the in-situ intact rock strength for a particular horizon? Or would the sum of all energies contributing to breaking rock in drilling be a more appropriate index for "true" rock strength. It is clear for this study and others conducted in the past, that measured compressive strengths on supposedly "homogeneous" specimens can and usually do vary widely (see section 5.3). This is mainly due to a combination of errors in the test procedure and microdefects in the selected specimens. Therefore, how is it possible to correlate laboratory compressive strength values, obtained on core from scattered locations along a borehole, with the continuous parameter logs generated from drill monitoring? One solution is to attempt to sample the entire length of core ie. closely spaced and numerous test data. However, this is generally seen to be a difficult task due to limitations imposed by the quality of the recovered core and the preparation of suitable test samples in friable, laminated rocks as was the case in this investigation. With these concepts in mind, point to point correlation and calibration of rock compressive strength to drill parameter response may not be possible.

6.1.2. Present Approach:

On the basis of the above ideas, it would appear difficult to correlate the known rock compressive strength with all the energies associated with drilling. It would be reasonable to state that rock breakage by drilling is complex and involves many different interacting mechanisms which cannot be represented by any existing forms of testing. However, by appreciating this statement, it is possible to utilize monitored drilling responses towards identifying zones of different "ease of drilling" or drillability. These zones in turn reflect relative differences in properties between the various rock units. The absolute ranges of rock strengths obtained are therefore not important, rather it is the relative differences in these values between the different rock types encountered at the mine that are. Therefore, if the relative differences in determined rock strength and drilling performance are the same for two rock types, then the influence of the other factors which constitute bulk rock strength can be assumed to be constant. These would therefore be accounted for in any relationship determined between intact rock strength and the drilling parameters.

In preliminary drill monitoring studies conducted at the mine, it was shown that variations in downpressure, torque and penetration rate demonstrated reasonable correlation with the changing geology. These parameters showed particular sensitivity in discriminating between soft coals and mudstones and harder siltstones and sandstones. The primary property which distinguishes these units at the site from one another are clear compositional contrasts, manifested by different colors and weathering properties but also by very sharp and well defined strength qualities. Since the drilling parameters were particularly responsive to the rock types present, it was proposed that this sensitivity was primarily controlled by the rock strength of the units.

Therefore, on this basis, a calibration of the drill responses to the rock was seen to be necessary to confirm this hypothesis. Such an approach would require that a "controlled" zone of rock be isolated where the properties are reasonably consistent and precisely identified in nature and location. This was accomplished through a detailed correlation of the results from core and gamma logs. Once a suitable test unit was selected, further confirmation of its homogeneity was obtained from the thin section analysis (section 5.4). These detailed microgeological studies therefore, were aimed at determining the extent to which the compositional variations of the test specimens influenced the ranges of rock strengths obtained on them. Additionally, the accurate isolation of drilling parameter signals for this same rock zone was required, in order to accurately correlate these responses with the rock strengths.

Many different approaches have been developed in the past in an attempt to relate rock strength to drilling performance. Several of these models demonstrated reasonable success and sensitivity in profiling changing rock mass strength in the present study and were reviewed previously in section 2.3. The forms of the equations are not the same, justified by the fact that they were developed under sets of very different conditions and for a variety of applications. Regardless of these factors, the selected models were applied to the drill performance data recorded in the current investigation. The calculated indices were subsequently compared to the individual parameters themselves to determine which of these were dominant for a particular model and rock type. In addition, the results from the various models were compared to one another to examine further the dependency of these on any particular drill performance parameters, see section 6.4. Finally, a correlation of the indices to measured compressive strengths was made in section 6.5 to determine the extent of any relationship which existed between these properties.

6.2 Determination of the Relationships Between Drilling Parameters for a 60R Drill at the Fording River Mine:

6.2.1 Introduction:

In order to determine precisely the relationships which existed between the various drilling parameters for this study, a selected borehole set up specifically for this purpose, was monitored while drilling in a controlled manner. The borehole which was chosen, EM476 (see Figure 5.1), was in an area consisting mainly of massive sandstones and siltstones with several thin coal stringers and mudstone partings also present. The natuie of the geology was confirmed by drill responses in boreholes adjacent to the testhole and by drill, gamma and core logs for holes located elsewhere on the bench, see section 5.1.

Relationships developed for rotary drill parameters in the past, and discussed in an earlier section, were developed primarily from controlled laboratory tests using homogeneous blocks of rock. These previous studies, therefore, are specific to the conditions for which they were determined, ie. the validity of their results is dependent upon the bit type and diameter, rock type, applied weights, air versus water flushing etc. used to establish the relationships. As a result, it was not considered appropriate to apply them to the current study, where a unique and different set of conditions were present.

Obtaining suitable and meaningful data to correctly establish the relationships between drill parameters was not a straightforward task in the present study. It required that the drill be made to operate in as controlled a manner as possible, while attempting to limit the influence of any geological variability on its performance as much as possible.

In order to reduce or eliminate the effect of the geology on drilling performance for the testhole, it was necessary to first identify a suitable rock unit which exhibited homogeneous properties. The area in which the testhole was located, was well known for the abundance of thick, massive sandstone rock units.

Therefore, based on the interpretation of the geology from both drill and gamma logged boreholes preceding the actual testhole, an appropriately homogeneous and thick sandstone/siltstone unit was isolated as a suitable "test block" sample of rock.

The compositional variability of the selected unit was determined in more detail, based on data from the same sandstone/siltstone unit encountered in both core (CHEM 1, Figure 5.2) and drill and gamma logs in the vicinity of the cored hole. These holes were located approximately 244 feet to the northeast along the bench from the position of the testhole (Figure 5.1). Figure 6.1 shows the drill and gamma logs for borehole EM188, and the geologic log based on the interpretation of the former data combined with that from core logging of CHEM 1. The sandstone/siltstone zone clearly identified in this hole by the drilling responses, at depths of 13 to 32 feet, was considered to be the stratigraphic equivalent of the unit shown in EM475 from 10 to 24 feet, see Figure 6.2. The interpreted core log for CHEM 1 (Figure 5.2), however, indicated that the area below this sandstone/siltstone horizon consisted of several 1 to 2 foot thick mudstone units and thinner coal stringers. This was also confirmed from the drill monitored data from borehole EM475, next to testhole EM476 (Figure 6.3).

A gamma log down borehole EM476 would have confirmed the geology encountered in this hole, yet was not possible due to production requirements for the logging truck elsewhere at the minesite.

The original design of the test called for controlled drilling and monitoring in a series of boreholes (4 to 6) all of which would penetrate the same homogeneous rock unit. This would have provided a suitably large data set from which the drilling parameter relationships would be clearly defined. However, a major factor which made such a program unfeasible, were the delays to production which would result from such a test period, where estimates of 1 to 2 hours per borehole were proposed. At

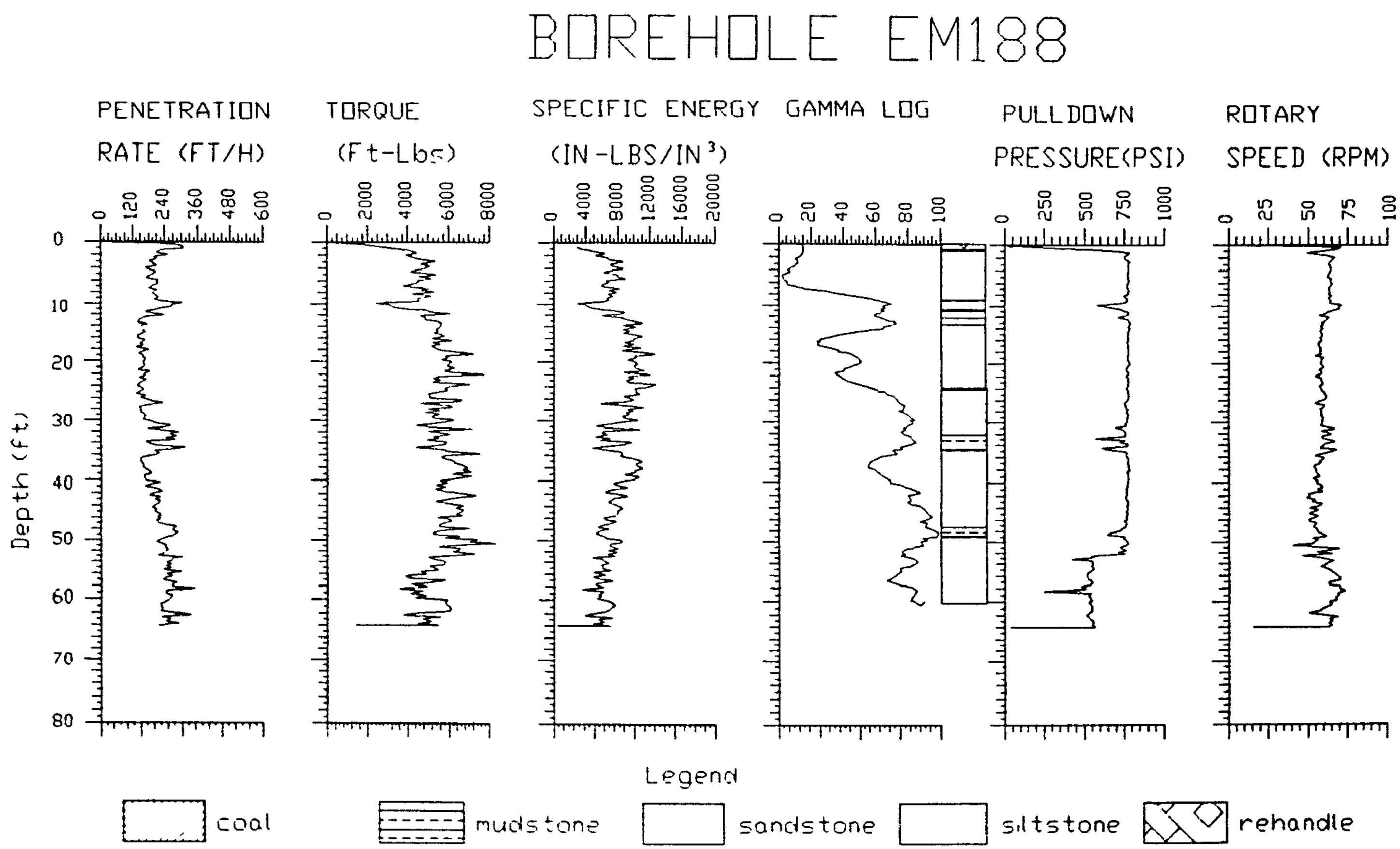

Figure 6.1 - Borehole Logs for EM188.

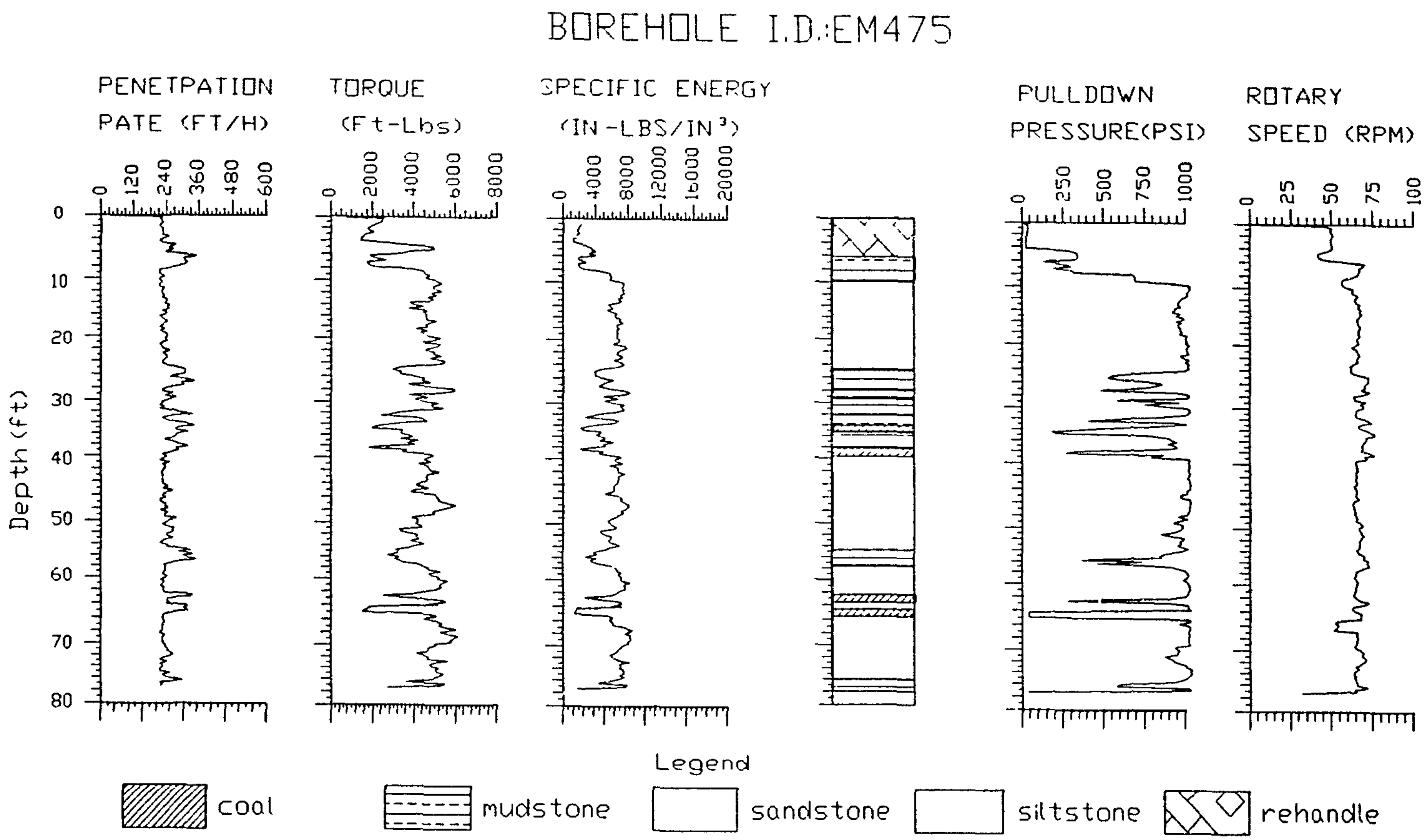

Figure 6.2 - Borehole EM475.

this point in time (July 4, 1988), the drill was far behind schedule, due to a major breakdown in mid-June. In addition, the mine was closing for a summer shutdown of 6 weeks on July 6 and had approximately 10000 more feet to drill off before this time. Therefore, very little flexibility was permitted in terms of delaying the drilling.

Within these limitations, permission was given to drill only a single controlled borehole ie. EM476. The results obtained from this limited test, therefore, are not considered to provide more than a preliminary examination of the relationships between the primary drilling parameters. They do, however, confirm similar trends identified during monitoring of routine production drilling, which are unique and specific to the geological environment and machine characteristics surrounding the monitoring program.

6.2.2. Controlled drilling:

It was interpreted that the sandstone/siltstone unit discussed earlier would be intersected in testhole EM476 at an estimated depth of 8 to 10 feet, for a thickness of 17 to 20 feet. Therefore, it was over this interval that the controlled drilling tests were to be conducted.

It was previously indicated in section 2.3 that W and N were the two drilling parameters dependent upon the driller, both being controlled from the operating panel of the drill. Therefore, the experiment involved making incremental adjustments to each of these two variables via the operator's panel, and monitoring the change in all the other drill performance parameters. The test drilling was aimed to be conducted within the sandstone/siltstone unit only, and so the geology was considered to be constant and thus controlled for this interval. Using this approach, variations in rock properties were assumed minimized as was their influence on the monitored changes in the drilling parameters.

The bit used during the test was relatively new (changed on July 3), also reducing any effects a worn bit might have on drilling performance.

The first part of the test involved setting a constant rotary speed, and increasing W in increments of 200 to 300 psi as indicated from the operator's gauge, up to a point at which either the maximum T or W was reached. The second part of the test involved maintaining constant levels of W and varying the value of N. A sampling interval of 4 inches was selected for both phases of the test. The acquired drill data is displayed in Figure 6.3 as logs, with the actual values shown in Table 6.1. The first part of the test was monitored from 11.16 feet to 25.92 feet for constant N, and constant W subsequently maintained from 26.26 feet to 34.37 feet. Although it was not clear at the time of monitoring, it became apparent from the drill logs of EM475, however, that below the hard test interval, softer rocks were present. This was apparently the case with the second half of the test, where the "constant" W varied without adjustment to the N, and therefore these results were not considered valid. Only the data from the first part of the test are referred to in the following discussion.

In this testhole, two different levels of constant N were monitored for variable W. Tests 1 to 4 were conducted for an initial operator panel gauge setting of 40 rpm, at gauge (downpressure) W of 175, 375, 600 and 800 psi. Tests 5 through 8 were run at an initial gauge setting of 60 rpm, for gauge W of 200, 400, 750 and 1000 psi. These operator panel settings for N and W and associated gauge readings for T (given as motor load in amperes) for all these tests are shown in Table 6.2.

There is a slight discrepancy between these analog gauge readings and the data acquired digitally using the drill monitoring hardware (Table 6.1). The drill gauges are damped thereby reducing their sensitivity and accuracy to changes in the performance parameters, and therefore, the actual (averaged)

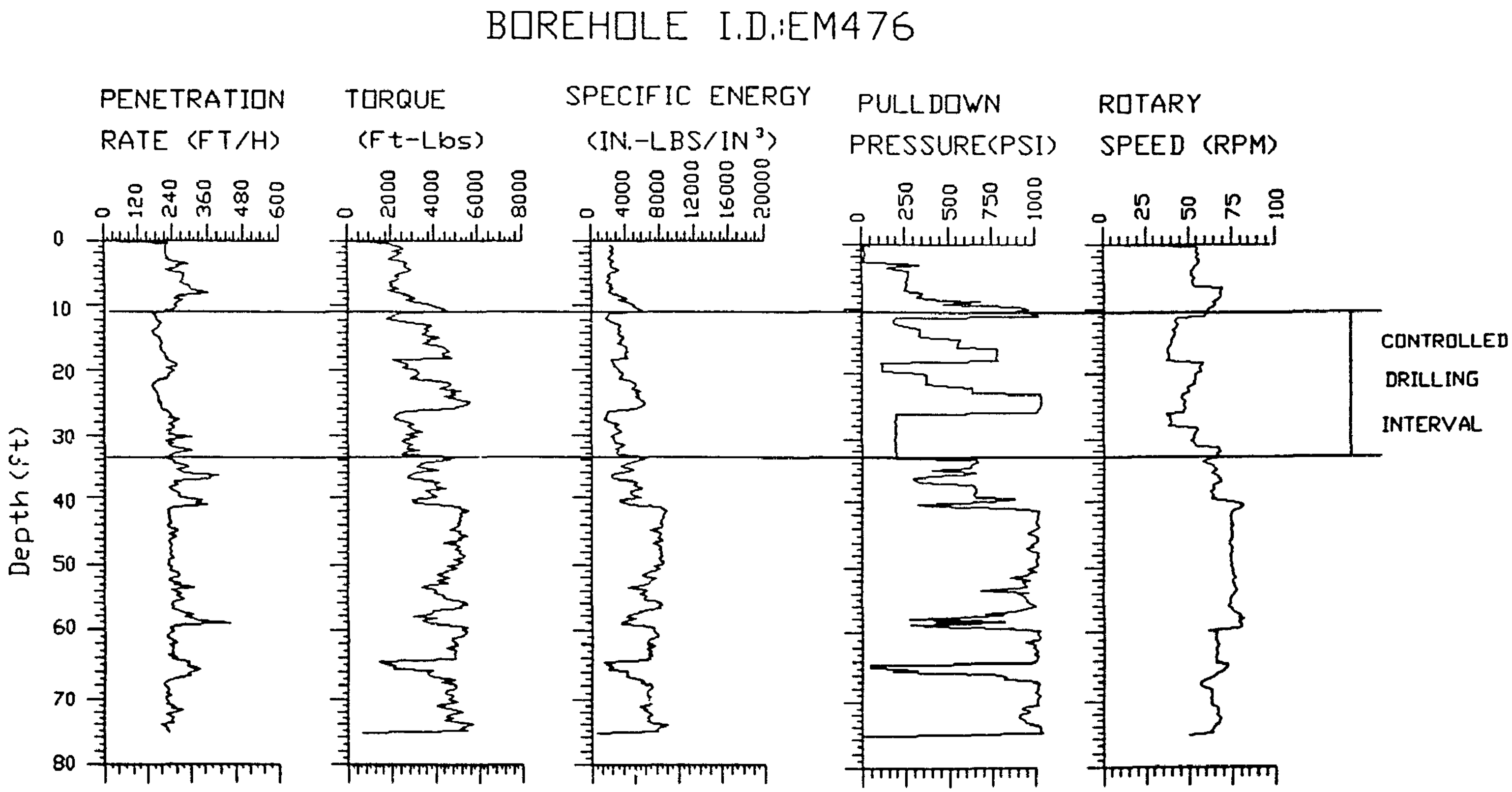

Figure 6.3 - Controlled Drilling Testhole EM 476.

Table 6.1 - Acquired Drill Data - Borehole EM476.

TEST#	DEPTH(ft):	R(ft/h):	I(psi):	W(psi):	N(rpm):	T(ft-lb):
1	11.16	134.29	23.24	198.00	43.44	2454.11
1	11.49	139.32	23.24	186.00	42.62	2118.73
1	11.82	152.21	23.24	185.00	42.66	1744.18
1	12.14	138.69	23.20	188.00	43.32	2160.47
1	12.48	142.01	23.20	259.00	42.84	2802.12
2	12.81	141.48	23.20	337.00	42.06	3718.17
2	13.13	138.95	23.24	337.00	40.90	3895.81
2	13.46	144.53	23.24	333.00	42.06	3502.00
2	13.78	139.37	23.24	329.00	41.32	3760.97
2	14.12	145.35	23.24	333.00	41.64	3454.91
3	14.44	193.36	23.24	567.00	39.86	3457.05
3	14.78	173.64	23.24	560.00	39.80	4227.56
3	15.09	186.17	23.24	556.00	40.12	3647.54
3	15.42	181.91	23.20	558.00	39.60	3825.18
3	15.76	189.81	23.20	549.00	38.88	3448.49
4	16.08	219.60	23.20	781.00	38.22	3979.28
4	16.42	206.68	23.24	779.00	38.24	4467.27
4	16.74	212.11	23.24	785.00	38.42	4591.41
4	17.06	202.68	23.24	783.00	38.36	4679.16
4	17.39	214.84	23.24	778.00	38.42	4418.04
4	17.72	208.47	23.24	780.00	38.32	4396.64
4	18.06	200.66	23.24	788.00	37.46	4792.59
5	18.38	115.45	23.20	112.00	58.40	2048.53
5	18.71	120.92	23.20	117.00	57.24	2410.88
5	19.04	125.39	23.24	114.00	56.28	2782.86
5	19.37	126.62	23.24	118.00	56.92	2748.62
5	19.69	109.10	23.24	115.00	57.36	2549.57
6	20.02	175.91	23.24	357.00	54.84	3138.15
6	20.34	178.30	23.24	369.00	54.06	3172.39
6	20.68	161.78	23.24	371.00	54.06	3270.85
6	21.01	164.96	23 24	369.00	54.00	3142.43
6	21.34	166.05	23.24	369.00	53.18	2868.47
6	21.66	147.11	23.24	367 00	54.36	3656.10
7	21.98	165.10	23.24	544.00	50.42	4544.32
7	22.32	177.67	23.24	638.00	49.70	4762.63
7	22.64	179.16	23.24	636.00	49.94	4662.04
7	22.98	189.58	23.24	637.00	50.72	4193.31
8	23.31	236.24	23.24	1034.00	46.62	5222.79
8	23.62	258.08	23.24	1040.00	46.18	4760.49
8	23.96	243.01	23.24	1040.00	47.00	5002.34
8	24.28	259.98	23.24	1043.00	48.32	4477.97
8	24.62	240.83	23.24	1041.00	47.02	5100.80
8	24.94	227.40	23.28	1032.00	47.26	5601.62
8	25.26	229.79	23.28	1032.00	47.76	5503.17
8	25.59	234.23	23.32	1019.00	47.62	5220.65
8	25.93	250.99	23.32	1011.00	47.36	4841.82

levels for each test interval are also shown in Table 6.2, as recorded by the drill monitoring system.

Table 6.2 - Drill Operator Panel Gauge Settings during Test Monitoring:

	Gauges:			Drill Monitor:		
Test #:	N:	W:	T:	N:	W:	T:
1	40	175	40	43.0	189.3	2119.4
2	34	375	60	41.8	321.3	3535.8
3	32	600	77	39.7	558.0	3721.2
4	30	800	107	38.2	782.0	4474.9
5	60	200	<30	57.2	115.2	2508.1
6	56	400	67	54.1	367.0	3208.1
7	51	750	115	50.2	613.8	4540.6
8	49	1000	130	47.2	1032.4	5081.3

6.2.3. Penetration Rate and Downpressure:

The effect of increasing W is clearly indicated by Figure 6.4 to result in a corresponding increase in R. The linear relationship determined between these parameters has the equation,

$$R\ (ft/h) = W\ (psi) \cdot (0.128) + 109.224 \quad \ldots\ 6.1$$

for a correlation coefficient of 0.97. The constant in this equation demonstrates that for downpressure equal to 0 psi (eg. when collaring the hole in rehandle), the weight of the drill steel, stabilizer, bit and head assembly is sufficient to promote penetration. This assumes, however, that the rotary speed is not equal to 0.

A multiplicative relationship between R and W was also determined as,

$$R = 24.53 \cdot W^{0.3169} \quad \ldots\ 6.2$$

for a correlation coefficient of 0.95.

Equation 6.2 has similar form to the results of work by past researchers, presented in section 2.3, where the general equation,

$$R = k \cdot W^{\beta} \qquad \ldots\ 2.2$$

was determined to describe the behaviour relating R and W, for values of β between 0.5 and 2.4; β was considered equal to 1.5 for hard ground, 0.6 for soft ground and 1.0 for medium hard rocks (Girard, 1985). Following the form of equation 2.2, for equation 6.2, the value of β is equal to 0.3169. The past observations were made under totally different conditions and modes of measurement from the present study and are therefore difficult to compare. This exponent was considered to be very dependent upon the strength of the material being drilled and the ranges of rotary speed and downpressure used in its determination (Brooks <u>et.al.</u>, 1963).

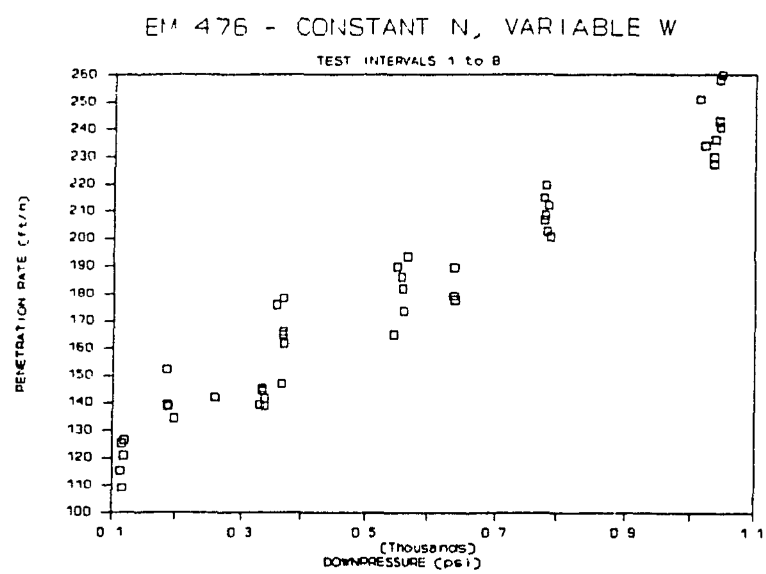

Figure 6.4 - Penetration Rate versus Downpressure.

6.2.4. Penetration Rate and Rotary Speed:

Figure 6.5 illustrates the data from all 8 test intervals of borehole EM476 for R versus N. The two lines in the figure represent test groups 1 to 4 (lower line) and 5 to 8 (upper line), and are the result of two different initial settings of rotary speed of 40 and 60 rpm respectively, used during the test. It is apparent from Figure 6.5 that although the rotary speed is "set" at some value at the beginning of the test, with increasing downpressure from interval to interval, it automatically decreases. These changes are accompanied by an increase in R.

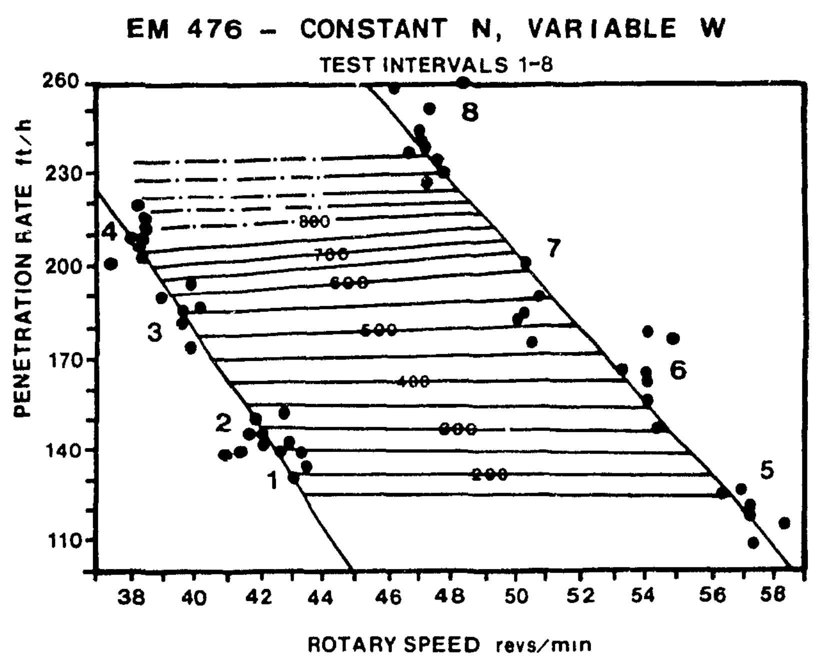

Figure 6.5 - Penetration Rate versus Rotary Speed.

The relationship between W and N is shown in Figure 6.6. Lines of equal W can be drawn to link the two lines in this plot by interpolation between data clusters of equal W. It is obvious from the vertical (constant W) lines, that any increases in N, has absolutely no effect on the values of W. This clearly indicates the independence of W with respect to N. The negative slopes of the two main lines of test interval data do, however, demonstrate the dependency of N on W, ie. decreasing speed with increasing applied load.

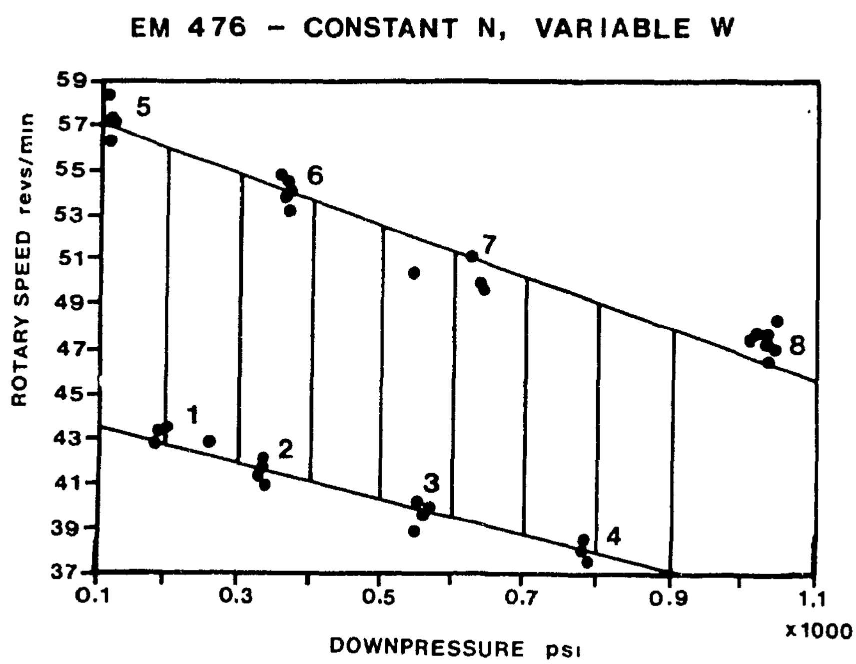

Figure 6.6 - Rotary Speed versus Downpressure.

The two R vs. N lines in Figure 6.5 are based upon groups of data acquired for both constant levels of W and N. Therefore, points on these lines (using interpolation between the medians of each test interval), having equal values of downpressure can be joined, thus developing the lines of "equal downpressure" shown in this diagram. These indicate that as rotary speed is increased for constant W, there actually is little or no effect on R. They also demonstrate that with increasing W, R increases, while N decreases. Therefore, it is apparent that R and N (once set by the operator) are both dependent upon the level of W. As a result, a multiple regression analysis between these parameters gives an equation similar to 6.1 except for the term for N as,

$$R = (W \cdot 0.128) + (N \cdot 0.027) + 107.887 \quad \ldots 6.3$$

with a correlation coefficient of 0.97. Comparison of these equations demonstrates that R will increase considerably for increasing W. However, changes in N contributes little to R. Also this contribution diminishes with increasing W.

Equation 6.3 is also only valid for when N is not equal to 0. Penetration for W = 0 is possible, but requires minimal bit rotation, which for this testhole was always > 30 rpm.

6.2.5. Penetration Rate and Torque:

The relationship between R and T, shown in Figure 6.7, was determined to be linear with an equation equal to,

$$R\ (ft/h) = T\ (ft\text{-}lbs) \cdot (0.034) + 52.61 \quad \ldots 6.4$$

and a correlation coefficient of 0.82.

Using the median values of the data from each test interval, a correlation coefficient of 0.88 is obtained for regression analysis, giving the equation,

$$R\ (ft/h) = T\ (ft\text{-}lbs) \cdot (0.034) + 48.71 \quad \ldots 6.5$$

which is nearly identical to equation 6.4. This relationship is similar to that determined for these parameters by other researchers in the past, whereby an increase in applied T resulted in a corresponding increase in R (section 2.3). This trend is shown by the regression line drawn through the points in Figure 6.7.

Equations 6.4 and 6.5 are valid only for $T > 0$ ie. a situation in which drilling is actually occurring. In addition, T is always greater than 0 when there is bit rotation, even for $W = 0$. In such cases the weight of the drill column with rotation will develop the necessary torque for minimal penetration rates to be achieved as shown by the constants in eqns. 6.4 and 6.5.

The regression equations above, therefore, are applicable only for the conditions under which they were established ie. $W > 100$ psi and $N > 30$ rpm.

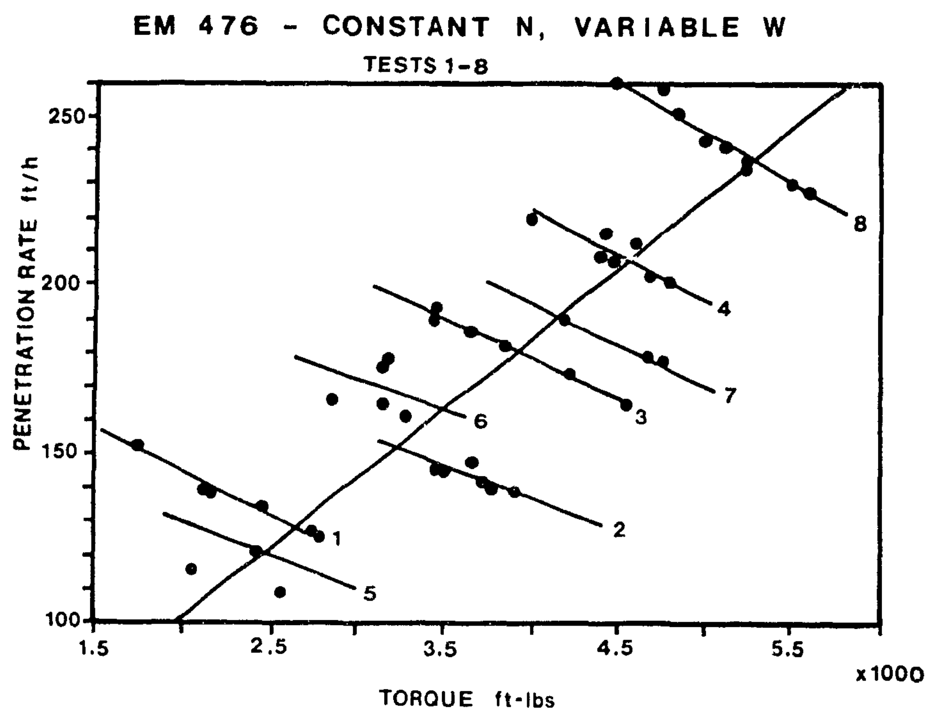

Figure 6.7 - Penetration Rate versus Torque.

6.2.6. Downpressure and Torque:

Figure 6.8 illustrates the linear relationship between downpressure and torque, with the regression equation, W (psi) = T (ft-lb)·(0.1544) ...6.6

and a correlation coefficient of 0.81.

As shown in this diagram, the general trend is increasing torque with increasing downpressure. However, it is also apparent that for constant downpressure (and rotary speed), represented by the horizontal lines in Figure 6.8, torque still exhibits some variation. Calculated COV's (coefficient of variation) for each test interval range from 15.7 percent at low downpressure, to 6.6 percent at higher levels. The higher COV may reflect the effect of insufficient applied downpressure on the bit resulting in it bouncing against the rock and thus producing the scatter in the torque data. The dispersion in the torque values may also be a result of inhomogeneities in the rock, which was

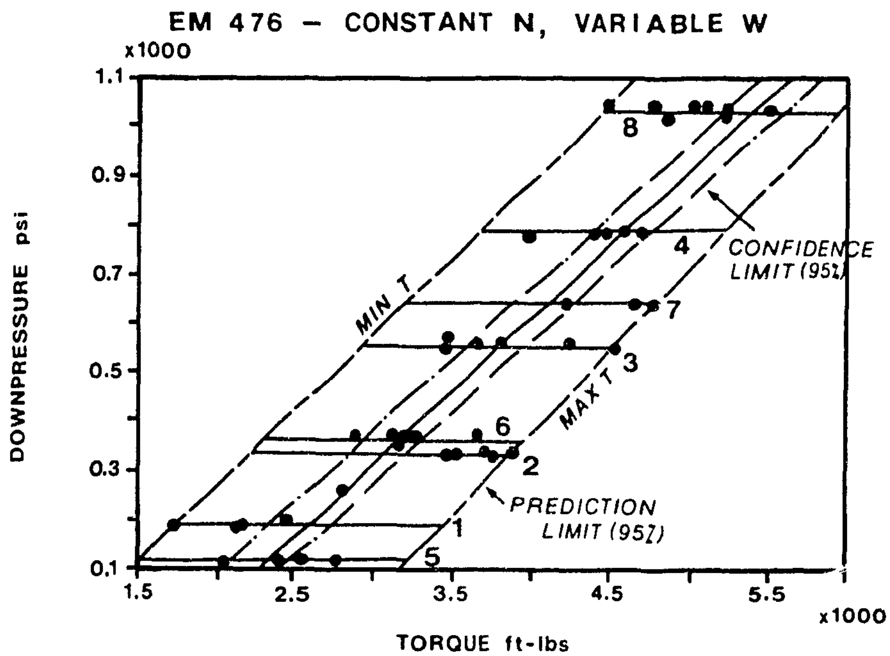

Figure 6.8 - Downpressure versus Torque.

previously assumed to be homogeneous. Torque is very sensitive to any changes in rock properties (see sections 6.3 and 6.4), and the presence of thin zones of variable composition, strength or structure could affect this parameter, generating the degree of variation observed.

Figure 6.8 shows the maximum and minimum torque boundaries, drawn through the lows and the highs in the data and parallel to the best fit line, which encompass the recorded spread in this data for each level of constant downpressure. These lines were also determined to be the prediction limits (95%) calculated from the regression analysis for downpressure and torque, based upon equation 6.6.

The zone delineated by these boundaries, therefore, should be the expected dispersion of monitored torque within the "homogeneous" sandstones to be encountered at the mine when drilling at constant downpressure and rotary speed. A greater spread in monitored torque data would be predicted as the rock properties become more variable.

The relationships between R, W and T as demonstrated from routine production blasthole monitoring data indicated trends very different from these established for drilling under controlled conditions. It was clearly seen that when drilling in the harder rocks, R was low for both high T and W. In softer rocks, for example coal, R increased for substantial decreases in both T and W.

The decreases in W observed when drilling in soft rocks, is without operator intervention. The high level of W normally set for routine drilling, will decrease automatically upon entering the coal seams. This is speculated to be the result of the low compressive strengths of these rocks which are unable to support the level of applied bit load. Since W in this case decreases, so does T, due also to the lower frictional properties of these units. Therefore the increases in R are due to the rate of excavation exceeding the rate of loading in the soft rocks at low levels of T and W.

Thus it is apparent that the rock properties effect a major influence on the behaviour of the drilling parameters, primarily

T and W, with associated changes to R resulting.

Evidence for this phenomenon is indicated by a closer examination of the R versus T data shown in Figure 6.7. An obvious spread in the T and R data for constant W is apparent. Theoretically, these data points should be clustered around the regression line shown due to assumed conditions of rock homogeneity and constant levels of N and W.

Isolating the data for test interval #8, indicated that R actually <u>decreased</u> for increasing T, as shown in Figure 6.9. This is the same relationship observed in routine monitoring, that for drilling in hard rocks, T is high while R is low. Conversely as T decreases in soft rocks, R increases. The equation of the regression line in Figure 6.9 is,

$$R\ (ft/h) = T\ (ft\text{-}lb) \cdot (-0.0323) + 406.37 \quad \ldots 6.7$$

with a correlation coefficient equal to -0.97, for average values of W = 1032 psi and N = 47.2 rpm.

However, this test interval was clearly identified as consisting of hard sandstone/siltstones only. In addition, as shown by the data in Table 6.1, there was little or no variation in both W and N for this interval, certainly not enough to effect the changes observed in R and T in Figure 6.9. Therefore, only one other possibility remained; the rock unit must not have consistent properties over this particular interval. Table 6.1 also indicates that the increases in R and T occur with

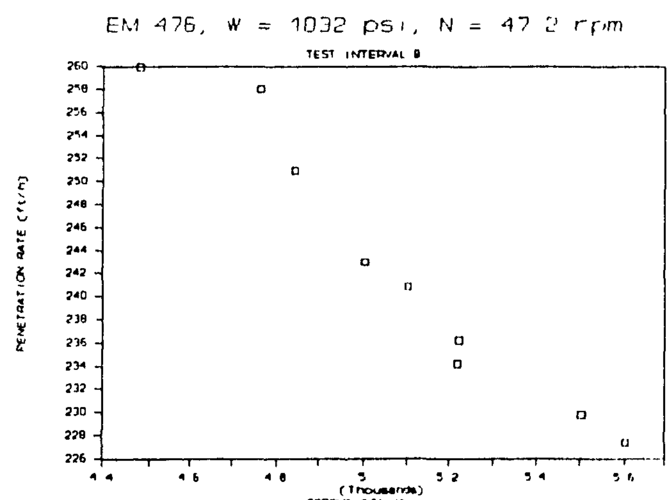

Figure 6.9 - Penetration Rate versus Torque; Test Interval 8.

increasing depth, from 23 feet to 26 feet.

In section 5.3 it was demonstrated that changes in the percentage and size of quartz grains in the sandstone/siltstones of the test area resulted in an overall increase in their measured compressive strengths. It is possible therefore, that the composition of the rock has changed somewhat over this zone giving rise to an increase in the compressive strength. Further evidence of this hypothesis is provided from several sources. Firstly, it is known from previous detailed petrographic studies of the sandstone and siltstones in this region of the mine, that vertical grading of quartz grain size and percentages is the rule rather than the exception. Decreasing or increasing of these compositional factors with depth is therefore a possibility (Donald, 1984).

Secondly, it is proposed that in this test interval, a combination of increasing quartz grain size and percentage has resulted in the changes in R and T monitored for constant W and N. These variations would be the result of a localized increase in rock strength at depths from 23 feet to 26 feet.

Without having a gamma log in this same borehole, the presence of grading for this particular interval cannot be directly established. However, examination of the drill responses for the equivalent horizon in the adjacent borehole EM475, indicates that T is increasing and R is decreasing (less dramatically) over this length for constant set W and N. Figure 6.10 is a zoom of the drill parameters for this interval in EM475. The zone from 22 to 25 feet, the same horizon as test interval 8 in EM476, is zoomed in Figure 6.11 where median lines have been drawn through the log traces for R and T to indicate the general trends in the data. It is interesting to note that the log for N shows a considerable decrease in its data at this location, also possibly reflecting the compositional changes proposed.

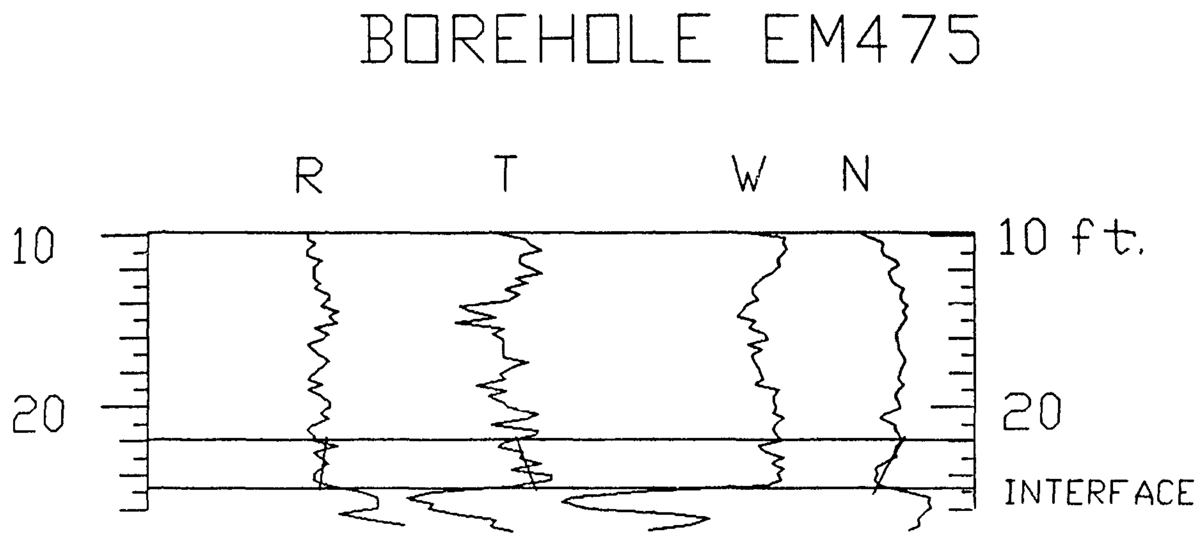

Figure 6.10 - Zoom of Borehole EM475.

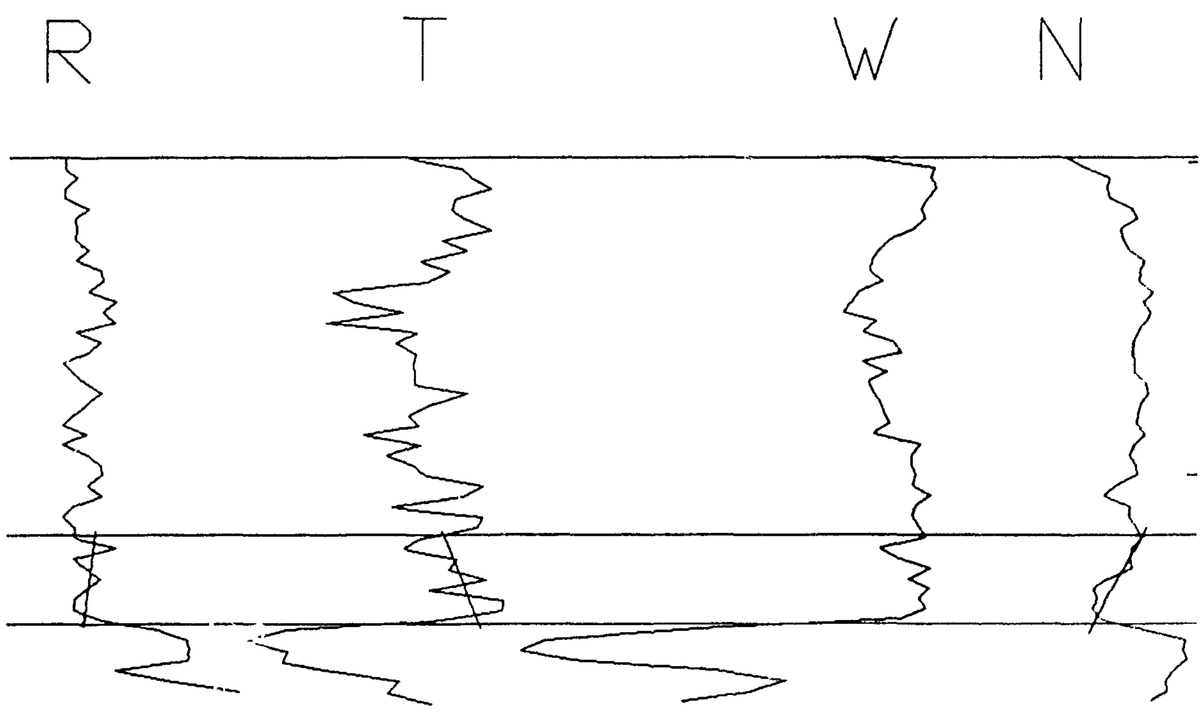

Figure 6.11 - Interval Between 22 and 25 feet; Borehole EM475.

Similar regression analyses through the data sets for other test intervals from borehole EM476 have calculated the correlation coefficients (r) shown in Table 6.3 below. However, here the trends in these constant downpressure test intervals are less the response to changing rock properties but more a result of the bit not being continuously in contact with the rock at low applied loads, resulting in a wider range of monitored values for T and R. This is apparent in this table, where the correlation coefficients are (generally) very high between these two parameters at higher W and poorer at lower W. The trends shown between R and T cannot be confirmed any further, with the data that was collected during the field period, yet they do indicate some very interesting concepts. The influence of rock properties to drilling performance will be addressed more fully in sections 6.3 to 6.5. The main conclusion that can be drawn is that at constant W, the properties of the rocks do influence T but not independently of R. Similar conclusions were made by Warren (1984) previously described in section 2.3.

Table 6.3 - Correlation Coefficients for Lines of Equal Downpressure.

Test Interval:	r:	W: (psi)
1	-0.57	189
2	-0.98	321
3	-0.98	558
4	-0.86	782
5	-0.53	115
6	-0.68	367
7	-0.53	614
8	-0.97	1032

6.2.7. Rotary Speed and Torque:

Also related to higher T from increasing W, shown in section 6.2.6, are decreases in N due to greater friction at the bit-rock interface. Figures 6.6 and 6.12 illustrate the relationships between N and W and N and T, where in each diagram two separate lines are seen, each related to the initial gauge settings of 40 and 60 rpm for the two test groups of data. The multiple regression of T as a function of W and N, gives the equation,

$$T = (W \cdot 2.95) + (N \cdot 2.36) + 2063.88 \quad \ldots 6.8$$

and a correlation coefficient equal to 0.912. As for eqns. 6.4 and 6.5, for W = 0, T values > 0 are possible only if N > 0. Equation 6.8 indicates only a slight increase in T will result for increasing N. However, substantial increases in T will develop for increased W.

As for some of the previous figures, Figure 6.12 shows lines of equal downpressure, which join points on the two rotary speed lines of similar downpressure value. These points are determined

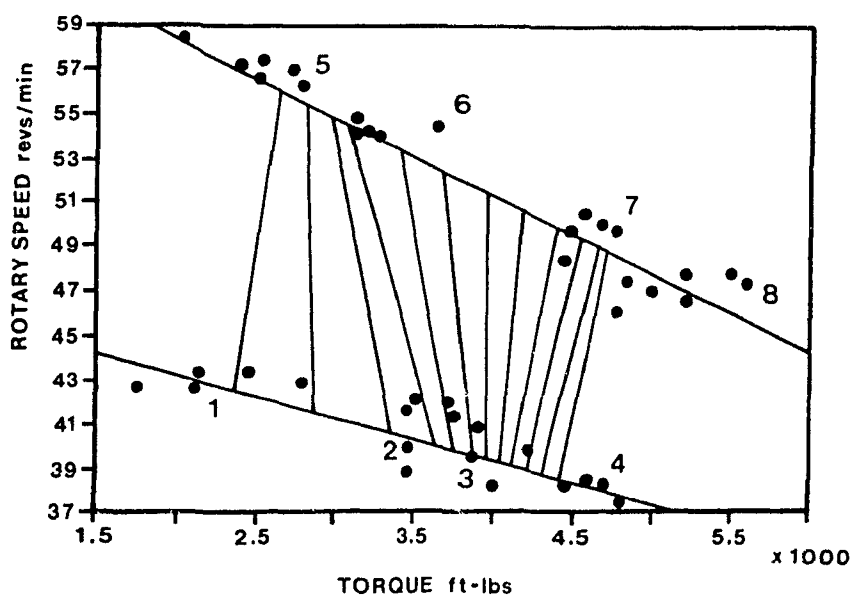

Figure 6.12 - Rotary Speed versus Torque.

by interpolating between the median values of the data for each test interval.

These constant value lines appear to have negative slopes at low downpressures and positive slopes for higher downpressures, with the midpoint between these conditions located at the line for 500 psi (vertical line at ≈ 4000 ft-lbs).

It is considered that at the low settings of downpressure, the bit is not firmly in contact with the rock, where with increases in rotary speed the bit begins to bounce, producing slightly lower torque values (seen by the negative slopes for downpressure less than 500 psi). This was the same mechanism proposed for the relationship of downpressure to torque, to account for the data scatter in the latter parameter.

For higher downpressures, where the bit is in continuous contact with the rock, an increase in the rotary speed results in slight increases in the torque, as indicated by the positive slopes of the lines in Figure 6.12.

Figures 6.9, 6.10 and 6.11 also illustrated the influence that increasing rock strength (or abrasivity giving an increase in friction) may increase T and thus decrease N for constant W.

6.2.8. Conclusions:

The main conclusion from this testhole is that W is clearly the critical parameter for the conditions of constant rock properties and the particular drill and bit type used. Increasing W produces corresponding increases in both R and T and decreases in N. The reasoning being that with increasing W, the depth of penetration of the bit inserts increase, as do the lateral forces needed to rotate the bit reflected by the increase in applied T. These mechanisms in turn produce an increase in the volume of material excavated per revolution due to enhanced rock breakage, with correspondingly higher values for R. However, a further result of increased W and thus increased friction at the bit-rock interface, is that N decreases (also indicated by the increase in T necessary to overcome this increased resistance to bit rotation).

The correlations above demonstrate that the relationships between the parameters, are solely the result of the applied load. In this regard, it is apparent that R, T and N are all dependent on the value of W, with this last parameter being independent of all the others. Therefore, W is clearly dependent upon the drill operator, as initially indicated in section 2.1.

However, it was also conclusively illustrated, that the relationships between W, T, N and R are dependent on the properties of the rock being drilled. Therefore, the conclusions made above are valid only if the rock is of a constant nature. These mechanisms are discussed in greater detail in sections 6.3 to 6.5 in reference to changing rock properties.

Reference is made to section 2.3 on past drilling research in order to compare the derived relationships in this study with those from other investigations.

6.3 Relationships Between Drill Performance Parameters and Variations in Rock Type:

6.3.1. Introduction:

It was indicated in section 2.3 that both shear and axial mechanisms are operating to break the range of rock types and strengths encountered in the present study. These concepts were also suggested from the results of section 6.2. Core testing results in section 5.3 clearly indicate that the absolute strength differences between hard siltstone/sandstones and softer mudstones/coals can be as high as 20,300 psi. In addition, the sedimentary rocks present at the study site are defined by sharp bedding contacts, with gradational variations at a range of scales but generally within a particular unit.

Therefore, these clear differences in both lithological and strength properties should logically be reflected by related pronounced contrasts in the recorded drilling performance parameters. The important item for successfully achieving such a correlation between rock properties and drill response is to know precisely where and what rock types are being intersected, as will be subsequently demonstrated.

The data from both gamma and core logs enabled the preliminary identification of the geological nature of the study area (section 5.3). Once this was clearly established, a more detailed correlation by depth between gamma and drill log responses permitted the classification of unique drill parameter patterns for coal, mudstone and sandstone/siltstone. These drill log patterns were determined not only to be highly characteristic of the various rock types, but also highly reproducible from borehole to borehole. A calibration of the drill responses in one borehole with the gamma log from the same or adjacent hole was performed at the outset. Following this, the monitored responses in the other boreholes were visually compared to this "key" and the particular rock types at depth were recognized by their correspondence to these characteristic drill parameter patterns. Utilizing this approach, the various rock types were accurately identified in 20 boreholes (out of 186), with confirmation provided by a comparison with gamma, drill and core logs throughout the study area. The drill parameter data was extracted for each of the different rock types from each monitored borehole, and compiled in a large database. The data was also compared to manual logs maintained by the author for every borehole throughout the monitoring period. These enabled the elimination of any responses in the drill logs which were the result of operator adjustments or related to the bit ie. jamming or caved hole.

Subsequently, the drill data was treated using the Statgraphics software package (1987).

The results of this statistical analysis confirmed what was already apparent from the unique patterns of the graphical drill log responses; that for each rock type, there was a characteristic range over which the individual drilling parameters varied.

The results of this analysis are discussed in the following section 6.3.2. In addition, an examination of how the observed responses in drill parameters are related to the particular rock breakage mechanisms for both soft and hard rocks will be attempted. A brief examination of pattern recognition techniques (star symbol plots) is presented in sections 6.3.3 and 6.3.4, to illustrate how the different rock units can be readily identified. Section 6.3.5 demonstrates the sensitivity of the monitored parameters to identify particular drilling situations.

6.3.2. Identification of Unique Drilling Parameter Data Ranges for Sandstone/Siltstone, Mudstone and Coal:

A - Hard Rocks: Sandstones and Siltstones

It is generally accepted that rock resistance to rotary drilling can be resolved into: (1) the reaction to the applied load, and (2) the frictional resistance that opposes the torque applied to the bit (Clark, 1987). The dominance of one of these factors over the other will depend on the bit type and design and the properties of the rocks being drilled.

One of the proposed mechanisms of rock breakage in these hard rocks is compressive failure by insert impaction. The impaction of inserts on these brittle rocks, results in the development of a zone of crushed material directly beneath the tooth (Figure 6.13).

The high compressive strength of the rocks prevent the inserts from penetrating very deeply, thus inhibiting the extensive development of fractures away from the initial impact point. Chips are eventually developed through the propagation and coalescing of fractures created through repeated impacts and other operating mechanisms (Maurer,1962).

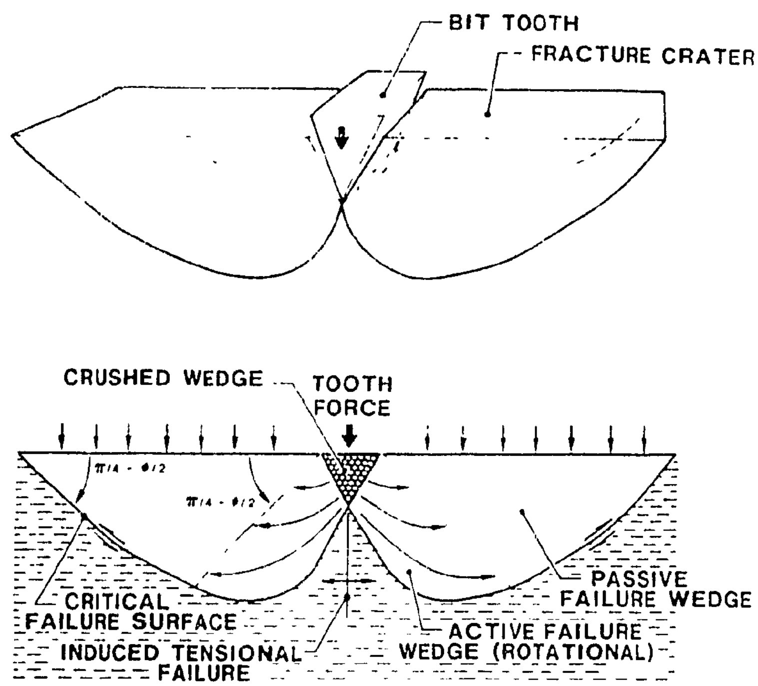

Figure 6.13 - Rock Fracture Model for Tricone Bits (MacPherson et.al., 1986)

In addition to the compressive stresses generated from impaction, tensile forces are propagated outwards from the point of tooth contact with the rock. These forces assist the development of shallow seated fractures originally created from impacting (Hartman, 1966).

The rotation of the bit also contributes horizontal forces through the applied torque, which act at the points of contact between the inserts and the rock to induce failure of the material along previously developed fracture planes. With propagation of these failure planes to the base of the borehole (free surface) a chip is formed (Hartman, 1966). In addition, the upward movement of the inserts on the bit cones with rotation, serves to lift and clear away the broken fragments or chips, and thus provide a clean surface for subsequent impacts. The fluctuations in monitored torque may also be reflective of chip formation ie. as the material fails, torque will momentarily decrease. Also regrinding of previously broken material (due to inefficient cleaning) may also contribute to some of the observed variations in recorded torque (Warren, 1984).

From a statistical analysis of the drill performance parameters acquired continuously while drilling these rocks, it was determined that the unique responses of these were related in part to the mechanisms involved with the rock breakage process. Table 6.4 illustrates the sample statistics generated from a data set of recorded drill monitored performance parameters in the identified sandstone/siltstone units of 20 production blastholes. The data for the 4 parameters have reasonably low dispersion as indicated by their corresponding low variance, standard deviations, ranges and interquartile ranges[1]. Coefficients of variation[2] (COV), indicative of the degree of data scatter, are for these rocks, highest for torque (10.57%) and penetration rate (7.8%) and lowest for rotary speed (3.85%) and downpressure (3.32%). The interquartile ranges also

---

[1] the <u>Interquartile Range</u> measures the spread or dispersion in the data, the lower the value the lower the discrepancy between data points.

[2] - <u>Coefficient of Variation</u> is a measure of the relative variation within a particular data set, and since it is independent of the scale of measurement, it can be used to examine the variation between several sets of data; = standard deviation/median x 100.

demonstrate that the bulk of the monitored data for most of these parameters falls within a very narrow window. These trends are consistent with the drilling responses observed in hard rocks, where both downpressure and rotary speed remain essentially constant, and changing rock mass (bulk) properties are best reflected by variations in torque and penetration rate.

Table 6.4 - Summary statistics for sandstone/siltstone units:

Sandstone/Siltstone:

	R (ft/h)	N (rpm)	W (psi)	T (ft-lbs)
Sample Size:	560	560	560	560
Average:	219.72	63.52	1017.87	4867.49
Median:	222.59	63.12	1027.00	4839.68
Mode:	216.53	62.94	1042.00	4820.42
Variance:	302.47	5.91	1161.41	261885.00
Standard Dev:	17.39	2.43	34.08	511.75
Standard Err:	0.80	0.12	1.57	23.43
Minimum:	154.45	55.94	800.00	2866.33
Maximum:	276.48	69.58	1057.00	6506.97
Range:	122.03	13.64	257.00	3640.64
Lower Quartile:	215.34	62.08	1014.00	4490.81
Upper Quartile:	227.14	64.74	1038.00	5177.85
Range:	11.80	2.66	24.00	687.04
COV:	7.8%	3.85%	3.32%	10.57%

These selected sandstone/siltstone units do contain some very thin, soft mudstone and coal stringer partings, which may account for the data below the lower quartile value[3], as well as the width of the interquartile range. Torque data in excess of the upper quartile value[4] could relate to rare situations of jammed

[3] - Lower Quartile - 25 percent of the data has values lower than the reported value.

[4] - Upper Quartile - 25 percent of the data has value in excess of the reported value.

bits, caved holes or very hard sandstone bands. Note that the influence of bit wear in generating any excessively high recorded torques is not a factor in this case, as a new bit was installed at the beginning of the particular monitoring period. In addition, the bit was examined at the beginning of each day of monitoring to ensure that cone bearings and teeth were still in good condition. Refer to section 8.2 and 8.3 for a more complete discussion of this phenomenum.

In hard siltstones and sandstones, identified from both gamma and core logs, the downpressure or applied load, was generally stable, averaging 1017.9 psi, and indicating that the rate of bit loading was equivalent to the rate of material excavation. The rotary speed in these rocks was comparatively low and constant, on average equal to 64.6 revs/min, indicating an essentially homogeneous rock with high strength both in compression and shear. The applied torque was high, yet with a greater dispersion than for the other parameters (COV=10.6%), reflecting not only the overall high strength of the material, but also the high frictional forces associated with these very abrasive rocks (high quartz content - also affects the rotary speed). The torque is also high as a result of the high applied load on the bit required to achieve good coupling and thus maximum energy transfer between the bit and the rock. According to Warren (1984), it is largely the rolling resistance between the bit and the rock which opposes the lateral force (due to applied torque) required to rotate the bit. This force is related to the applied vertical load (downpressure), tooth geometry and depth of tooth penetration. For high applied loads, as is the case here, the lateral force necessary to roll the tricone bit is high, as reflected by the high torque. Since torque is a primary parameter affecting the rock breakage, any small-scale variation in the rock properties will be reflected by more dramatic changes in this parameter than by those for penetration rate and rotary speed. This is valid since penetration rate is in effect the result of the efficiency of the applied torque to break the rock. The sensitivity of torque to variable rock properties may also account for the higher dispersion (high COV and wide interquartile range) demonstrated in the recorded torque data. This relationship was apparent in Figure 6.8 of section 6.2.

If insufficient torque is available (accompanied by low downpressure), further rock breakage will not occur and the bit will bounce on the rock during rotation creating severe drill vibration. Therefore the applied lateral and vertical forces should be sufficient to overcome both the compressive and shear strengths of the material to achieve excavation of the rock and thus penetration. In hard rocks, the tooth-shaped inserts for the bits used do not penetrate very deep (due to the high strength of these rocks in compression, indicated by stable, high applied downpressures). The area of contact between insert and rock is thus small and therefore the lateral forces high, as shown by the high torque. Since the volume of excavated material per revolution is low, due to both the strength properties of the material and the design of the inserts, then penetration of the bit per revolution is also low. This is readily confirmed from monitored results by the substantially lower rates of penetration witnessed in sandstones/siltstones as opposed to mudstones and coals.

B - Soft Rocks: Coal and Mudstones:

In soft rocks, i.e. mudstones and coals, the mechanism of rock breakage is primarily a combination of gouging-shearing actions. Impact mechanisms may also be important in the higher strength mudstones, but overall would appear to be secondary. This aspect is apparent by the generally low to very low downpressures associated with drilling soft rocks. Table 6.5 indicates that the hydraulic downpressure in coal averages 548.42 psi with a COV of 30.9%. This variation can be attributed to the heterogeneous nature of these rocks, where numerous thin and hard partings of both mudstone and siltstone are commonly interbedded with the coal. Downpressures in mudstone are higher, averaging 826.12 psi, with a lower COV than for coal of 20.9%. The lower dispersion in recorded downpressures is due to the overall greater homogeneity of both composition and strength exhibited by the mudstones, as compared to the coals. However, the lower quartile region of the data results from the presence of soft coal partings within the more pure mudstone units, as well as transitional horizons of muddy coal. Following the same logic, the data above the upper quartile for downpressure, represents the influence of higher strength transitional zones of muddy siltstone units. The variable low downpressures recorded in both coal and mudstone are a result of excavation rates exceeding the loading rate due to little or no opposing force to the axial load (ie. rocks are weak in compression). It can be assumed under these conditions therefore, that the bit is not in continuous contact with the rock. A result of this and the fact that the frictional forces opposing rotation are lower in these softer materials, higher rotary speeds and lower torques as compared to harder rocks would be apparent. Table 6.5 shows that for coal, rotary speeds are high with an average of 68.41 revs/min and generally stable as indicated by the low COV of 6.17%. The recorded rotary speeds in mudstones, are lower and more widely dispersed, with an average of 64.64 revs/min and a COV of 10.76%. However, the interquartile range is lower in the mudstones than for coal (2.83 revs/min versus 6.32 revs/min), indicating that the frictional properties of coals are more variable.

In addition, due to the low strength of these rocks under compression, penetration of the tooth-shaped inserts is at a maximum (for even low downpressures). The bit, therefore, gouges its way through the rock using the inserts as scrapers to shear the material along natural planes of weakness (common in the coals and mudstones of the study area) and/or fractures induced

Table 6.5 - Summary statistics for coal and mudstone units.

Coal:

	R (ft/h)	N (rpm)	W (psi)	T (ft-lbs)
Sample Size:	497	497	497	497
Average:	288.99	68.41	548.42	2893.77
Median:	287.40	69.80	536.00	2741.13
Mode:	277.28	71.04	408.00	2558.13
Variance:	1597.33	18.61	27491.30	435689.00
Standard Dev:	39.97	4.31	165.81	660.07
Standard Err:	1.86	0.21	7.75	30.84
Minimum:	250.57	58.00	5.00	518.01
Maximum:	430.25	76.10	931.00	5616.61
Range:	273.50	18.10	926.00	5098.60
Lower Quartile:	273.50	65.44	419.00	2457.54
Upper Quartile:	306.15	71.76	672.00	3232.32
Range:	32.66	6.32	253.00	774.78
COV:	13.9%	6.2%	30.9%	24.1%

Mudstone:

	R (ft/h)	N (rpm)	W (psi)	T (ft-lbs)
Sample Size:	202	202	202	202
Average:	250.28	64.64	826.12	4150.77
Median:	244.68	64.78	880.43	4151.58
Mode:	261.89	65.24	943.94	3756.69
Variance:	566.05	6.97	34165.15	417034.00
Standard Dev:	23.79	2.64	184.84	645.78
Standard Err:	1.81	0.20	47.56	49.24
Minimum:	180.78	56.94	353.00	2538.87
Maximum:	326.35	71.62	1029.44	5931.23
Range:	145.57	14.68	673.44	3392.36
Lower Quartile:	232.91	63.39	783.50	3723.52
Upper Quartile:	264.67	66.22	926.75	4523.99
Range:	31.76	2.83	143.25	800.47
COV:	9.7%	10.8%	20.9%	15.6%

by axial loading. The lateral force applied by the inserts promoting shear rock failure during this scraping action, is due to the applied torque. Similar mechanisms operate for drilling in the mudstones; for the lower strength end of the mudstones, mechanisms similar to those in coal would operate, but to a lesser degree than for coal as observed by the different ranges of the recorded parameters in each rock type. For higher strength mudstones (transitional zones to siltstone), these drilling mechanisms would more closely resemble those working to break rock in the sandstone/siltstone units.

The variation of properties in both rock types is also manifested by their ranges of variation for recorded torque. The average torque in the softer coals is 2893.77 ft-lbs with a COV of 24.1%, and an interquartile range of 774.78 ft-lbs. For mudstones, torque averages 4150.77 ft-lbs, with a COV of 15.56% and an interquartile range of 800.47 ft-lbs. This data again points out the greater material property variability of coal compared to mudstone. The data greater than the torque upper quartile value in coal, represents the transition zones and hard partings of coaly mudstones and mudstones. This same region in the mudstones reflects the presence of silty mudstones to siltstones either as inter-bedded partings or gradational zones.

Since penetration of the inserts in soft rocks is at a maximum, so therefore is the volume of material excavated per revolution of the bit. Also, since the contact area of insert to rock is large, and the shear strengths low, the lateral force required to induce failure and produce chips is low, as indicated by the low applied torque recorded while monitoring. These factors contribute to the high to very high rates of penetration thus achieved when drilling in these rocks. Average penetration rates for coal are equal to 288.99 ft/h with a COV of 13.9%. In mudstone, average rates of 250.28 ft/h are achieved with a COV of 9.72%. This latter value again reflects the greater homogeneity of the mudstone units over coal.

6.3.3. Box and Whisker Plots:

Box and Whisker plots for the statistical data in Tables 6.4 and 6.5, shown in Figures 6.14 to 6.17, reiterate in a graphical manner the trends discussed above. These diagrams clearly indicate the unique ranges of drilling performance parameters established for sandstones and siltstones, mudstones and coals.

Box and Whisker plots enable the quick identification of certain key items, such as the range of the data and the median. The range of the data is represented by the total height of the plotted values, where the median is the middle line in the box. The lower end of the box is the lower quartile value and the upper end represents the upper quartile. The box defined by these lines is therefore equal to the interquartile range, which includes the middle 50% of the data values. The endpoints of the "whiskers" or lines extending out from the box are the minimum and maximum values for the data set. Extreme values are plotted as separate points, as the whiskers extend only to those points that are within 1.5 times the interquartile range. Skewness of the data can also be visualized by noting the position of the central line (median) of the box with respect to the end lines (Statgraphics Manual, 1987).

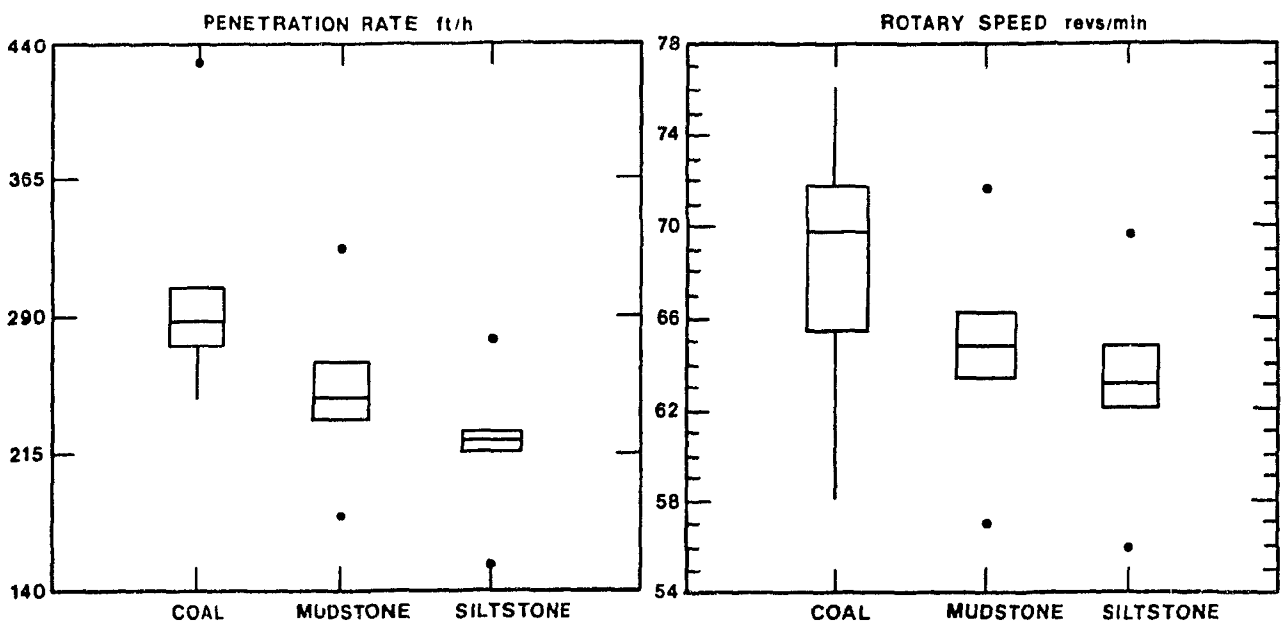

Figure 6.14 and 6.15 - Box and Whisker Plots for the Summary Statistics in Tables 6.4 and 6.5.

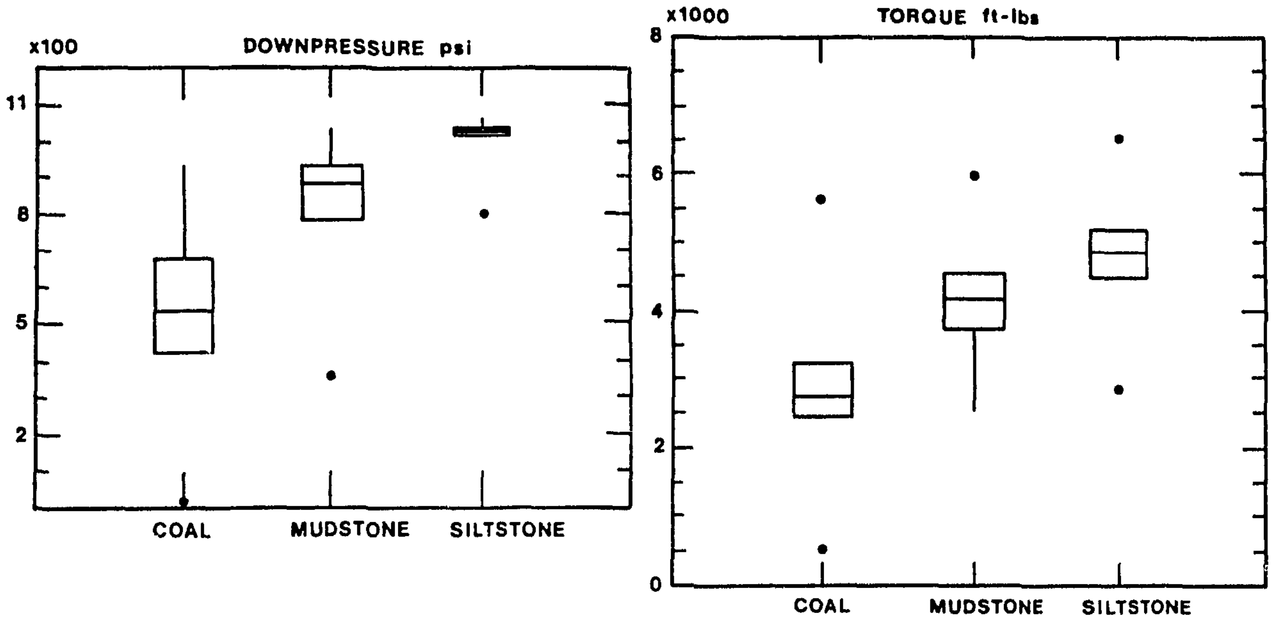

Figure 6.16 and 6.17 - Box and Whisker Plots for the Summary Statistics of Tables 6.4 and 6.5.

6.3.4. Star Symbol Plots:

An alternate method of displaying multivariate data enabling visual comparisons to be made, are through the use of star symbol plots. These stars consist of a series of rays drawn from a center point, with each ray representing one variable starting at the three o'clock position and moving in a counter-clockwise direction. The smallest value in each variable is plotted with the shortest ray, while the largest value receives the longest ray. Therefore, in this manner, a star symbol can represent one observation in the data set, ie. the five recorded drill parameters for each sampling interval can be shown as one star symbol. Figure 6.18 indicates the order in which the parameters are plotted for this study.

This technique is illustrated using the summarized statistics for the sandstone and siltstone, mudstone and coal rock units in Tables 6.4 and 6.5. Figure 6.19, therefore represents the "expected"or standard shapes of the star symbols for the different rock types, based on the determined ranges of drill performance parameters for each.

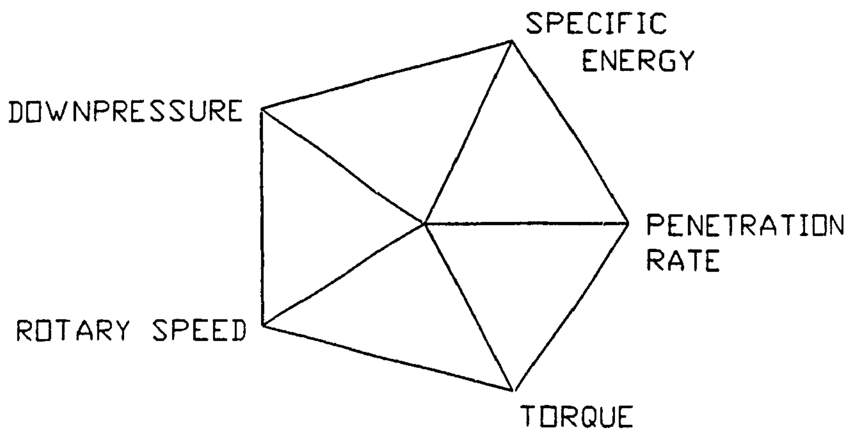

Figure 6.18 - Key to Star Symbols.

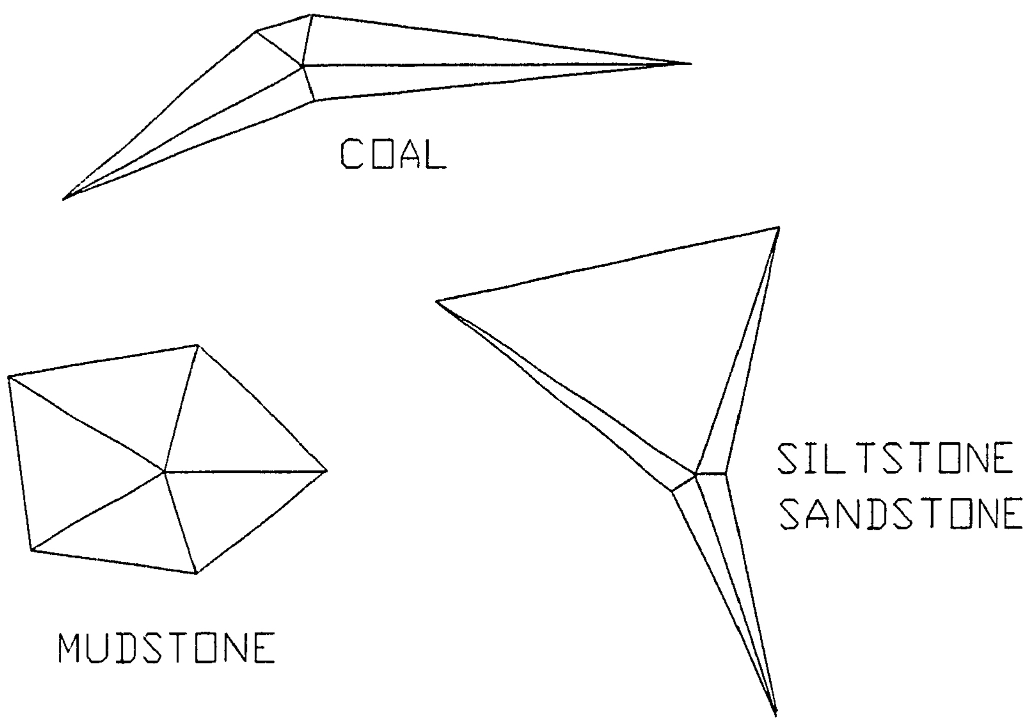

Figure 6.19 - Standard Star Symbol Shapes for Different Rock Types.

The application of this method to data from monitored boreholes, illustrates the effectiveness of the star symbols to enable an immediate recognition of the nature of the rock being drilled. In addition, since the drill parameters were previously determined to have reasonably well established ranges for each rock type, it would be expected therefore, that the shapes of the star symbols would reflect the consistency in this data. This would permit comparisons of the changing rock types within boreholes to be made, and subsequently, correlations between adjacent boreholes, based on recognized similar shaped star symbols. Such a technique takes advantage of the inter-relationships between drill parameters, in that this method relies upon the relative changes amongst these variables for the shapes of the symbols, rather than their absolute values.

Figures 6.20 to 6.23 show the results from the application of this method to the data of boreholes EX2078 and EX2052 (see Figure 7.1). The depth locations of the various rock units were initially determined from a correlation of the drill and gamma log responses, with the latter being obtained in the same borehole. The drill data within these intervals were subsequently averaged and their star plots determined. Figures 6.20 and 6.21 display the entire range of drill, gamma and geologic logs for boreholes EX2078 and EX2052 respectively. The calculated star symbols are displayed beside the geologic log in each of these diagrams. A boxed-in area on the downpressure log in Figure 6.20, indicates where the fluctuations in this parameter were not due to the rock but were adjustments made by the operator to reduce the observed high level of torque.

Figures 6.22 and 6.23 illustrate close-ups of the star symbols next to the geologic and gamma logs for the complete length of the boreholes. The coal and waste rock units intersected in the two boreholes are in the same stratigraphic sequence of rocks. Therefore, the drill performance responses should be very similar, as should the shapes of the star symbols. The apparent differences in the star plots between the two boreholes in these figures are minor. These boreholes are separated horizontally by a distance of 30.5 feet, and therefore, some lateral and vertical

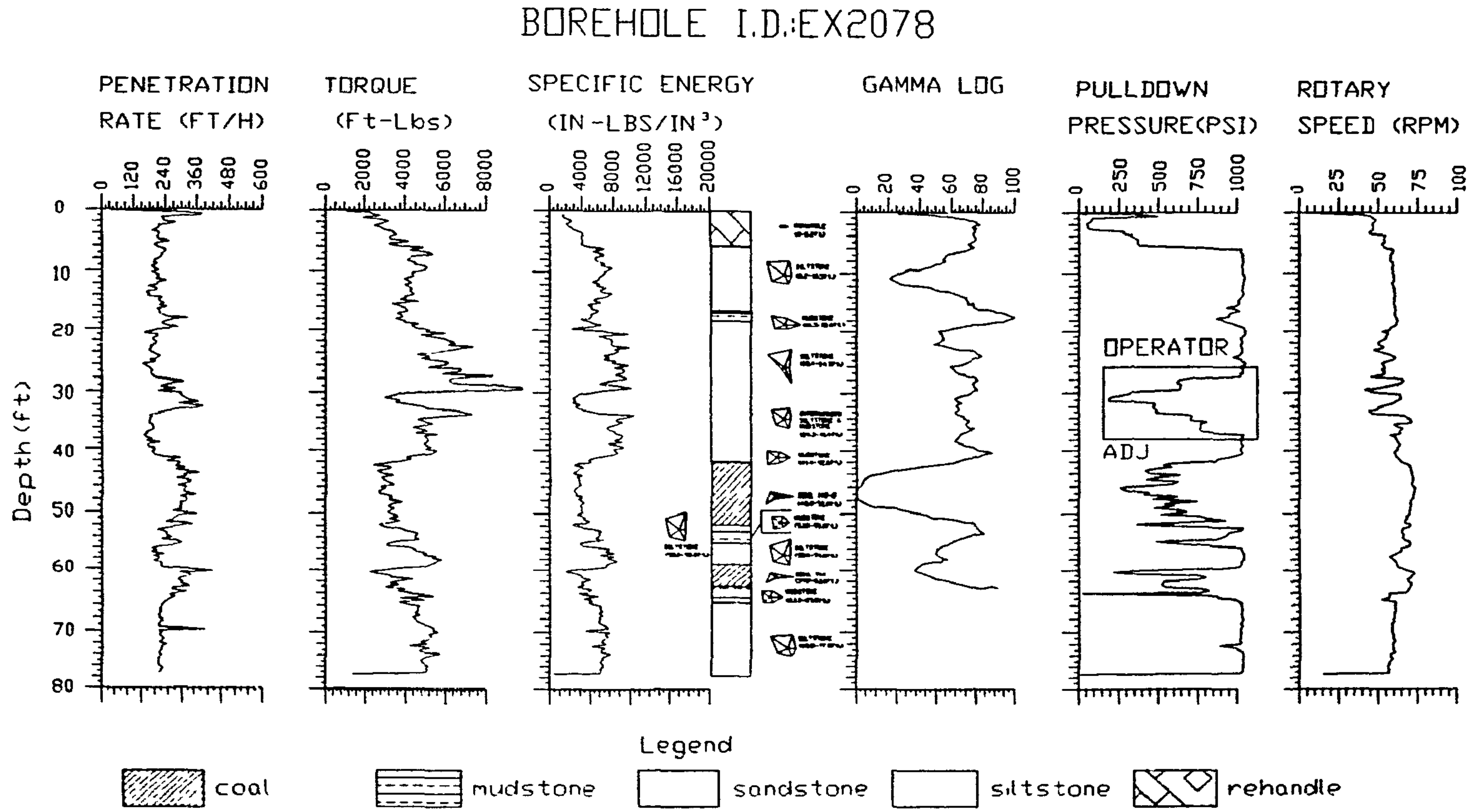

Figure 6.20 - Borehole EX2078.

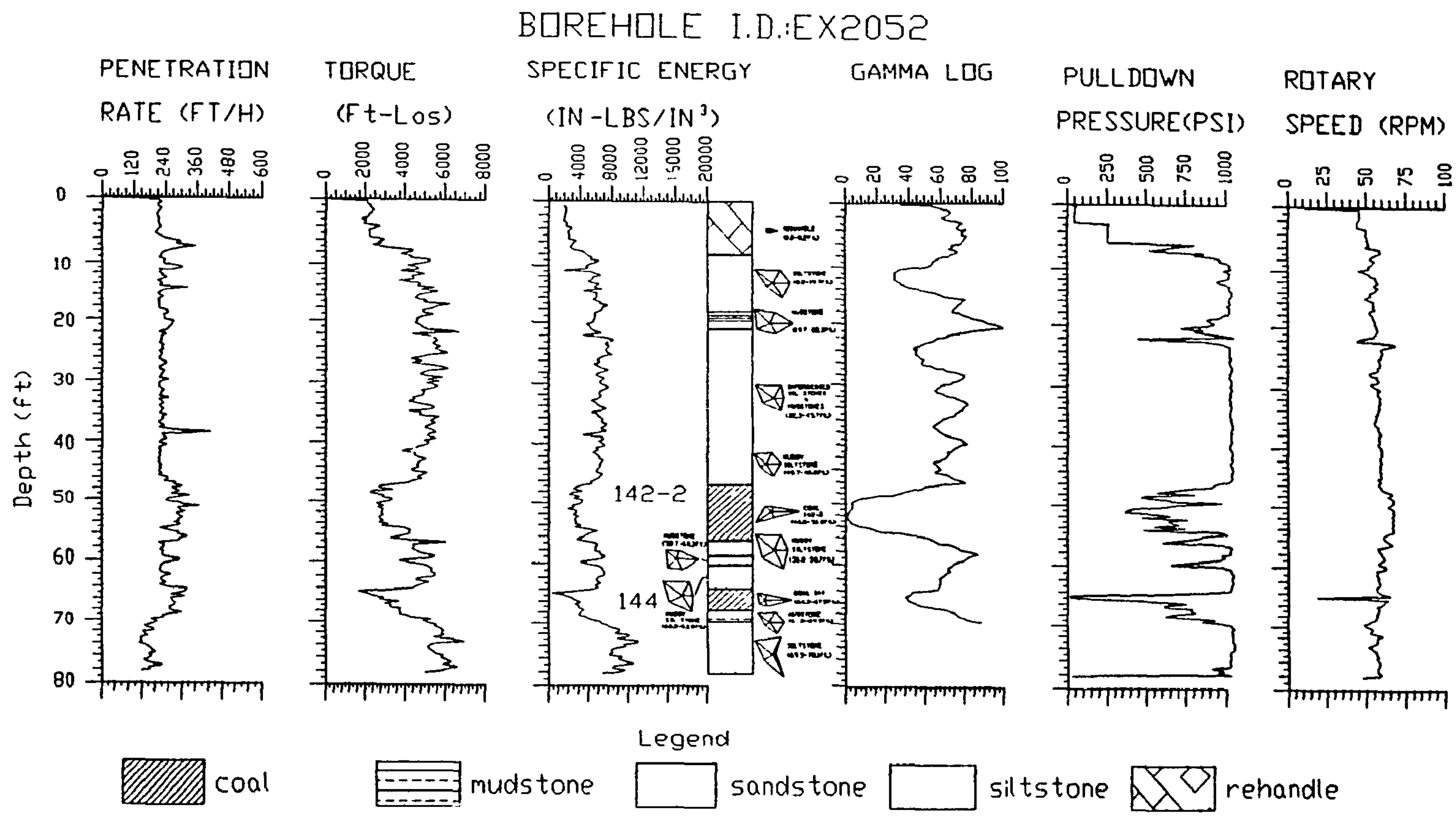

Figure 6.21 - Borehole EX2052.

gradations in the waste rock units from more homogeneous to muddier siltstones (or vice versa) are to be expected. The gamma logs indicate that the geology is essentially identical in each of the boreholes. However, the zone of interbedded siltstones and mudstones in borehole EX2073 may have a higher overall mud content, as witnessed by the high gamma response above coal seam 142-2. This soft mudstone unit subsequently resulted in higher penetration rates and rotary speeds at lower torque to be achieved, as indicated by the corresponding star symbol shape at this location in Figure 6.22. In borehole EX2052 (Figure 6.23), at the same location with respect to coal seam 142-2, the drill and gamma responses are more reflective of a muddy siltstone to siltstone horizon, indicated by a less distorted star symbol. Regardless of these anomalies, the correlation of the plotted star symbols between each of the boreholes is very good.

A comparison of these boreholes with the standard shapes shown in Figure 6.19, indicate the effectiveness of these plots to enable an immediate recognition of the rocks being drilled. As well, the reproducibility of the star symbol shapes again establishes the unique and consistent ranges of drill parameter variation which are associated with a specific rock type.

Several other examples of these star plots are provided in Appendix III.

6.3.5. Identification of Particular Drilling Situations:

A potential phenomenon associated with the rotation of the bit and steel against rock, is the development of torsional energy in the drill string. For example, when drilling in hard rock, as a result of the high frictional forces opposing the rotation of the bit and steel (seen by the recorded high torque and low rpm in sandstones and siltstones), torsional energy is developed and stored as potential energy in the drill system. As the bit passes from a hard to a softer rock unit e.g. sandstone to coal, the stored energy is proposed to be released at the bit as the

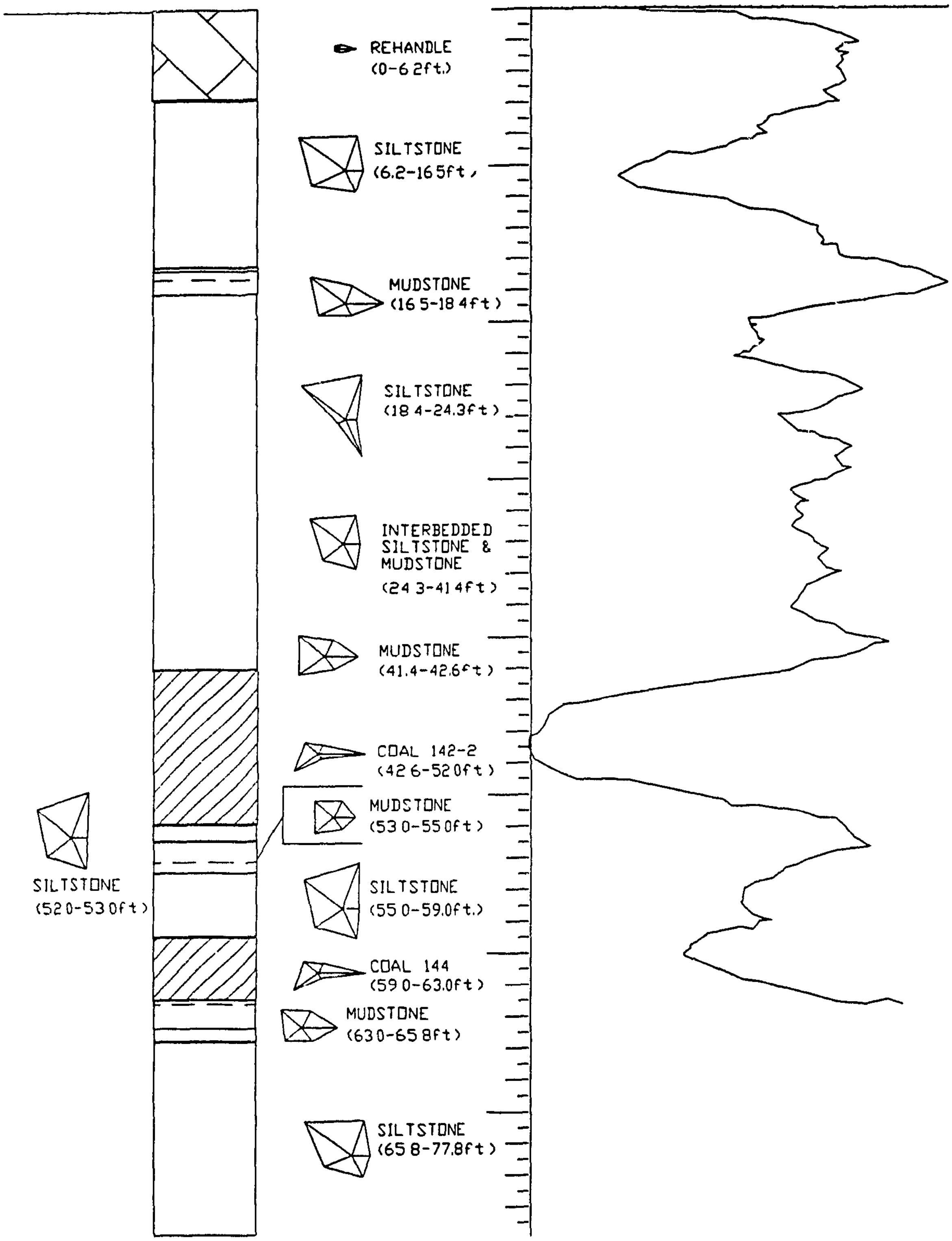

Figure 6.22 - Star Symbol Plots for Borehole EX2078.

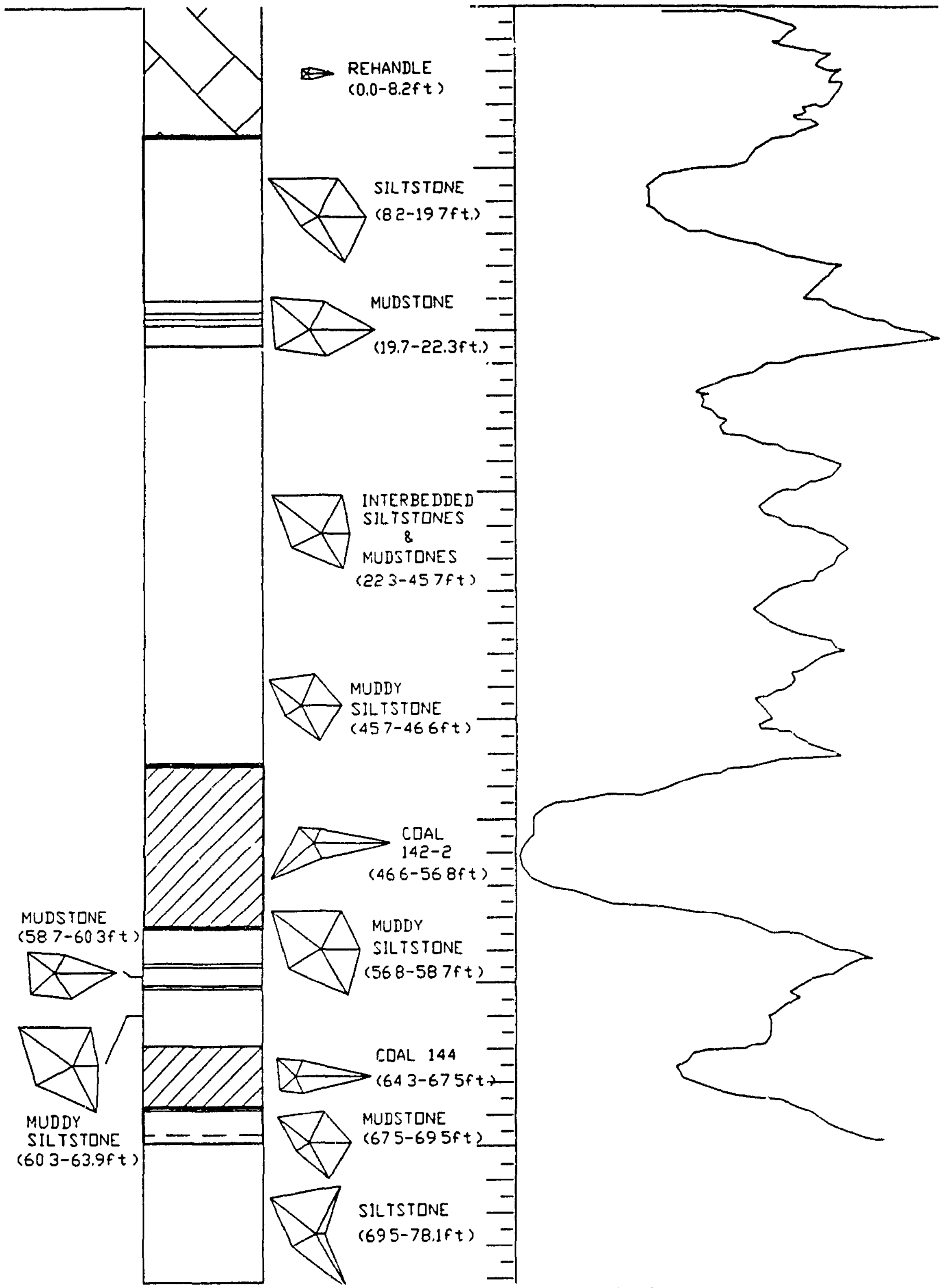

Figure 6.23 - Star Symbol Plots for Borehole EX2052.

frictional forces resisting rotation diminished. This energy, since it is a elastic torsional component, would be manifested by a sudden increase in both the rotary speed and penetration rate and decrease in the applied torque (Eronini et.al., 1981).

Surging of monitored drill rates, torque and rotary speed was identified in past studies where drilling parameters were acquired using an instrumented section of drill pipe directly behind the bit. Reasoning for these responses was considered to be the result of torsional deformation of the drill string. The increases or decreases in these parameters was observed to occur when the built-up energy would be released through unwinding (Miller and Rollins, 1968). However, Eronini et.al. (1981) concluded that the majority of torsional energy build-up was the result of friction developed between the drill steel and the borehole walls in very deep and deviated boreholes.

Maurer (1962) proposed that the sudden peaks in the parameters could also be the result of the accumulation of cuttings under the bit teeth, thus reducing the friction between the bit and the rock. This could be a possible mechanism when the bit suddenly exits the hard waste rock unit and suddenly is faced with much higher excavation rates. There would therefore be a slight lag in the cuttings removal as the system becomes momentarily overwhelmed, resulting in a sudden change in drilling performance.

The instantaneous changes in the drill parameters, by either (or a combination) of these mechanisms can be observed in the present thesis study when the bit enters a coal seam from a harder sandstone unit. Initial instantaneous increases (peaks) in penetration rate and rotary speed are observed, along with associated decreases in torque, mainly in boreholes which were drilled from collar to depth without interruption i.e. continuous applied load on the bit. Maximum parameter responses are seen when drilling through coal and sandstone units which are divided by sharp bedding contacts rather than a transitional boundary of coaly mudstone or muddy siltstone. Figure 6.24 illustrates the overall parameter responses for drilling in borehole EX1025, where a thick coal seam (142-2) is overlain by a zone of massive siltstones. In a zoom of this diagram, Figure 6.25, the marked interval (box) shows that as the bit intersects the interface between the different rock units at 46 feet, the penetration rate increases dramatically (peak), with a related increase in rotary speed and decrease in torque.

Eronini et.al. (1981) also noted that torsional vibrations can develop with rotation as the wobbling of the drill string above the bit increases. The resistance to rotation due to rubbing contact between the drill string and borehole will also increase in this situation. This phenomenon could result in very large power losses between the surface and the bit. In this regard, unless drill performance was monitored at the bit rather than at surface as for the present investigation, these torsional effects could effectively mask the response of the drill to changing rock properties. However, his concept was developed for drill strings of lengths in the thousands of feet rather than for blasthole lengths of tens of feet. In this thesis study, the influence of frictional forces between drill steel and borehole were seen to have only a negligible effect on the drill performance. Excessive torque and reduced rotary speed were apparent in situations where the borehole caved. Here, due to the layered nature of the rocks, blocks of ground would fall or shift into the borehole along bedding and/or joint surfaces, thus pinning the drill steel. The bailing air pressure, in combination with high torque and low rotation speed resulting from increased friction between steel and borehole walls, would rise. The increase in air pressure enabled the occurrence of caving to be readily identified and not mistaken, due to the similar drill parameter responses, for drilling in hard rock.

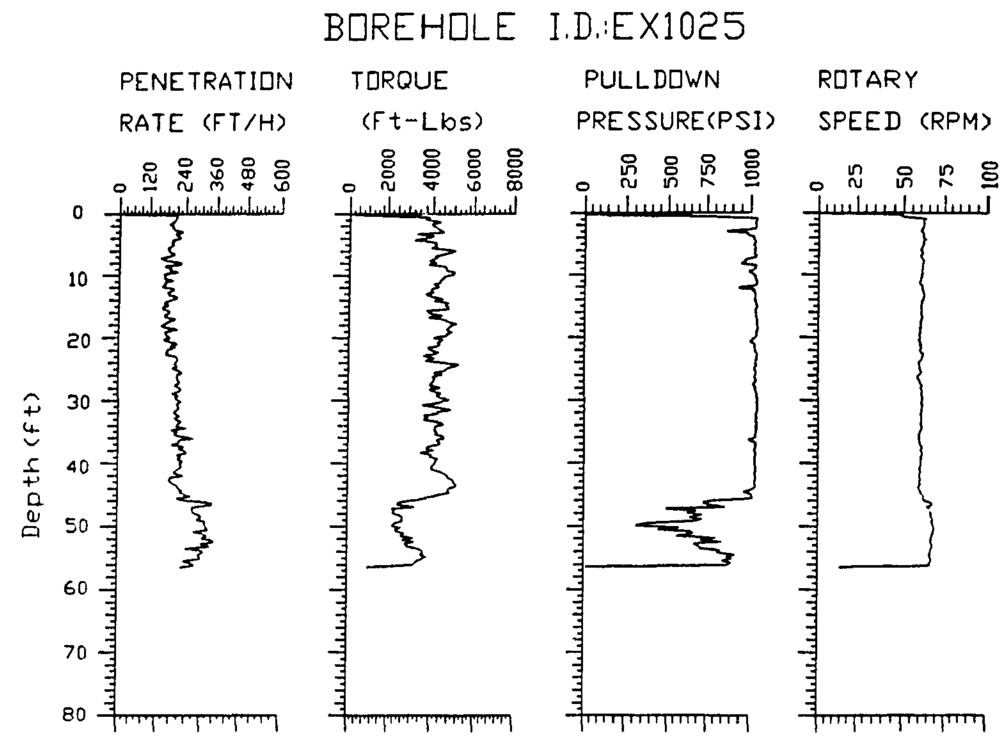

Figure 6.24 - Drill Logs for Borehole EX1025.

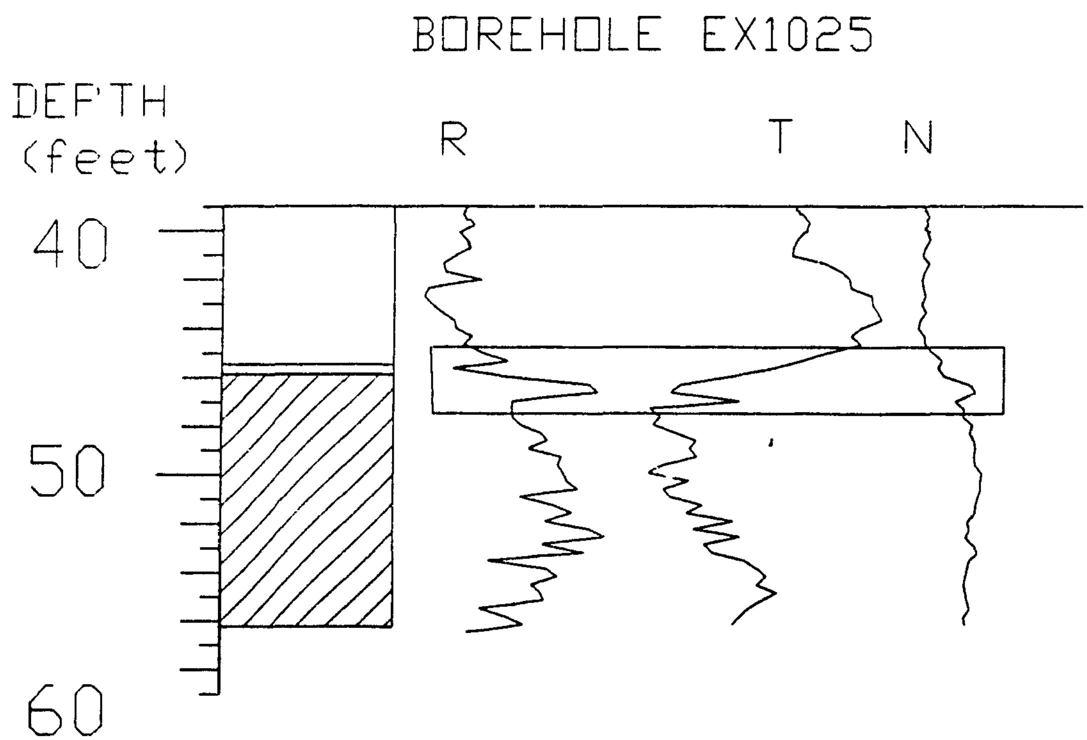

Figure 6.25 - Interface Between Siltstone and Coal.

6.3.6. Conclusion:

It has been demonstrated from the summary statistics of the recorded performance parameters that very well defined and consistent ranges of data exist for the various rock types drilled in this thesis study. Variation in the material properties of a particular rock unit appears to be reflected by an associated dispersion in the monitored performance parameters.

Examination of the interquartile ranges and the quartile limits further indicates the overall stability of the sample data for most parameters, when drilling in relatively homogeneous rocks. On this basis, unique ranges of drilling parameters can be isolated for the various rock types. The consistency of the inter-relationships between the drilling parameters for each rock type is clear from the statistical analysis, but further reinforced by the reproducibility of their respective star symbol plots from borehole to borehole.

This section validates at a macro (bulk) scale the hypothesis proposed in section 1.2. Section 6.5 will examine further the relationships between drilling parameters and rock properties using measured rock strengths.

6.4 Identification of Dominant Drill Parameters in Hard Versus Soft Rocks:

6.4.1. Introduction:

Section 6.3 identified that there were well-defined ranges for the drilling parameters in hard versus soft rocks. Also discussed was the role of each drilling parameter in the process of rock breakage in the different rock types. This section will further examine this point, by incorporating the data into several drilling models, originally discussed in section 2.3. The combined drilling responses, using these models, will be correlated to the individual parameters and to themselves. These should clearly define those parameters that control the outcome of the selected model. These results in turn, should reflect the dominant parameters involved in the rock breakage processes for soft versus hard rocks.

This is an important phase towards developing a complete understanding of the mechanisms of rock breakage for the type of drill and bit being used in this study.

6.4.2 Drilling Models:

There are many different drilling models which are published in the literature which incorporate a "drilling strength" or other rock property related variable. However, the majority of these had been developed under very controlled conditions and as such were considered inapplicable to data from the present investigation.

The drilling models discussed in section 2.3, and used for more detailed analyses below, were chosen for several basic reasons. Equation 2.10 for the specific energy, SE(T) was selected due to its simplicity. It did not involve any constraints in terms of coefficients or correction factors for bit wear or rock strength etc., yet combined the basic drilling parameters together into a logical formula. This fact made the equation that much more adaptable to any drilling situation, due to the minimum amount of limitations imposed by its form.

In addition, eqn.2.10 for example, was one of the few equations which accounted for the torque. Torque in this study, was determined from the outset (see section 4.3) to be one of the key parameters in identifying changing rock properties. Therefore it was essential to utilize its responses in combination with those of the other parameters to improve this capability. The equation for SE(T) allowed the importance of the torque responses to be maintained, and not diminished by variations in the other parameters.

The form of the equation for SE(T) was simply the sum of the axial and rotational components of energy applied to the bit to achieve penetration. For the drills monitored in this investigation, the product $2\pi NT$ is very important, as it determines the power output of the electric rotary motors based on the variations in both torque T and rotary speed N. This power equation forms part of the rotary energy component for SE(T), and therefore realistically accounts for the actual energy output applied to the bit by the drill. Therefore, the overall arrangement of the SE(T) formula enabled the changes in one component to not minimize the effect of the other when different conditions of rock breakage were encountered eg. soft vs. hard rocks. The units of measurement for this model were in terms of in-lb/in^3, which were equivalent to those normally reported for rock strength.

Rabia (1987) noted that the work done by the component W/A in the eqn.2.10 was commonly 1 to 2 percent of the total work done in rotary drilling and so can be neglected. However, in the present work, this component was seen to contribute up to 15 percent of the total calculated specific energies in harder sandstones and siltstones.

The model for SE(R) in eqn.2.31, represents the typical relation which does not include the torque. This equation was developed for the petroleum industry, and the prominence of the product of weight on bit, W, and rotary speed, N, related to penetration rate, R, as for most past investigations in this field, was evident. However, the advantage of this model compared to others, as for eqn. 2.10, was its simplicity. In addition, it was an energy equation, whereby the calculated SE(R) data was in proportional measurement units for both SE(T) and rock strength.

The Dx exponent model (eqn.2.22) also represents the typical form of equation from the oil industry, relating only the parameters of R, W and N with bit diameter, D, to derive a unitless and site specific index. However, this equation did exhibit reasonable sensitivity to profile changing ground during preliminary monitoring studies and so was selected for closer examination.

The Energy formula in eqn.2.39, was simply an attempt to examine the basic kinetic energies which are proposed to be generated by a simplistic drilling system, ignoring all outside influences. As will be demonstrated in subsequent sections, this particular index demonstrated very poor correlation with rock strength and was generally dominated by the variations in W.

6.4.3. Correlation of the Calculated Indices to Drill Parameters:

An analysis of the correlation between the calculated specific energies (SE(T) and SE(R)), Dx exponents, kinetic energies[1] and drilling performance parameters gives the correlation coefficients in Table 6.6.

Correlation coefficients provide a normalized and scale-free measure of the association between two variables. The coefficient

[1] The specific energy of Mellor (1972), W_s, is not included as it relies on the monitored drilling performance parameters indirectly for the purpose of estimating compressive strength and subsequent determination of Young's modulus.

values are between -1 and +1, where a positive number indicates the variables vary in the same direction (directly), while a negative correlation identifies variables which vary in opposite directions (indirectly). Statistically independent variables have an expected correlation of zero (Statgraphics Manual, 1986).

Dx Correlation: The correlation between Dx and W, is both positive and high in the softer coals (0.89) and mudstones (0.88), yet is very low in the harder sandstone/siltstones (0.24). This can be explained by equation 2.22 for calculating Dx values, where downpressure is one of the dominant parameters for this index, in addition to the degree of importance of this parameter in the rock breakage mechanisms of hard vs. soft rocks. Variations in downpressure in coal have been demonstrated to be a reflection of inhomogeneity of these units. Therefore, in these rocks, the recorded changes in downpressure will dominate in eqn. 2.22, with the responses in the other parameters contributing little or not at all to the calculated Dx values. This concept is exhibited by the high correlation in Table 6.6 between Dx and downpressure, and by the poor correlation of Dx with penetration rate (-0.67), rotary speed (-0.11) and torque (0.41).

In the harder mudstones, both penetration rate and downpressure appear to affect the calculated value for Dx, as demonstrated by their high correlation coefficients of -0.88 and 0.88. Yet as for coal, the rotary speed and torque do not appear to play a major role in Dx value calculation, as shown by the very low correlation coefficients of -0.11 and 0.42 respectively. This should be expected in the softer rocks, where rotary torque is very low, and calculated Dx is very dependent upon the variations in downpressure.

However, in the harder sandstone/siltstones, downpressure is essentially constant and high. Therefore, the variations in other drill parameters contribute more towards determining any variation in the Dx exponent and thus changing rock properties, than does downpressure. The high correlation coefficient between Dx and penetration rate of -0.92, indicates that in hard rocks, this drilling parameter becomes the dominant variable in equation 2.22. As for the softer rocks, rotary speed has low correlation with Dx data (-0.14), and therefore has little effect in determining changing Dx values. In harder rocks, torque is high yet sensitive to changing rock properties for (essentially) constant downpressure and rotary speed. Therefore, variation in

Table 6.6 - Correlation matrix between calculated indices and drilling parameters.

Coal: 457 Data Points

	R	N	W	T
Dx	-0.67	-0.01	0.89	0.41
SE(T)	-0.37	0.28	0.57	0.92
SE(R)	-0.61	-0.06	0.94	0.42
Energy	-0.35	0.09	0.95	0.49

Mudstone: 172 Data Points

	R	N	W	T
Dx	-0.88	-0.11	0.88	0.42
SE(T)	-0.66	0.03	0.62	0.89
SE(R)	-0.87	-0.12	0.88	0.41
Energy	-0.59	0.04	0.94	0.48

Sandstone/Siltstone: 477 Data Points

	R	N	W	T
Dx	-0.92	-0.14	0.24	0.71
SE(T)	-0.88	-0.33	0.04	0.89
SE(R)	-0.92	-0.34	0.02	0.69
Energy	-0.72	-0.18	0.07	0.65

R = penetration rate; N = rotary speed;
W = downpressure; T = torque;

recorded penetration rate will be mainly dependent upon the changes in torque. Since for these rocks, changes in Dx are very dependent upon the variation in penetration rate (corr.coef.= -0.92), it follows that Dx would have a corresponding (lesser) dependency on torque as indicated by a correlation coefficient of 0.71.

SE(T) Correlation: Relationships between SE(T) and torque however, are highly correlatable in all rock types. Correlation coefficients calculated between these two variables in coal, mudstone and sandstone/siltstone are 0.92, 0.89 and 0.89 respectively. These high coefficients should be expected since torque is the primary controlling parameter (along with penetration rate) in equation 2.10 to calculate SE(T).

Correlation between SE(T) and penetration rate is highest in sandstone/siltstone units having a coefficient of -0.88, and -0.66 and -0.37 in mudstone and coal respectively. The high correlation in the harder rocks is based upon the dependency of penetration rate on applied torque for the mechanisms of rock breakage which are operating (section 6.2). Since downpressure and rotary speed remain steady, the rate of penetration is wholly dependent on the applied torque under these conditions. Therefore since penetration rate is controlled by torque, the calculated SE(T) values as a result will also show high correlation with this parameter.

In the softer rocks, the poorer correlation of penetration rate to SE(T) is the result of this drill parameter no longer being solely a result of the applied torque, but where the variation in both downpressure and rotary speed (and efficiency of cuttings removal) also influence the calculated specific energy. This concept is demonstrated by the higher coefficients of correlation seen for SE(T) to downpressure for both coal (0.57) and mudstone (0.62), versus the low value (0.04) for sandstone/siltstones

(Table 6.6). However, it is clear that rotary speed has very poor correlation with the calculated specific energies in both hard and soft rocks. This fact can be explained by the very low COV's calculated for the rotary speed in all rock types and shown in Tables 6.4 and 6.5 of section 6.3. These COV's indicate that the recorded rotary speeds do not vary substantially when drilling in a particular rock unit. Therefore, it can be concluded that this parameter does not affect the extent of the calculated variations in SE(T) or any other index.

SE(R) Correlation: SE(R) correlated to penetration rate shows an increasing coefficient from softer to harder rocks. In coal, a low correlation coefficient of -0.61 was calculated, with higher values of -0.87 for mudstone and -0.92 for sandstone/siltstone. The trend for coal can be explained by the high dependency of SE(R) on downpressure when drilling in coal, as indicated by their high correlation coefficient of 0.94. It follows therefore, that the more downpressure varies in relation to the changing properties of the rock being drilled, the less important are the variations in penetration rate (and the other parameters) on the range of the calculated SE(R) data. This is clearly exhibited by the data of Tables 6.4 and 6.5 in section 6.3, where the downpressure varies considerably (COV = 30.9%) in coal, while the other parameters have less dispersion in their recorded data.

For mudstone, Table 6.5 indicates a narrower spread in the recorded downpressure data (COV = 20.99%) as compared to coal, and thus Table 6.6 shows a lower coefficient value of SE(R) to downpressure of 0.88.

In the sandstone/siltstones, the stability of the applied downpressure (COV = 3.32%, Table 6.4) results in the very low correlation coefficient of 0.020, for the relationship of SE(R) to downpressure W. Therefore, variations in penetration rate become the controlling factor in the calculated variations in SE(R), as confirmed by the very high correlation coefficient between these two of -0.92.

Poor correlation between torque and SE(R) should be expected overall, since the equation to calculate this index does not involve this parameter. This poor relationship is clear in coal (corr.coef.=0.42) and mudstone (corr.coef.=0.41), where downpressure dominates the range of data calculated for SE(R). As downpressure becomes more constant, as in sandstone/siltstones, the correlation coefficient between SE(R) and torque increases (=0.69). This is due to the pronounced influence of the variations in torque on the recorded changes in penetration rate (which affects SE(R)), and the reduced effect of the downpressure as it stabilizes.

Energy Correlation: The calculated Energy values are seen from equation 2.39 to be dependent upon W, N and R. The magnitude of W in this equation makes it the dominant term in determining the calculated Energy values. However, as previously explained, depending upon the strength of the material being drilled, the calculated **range** (ie. sensitivity to changing rock properties) of variations in Energy may or may not be dependent on downpressure. As for the other calculated indices, for the high, constant levels of recorded downpressure in hard rocks, variations in the next most important variable in equation 2.39, ie. the penetration rate, will determine the spread in the Energy data.

In soft coals, however, since the dispersion of the downpressure data is higher than for other parameters, it will therefore determine the variation in the Energy data. This relationship is shown by the high correlation coefficient for Energy and downpressure of 0.95. In harder sandstone/siltstones, where downpressure remains constant, the correlation is very poor and the coefficient equals 0.074. The trend of Energy and penetration rate follows the same logic discussed above. Correlation of Energy to penetration rate in coals is poor (-0.35), due to dominance of downpressure, and good in sandstone/siltstones

(-0.72) where drill rates are related mainly to the applied torque. These points are confirmed by the higher correlation coefficient of Energy to torque in sandstone/siltstones of 0.65, versus 0.48 and 0.49 in coal and mudstone respectively. As for Dx and SE(R), torque is not accounted for in the Energy equation, a fact indicated by their poor overall correlation with the responses in this parameter.

6.4.4. Correlation Between the Calculated Indices:

Table 6.7 illustrates the coefficients determined for the correlation of the calculated indices amongst themselves. It is quite apparent that those indices, sharing the same dominant drilling parameter (that drill parameter with the highest variance) for their determination, will also have the same degree of variation (COV's etc.) in their calculated data, and thus will show high correlation. This is clear from this table that in soft rocks, where downpressure has the highest data spread, the indices of SE(R), Dx and Energy show high correlation with each other. SE(T), dominated by the variance in applied torque, however, demonstrates lower correlation with all other indices as a result. However, as the variation in downpressure decreases with increasing rock strength, the correlation between the downpressure dependent indices also decreases. This is a result of other drilling parameters becoming more important in determining the particular index, as the influence of downpressure decreases.

An exception to this is for the relationship of Dx to SE(R), which has high correlation coefficient for all rock types. This fact is probably related to the similarity of their equations, where the same ratios between drilling parameters are calculated. The generated data for Dx and SE(R), vary therefore, by only a scalar or constant.

The Energy index, due to the form of its equation (being a sum of two products rather than a sum of ratios between drill

Table 6.7 - Correlation matrix between the different indices.

Coal: 457 Data Points

	Dx	SE(T)	SE(R)	Energy
Dx	1.000	0.688	0.985	0.919
SE(T)	0.688	1.000	0.679	0.683
SE(R)	0.985	0.679	1.000	0.949
Energy	0.919	0.683	0.949	1.000

Mudstone: 172 Data Points

	Dx	SE(T)	SE(R)	Energy
Dx	1.000	0.754	0.995	0.897
SE(T)	0.754	1.000	0.744	0.698
SE(R)	0.995	0.744	1.000	0.899
Energy	0.897	0.698	0.899	1.000

Sandstone/Siltstone: 477 Data Points

	Dx	SE(T)	SE(R)	Energy
Dx	1.000	0.728	0.979	0.688
SE(T)	0.728	1.000	0.727	0.545
SE(R)	0.979	0.727	1.000	0.675
Energy	0.688	0.545	0.675	1.000

R = penetration rate; N = rotary speed;
W = downpressure; T = torque;

parameters), does not properly compensate for changes in one parameter by corresponding changes in another. As a result, its coefficients of correlation with all other indices decreases from softer to harder rocks as the role of downpressure also decreases.

The relationships between SE(T) and SE(R) and Dx do improve slightly for drilling in harder rocks. This can be attributed to the reduced influence of downpressure and the increased effect of penetration rate variations (due to applied torque). This point is substantiated by the improved correlation of SE(R) and Dx to torque and thus SE(T) from coal to mudstone, shown in Tables 6.6 and 6.7.

6.4.5. Conclusion:

On the basis of these correlations, it is possible to define which of the calculated indices best reflects the changes in rock properties. It appears that the variations in SE(T) show the highest sensitivity to changing rock strength due to;

1 - its high correlation with torque for all rock types (Table 6.6), indicating the prominence of this parameter in rock breakage mechanisms for both soft and hard rocks,

2 - its dependency on applied torque (eqn.2.10), a parameter which was demonstrated in sections 6.2 and 6.3 to be highly sensitive to changes in rock properties at constant W.

The high variation demonstrated in Tables 6.4 and 6.5, and good correlation with SE(T) in all rock types makes torque one of the best parameters to reflect the changing properties of rock. Since SE(T) is dependent on torque, it also provides a good indication of rock mass characteristics. In addition, SE(T) also accounts for the variations in other parameters other than torque, which further enhances its sensitivity to the rock.

It would appear that the downpressure dependent equations are more suitable to truly reflect the nature of the softer rocks. This is due to its sensitivity, as indicated by the high dispersion of this parameter in Table 6.5, to respond to the changing rock properties in soft rocks. Since these equations do not account for the torque, downpressure is the dominant variable.

The poor correlation of SE(T) to downpressure in soft coals is an exception to this theory, due to the domination of torque.

For harder rocks, downpressure is stable, and therefore variations in other drill parameters will determine the responsiveness of the particular index to the rock.

Further conclusions of this analysis indicate that it is that drill parameter which exhibits the greatest range of variation (ie. highest COV, variance, interquartile range etc.) which appears to be best suited to identify changing rock properties. This statement is valid if it has been previously established that the variations are due to the changing rock properties. Therefore, the index dominated by the relative variations in the particular parameter, will provide the highest response to heterogenous rock.

6.5 Correlations Between Drilling Performance Parameters and Measured Rock Properties:

6.5.1 Introduction:

Section 6.3 involved the correlation between drilling parameters and the bulk properties of rock, where the absolute strength values were not considered. Only the relative rock strengths in terms of hard versus soft were compared to characteristic drilling parameter patterns. Based on these and the geological boundaries between the different rock units, as defined by core and gamma logs, unique ranges of drill parameters were identified.

Section 6.4 demonstrated further some of the conclusions made in section 6.3, by again identifying the dominance of particular parameters in rocks of different relative strength. This section also indicated the usefulness of selected drilling models, which enable the responses of more than one parameter to be accounted for by one calculated index. Section 6.4 also presented the possibility of using only this calculated parameter to properly assess the changing nature of the rock.

In this following section, the correlation between drilling performance and rock properties will also be attempted. Here, however, the drilling parameters, both individually and combined, will be related to the measured compressive strengths of rock. The nature of the measured compressive strengths was discussed in section 5.3.

The combined parameter responses, as discussed in section 6.4, are re-examined here in terms of their sensitivity to reflect variations in rock strengtl.. As in previous sections, a strong bias is shown by these calculated indices, with respect to the particular drilling parameter the model is dependent upon. This bias in turn is increased or decreased, according to the prominence of the particular parameter in the rock breakage mechanisms which depends on the strength of rock being drilled.

As for section 6.2, where a homogeneous interval of sandstone/siltstone was isolated for controlled drilling tests, a unit of similar composition was selected for this analysis. This approach would minimize as much as possible the variation in measured strength and thus monitored drilling performance data due to compositional changes in the rock. This in turn would enable a more valid correlation between rock properties and drill parameters to be made.

6.5.2. Sandstone/Siltstone Test Interval:

The same sandstone interval encountered in both cored holes CHEM 1, from 39.1 to 48.3 feet, and CHEM 2, from 43.5 to 53.5 feet, was used for more detailed analysis. The geologic logs for these holes were shown and described in section 5.1, see Figures 5.2 and 5.3.

This unit was seen from gamma logs to consist primarily of clean (low argillaceous content), massive sandstone, with some gradations to siltstone. Thin section analysis further confirmed that these rocks were sandstone/siltstone with considerable compositional variation. Section 5.3 and Appendix I provides the complete thin section analyses for all the test samples.

Within the CHEM 1 sandstone unit, a total of 4 valid unconfined compressive strengths were obtained. In CHEM 2, a total of 10 compressive strengths were derived from testing, yet only 3 were considered valid based upon thin section data and examination of the failure mode. Table 5.1 presents the strength, moduli and depth location data for the test samples from cored holes CHEM 1 and CHEM 2.

The same sandstone/siltstone horizon seen in both cored holes, was isolated in the drill monitored boreholes. A total of 5 monitored boreholes were examined around CHEM 1 and 6 adjacent to CHEM 2, see Figure 5.1. Table 6.8 shows the averages of the acquired drill data for the approximate 10 foot thickness of the sandstone unit in each of the monitored boreholes. The specific

Table 6.8 - Averaged Drill Performance Parameters for the Sandstone/Siltstone Test Interval.

DATA FROM BOREHOLES AROUND CHEM #1:

BH:	DEPTH:	R:	I:	W:	N:	T:
EM127	41.01-45.61	202.64	23.05	882.73	62.54	4990.78
EM127	45.93-51.52	200.66	21.96	824.84	56.41	5091.31
EM128	41.01-45.94	228.58	22.95	849.97	67.09	5204.79
EM128	46.27-47.90	227.02	23.03	871.33	59.25	7106.96
EM128	48.24-56.43	231.42	23.12	729.54	64.21	5353.35
EM186	41.99-48.89	172.71	26.18	483.18	62.35	5973.55
EM186	49.21-54.14	193.01	26.31	477.99	61.62	5801.34
EM187	36.75-41.99	152.39	25.53	419.24	59.08	5133.53
EM187	42.33-44.29	160.38	25.64	418.86	55.45	5799.45
EM188	36.42-45.93	189.17	24.18	772.03	54.88	6269.89
	AVERAGE:	195.80	24.20	672.97	60.29	5672.50
	MAX:	231.42	26.31	882.73	67.09	7106.96
	MIN:	152.39	21.96	418.86	54.88	4990.78
	STD:	26.67	1.51	188.08	3.78	628.61

DATA FROM BOREHOLES AROUND CHEM #2:

BH:	DEPTH:	R:	I:	W:	N:	T:
EM894	42.01-54.79	228.86	22.79	858.50	65.39	4689.27
EM895	43.64-57.42	227.86	23.04	913.87	59.39	5064.81
EM896	46.26-58.39	229.75	23.18	875.84	74.02	4879.95
EM897	47.91-58.39	230.41	23.42	550.47	78.22	3541.54
EM953	34.13-46.59	226.89	22.48	826.44	72.71	4826.02
EM954	38.72-49.22	232.44	22.43	884.82	74.98	4929.25
	AVERAGE:	229.37	22.89	818.32	70.79	4655.14
	MAX:	232.44	23.42	913.87	78.22	5064.81
	MIN:	226.89	22.43	550.47	59.39	3541.54
	STD:	1.80	0.36	122.67	6.40	510.55

BH:	SE(T):	SE(R):	Dx:	Energy:
EM127	5665.35	3553.12	0.64	25742.81
EM127	5255.83	3059.32	0.61	23722.50
EM128	5622.98	3274.35	0.63	24825.95
EM128	6648.26	2972.32	0.60	25019.44
EM128	5388.67	2731.69	0.59	21148.56
EM186	7420.70	2586.22	0.60	14272.02
EM186	6410.22	2269.12	0.57	13960.49
EM187	6780.91	2507.59	0.59	12402.63
EM187	6819.59	2234.80	0.57	12208.60
EM188	6577.56	2990.39	0.61	22209.45
AVERAGE:	6259.01	2817.89	0.60	19551.24
MAX:	7420.70	3553.12	0.64	25742.81
MIN:	5255.83	2234.80	0.57	12208.60
STD:	687.96	407.35	0.02	5359.29

BH:	SE(T):	SE(R):	Dx:	Energy:
EM894	4995.09	3214.06	0.62	24974.06
EM895	4983.81	3089.04	0.61	26242.27
EM896	5750.22	3684.96	0.65	26007.29
EM897	4352.09	2680.64	0.60	16520.00
EM953	5635.03	3493.06	0.64	24487.40
EM954	5826.65	3721.08	0.65	26308.94
AVERAGE:	5257.15	3313.81	0.63	24089.99
MAX:	5826.65	3721.08	0.65	26308.94
MIN:	4352.09	2680.64	0.60	16520.00
STD:	528.01	364.49	0.02	3451.48

energies (Teale, 1965; Rabia, 1982, 1987), Dx exponents (Bingham, 1964) and kinetic energies were also calculated for these units from the drill data, and are presented in the table. The reason for selecting this particular sandstone unit for closer study is due to several factors. First, this particular horizon was clearly recognizable in core, and gamma and drill logs. Secondly, the reasonably consistent high strength and compositional homogeneity exhibited from core testing and confirmed in thin sections made it the most suitable zone to enable a correlation of its properties to the recorded drilling responses. Thirdly, a greater number of compressive strengths were obtained from laboratory testing of sandstone/siltstone samples, and therefore this data set was considered more reliable than for the other rock types.

Selection of this rock unit, also minimized the effect of any large scale compositional variations on drilling performance and rock strength. Since an attempt was being made to correlate rock properties to drill performance, the chances of succeeding were greatly enhanced by reducing the number of variables surrounding the experiment, most importantly those related to the composition of the rocks.

Detailed microgeological thin section studies were conducted to examine the reasons for the observed dispersion in the measured compressive strength data for this sandstone/siltstone interval. Since it had been assumed that the valid strengths were unaffected by platen end-effects or related phenomena, then the spread in strength data was speculated to be the result of compositional variations in the test specimens. The extent of these variations and influence on the strength were determined by the petrographic studies discussed in section 5.3.

The approach taken therefore, was that successful correlations achieved between rock properties and drill data in this "controlled" rock environment could subsequently be applied to the less ideal mudstone and coal units elsewhere. This appeared to be a valid assumption, in that the correlation of drilling to rock properties was established in a rock unit having the least amount of variation. The mechanisms of rock breakage in such a situation could be assumed to be optimal. Therefore any relationship determined should be applicable to drilling in softer rocks where conditions were less than ideal.

6.5.3. Correlation Between Measured Compressive Strength and Drill Parameters:

The raw data acquired while drilling through the sandstone/siltstone test horizon is shown in Table 6.8. A regression analysis of the parameters of penetration rate R, rotary speed N, torque T and downpressure W to measured compressive strengths σ_c(meas), give the correlation coefficients in Table 6.9.

Table 6.9 - Correlation Coefficients for Compressive Strength to Drilling Parameters.

	R	N	W	T
σ_c	0.346	0.336	0.664	0.924

It is clear from these results, that for the hard sandstone/siltstones, there is a strong relationship between the applied torque and the rock strength. Therefore the variations in this parameter alone should reflect changing rock properties. This was also demonstrated in sections 6.2 to 6.4.

A weaker relationship exists between the compressive strength and the applied downpressure, since this parameter is essentially constant when drilling in hard rocks. Therefore, it does not provide a sufficient response to varying ground conditions as does the torque. Correlation with the penetration rate and rotary speed showed very poor correlation, reflecting the stability of these responses in rock that has consistent properties.

It is interesting to note, that although this test interval demonstrated an overall homogeneity, the high correlation of torque to σ_c(meas) indicates that at a certain scale it is not. It was suggested from the thin section analysis that there existed considerable compositional variation in the test samples at a microgeological level which were clearly responsible for the range in the σ_c(meas) data. Since σ_c(meas) and torque are highly correlatable, the same compositional anomalies accounting for the variation in σ_c(meas) must also contribute to the observed dispersion in the monitored torque data. This fact was also indicated as a possibility for the trends in torque shown in Figure 6.8.

As discussed in sections 6.2 to 6.4, the variations of drilling performance in hard versus soft rocks is a combined response of more than one parameter. Therefore a simple comparison of rock strength to the individual parameters is insufficient. Using the same drilling models as for section 6.4, the combined response of the parameters to measured compressive strengths are examined in the following section.

6.5.4. Combined Drilling Parameter Response to Measured Compressive Strength:

The drilling models discussed in detail in section 2.3 and correlated to the drill parameters in section 6.4 were subsequently applied to the recorded drill data for this test interval. These equations were seen in this latter section to compensate for variations in the drilling performance, based on the concept of energy balancing and the inter-relationships between the parameters. The index thus calculated will reflect the variations displayed by that drilling parameter which dominates the rock breakage process for the particular rock type.

An assumption made prior to comparing the results from the drilling models and measured compressive strengths, was that the relationship based on Mohr's Failure Criteria, and described by Bingham (1964) as equation 2.20 was valid. This equation relates the shear strength of the rock to the compressive strength for a known angle of internal friction. Therefore, using the measured compressive strengths, shear strengths were estimated using this relationship.

In order to apply this equation to the data of this study, angles of internal friction were selected for sandstones and siltstones as 28.64° and 31.46° respectively, based upon the data in Table 5.2. Since it was also assumed that in most cases the sandstones graded into siltstones (and vice versa), an average value of these equal to 30.05° was used in all subsequent calculations. This approach was considered acceptable as the angles of internal friction in the types of sedimentary rocks (detrital) encountered are generally in the range of 25° to 35° (Bingham, 1964; Vutukuri et.al., 1974; Lebel, 1984).

The techniques discussed below are therefore to illustrate how drilling performance data could be used towards:

a - providing estimates of compressive and shear strength of the rock types present and,

b - based on the results in (a) estimates of both tangent and secant modulus could subsequently be determined.

The estimated rock property data will be shown in the following section to be in very close agreement with data obtained from laboratory testing of core. The relationships established between intact rock properties and performance parameters, however, are dependent upon the particular drill and bit type and bit diameter used throughout these investigations. As such they are only applicable for when N, W and thus R and T are greater than 0 ie. the drill is actually operating.

6.5.5. Estimation of Shear and Compressive Strengths:

A - Specific Energy, SE(T) - (Teale, 1965): For the purpose of the following analysis, it was proposed that the calculated specific energies, SE(T) are proportional to the shear strengths, τ, of the rocks being penetrated. This assumption is based on the principles of rock breakage by a tricone bit, where shear forces due to the applied torque were identified as the dominant mechanism promoting rock failure in the sandstone/siltstones (sections 6.2 to 6.4). Since Teale's equation is based on torque, indicated in section 6.4 to govern the outcome of this equation, such an hypothesis can be considered valid for this discussion.

Table 6.10 illustrates the range of τ_a calculated (using eqn.2.20) from σ_c(meas), and compared to SE(T) determined from recorded drill parameters. All data is for the sandstone/siltstone units previously described.

Table 6.10 - Calculated τ and SE(T) for Sandstone/Siltstone.

Sandstone/Siltstone:

	SE(T)	σ_c (meas)	τ_a	τ_b	σ_c (calc)
Min:	4351.45	10453.05	6065.35	5449.10	12590.35
Max:	7419.65	27084.55	11721.80	11569.55	26730.75
Avg:	5757.95	18136.60	8193.95	9252.45	21278.80
Std:	607.55	3046.45	1999.55	-	-

All data in psi;

$$\sigma_c \text{ (psi)} = \text{SE(T) (psi)} \cdot 4.61 - 7464.60 \quad \ldots 6.9$$
$$\tau_b \text{ (psi)} = \text{SE(T) (psi)} \cdot 1.99 - 3230.60 \quad \ldots 6.10$$

The correlation coefficient for the relationship between σ_c(meas) and SE(T) (siltstone/sandstone) was calculated to be equal to 0.970, with a regression equation,

$$\sigma_c \text{ (psi)} = 4.61 \cdot \text{SE(T) (psi)} - 7464.60 \quad \ldots 6.9$$

The same coefficient of correlation was obtained for τ_a versus SE(T), with an equation equal to,

τ_b (psi) = SE(T) (psi) $\cdot$ 1.994413 - 3230.60 ... 6.10 Both these regression equations are valid only for values of SE(T) > 0, which implies drilling is taking place.

Values for τ_b were calculated by substituting SE(T) data into equation 6.10, in order to compare these with the τ_a data calculated using σ_c(meas). The average, minimum and maximum

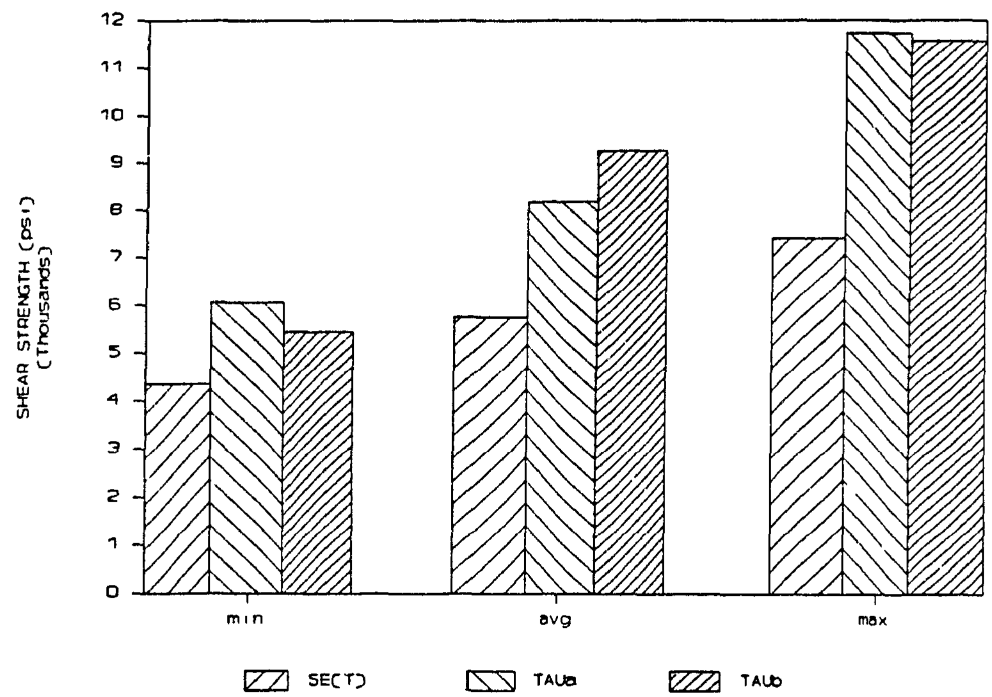

Figure 6.26 - SE(T) vs. τ_a and τ_b.

values of SE(T), τ_a and τ_b are shown in Figure 6.26.

It is apparent from this diagram, that the average calculated SE(T) value is very close to those for τ_a and τ_b. However, a greater dispersion in the overall ranges of the τ data is clear. This reinforces the concept presented earlier that this particular specific energy equation may not account for all the energy inputs and losses associated with drilling (section 2.3). However, this is assuming that τ_a data based on eqn.2.20 and σ_c(meas) are valid estimates of the actual shear strengths for these rocks. It may be in fact that "true" τ are lower (or higher) than τ_a and therefore would be in better (or worse) agreement with the calculated values for SE(T). Regardless of this, the calculated values for τ_b, using eqn.6.10, can be stated to be reasonable estimates of true shear strengths.

Using the data for τ_b , corrected compressive strength values, σ_c(calc), were determined from equation 2.20. These are compared to the values of σ_c(meas) in Figure 6.27, which demonstrates the good agreement of the data. All the estimated values are given in Table 6.10.

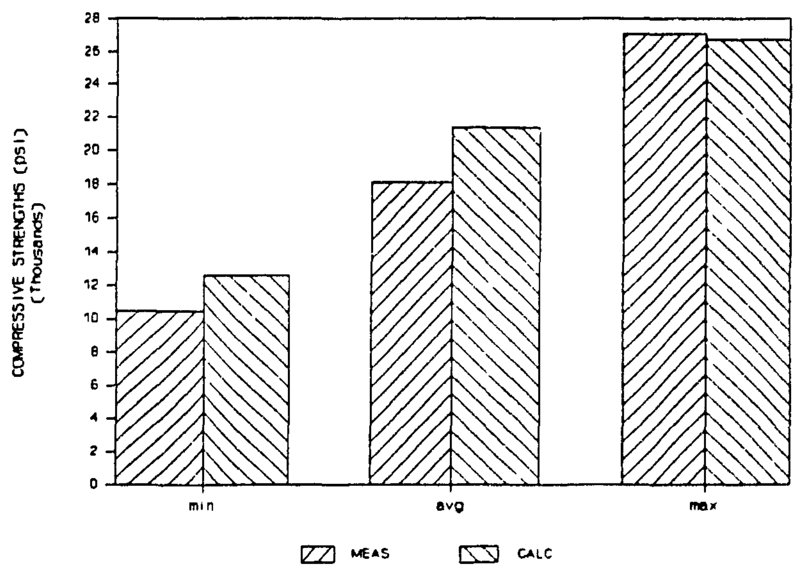

Figure 6.27 - σ_c(meas) vs. σ_c(calc).

Applying equation 6.9 to the ranges of SE(T) calculated from monitored drilling in 20 borehole for <u>all</u> rock types at the mine, values for σ_c(calc) were determined. These were also calculated for the complete range of rock types assuming, however, that the SE(T) data were proportional to τ in equation 2.20.

Comparison of the above strength data with those given in Tables 5.1 and 5.2 of section 5.3 indicate that these "estimated" values are within the ranges of the "measured" data[1].

The higher values of σ_c(calc) for mudstones and coals based on equation 6.9 compared to the σ_c(meas) data, shown in Figures 6.28 and 6.29, are probably due to the inclusion within the drill data

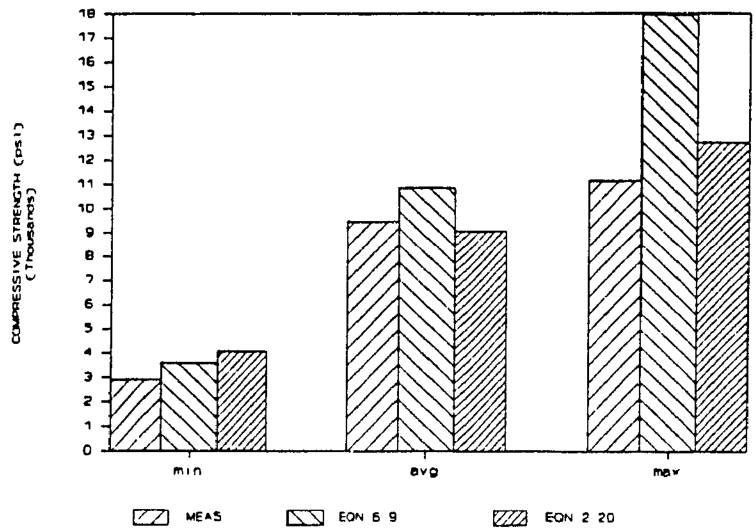

Figure 6.28 - σ_c(meas) vs. σ_c(calc) - Mudstone.

[1]Note that no σ_c(meas) data were obtained for the coal seams encountered in the current study. The data used for comparison with the estimated values were data measured on coal core samples taken from a different stratigraphic level at the mine. Therefore, it is not known whether or not this data is directly comparable to the coals of the more recent thesis field study.

used in determining SE(T), of harder interburden zones. The drill responses for these thin, discontinuous mudstone (in coal) and muddy siltstone (for both coal and mudstone) partings are sometimes difficult to separate from the parameters for the softer rocks. In addition, due to the nature of these units, it would be difficult to both prepare and test such samples in the laboratory to derive any meaningful results.

Figure 6.28 indicates that the σ_c(calc) data for mudstones, based on equation 2.20, gives better results than using the regression equation 6.9. These former SE(T) based σ_c(calc) values better reflect the predominant type of energy input (ie. shear) used in breaking these softer rocks. From the data plotted in Figure 6.29, it would appear that the σ_c(meas) values do not accurately reflect the actual strengths of the coals in the study area. Based on the good correlation of the SE(T) data for mudstones and sandstone/siltstones, it would be reasonable to state that the σ_c(calc) data determined from eqn.2.20, more accurately reflects the true range of coal strengths.

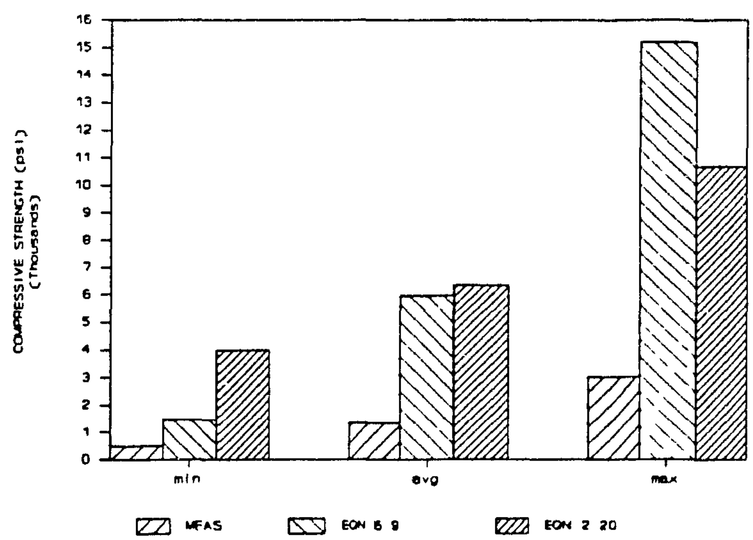

Figure 6.29 - σ_c(meas) vs. σ_c(calc) - Coal.

The values of σ_c(calc) using equation 6.9 for the sandstone/siltstone data, gave the best results when compared to σ_c(meas). This is reasonable, since this equation was based upon data from a hard sandstone/siltstone test interval. The underestimated σ_c(meas) data obtained using eqn.2.20, indicates that the rock breakage in harder rocks involves more than simply shear processes. The data using both approaches are compared in Figure 6.30.

The calculated data from the different equations and for the various rock types are summarized in Table 6.11 where the number of data points used in the calculations is indicated by "Pts.".

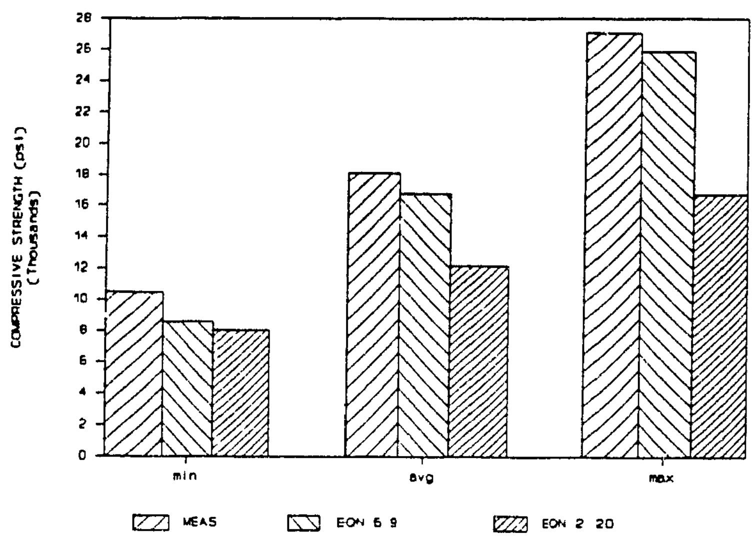

Figure 6.30 - σ_c(meas) vs. σ_c(calc) - Sandstone/siltstone.

Table 6.11 - Estimated σ_c based on calculated τ and SE(T) for all rock types.

	Sandstone: (Pts: 562)	Mudstone: (205)	Coal: (493)
Calculated SE(T):			
Min:	3481.45	2401.20	1935.75
Max:	7234.05	5518.70	4919.85
Avg:	5256.25	3939.65	2913.05
Std:	623.50	800.40	655.40
Calculated σ_c: (eqn.6.9)			
Min:	8572.40	3600.35	1457.25
Max:	25872.35	17966.95	15206.15
Avg:	16756.20	10856.15	5955.15
Std:	2865.20	3105.90	2860.85
Calculated σ_c: ($SE(T) \approx \tau$)			
Min:	8056.20	4078.85	3988.95
Max:	16715.60	12694.75	10680.70
Avg:	12145.20	9056.70	6342.30
Std:	1441.30	1840.05	1423.90

Min: = minimum value (all data in psi)
Max: = maximum value
Avg: = average value
Std: = standard deviation

B - Specific Energy, SE(R) - (Rabia, 1982,1987): Correlation of σ_c(meas - sandstone/siltstone) with the SE(R) data calculated using equation 2.31 was good, having a coefficient of 0.8984. It was also demonstrated that SE(R) data was highly dependent upon the downpressure, with a correlation coefficient between these two parameters equal to 0.998, a fact also apparent from the form of equation 2.31 and discussed in section 6.4.

The regression equation for σ_c(meas) and SE(R) is,

$$\sigma_c \text{ (psi)} = \text{SE(R) (psi)} \cdot 7.84 - 5009.52 \quad \ldots \; 6.11$$

As for the regression equations using SE(T), equation 6.11 is valid only for SE(R) > 0.

Shear strengths τ_a, as for the previous section, were estimated using the data for σ_c(meas) for this interval and equation 2.20, and then correlated to the calculated SE(R) data. A correlation coefficient of 0.898 (same as for eqn.6.11) and a regression equation was obtained as,

$$\tau_b \text{ (psi)} = \text{SE(R) (psi)} \cdot 3.39 - 2167.75 \quad \ldots \; 6.12$$

Values for τ_b were calculated using eqn.6.12, with the results

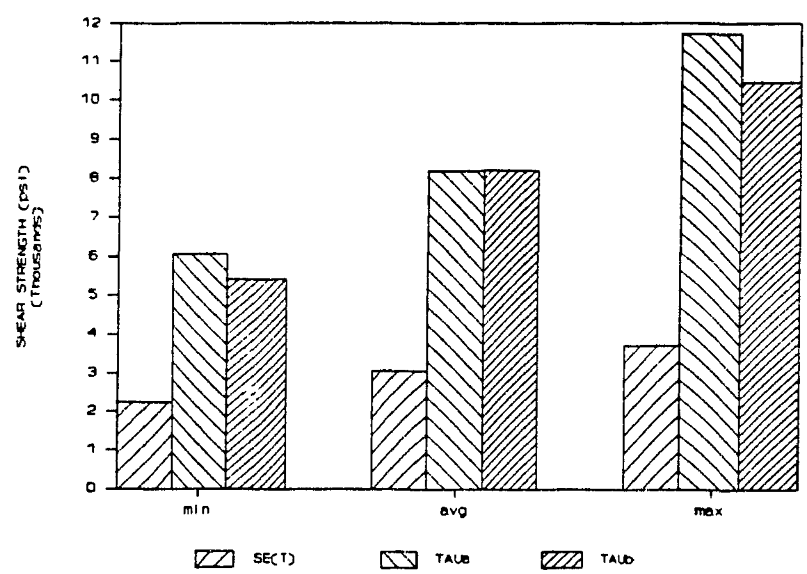

Figure 6.31 - SE(R) vs. τ_a and τ_b.

compared to both SE(R) and τ_a in Figure 6.31. It is obvious that the values of SE(R) show very poor correlation with both τ_a and τ_b. This is due in part to the exclusion of torque in the equation to calculate SE(R). In addition, since SE(R) is very dependent on downpressure, it is apparent from Figure 6.31 that the low dispersion in SE(R) is due to the stability of this parameter in harder rocks.

Values for σ_c(calc) were determined based on the data for τ_b. A comparison of σ_c(meas) to σ_c(calc) is shown in Figure 6.32, where the agreement between the data is very high.

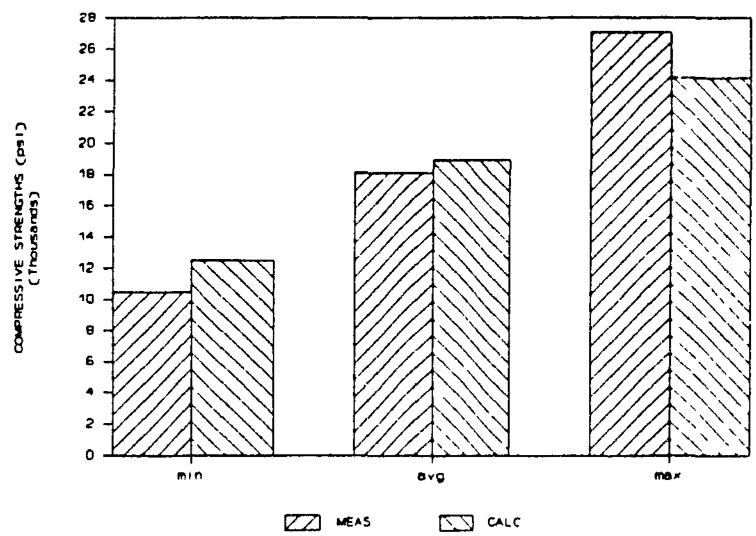

Figure 6.32 - σ_c(meas) vs. σ_c(calc).

All the data calculated for this particular test zone of sandstone/siltstone using the regression equations 6.11 and 6.12 are shown in Table 6.12.

Data for σ_c(calc) was calculated for all of the rock types, based on equation 6.11 and the substitution of SE(R) for τ in eqn.2.20.

Figures 6.33, 6.34 and 6.35 compare σ_c(meas) with σ_c(calc) calculated using these methods. The best results for the coals and mudstones are seen for the σ_c(calc) data determined using equation 2.20 and plotted in Figures 6.33 and 6.34. (Note that comparing σ_c(meas) to σ_c(calc) for coal, has the same limitations as indicated in the previous section). The reason is due the fact that shear mechanisms are dominant for the soft rocks. Therefore, the responses and magnitudes of the parameters should be a reflection of this process. For these reasons the values σ_c(calc) estimated using SE(R)$\approx\tau$, show a higher sensitivity to variation of material properties in softer rocks.

Table 6.12 - Calculated τ and SE(R) for sandstone/siltstones.

	Sandstone/Siltstone:				
	SE(R)	σ_c (meas)	τ_a	τ_b	σ_c (calc)
Min:	2234.45	10453.05	6065.35	5415.75	12510.60
Max:	3720.70	27084.55	11721.80	10458.85	24165.70
Avg:	3053.70	18136.60	8193.95	8195.40	18935.55
Std:	520.55	3046.45	1999.55	-	-

All data in psi;

σ_c (psi) = SE(R) (psi) $\cdot$ 7.84 - 5009.52 ... 6.11

τ_b (psi) = SE(R) (psi) $\cdot$ 3.39 - 2167.75 ... 6.12

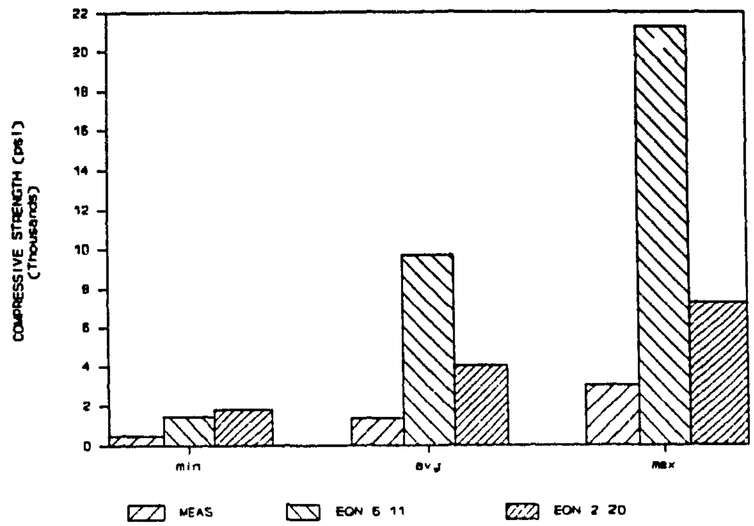

Figure 6.33 - σ_c(meas) vs. σ_c(calc) - Coal.

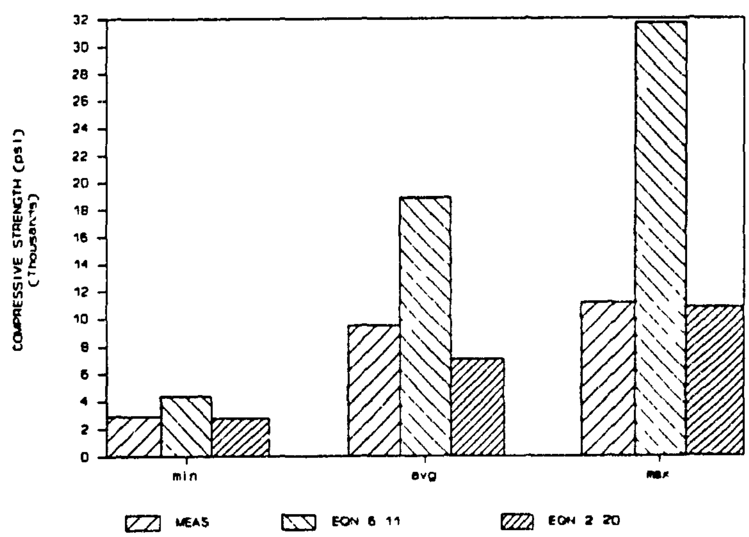

Figure 6.34 - σ_c(meas) vs. σ_c(calc) - Mudstone.

The underestimated values for σ_c(calc) for sandstone/siltstone using eqn.2.20 and illustrated in Figure 6.35, indicates the differences in rock breakage processes for hard versus soft rocks. It is clear that other mechanisms besides shearing are operating, as witnessed by the low σ_c(calc). These trends are similar to those discussed in the previous section for SE(T) vs.σ_c(calc).

In hard rocks, since downpressure is high, and both rotary speed and penetration rates are low, very high values for calculated SE(R) result. Since equation 6.11 is based on drill data from the hard sandstone/siltstone test interval, the overestimated values of σ_c(calc) in Figures 6.33 and 6.34 calculated using this relationship reflect these particular conditions.

Deviations between σ_c(meas) and σ_c(calc) are therefore greatest in the softer rocks where the responses of the performance parameters are very different. The σ_c(calc) data for the sandstone/siltstones, however, are within an acceptable range of the σ_c(meas) values (Figure 6.35).

The estimated data for the different rock types are presented in Table 6.13 below.

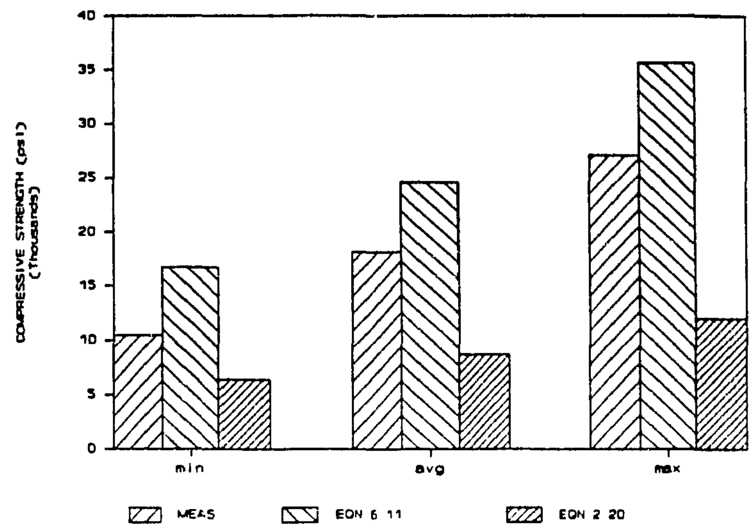

Figure 6.35 - σ_c(meas) vs. σ_c(calc) - sandstone/siltstone.

Table 6.13 - Calculated σ_c based on calculated τ and SE(R):

	Sandstone: (Pts: 562)	Mudstone: (205)	Coal: (493)
		Calculated SE(R):	
Min:	3481.45	2401.20	1935.75
Max:	7234.05	5581.70	4919.85
Avg:	5256.25	3939.65	2913.05
Std:	623.50	800.40	655.40
		Calculated σ_c (eqn.6.11):	
Min:	16724.30	4365.95	1444.20
Max:	35633.75	31681.05	21233.80
Avg:	24597.80	18851.45	9688.90
Std:	2676.70	4265.90	3919.35
		Calculated σ_c (eqn.2.20; SE(R)≈τ)	
Min:	6404.65	2766.60	1786.40
Max:	11975.55	10828.60	7265.95
Avg:	8724.65	7041.20	4070.15
Std:	788.80	1260.05	1084.60

(All data in psi)

6.5.6. Estimation of Young's Modulus:

A - Specific Energy, W_s - (Mellor, 1972): Using equation 2.29, the specific energy, W_s, was calculated for the range of measured tangent moduli (E_t(meas)) and compressive strengths for sandstone/siltstone (σ_c(meas)) shown in Tables 5.1 and 5.2. The constant C in eqn.2.29 was set equal to 1.5, as indicated by Mellor (1972).

The correlation of W_s to σ_c(meas), gave a coefficient of 0.983, and the regression equation,

$$W_s \text{ (psi)} = \sigma_c \text{ (psi)} \cdot (0.003013) - 11.74 \quad \ldots 6.13$$

Although W_s is referred to as specific energy, the calculated values are not considered related to the SE(T) or SE(R) data calculated previously. This index is used here to permit the estimation of modulus, based on monitored drilling performance parameters.

Due to the reliability of using SE(T) data to estimate σ_c, this approach has been used here to estimate values for W_s. This phase involves using the drilling performance parameters in an indirect way to provide estimates of E_t.

Using the regression equation 6.13, estimated values for W_s can be calculated based on the calculated values for σ_c(calc) determined using SE(T) in eqns.6.9 and 2.20 and shown in Table 6.14.

Table 6.14 also illustrates estimated values for E_t(calc) and E_s(calc) calculated for sandstone/siltstones using eqns.2.28 and 2.29. Comparison of these estimated values with the measured data for E_t and E_s in Table 5.2 indicates a high degree of correlation.

Figure 6.36 illustrates more clearly the close correspondence of E_t(meas) and E_t(calc). The best agreement with E_t(meas) is demonstrated by the values for E_t(calc) determined using σ_c calculated from eqn.6.9. Poorer correlation was obtained when comparing E_t(meas) with E_t(calc) derived using eqn.2.20. This equation was shown previously to be more appropriate for soft rocks.

Table 6.14 - Estimated E_t and E_s.

Sandstone/Siltstone:

	σ_c (Eqn.6.9) (psi)	W_s	E_t(calc) (psi)	E_s(calc) (psi)
Min:	8572.40	14.07	1.74×10^6	2.61×10^6
Max:	25872.35	66.27	3.37×10^6	5.06×10^6
Avg:	16756.20	39.44	2.42×10^6	3.62×10^6
Std:	2865.20		-	-

	σ_c (Eqn.2.20) (psi)	W_s	E_t(calc) (psi)	E_s(calc) (psi)
Min:	8056.20	12.47	1.73×10^6	2.59×10^6
Max:	16715.60	38.57	2.41×10^6	3.62×10^6
Avg:	12145.20	24.80	1.97×10^6	2.97×10^6
Std:	1441.30	-	-	-

$$W_s = \sigma_c \text{ (psi)} \cdot (0.003013) - 11.74 \quad \ldots\ 6.9$$

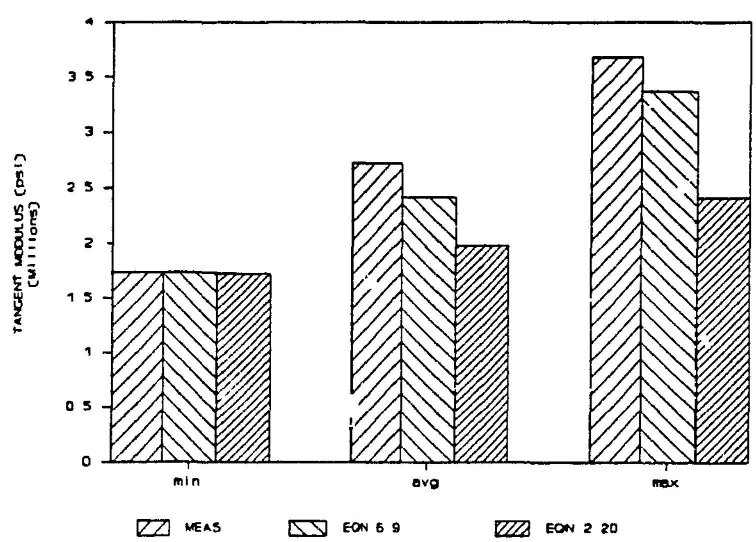

Figure 6.36 - E_t(meas) vs. E_t(calc).

In the same manner as equation 6.13 was determined based on σ_c(meas) for sandstone/siltstone, a relationship was established for W_s and σ_c(meas) for mudstones. However, only 3 valid compressive strengths were obtained from testing the mudstone samples. Therefore this regression analysis cannot be considered statistically sound, yet the results do show good correlation with the measured data. Table 6.15 illustrates a correlation coefficient of 0.995 and a regression equation for W_s and σ_c(meas),

$$W_s = \sigma_c \text{ (psi)} \cdot (0.002635) - 6.0871 \quad \ldots \; 6.14$$

Using this equation, and estimated σ_c data from equation 6.9, W_s and thus E_t(calc) and E_s(calc) values were determined. It is apparent that the E_t(calc) data, based on eqns.6.9 and 2.20, compare very well with the measured values of E_t obtained from mudstone core testing in the current study. Best agreement was obtained using eqn.2.20, where SE(T)≈τ, which in all previous situations determined estimated data which showed the highest correlation with measured rock properties in soft rocks. This data is shown in Figure 6.37.

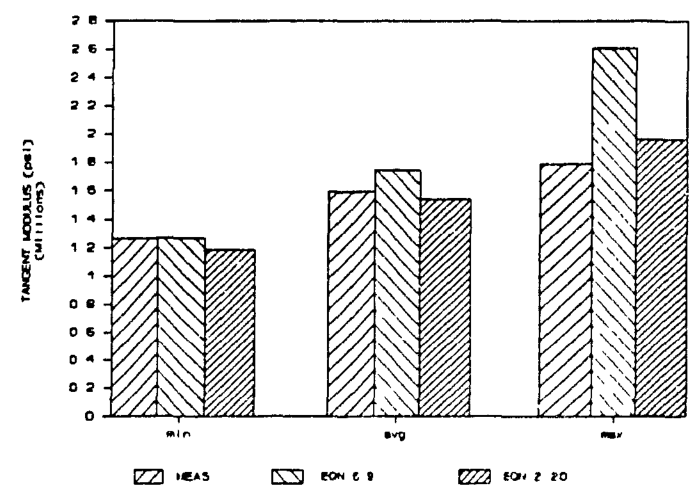

Figure 6.37 - E_t(meas) vs. E_t(calc); Mudstone.

This approach therefore enables <u>estimates</u> of both tangent modulus, E_t, and secant modulus, E_s to be obtained directly from monitored drill data. The proposed method is based on previously established relationships between calculated specific energies and measured rock compressive strengths.

Table 6.15 - E_t(calc) and E_s(calc).

Mudstone:

	σ_c (meas) (psi)	E_t (meas) (psi)	W_s(eqn.2.29)
Min:	6477.15	1.27×10^6	11.02
Max:	11136.00	1.79×10^6	21.61
Avg:	9468.50	1.59×10^6	18.85
Std:	2119.90	2.34×10^5	5.66

R = 0.995;

$$W_s = \sigma_c\ (\text{psi})\cdot(0.002635) - 6.0871 \quad \ldots\ 6.14$$

	σ_c(eqn.6.9) (psi)	W_s	E_t (psi)	E_s (psi)
Min:	3600.35	3.48	1.27×10^6	1.91×10^6
Max:	17966.95	41.33	2.61×10^6	3.91×10^6
Avg:	10856.15	22.48	1.75×10^6	2.62×10^6
Std:	3105.90	2.18	1.53×10^6	2.29×10^6

	σ_c(eqn.2.20) (psi)	W_s	E_t (psi)	E_s (psi)
Min:	4078.85	4.64	1.19×10^6	1.79×10^6
Max:	12694.75	27.41	1.96×10^6	2.95×10^6
Avg:	9056.70	17.84	1.54×10^6	2.31×10^6

<u>6.5.7. Relative indicators of rock strength:</u>

A - Dx Exponent: Dx data was calculated using equation 2.22, and the recorded drill parameters from the sandstone/siltstone test interval, see Table 6.8. The correlation coefficient relating these Dx values to measured compressive strengths was equal to 0.60. The low correlation is similar to that obtained between compressive strength and downpressure, shown in Table 6.9. It is obvious that equation 2.22 is highly dependent upon the downpressure, as confirmed by a coefficient of correlation in sandstone/siltstone of Dx with this parameter of 0.987. The high downpressures measured while drilling in hard rock, cause the response in calculated Dx to be insensitive to rock strength variations. In addition, the rotary torque is not taken into account, further reducing the sensitivity of the model, especially for very high downpressures associated with the harder rock units. This was discussed in sections 6.4.3 and 6.4.4.

B - Kinetic Energy: Comparison of the kinetic energy of drilling using equation 2.39 and 2.40 and the measured compressive strengths gives a correlation coefficient of only 0.437. Regression with respect to downpressure data from the test interval indicates that the kinetic energy is very dependent upon this parameter, where a correlation coefficient of 0.944 is determined. Similar reasons, as for the Dx exponent above, account for its poor correlation with σ_c(meas), see sections 6.4.3 and 6.4.4.

6.5.8. Conclusions:

It is noted that this section is presented only to indicate the potential of estimating rock properties from field monitored drilling performance parameters. The correlations obtained between the combined drill parameters and compressive and shear strength and Young's modulus data were good, yet were based on a relatively small data set of measured rock property values. The correlations also indicate, as in section 6.3 and 6.4, that the mechanisms of rock breakage in hard and soft rocks are different. In soft rocks, it is clear that shear mechanisms predominate, based on the close correlation of combined parameter responses to the shear strength of rock. In harder units, deviations between the shear strength and combined responses is greater, indicating other mechanisms, ie. compressive processes are also operating to break the rock.

The best results were obtained between measured rock strengths and the data from eqn.2.10 for calculated SE(T). It was previously demonstrated in earlier sections that torque was an important parameter in rock breakage processes. This fact was also suggested by its very high correlation with compressive strength in Table 6.9. Therefore, for these reasons and since eqn.2.10 incorporated torque, this equation was considered to be the most appropriate model to simulate the drilling processes operating for this study.

The relationships thus developed demonstrate the possibilities of such an approach, and present the opportunity for more detailed and comprehensive studies to be undertaken in the future.

7.0 APPLICATION OF DRILL PARAMETER RESPONSES TO EXPLORATION:

7.1 Geology of EX Bench, Eagle Mountain:

The relationship between the variations in drilling performance parameters and the properties of rocks at the study site was established in Chapter 6.0. This section will demonstrate how the characteristic patterns of drill parameter response can be used in a practical manner to identify the changing geology on a working bench.

It was shown previously in chapter 4.0 how the patterns in drill parameters were used to identify the changes in the lateral and vertical stratigraphic position of coal seams. These results were illustrated in Figure 4.7, whereby similar patterns of drill parameters for a particular coal seam were correlated between adjacent boreholes to create the cross-section.

In this more recent study, the responses of the drill parameters to rock type was much more clearly established. This was due primarily to the amount of drill data collected in a variety of rock environments and the detailed geological investigations undertaken to confirm these results. Therefore, more accurate stratigraphic sections could be constructed, as will be demonstrated.

In the most recent drill monitoring study at the mine, 58 boreholes, of depths ranging from 64 to 113 feet and spacings of 28 to 35 feet, were drilled in an area having coal seams of up to 13 feet thick. Gamma logs were also obtained in 15 of these previously monitored boreholes. The locations of the drill monitored and gamma logged boreholes are shown in Figure 7.1.

The elevations of the collars of the monitored boreholes were surveyed, and determined to all be at heights of 2255 meters ± 10 cm (see Figure 7.1). The fault trace indicated in this figure at the east end of the bench was inferred by the Geology group at the mine, based on an interpretation of gamma logs from bench levels above the 2255 meter level illustrated.

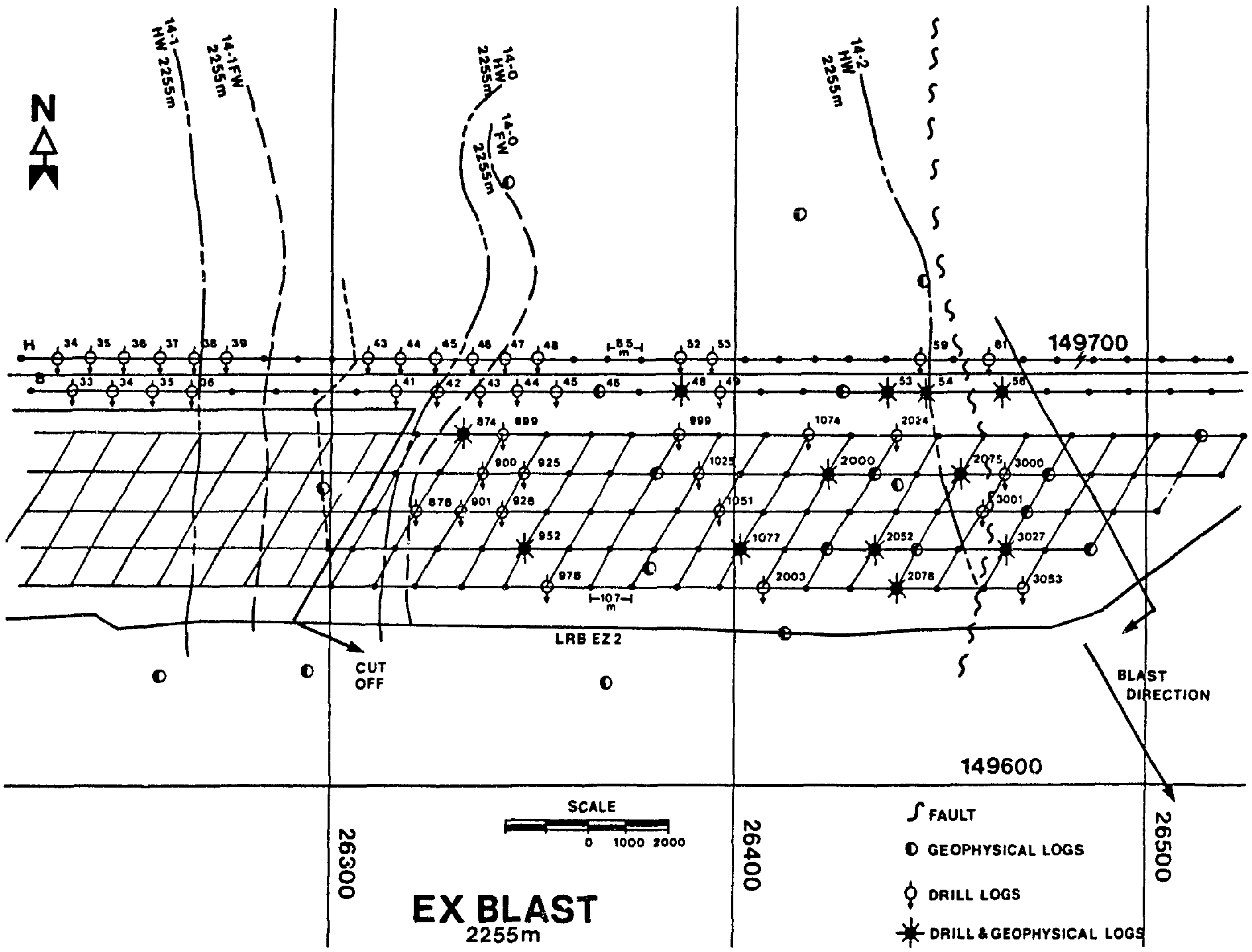

Figure 7.1 - EX Bench, June-July 1988.

Contour lines for the coal seams encountered on this bench are also shown. Note that the bench is oriented in the same direction as the dip for the coal seams, both being parallel to the lines of latitude.

Mapping of exposed faces revealed that bedding dipped 15° to 20° to the west in areas unaffected by localized faulting and folding. However, in the more structurally complex bench locations, bedding was occasionally near vertical as well as overlapped. These results were confirmed by both monitored drilling and gamma logs.

Figure 7.2 shows the drilling, gamma and geologic logs, the latter based on interpretation of the first two logs, for one of the monitored boreholes in this area, EXB54, which intersected two exploitable coal seams 142-2 and 144. Note that seam 144 is divided into two units by a parting of siltstone. A smaller seam is also located at the bottom of the borehole and based on mine cross-sections for the area would most probably be seam 130.

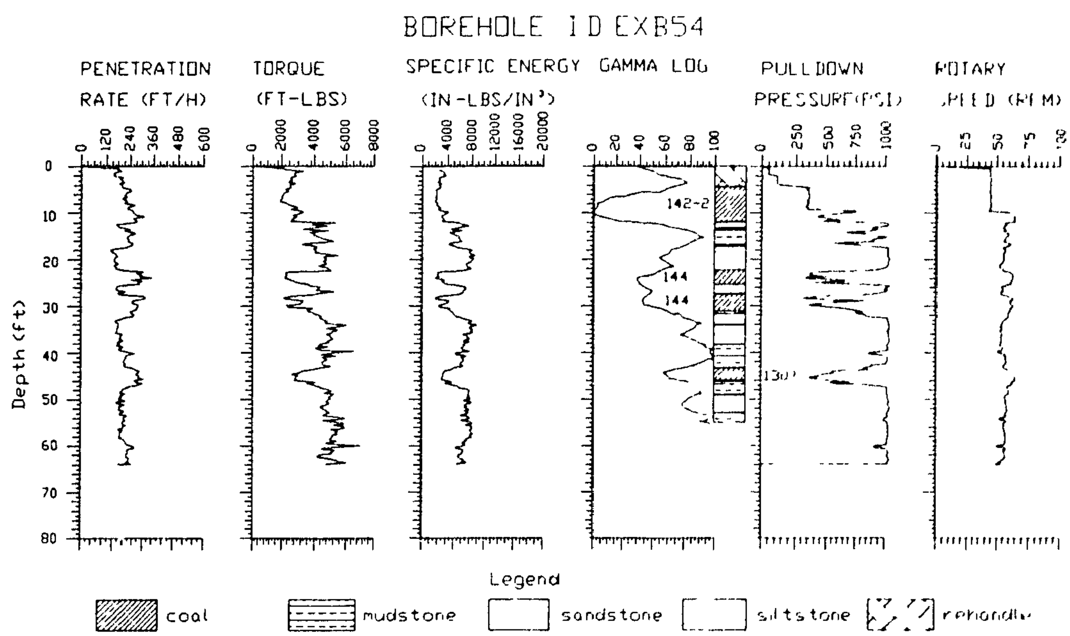

Figure 7.2 - Drill, Gamma and Geologic Logs for Borehole EXB54.

Additional plots of monitored boreholes for this bench are provided in Appendix III.

The stratigraphic section shown in this figure is typical for this bench location, ie. thick coal seams and interburden units of sandstone, siltstone and mudstone. The coal seams are commonly bounded on either their upper or lower (or both) bedding contacts by mudstone units. An example of this feature is indicated in Figure 7.2 for the lower boundaries of seams 142-2 and 144.

In order to examine in more detail the capabilities of drilling parameter responses to identify variations in rock type, a comparison between the drill data and mapped data will be made. With reference to Figure 7.1, the contour line for the hanging wall (HW) of seam 14-1 can be located at the western end of the bench. This line indicates the intersection of this seam with the 2255 meter level, which is the bench level from which all boreholes were monitored in this investigation. This coal seam dips below the bench closest to monitored boreholes EXH38 and EXB36, as shown by the photograph in Figure 7.3.

Figure 7.3 - Coal Seam 141.

Mapping of the face at this location, gave a clear view of the upper contact between the overlying waste rocks and the 141 seam. It was evident that the upper 3 to 5 feet of the coal seam consisted of thin interlaminations of coal, mudstone and siltstone. The zone above this horizon was mainly a thinly bedded and blocky siltstone, with a gray to buff-orange color on its weathered surface. A close-up photograph of the highlighted area in Figure 7.3 is seen in Figure 7.4, which clearly illustrates these features. (The darker bands are coal and mudstone, with the light gray streaks siltstone).

Figure 7.4 - Upper Boundary of Coal Seam 141.

A sketch of the complete section through coal seam 141 as mapped, including its upper and lower waste rock units, is shown in Figure 7.5. This diagram indicates that both the upper and lower contacts of the coal are bounded by mainly mudstone, with smaller partings of siltstone also present. This sequence is similar to what was mapped by Donald (1984) in an extensive study of the relationships between coal seams and waste rock units on Eagle Mountain.

Examination of this section with reference to the drill monitored logs EXH37 and EXH36 revealed remarkable sensitivity of the parameter responses to the variation in rock types. In addition, the pattern of these responses from borehole to borehole was identical, as was the geology within and around coal seam 141. Figures 7.6 and 7.7 are zooms of logs for downpressure (to the right in the figure) and specific energy (SE(T) - left hand side) for drilling through seam 141 in holes EXH37 and 36. The depth increments are in feet. A legend to the patterns for the different rock types is given in Figure 7.8. It was demonstrated in chapter 6.0 that this SE(T) value is very dependent upon torque, which on its own is highly sensitive to the changing strength of rock. Since calculated SE(T) also accounts for changes in the other parameters such as penetration rate, rotary speed and downpressure, it should therefore reflect the net response of the drill to the ground. It was also shown that specific energy is highly correlatable to compressive strength in section 6.5. Therefore, this log should reflect the variations in rock strength within the sequence. Downpressure was previously indicated to be responsive to hard versus soft materials, and therefore higher values would be expected in siltstones and mudstones versus coal.

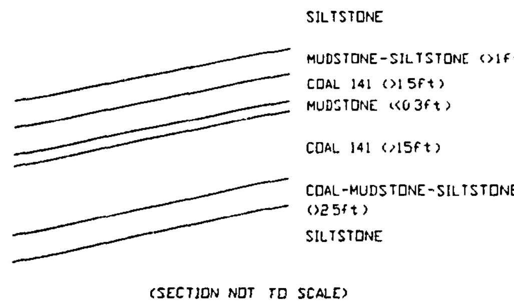

Figure 7.5 - Mapped Sequence for Coal Seam 141.

The boreholes in Figures 7.6 and 7.7 can be seen on the bench plan in Figure 7.1 to be located west of the point where coal seam 141 intersects the 2255 meter level. Since borehole EXH36 is positioned further along the bench (28 feet west of EXH37) and downdip from seam 141, it should be expected to intersect coal

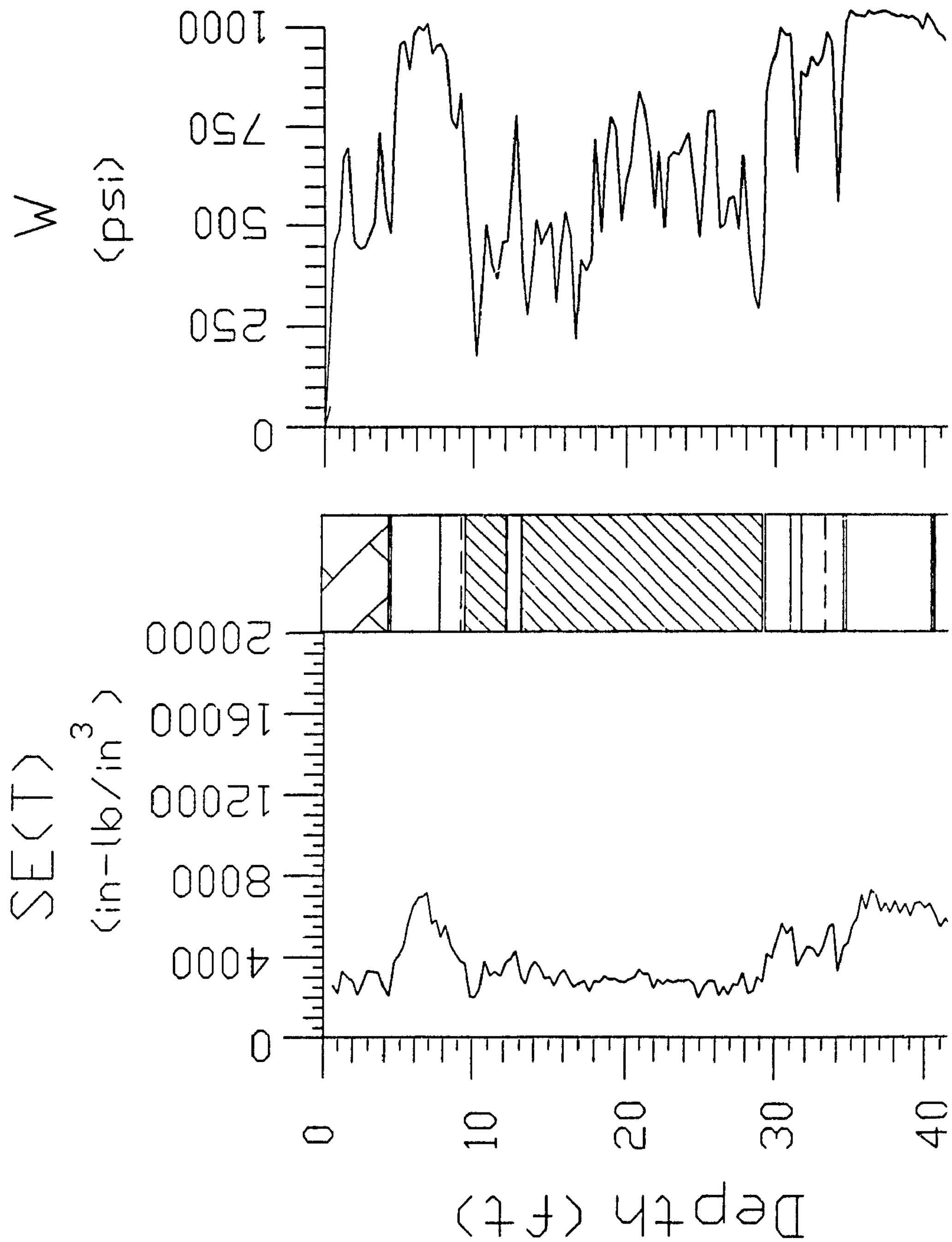

Figure 7.6 - Drill and Geological Logs for Borehole EXH37.

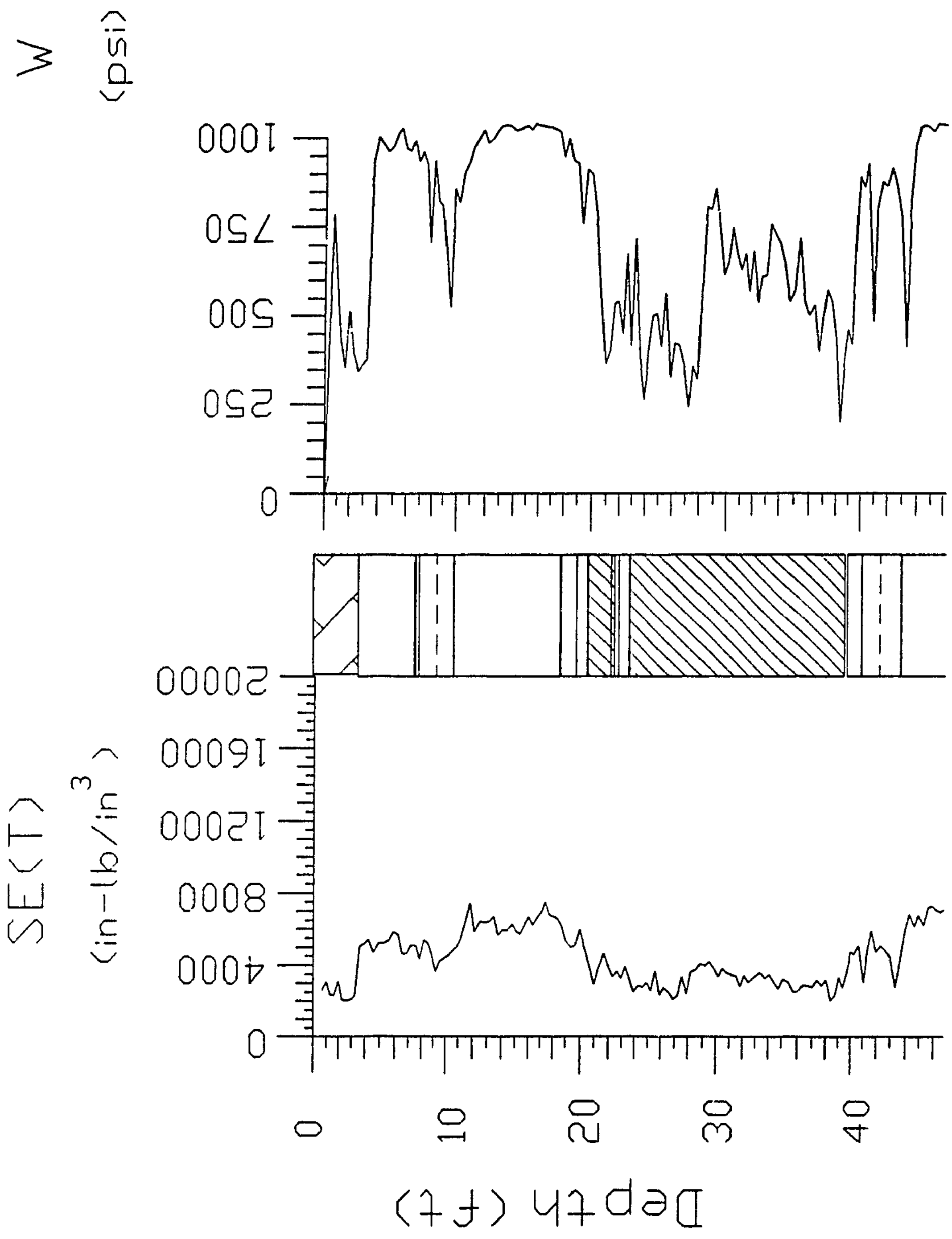

Figure 7.7 - Drill and Geological Logs for Borehole EXH36.

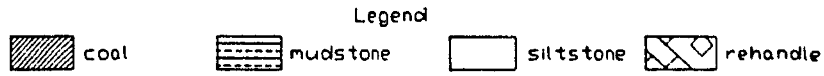

Figure 7.8 - Legend for Patterns in Figures 7.6 and 7.7.

at a depth below where it is encountered in borehole EXH37. Figure 7.6 shows the coal at a depth of 9 to 29.5 feet, while Figure 7.7 encounters the coal from 20.5 to 40 feet confirming this hypothesis.

Comparing these two figures, it is readily apparent that the patterns for specific energy and downpressure for this horizon are identical. The interpreted geologic log indicates the same succession of rock units for each borehole; ie. overlying waste rock bands of siltstone and mudstone (2 to 3 feet thick), followed by an interval of coal seam 141 (2 to 3 feet), separated from the thicker unit of 141 by a thin (1 to 1.5 feet) mudstone parting. Below this parting, 141 seam continues for another 15.5 to 16.5 feet, until a lower contact of thin siltstone and thicker mudstone partings is reached. After this, thicker units of siltstone are present.

All these features are shown by the responses in the two parameters plotted. The sensitivity of the specific energy log as compared to the downpressure, is more subdued, yet is capable of detecting the upper and lower boundaries of the coal with good resolution. (Note: resolution for this case refers to the closeness of the identified depths of coal seams from drill logs with those indicated on mine cross-sections and from gamma logs in adjacent boreholes on the bench). Here, the high specific energies in the harder siltstones and transitional strength mudstones are reasonably contrasted by the lower values in coal. However, the variation in downpressure illustrates much more clearly the differences in the various rock units. As well, the depth locations of even thin partings of mudstone in coal, for example the one in borehole EXH37 at 12 to 13 feet and in EXH36 at 22.5 to 23.5 feet can be detected.

A comparison of these two sequences with the one determined from mapping the face and shown in Figures 7.4 and 7.5, indicate that the drill monitored responses accurately reflect the true geology for this interval. An in-depth analysis of the drill logs for the other 9 boreholes also intersecting coal seam 141, revealed the same degree of accuracy and reproducibility between holes as shown above.

7.2 Statistical Analysis:

An alternate way of viewing the similarities between the drill parameters responses in each of these boreholes, is to examine Box and Whisker plots. These were used in section 6.3.3 to illustrate graphically the particular variations in the drill performance parameters for different rock types.

The statistical data calculated for boreholes EXH37 and 36 are shown in Table 7.1.

Figures 7.9 to 7.12 compare the statistics shown in Table 7.1, calculated on data obtained in EXH37 and 36 while drilling through the same 35 foot section around coal seam 141 (Figures 7.6 and 7.7)

Figure 7.9 shows the penetration rates measured in the two boreholes, where median values of 264.67 ft/h and 265.75 ft/h were obtained in EXH37 and EXH36 respectively. Maximum and minimum drill rates were also comparable, as were the upper and lower quartile values and interquartile ranges.

Recorded torque was slightly higher in EXH36 as shown in Figure 7.10, resulting from the higher rotary speed set by the operator in this borehole. The rotary speed box and whisker plot is not shown, but the median values were 69.1 revs./min in EXH36 versus 62.6 revs./min in EXH37. Figure 7.11 compares the downpressure, and clearly indicates the high correlation in data between the boreholes. Median values of 719 psi and 758 psi in EXH37 and EXH36 were determined. In addition, the median values were

Table 7.1 - Summary Statistics for Boreholes EXH37 and EXH36.

EXH 37:

	R (ft/h)	N (r/min)	W (psi)	T (ft-lbs)	SE(T) (inlb/in^3)
Sample Size:	107	107	107	107	107
Average:	246.87	64.49	715.09	3069.29	3067.57
Median:	264.67	62.60	719.00	2725.07	2609.28
Variance:	6224.33	30.19	60282.90	786357.00	1.3×10^6
Std.Dev.:	78.89	5.49	245.53	886.77	1128.75
Std.Err.:	7.32	0.53	23.74	85.73	109.12
Minimum:	216.75	48.34	179.00	1701.59	1569.74
Maximum:	377.58	76.10	1041.00	4935.99	5513.66
Range:	160.83	27.76	862.00	3234.40	3943.92
Lower Quart:	231.91	60.96	490.00	2408.95	2176.66
Upper Quart:	287.40	68.12	959.00	3814.48	4133.04
Quar.Range:	55.49	7.16	469.00	1405.53	1956.38
COV:	29.8%	8.8%	34.1%	32.5%	43.3%

EXH36:

	R (ft/h)	N (r/min)	W (psi)	T (ft-lbs)	SE(T) (inlb/in^3)
Sample Size:	116	116	116	116	116
Average:	268.97	67.21	742.61	3453.31	3482.21
Median:	265.75	69.10	758.00	3237.67	3096.04
Variance:	1802.24	16.74	62864.50	991688.00	1.4×10^6
Std.Dev.:	42.46	4.09	250.73	995.84	1193.78
Std.Err.:	3.94	0.38	23.28	92.46	110.84
Minimum:	214.35	60.84	199.00	2045.75	1651.15
Maximum:	377.21	72.36	1039.00	5308.40	5681.04
Range:	162.87	11.52	840.00	3262.65	4029.89
Lower Quart:	228.39	62.44	536.00	2521.74	2462.74
Upper Quart:	295.12	70.92	1015.00	4367.75	4655.47
Quar.Range:	66.73	8.48	479.00	1846.01	2192.73
COV:	15.9%	5.9%	33.1%	30.8%	38.6%

bounded by nearly identical maximum, minimum, lower and upper quartile values (see Table 7.1). Calculated COV's also indicate the high degree of similarity in the dispersion in the monitored data between the holes.

Calculated specific energy (SE(T)) is plotted in Figure 7.12, where the median value is higher in EXH36, due to both the higher rotary speed and torque in this hole. However, regardless of this, the absolute values for the maximum, minimum and lower and

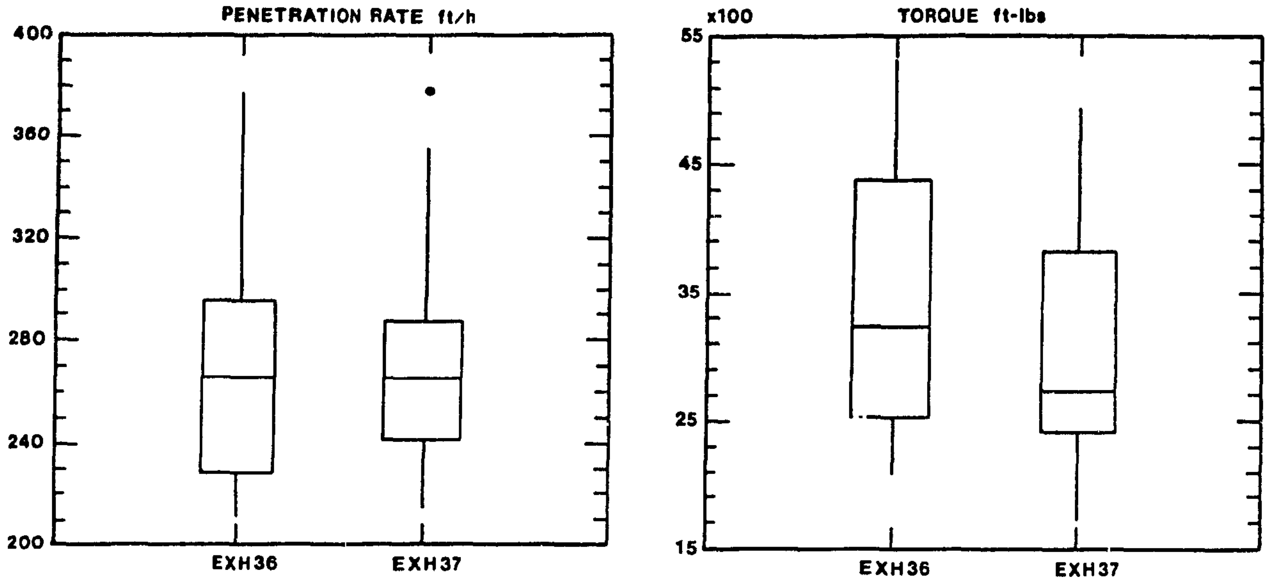

Figure 7.9 and 7.10 - Box and Whisker Plots for Boreholes EXH37 and EXH36.

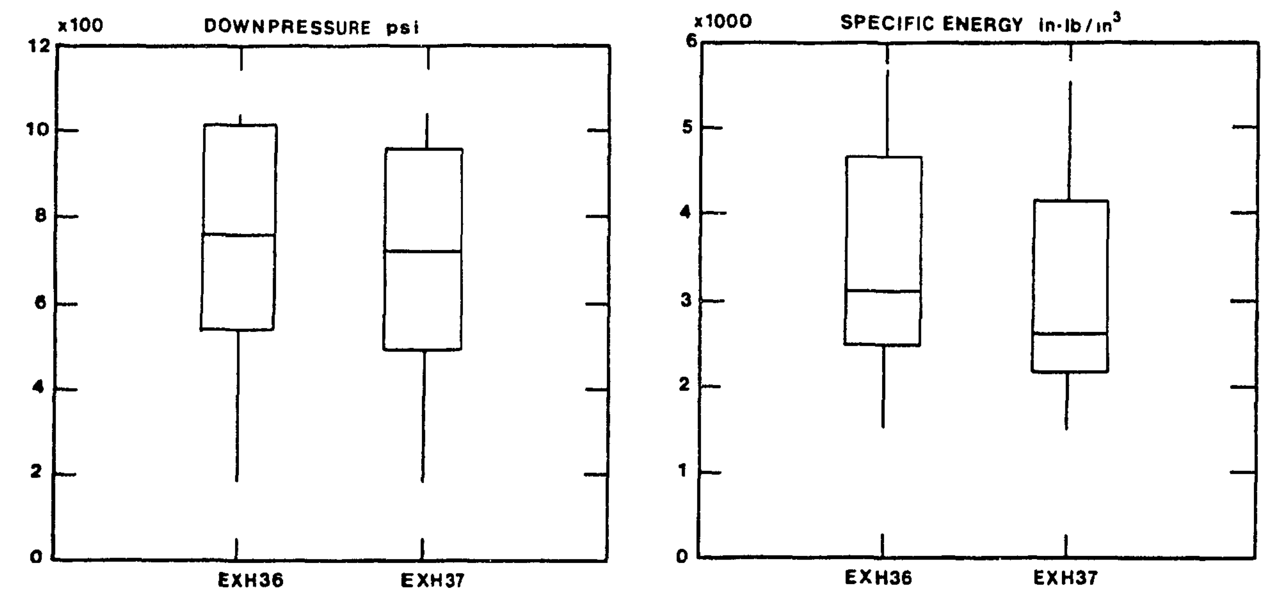

Figure 7.11 and 7.12 - Box and Whisker Plots for Boreholes EXH37 and EXH36.

upper quartiles are very close. The spread in this data in each borehole is also very similar as indicated by the COV's of 43.3% and 38.6% in EXH37 and 36. This point is further demonstrated by both their ranges and interquartile ranges in Table 7.1.

Another visual technique to compare multivariate data sets is to use star symbol plots. These plots were demonstrated in section 6.3.4. These symbols enable a quick, cursory comparison to be made on data sets, both between and within boreholes. Such a visual technique allows the relationships between the various drill parameters and in different rock types to be identified and then compared in a relative manner, without extensive statistical treatment of the data. Figure 7.13 illustrates the key to the star plots developed, using the parameters of penetration rate, downpressure, rotary speed, torque and calculated specific energy (SE(T)).

The data in boreholes EXH37 and 36 for the intervals around coal seam 141, were divided into groups of data sets corresponding to each of the identified rock types previously shown in Figures 7.6 and 7.7. These data intervals were averaged and the star symbols determined and plotted next to the drill and geological logs for each hole in Figures 7.14 and 7.15.

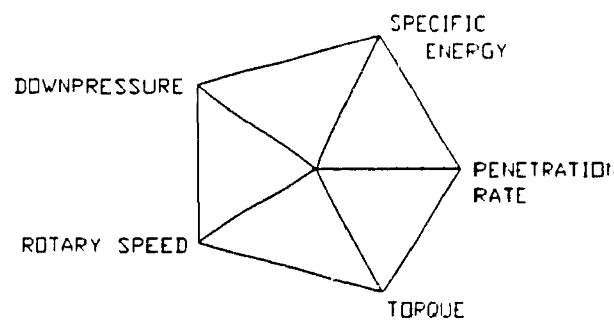

Figure 7.13 - Key to Star Symbol Plots.

Examination of Figures 7.14 and 7.15, reveal that the star symbols for the different rock types are uniquely characteristic. This should be expected since these figures are based upon the ranges of drill parameters, which were demonstrated earlier to be quite distinctive for the various rock types encountered. Comparison of these star symbol shapes with those determined from the extensive statistical treatment of drill data in section 6.3 (see Figure 7.16), indicates the high degree of similarity with the characteristic shapes for siltstones, mudstones and coals. This fact immediately demonstrates that the range of drill parameters acquired from these boreholes correspond to the expected ranges for the rocks present. A comparison of Figure 7.14 and 7.15 further illustrates the similarities between these boreholes, demonstrated earlier using statistical data. Here the drill parameters in the various rock intervals are clearly seen to be nearly identical, based on the likeness of the star symbol shapes in holes EXH37 and 36. Several other examples of this technique are provided, including the complete borehole logs for holes EXH37 and EXH36, in Appendix III.

7.3 Cross-Sections:

On the basis of the interpretation of all the boreholes in this area, using similar techniques to those outlined above, an east-west cross-section was drawn at latitude 149700 (see Figure 7.1). This particular section was selected in that it included the highest number of monitored boreholes (28 out of 58), with all of these intersecting a major coal seam. In addition, the results from 23 gamma logs were also available, either having been logged in drill monitored holes or adjacent to them. It was discussed earlier that this particular bench was complicated by both localized folding and faulting, and therefore the attempt was made to determine the extent to which this deformation had affected the coal seams based solely on the drilling log responses.

The mine had cross-sections developed for this location from their mainframe-based modelling system. These were dependent upon interpreted exploration and production gamma logs and driller reports from adjacent areas and/or levels above the present 2255 meter bench. The cross-section for latitude 149700 (looking north) generated by the mine in this manner, was based on the results from 2 exploration and 9 production gamma logs and is illustrated in Figure 7.17. This vertical section shows the major

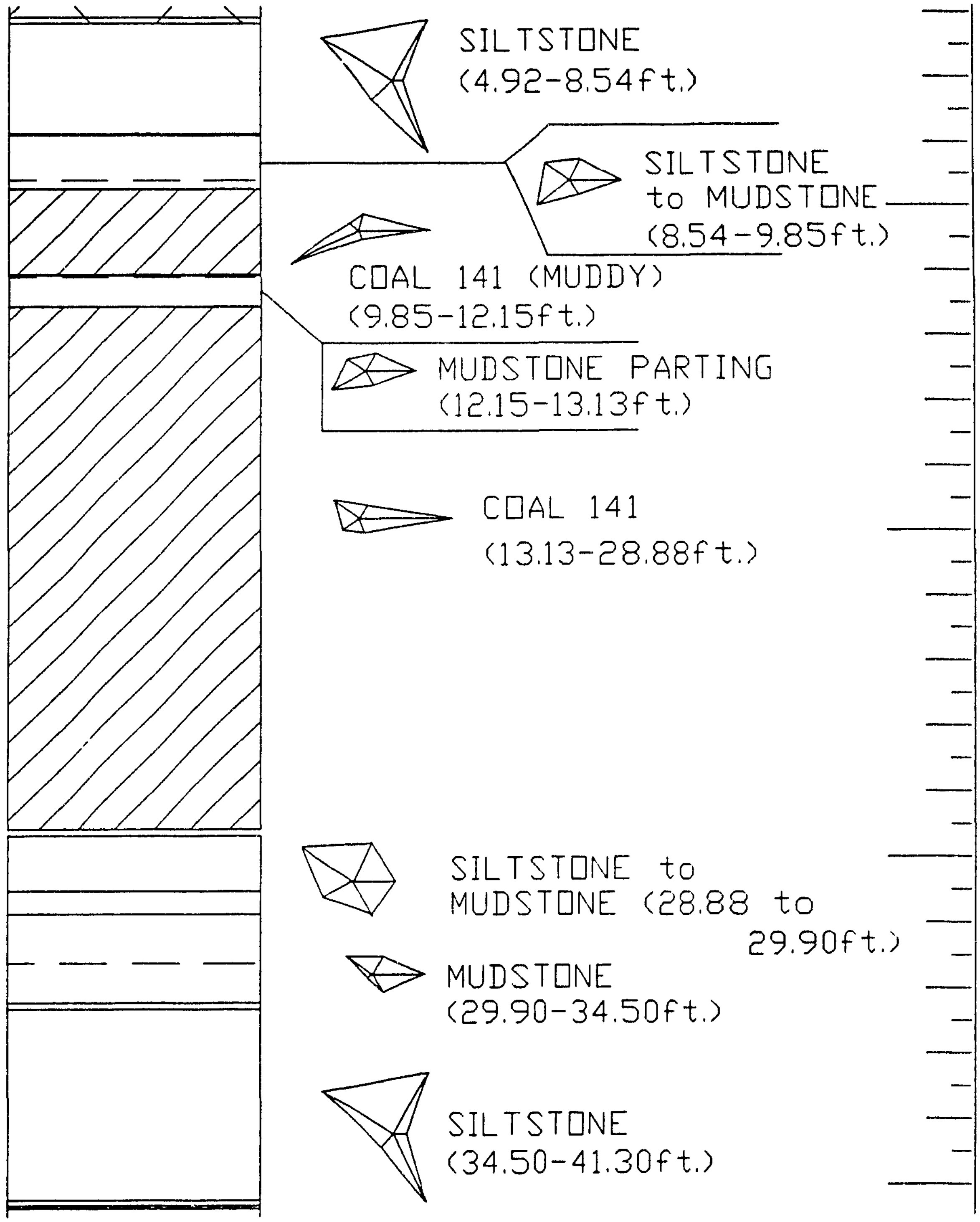

Figure 7.14 - Star Symbols for Borehole EXH37.

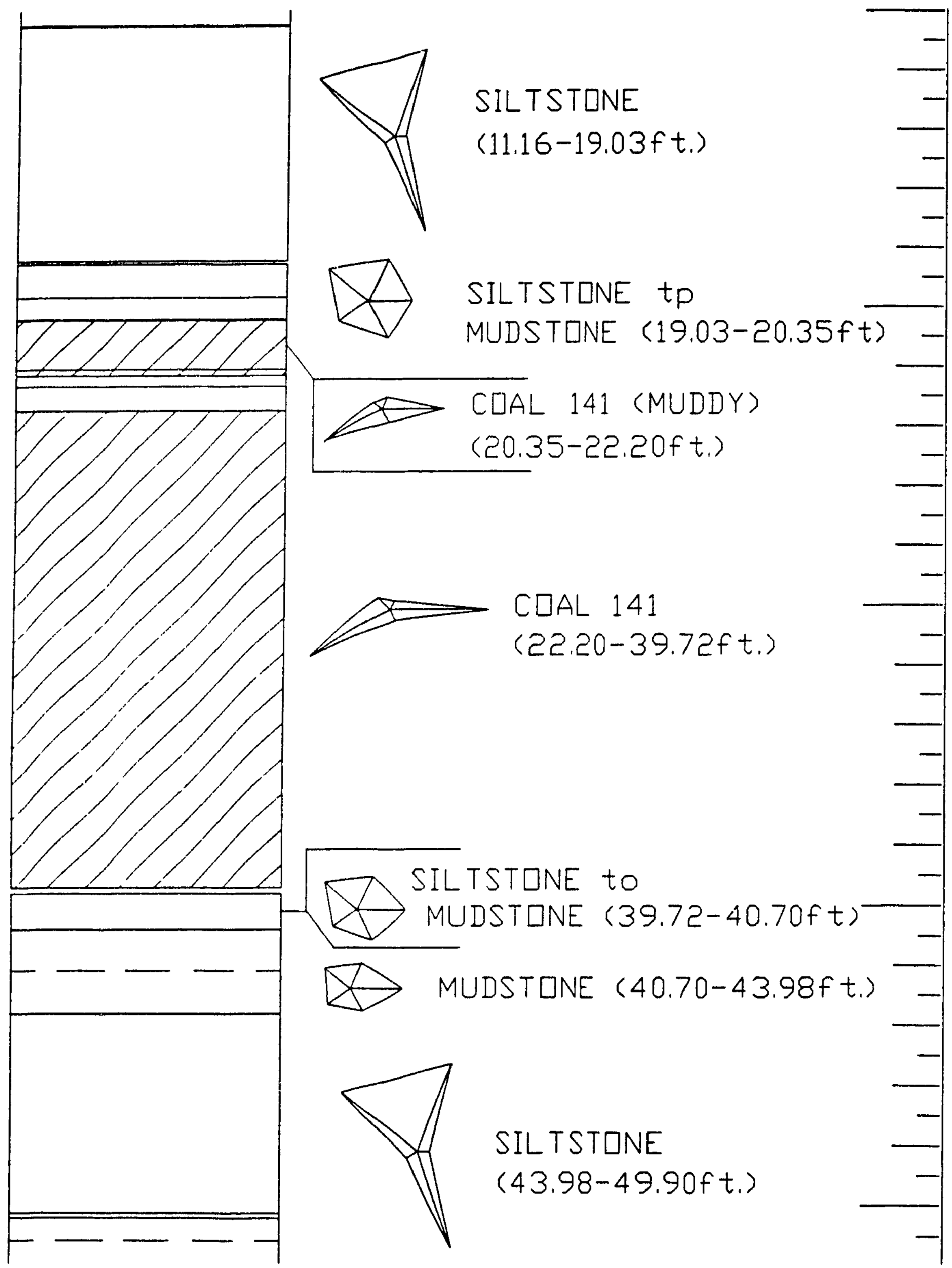

Figure 7.15 - Star Symbol Plots for Borehole EXH36.

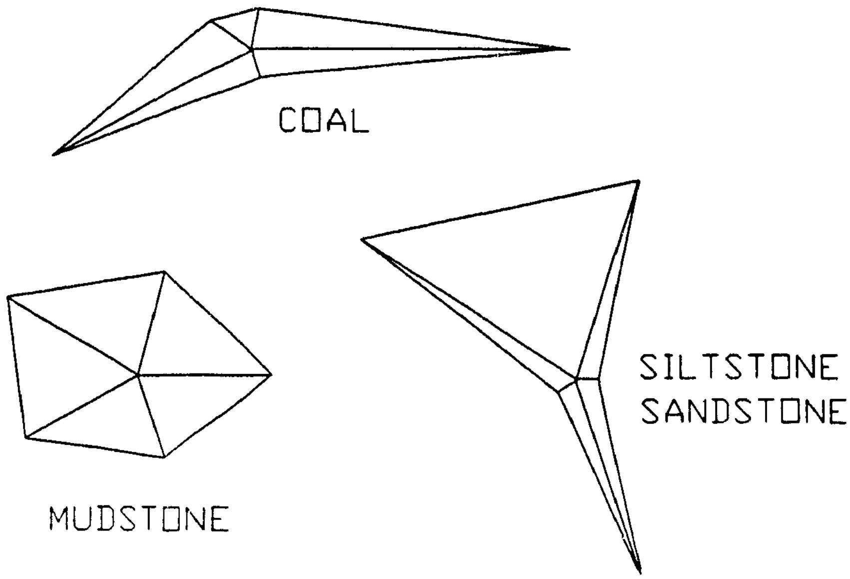

Figure 7.16 - Standard Star Symbol Shapes for the Different Rock Types

coal units for the bench including seams 142-2 and 141 discussed above. A reverse fault is indicated to have displaced the bedding in 142-2 seam, with bedding appearing to be relatively undisturbed.

However, based on drill and gamma log responses obtained in the current study, a vertical section along latitude 149700, shown in Figure 7.18 was created. This figure is clearly very different from the section in Figure 7.17. The same major coal seams are all indicated, except here, seam 199 is also shown. The structure proposed is much more complex than originally indicated. A series of reverse and normal faults and folds were inferred to account for observed vertical displacements of the bedding. These bedding offsets, occurring primarily at the eastern end of the bench, were interpreted from coal intersections identified in drill and gamma logs. The complexity of this area is well known to the mine, yet bench plans do not properly indicate the extent of the structure due to an insufficient amount of exploration drilling.

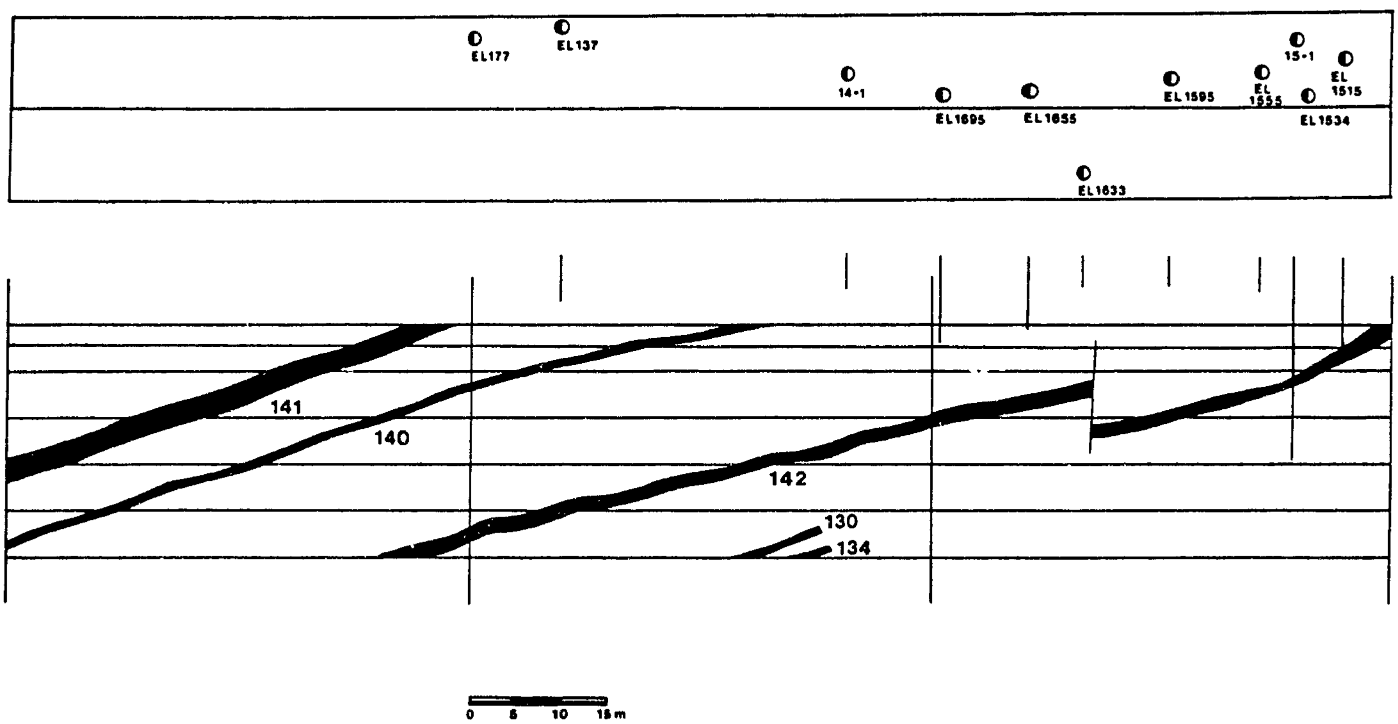

Figure 7.17 - Cross-Section Along 149700; Fording Coal Ltd.

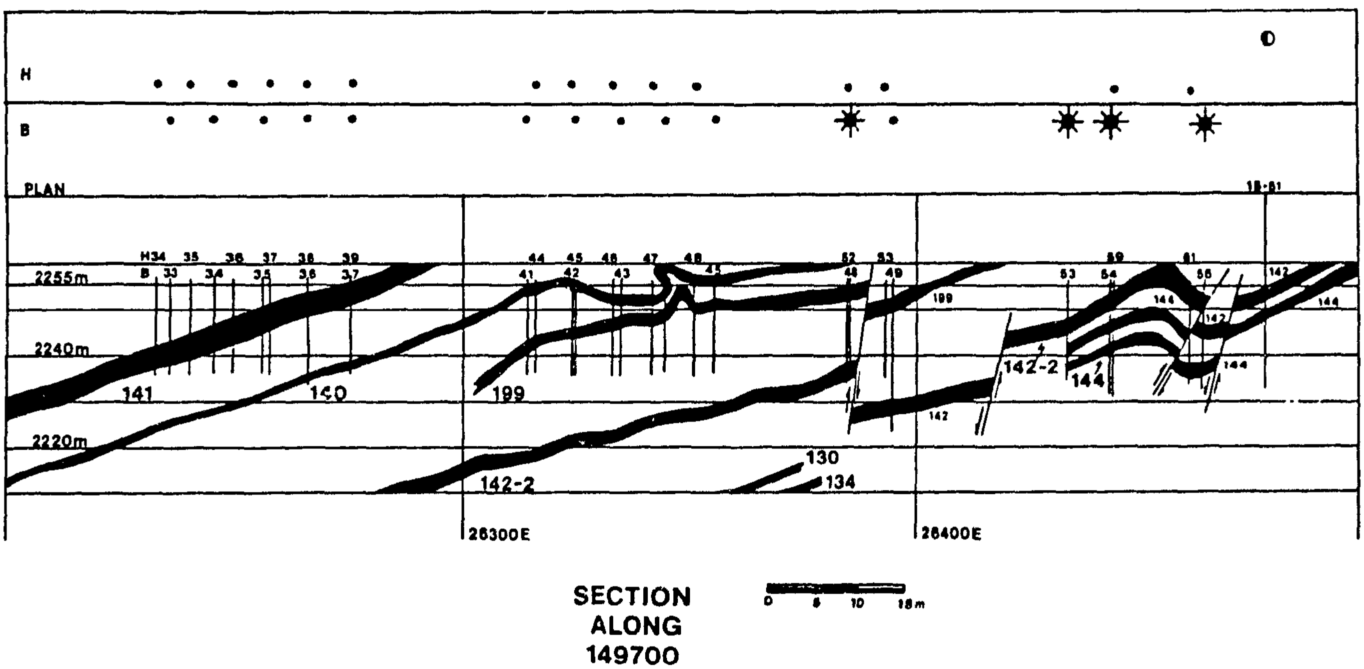

Figure 7.18 - Cross-Section Along 149700 Based on Drill Logs.

The origin of the structures in this area, is the major thrust fault which daylights close (<100 feet) to the eastern end of the EX bench. This thrust is shown on the general east-west cross-section for the mine property, nearly bisecting Eagle Mountain (Figure 4.3). The localized folding and faulting can therefore be related to movement along this main thrust as well as along splays, which branch off from the larger structure.

The section in Figure 7.18 shows the intersection of coal seam 141 by the two boreholes discussed above, EXH37 and EXH36. East of this location, a small drag fold was indicated near the positions of boreholes EXH47 and 48 and EXB44 and 45. This fold was not only based on the displaced locations of coal seams as shown in the drill logs, but was also confirmed by examining the highwall, 15 feet to the north of these boreholes. Figure 7.19 exhibits the geometry of this fold, whereby the bedding, due to the tightness of the structure, can be seen to be nearly folded back over itself. The influence of this fold is very local, and does not extend much below the 2255 meter bench level. Figure 7.18 has drawn in the fold as it is observed above this elevation, to provide a better picture of its effect on the underlying lithologies, ie. seam 199.

Further east of this fold, is an area where monitored boreholes EXH53 and EXB49 had initially intersected seam 199 at depths of 4 and 12 feet. Borehole EXB49 had also encountered seam 142-2 at a depth of 82 feet. In boreholes EXH52 and EXB48, 28 feet to the west of these first holes, seam 199 was located at surface, and seam 142-2 at 58.7 feet in EXB48.

The coal seams 199 and 142-2 should have been intersected in the second pair of boreholes, at greater depths, based upon projecting these units along dip from the initial depth intersections in holes EXH53 and EXB49. Therefore, the offsets observed in the vertical positions of the coal seams were inferred to be the result of a reverse fault located between the two groups of boreholes.

Mapping of the 50 feet high bench face, 15 feet to the north of these boreholes, indicated that a reverse fault at this location was possible. Figure 7.20 shows a reverse fault clearly offsetting the bedding, with an estimated dip separation of 10 to 13 feet.

Other reverse and normal faults were also proposed for the anomalous intersection depths obtained in drill monitored holes for coal seams 142-2 and 144, and are illustrated in Figure 7.18. A fold and its associated faults, were assumed to be the cause of the anomalous coal intersections acquired in boreholes EXH59 and 61, and EXB53, 54 and 56. This fold is displayed in a photograph in Figure 7.21, as exposed on the bench highwall to the north of the monitored borehole locations. A photograph of a combined bedding and drag fault, which results in bedding planes being orthogonal to one another, is shown in Figure 7.22. This fault was located further east of the fold, outside of the EX bench area, and indicates the increasing amount of bedding distortion and displacement as the distance to the major thrust fault diminishes.

Figure 7.19 - Drag Fold, EX Bench.

Figure 7.20 - Reverse Fault, EX Bench.

Figure 7.21 - Fold, EX Bench.

Figure 7.22 - Bedding Fault, EX Bench.

7.4 Conclusions:

This chapter illustrated the capabilities of the interpreted drill monitor data towards geological exploration. Firstly, the reproducibility of the drill data in parallel boreholes was clearly indicated. This was in terms of the similar patterns of SE(T) and W recorded when penetrating both thick coal seams and surrounding waste rock units. Statistical methods further demonstrated the similarities in drilling response in these holes as shown by both Box and Whisker and star symbol plots.

Based on the coal seams identified from the interpreted drill and gamma logs, a revised east-west cross-section was determined. In addition, the correlation of these results with those from face mapping identified several folds and faults. These structures were related to the major thrust daylighting to the east of the monitored area.

8.0 ROTARY TRICONE BIT WEAR STUDIES AT THE FORDING RIVER MINE:

8.1 Introduction:

In this section, bit wear studies conducted during the present thesis studies are reviewed. They were associated with the monitored drilling investigations in order to:

a - determine the nature of the failure, whether progressive or catastrophic,

b - evaluate the possibility of predicting or forecasting bit failure on the basis of specific behaviour in one or several of the monitored parameters (related to a),

c - to assess the overall effect bit wear had on the monitored performance parameters to affect their capability of identifying changing rock mass properties and,

d - to examine the possible causes of the bit wear related to bit design and operation.

An examination of tricone bit wear will be presented based on the monitored drilling investigations conducted at the Fording River Mine. Firstly, a brief review of past studies on this topic will be presented in section 8.2.

8.2 Past bit wear studies:

Very few studies have been conducted to investigate the bit wear characteristics of roller cone bits. Most work with respect to rotary drilling have been undertaken to examine the wear mechanisms of drag or diamond bits, but due to the dissimilarity in their mode of rock breakage compared to tricone bits, they will not be reviewed. Extensive discussions on the wear of these types of bits are given in Clark (1987) and Fish (1961).

Discussion will therefore focus on roller bit studies conducted using primarily steel milled-tooth bits, which have some similarities in terms of wear characteristics with tungsten-carbide insert bits. However, considerable differences are also apparent with respect to the nature of the wear for these two types of bits.

Laboratory investigations by Cunningham (1960) were aimed at evaluating the causes of premature rock-bit bearing and teeth wear. These studies involved the drilling of homogeneous gray granite samples using 7 7/8 inch diameter bits over ranges of rotary speed and weight on the bit. His approach was to measure the tooth height at frequent intervals to determine the level of tooth wear throughout the life of the bit. Tests were stopped when the bit was either 0.180 inch under gage or the teeth were very dull. In these tests the bearings were considered to not be a limiting factor to overall bit life. The results of this work indicated that for constant weight on the bit, bit footage decreased dramatically for higher levels on rotary speed. The drilling rate at any degree of teeth dullness was also observed to be directly proportional to the rotary speed. Similar results were obtained by Morlan (1962).

Studies by Somerton (1959) examined the mechanisms of rock breakage by rotary drilling. In these investigations an evaluation of the effect of bit wear on the drilling performance parameters was attempted. This work involved the use of milled-steel tooth bits, whereby the degree of wear was determined by the reduction observed in the depth of penetration of the teeth for a given weight on bit. The procedure was to weigh the bits prior to the tests, photograph the teeth, and make bottom-hole impressions using modelling clay. Five different test runs were conducted for different levels of rotary speed and bit weight, with weighing, photographs and impressions made after each run. Photographic transparencies were made from the impressions and from these, the cross-sectional areas of the teeth were determined for measured depth of penetration. It was thus determined that the depth of penetration decreased as bit wear progressed, a result of the rounding (dulling) of the individual teeth. Therefore, in order to maintain equal depth of penetration (ie. consistent drill rates) it would be necessary to increase the weight on the bit as the teeth wear. This would in turn speed up not only the further wear of the teeth, but would lead eventually to bearing failure. It was also noted that as bit teeth wore the chips developed became progressively finer. From these tests, Somerton (1959) expressed bit wear as a percentage of the wearable steel remaining on the cones.

Comments by Simon (1959) on the work of Somerton (1959), indicated that the penetration rate was at a maximum for a bit with sharp teeth edges, but so was the torque required to rotate the bit (related to the high depth of penetration of the teeth). Therefore, the power input to the rock is also at a maximum. As the teeth wear during a "break-in" period, the relative rate of decrease of power input to the rock is greater than the relative rate of decrease of penetration rate at constant weight on bit. As wear progressed, the penetration rate was seen to decrease more rapidly than the power input.

For tungsten-carbide insert roller-bits, unlike steel milled-tooth bits, failure is usually the result of bearing failure. Milled-tooth bits also undergo this type of failure but poor bit performance is generally the result of dull teeth. Insert bits, however, were designed to drill at the same rates as the day they were installed, due to the durability of the tungsten-carbide composition of the inserts. This is not always the case as inserts are frequently chipped or broken off due to excessive bit weights and rotary speeds, yet the overall performance is relatively unchanged. As a higher percentage of the inserts are removed, the bearing structures themselves can be damaged due to unbalanced loading and cone shell and excessive gage wear (Estes, 1971).

However, a relationship between the life of the bit and the level of rotary speed at constant weight, still holds true for these types of bits. It is seen that bit life is maximized for lower rotary speeds, while drilling rate is maximized at the highest rotary speed for a particular level of weight on bit. This is mainly related to the fact that higher rotary speeds will damage the inserts in hard or broken ground, which in turn can reduce the life of the bearing structure (Estes, 1971). Therefore, a compromise must be established between these factors to determine an acceptable bit life for suitable drill rates. In the oil industry, generally bit life is sacrificed for maximum penetration rates (Lummus, 1970).

Standards exist for the grading of the degree of wear for insert bits. The method proposed by the Rotary Drilling Committee of AAODC (American Association of Drilling Contractors) is a dull bit code to be used in the field to enable a relative identification of the nature and degree of wear of inserts, bearings and gage. Inserts are graded by the relative percent of total cutting structure gone, while an estimate of the total life taken out of the bearings is made to establish their remaining life. By maintaining records of the progressive wear of the bits, an evaluation of whether or not the bit being used is the most suitable design can be readily determined (Garner, 1971).

Based on a review of the literature, no scientifically based studies have been undertaken with respect to wear using insert bits. Most of the drillability studies conducted in the past account for the effect of bit wear but no one has at yet quantified this property in terms of drilling performance.

<u>8.3 Bit Wear Studies at the Fording River Mine:</u>

During the course of the field monitoring period conducted in the summer of 1988, a total of 186 production boreholes, equivalent to 12,600 feet of linear displacement, were monitored. Over the same period, 3 different bits were used, all of identical diameter, model, type and manufacturer (Table 8.1).

The first bit was monitored for 29.8% of its life or 2390 feet out of a total of 8023 feet drilled see Table 8.2. In addition, this bit failed while the daily monitoring was underway, enabling the recording of the drill performance at the precise moment of actual bit failure. As well, after changing this bit, drill data was acquired for drilling at the same spot as for the failed bit, providing a complete set of drill logs for "old" versus "new" bit conditions, for an identical geological environment. Data from these events form the substance of this chapter.

The second bit was monitored through to the time at which it also failed, equivalent to 6771 feet out of a total 18222 feet drilled, or 37.2% of the bit life (Table 8.2).

This approach enabled the collection of detailed records of the variations in drilling performance coupled with a knowledge of the history of each bit. This bit wear study was aimed towards identifying which of these drill parameters may be affected by and be of use towards actually predicting the degree of bit wear.

Table 8.1 - Tricone bit used during monitored drilling studies:

Manufacturer: - Security Division Mining Operations, Dresser Ind., Dallas, Tx.

Model/Type: - "S" Series, 12.25 inch (311mm) diameter, tricone blasthole bit, model S8M. - tooth-shaped tungsten-carbide inserts

Recommended Use: - formation hardness of: 0 - 20,000 psi (0 - 138 MPa)

(Dresser-Security, 1987)

The procedure thus followed by the author at the beginning of each day of monitoring, was to first determine whether or not the bit had been changed during the previous shift. If it had not, then an examination of the bit was conducted to assess its condition compared to the previous day's monitoring. This would involve the inspection of the tooth-shaped tungsten-carbide inserts on each of the cones, and the cone bearings to see if they turned freely and without grinding. As well the leg wear (gage) protection inserts were examined to see if an excessive amount of wear was developing. It was commonly seen that bit failure occurred most frequently due to excessive wear at this location with subsequent cone roller bearing failure resulting from rock fragments entering through the worn shirttail; see Figure 8.1 for the drill bit nomenclature used in this discussion.

If the bit had been changed, it would be visually examined, and the new serial number and the number of first hole drilled subsequently recorded in the manual logs maintained for each monitored borehole. In addition, the old or failed bit would be inspected in more detail at the end of the monitoring day, to determine the cause(s) of failure. Photographs were taken of the failed bit to record the nature of the failure.

Tables 8.2 and 8.3 show the details regarding 2 of 3 bits monitored during the present investigation. These tables indicate the bit serial number, the footage both drilled and monitored (in parentheses) on a day by day, shift by shift and blast basis, the cumulative footage per day and the total footage drilled and monitored over the life of the bit.

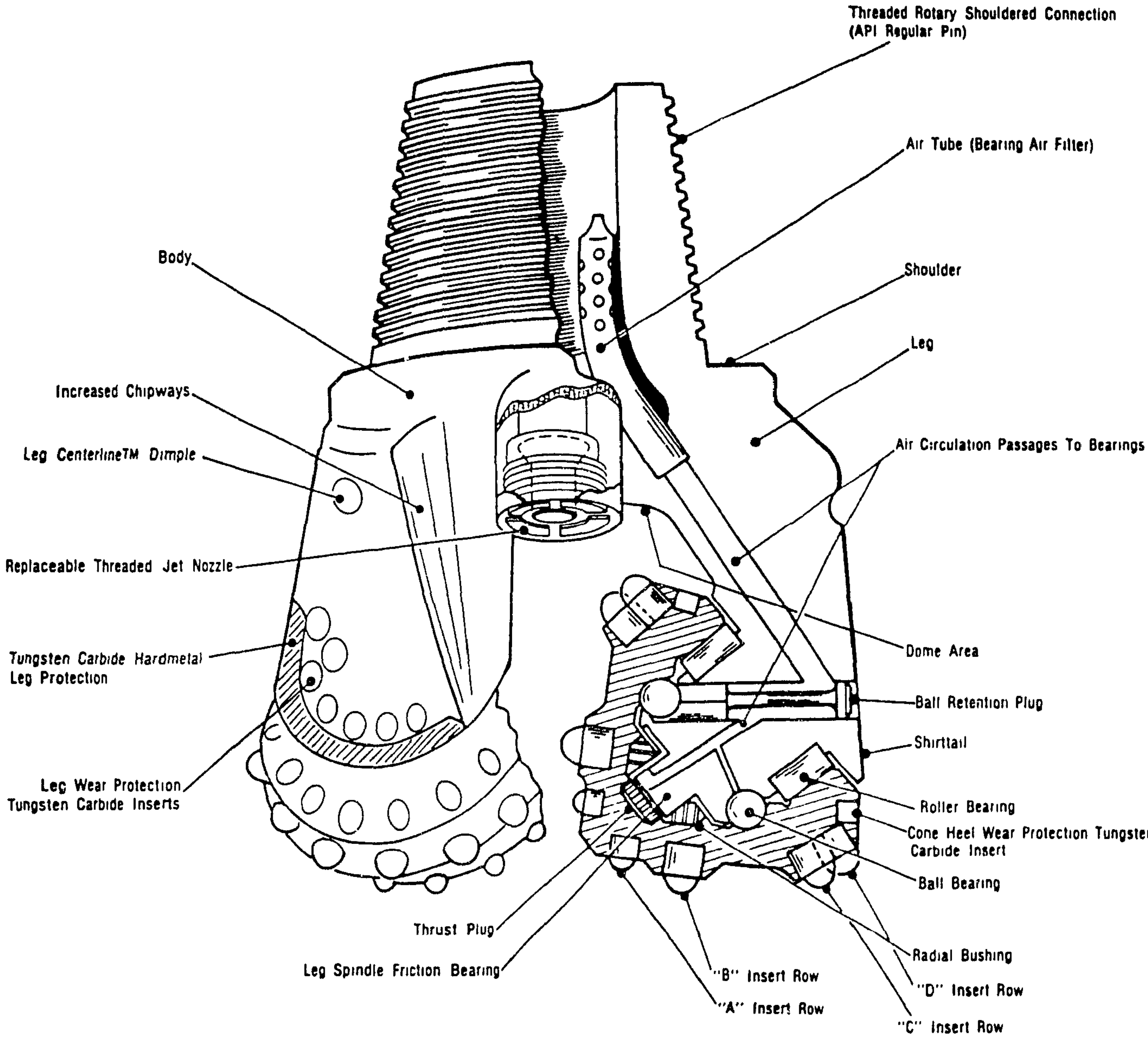

Figure 8.1 - Drill Bit Nomenclature (after Smith Tool International, 1987).

Table 8.2 - Bit Reports, June 1988.

Bit # 474980:

Date:	Shift Footage:	Cum. Depth:	Blast:
June 16	D - 419 (145) N - 865	419	EX
June 17	D - 668 (529) N - 1005	1284	EX
June 18	D - 778 (562) N - 900	2957	EX
June 19	D - 848 (556) N - 865	4635	EX
June 20	D - 726 (542) N - 893	6348	EX
June 21	D - 56 (56) - Bit Fails	8023	EX

Total Footage Drilled: 8023 feet
Total Footage Monitored (#): 2390 feet (29.8%)

Table 8.3 - Bit Report June to July 1988.

Bit # 476472:

Date:	Shift Footage:	Cum. Footage:	Blast:
June 21	D - 1020 (893) N - 896	1020	EX
June 22	D - 1170 (715) N - 213	1916	EX
June 23	D - 635 (128) N - 780	3299	EZ
June 24	D - 895 (780) N - 1102	4714	EZ
June 25	D - 925 (869) N - 975	6711	EZ
June 26	D - 832 (704) N - 1040	8611	EZ
June 27	D - 946 (704) N - 1088	10483	EZ
June 28	D - 50 (P.M.) N - 705	12517	EZ
June 29	D - 514 (514) N - 926	13272	EM
June 30	D - 968 (801) N - 893	14712	EM
July 2	D - 791 (636) N - 858 (bit fails)	16573	EM

Total Drilled Footage: 18222 feet
Total Monitored Footage (#): 6771 feet (37.2%)

The approach to be taken to examine the effects of bit wear, will concentrate mainly on drill monitoring data obtained during the life of bit number 476472. This was due to the fact that monitoring of the drill was essentially continuous from the time that this bit was installed until the day it failed. Thus a complete record of its performance during this period is available for analysis.

Bit #474980:

A preliminary discussion of drill data obtained from two boreholes drilled only 1.5 feet apart will precede this more detailed analysis. This first hole, EXB45, was drilled with bit #474980, which happened to be the last borehole drilled using this bit. The actual moment of failure of this bit was thus recorded in terms of the response exhibited by the drill performance parameters as shown in the plot in Figure 8.2.

This plot shows that the bit failed at a depth of 44 feet, as indicated by the sudden drop in penetration rate and increase in the specific energy. Signs that the bit was not performing properly prior to this point, however, are also very apparent from the very beginning of the borehole. The unusually high recorded torque indicates that the bit was not cutting effectively nor rolling smoothly across the rock. This was the result of the jamming of one or more of the cones due to failure of their roller bearings. The attempt in this case, to rotate a seized tricone bit against rock under an axial load necessitated the development of very high torques in order to overcome resistance to rotation and achieve penetration of the bit. This effort was also accompanied by severe drill vibrations, noted by the author during the monitoring.

The very low and ragged downpressure trace in Figure 8.2 was a result of continuous adjustments to this parameter by the operator to maintain the torque within acceptable limits. Rotary speed remained constant over the entire borehole, with little or no change shown, even at the point of bit failure. Penetration rates showed only a subdued response to the changing nature of the ground, primarily a result of the bit being no longer able to drill the rocks properly. Penetration rates were seen to increase slightly, however, as a coal seam is encountered from 9 to 16.5 feet, with a decrease in torque over the same interval. The response in penetration rate as the bit failed was clearly an indication that the cones were jammed, however, drilling continued for an additional 11.5 feet beyond this point, with associated high torque and vibration.

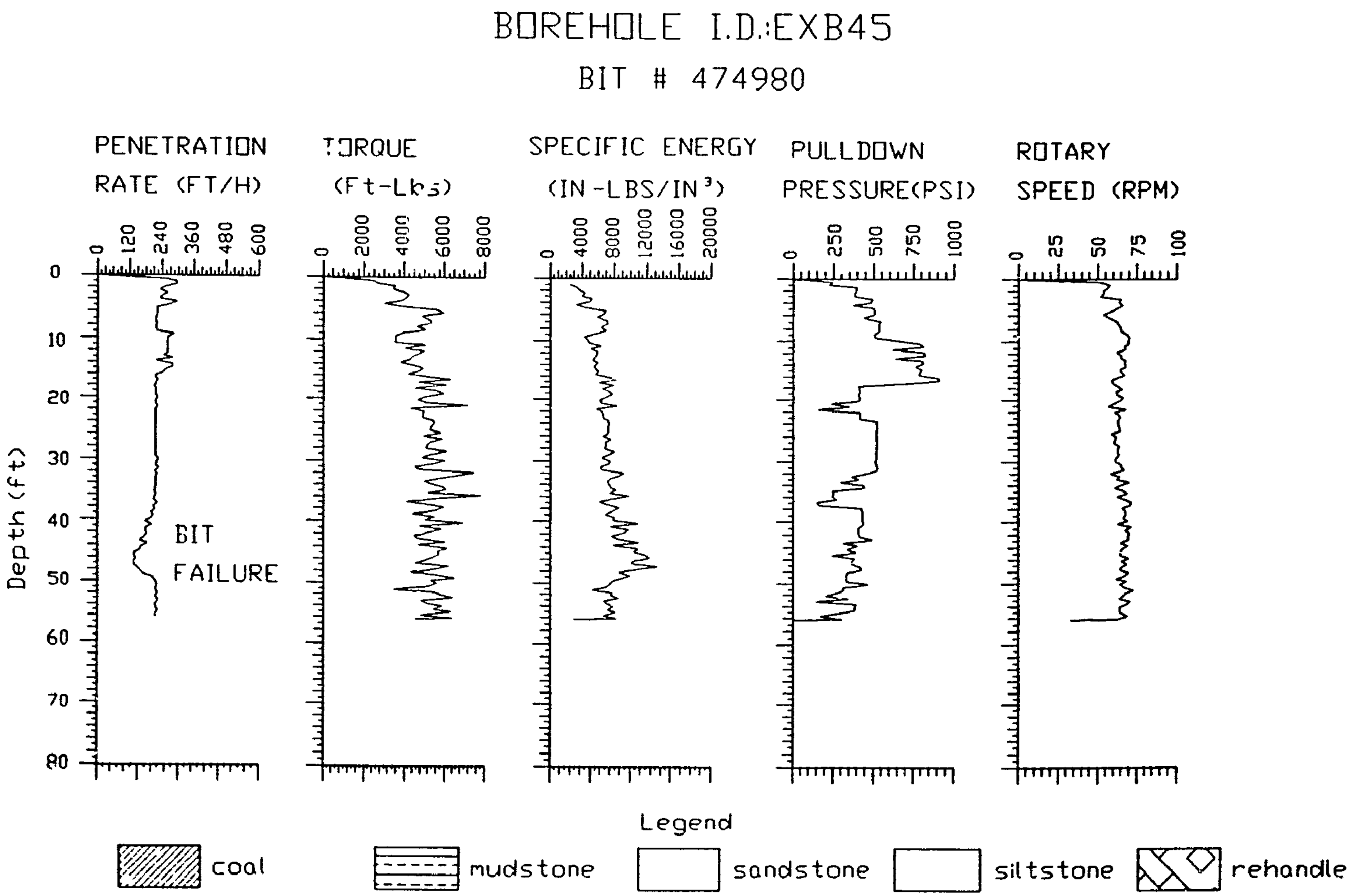

Figure 8.2 - Drilling Logs for Borehole EXB45.

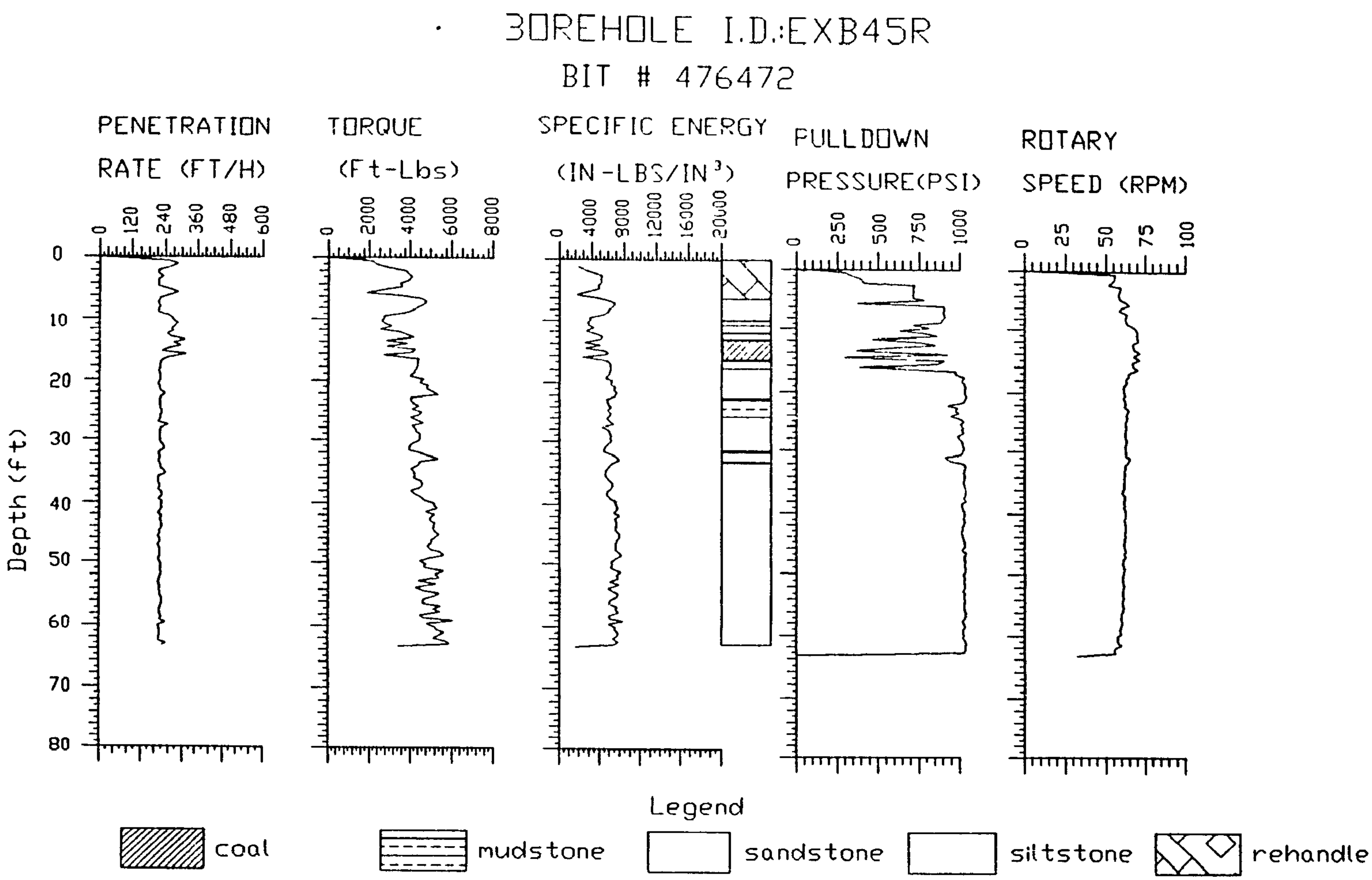

Figure 8.3 - Drilling Logs for Redrilled hole EXB45R.

Note that for these conditions of a severely worn or failed bit, the adverse effect this condition has on the recorded drill parameters negates any attempt at identifying the nature of the rocks being penetrated on the basis of their responses.

After completion of this hole, which caved as a result of the high vibrations generated by drilling with a damaged bit, the failed bit #474980 was changed for #476472. The first hole drilled with this new bit was the redrilled hole for EXB45, or EXB45R, located only 1.6 feet away from the original borehole position. The plot of recorded drill parameters for this borehole is shown in Figure 8.3.

The most apparent differences between Figure 8.2 and Figure 8.3 are the recorded responses in the drill parameters, namely torque and downpressure. In Figure 8.3, since a new bit is being used, normal levels of downpressure were set by the operator. The applied torque should be also lower for this level of applied load than for the previous hole due to the efficient breaking of rock using an undamaged bit. The log for the torque is seen in Figure 8.3 to be lower and more constant than for the same hole drilled with a worn bit (see Table 8.4 below).

The penetration rate in Figure 8.3 does not appear responsive to the changing ground, yet does increase as the coal seam 199 is penetrated from 9 to 16.5 feet. The geologic log shown for the borehole is based upon interpretation of the drilling parameter responses, mainly downpressure,torque and calculated specific energy, and correlation with the gamma log response from an adjacent borehole EXB46, see Figure 8.4. As seen from the geology for this borehole most of the drilling is in harder siltstones and sandstones, consistent with the high, stable torque and downpressure and the low, stable penetration rates thus recorded. Rotary speed does increase as the coal seam is intersected, but for the rest of the hole remains essentially constant.

A statistical analysis of the recorded parameters from borehole EXB45 and EXB45R, ie. for a worn and a new bit respectively,

Table 8.4 - Summary Statistics for Boreholes EXB45 and EXB45R.

EXB45:

	R (ft/h)	N (rpm)	W (psi)	T (ft-lbs)
Sample Size:	114	114	114	114
Average:	147.37	64.64	452.67	5112.08
Median:	136.59	64.65	420.00	5125.41
Variance:	2505.19	17.36	27554.30	872672.00
Std.Dev.:	50.05	4.17	165.99	934.17
Std.Error:	4.69	0.39	15.55	87.49
Minimum:	66.32	52.14	144.00	2476.37
Maximum:	296.14	73.02	911.00	7797.56
Range:	229.82	20.88	767.00	5321.19
Lower Quartile:	112.91	62.74	365.00	4535.76
Upper Quartile:	164.99	67.86	519.00	5697.94
Interquartile Range:	52.09	5.12	154.00	1162.18
COV:	36.64%	6.44%	39.52%	18.23%

EXB45R:

	R (ft/h)	N (rpm)	W (psi)	T (ft-lbs)
Sample Size:	128	128	128	128
Average:	260.98	62.14	934.01	4421.70
Median:	257.88	61.90	1022.00	4472.62
Variance:	884.97	10.81	33440.10	686335.00
Std.Dev.:	29.75	3.29	182.87	828.45
Std.Error:	2.63	0.29	16.16	73.23
Minimum:	153.85	51.98	295.00	1892.29
Maximum:	370.53	71.28	1041.00	6053.22
Range:	216.68	19.30	746.00	4160.93
Lower Quartile:	243.69	60.64	909.50	4075.59
Upper Quartile:	274.31	63.08	1030.50	5070.83
Interquartile Range:	30.62	2.44	121.00	995.24
COV:	11.54%	5.31%	17.89%	18.52%

shows much more clearly the differences in the monitored drill performances for each of these conditions. Table 8.4 shows the summary statistics for the monitored drill parameters in each of the boreholes.

The penetration rate in borehole EXB45 averages 147.37 ft/h versus 260.98 ft/h in borehole EXB45R ie. an improvement of 43.6%. Also it is apparent that the downpressure in EXB45R is 52% higher on average than in EXB45 drilled using a damaged bit. At the same time, the applied torque required to achieve penetration is 13.5% lower on average in hole EXB45R using the new bit.

The continuous adjustment of downpressure by the operator in EXB45, in order to compensate for high torque, is reflected by the large value of 39.52% for the COV in Table 8.4. This value (coefficient of variation) indicates that the variation in the recorded downpressure data in this hole has a much wider range than the data acquired for monitoring in EXB45R, where a COV equal to 17.9% was calculated. In this latter borehole, the variations which are observed were mainly a result of the drill reacting to changing ground characteristics, for example when drilling through softer coals and mudstone horizons and rehandle. The dispersion of the torque data in both the boreholes is about the same as seen by a COV in EXB45 of 18.23% and 18.52% in EXB45R. However, in EXB45 the torques are generally much higher.

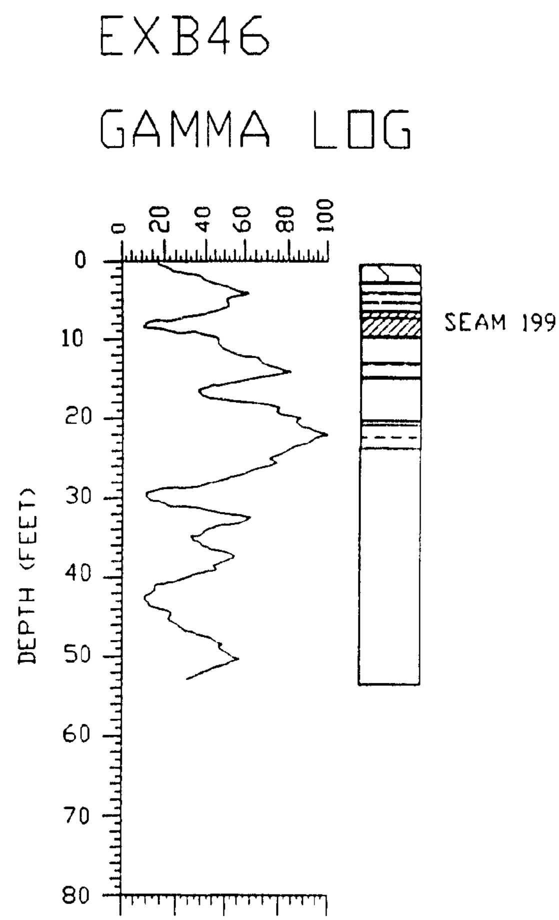

Figure 8.4 - Gamma and Geologic Log for Borehole EXB46.

A visual means of illustrating the differences in the drill performance parameters between the two boreholes is provided in Figures 8.5 to 8.8. These Box and Whisker plots were discussed in section 6.3.3.

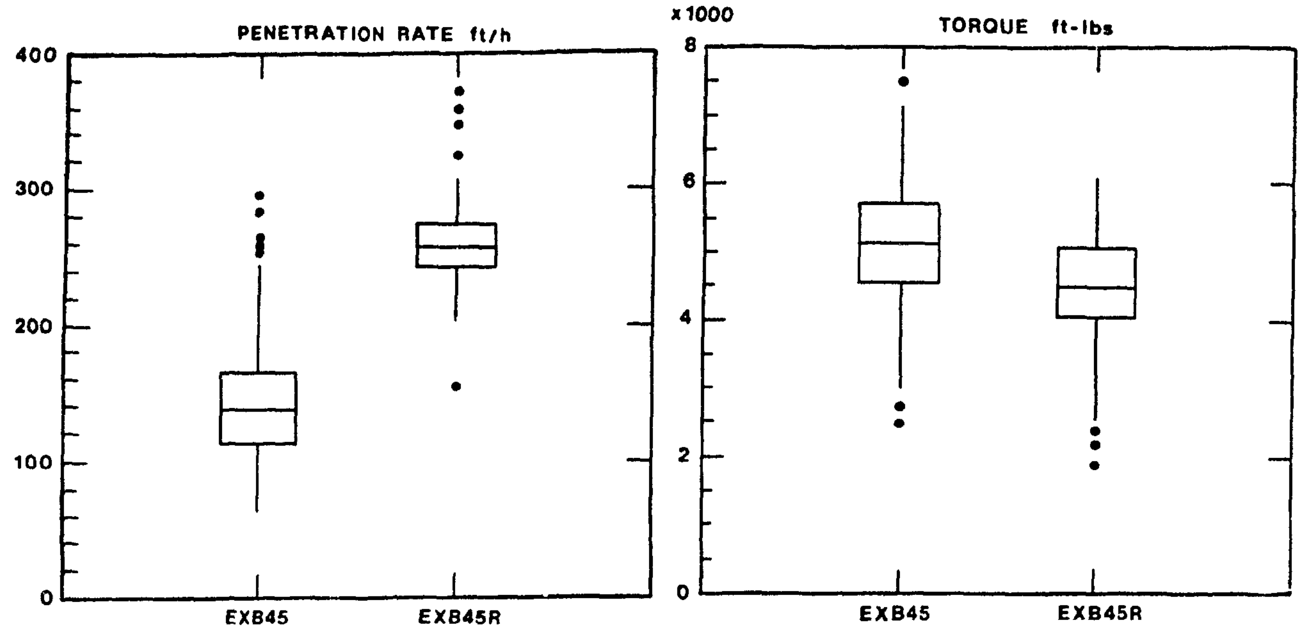

Figures 8.5 and 8.6 - Box and Whisker Plots for Boreholes EXB45 and EXB45R.

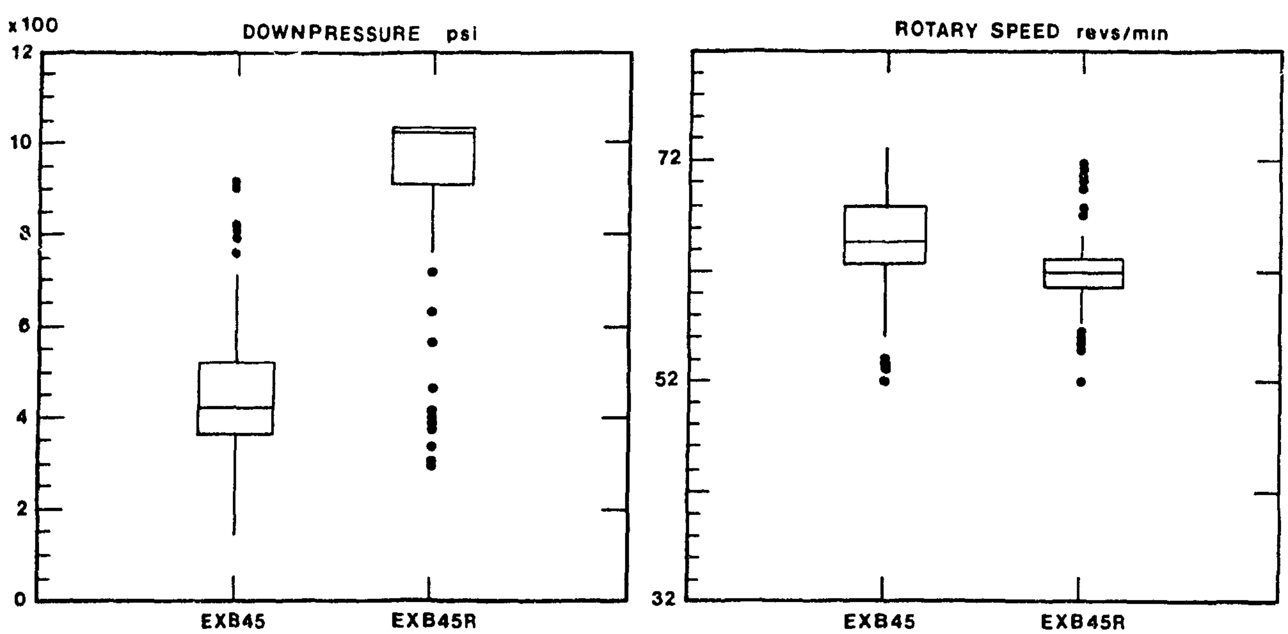

Figure 8.7 and 8.8 - Box and Whisker plots for boreholes EXB45 and EXB45R.

Figure 8.9 - Failed Bit #474980.

Examination of the failed bit #474980 (Figure 8.9) after it had been replaced revealed several interesting points. Two of the three cones were completely jammed, with the third cone able to rotate only slightly. With reference to Figure 8.1 and Figure 8.9, cone #1 had apparently been seized for a considerable period of time, as indicated by the degree (worn smooth) and irregularity of wear of its "C" and "D" row inserts and gage (cone heel) inserts. In addition, several of the inserts have been broken off as seen in Figure 8.10. This photograph also shows that the "A" row inserts, along with the actual cone material, have been worn/broken right off, exposing the actual end of the journal (thrust plug). The same type of wear was shown by cone #2 (Figure 8.11).

Breaking of individual inserts is usually an indication that (1) the bit was improperly broken-in; (2) the bit is the wrong type for the formation being drilled ie. a harder formation bit with shorter inserts may give better performance; and (3) improper use ie. lower applied weight and rotary speed should be used when drilling in rehandle and when collaring, as well as reducing bit vibrations whenever possible. Wear of the cones may be due to inserts which are too short or have been broken off previously, directly exposing the cone shells to the rock. The observed cone

Figure 8.10 - Cone #1, Bit #474980.

wear, could also be a result of the bit rotating about a line other than the center line of the bit. When this occurs, rings of uncut rock are left on the bottom of the hole which wear or break the inserts and subsequently wear against the cone shells. This condition usually is a result of using the wrong bit and/or rotary speeds which are too low. Instead a bit having a higher offset resulting in faster penetration rates should be used along with higher rotation speeds. This type of wear could also develop when drilling softer rocks, where the borehole wall could break down and the bit "walks". A stabilizer is used behind the bit at the minesite, and therefore this problem should be controlled or reduced.

Unbalanced cone wear could also develop from the "balling" of the bit. Excessive applied downpressures and resulting high

Figure 8.11 - Cone #2, Bit #474980.

penetration rates in softer formations, can result in bit floundering. When this occurs, the cones are restrained from rotating, and with further rotation those inserts protruding downwards are worn excessively or broken off. Continued use of the bit will result in excessive cone wear due to the lack of, or reduced protection offered by the broken or worn inserts. The use of the improper bit type may also create bit balling because of inadequate insert spacing. Here, the broken material packs between the rows of inserts, once again reducing or preventing cone rotation. The inefficient removal of cuttings from the hole is frequently a contributing factor to bit balling (Benston, 1956).

Figure 8.12 shows that the shirttail on the #3 cone was worn down to the point that the roller bearings of this cone were

Figure 8.12 - Shirttail of Cone #3, Bit #474980.

exposed. Subsequent jamming of the roller bearings of bit #474980 resulted due to the intrusion of dust/rock fragments etc. through the worn opening. Note in Figure 8.13 that the "C" and "D" row and gage wear protection inserts on this cone have been broken off or completely removed, probably after the cone bearings jammed.

The shirttail wear could have developed from the "milling" of cuttings around the bit prior to being lifted up the annulus. As well, excessive gage wear could also be due to the use of the wrong bit type, ie. possibly one with less offset and greater gage wear protection should be used. This condition could also be enhanced by excessive rotary speeds in highly abrasive formations (Benston, 1956; Garner, 1977).

Figure 8.13 - Cone #3, Bit #474980.

The presence of a few broken inserts should not affect the performance of this type of bit very substantially. The design of the bit enables good penetration to be maintained throughout the life of the individual tungsten-carbide inserts. However, as the number of broken inserts increases, the loading of the bit becomes uneven, resulting in insert and bearing damage. This imbalance in load distribution is manifested by bit bouncing, with the resulting vibration further affecting the roller and ball bearings in the cones. Excessive insert breakage, however, may reduce the protection provided to the cone shells thus also contributing to bearing damage.

As the bearings (roller and ball) of one cone become damaged, the load imbalance thus developed will be transmitted to the other cones. Therefore, the primary reason proposed for bit failure is due to cone bearing damage, caused by several related or independent factors: (1) excessive shirttail and/or cone wear allowing entry of cuttings onto bearings, (2) excessive downpressure (while collaring and during routine drilling) and rotation promoting premature failure of the bearings through overloading (also due to the use of the wrong bit not rated either for the encountered formation hardness or the applied weights), and (3) blocked air jets (a condition enhanced by poor cutting due to a worn bit or balling of the bit in softer formations), thus preventing sufficient cooling of the bearings and inefficient cuttings removal.

Excessive shirttail and gage wear are the reasons for the failure of bit #474980 as witnessed by Figure 8.12. Failure may have also been premature due to both the high strengths of rocks at the site and the applied loads being in excess of the rated values of formation hardness and downpressure for this bit. However, the progressive steps leading to the eventual total failure of this bit seems to have been the following; Excessive wear of the cones (possibly due to prior breakage of several "A" and "B" row inserts, bit balling etc.) for both cone #1 and #2, led to the jamming of the bearings from the entry of rock fragments through worn openings. Probably cone #1 was the first to jam, judging by the degree of wear of its "C" and "D" row inserts, followed by cone #2. The failure of cone #2 was probably also assisted by the imbalance created by the bearing failure in cone #1. Following this, the imbalance of the applied load promoted the rotation of the bit to become eccentric, causing excessive shirttail wear for cone #3, exposing its roller bearings. Jamming of these by rock chippings, and damage from load imbalances, eventually led to the complete seizure of the bit in borehole EXB45.

Bit #476472:

As shown in Table 8.3, 6771 feet of the total footage drilled with bit #476472 was monitored. This particular study was unique in that the majority of the boreholes drilled were in waste rock with only several thin, mudstone or coal partings present. The dip of the bedding in this area was shallow (< 10°) to sub-horizontal, and so the rock units encountered in each monitored borehole are assumed to be similar, both stratigraphically and compositionally. This approach is supported on the basis of results from both gamma and core logs in this area, that identify the predominance of thick, massive sandstone/siltstone units. The geology can therefore be considered reasonably constant for the study area, consisting of mainly sandstones and siltstones (up to 80% of intersected units). This assumption is further supported by the ranges of the data, determined from a statistical treatment of the <u>averaged</u> drill performance parameters for the complete length of borehole (Table 8.5). The ranges of data shown in Table 8.5 for 29 boreholes, conform to those determined for drilling in homogeneous sandstone/siltstones and shown in Table 6.4. Due to the inclusion of the drill data for mudstone and coal parting intersections, the average downpressure is lower (17% less) and more widely dispersed (COV = 18%) than would normally be expected in sandstone/siltstones. This variation is also the result of the bit wear, to be demonstrated in subsequent discussions. The recorded torque, however, shows an average value higher than that in Table 6.4, with a spread in data about normal for harder rocks (COV = 9.56% vs. 10.6%).

The philosophy used in analyzing the data from the monitored boreholes was that variations with time should reflect the wearing of the bit. Trend analysis techniques were utilized to determine if there were any "trend" relating the length of drilled footage (increasing with time) to the responses of the monitored data. These methods are useful for predicting the future values of a time series, and it was anticipated that such a technique would enable a means of forecasting bit failure on the basis of decaying drilling performance. Similar statistical

Table 8.5 - Summary Statistics for Monitored Boreholes Used in the Bit Wear Study.

	Bit # 476472:				
	R (ft/h)	N (rpm)	W (psi)	T (ft-lbs)	I (psi)
Sample Size:	29	29	29	29	29
Average:	215.15	59.91	848.89	4770.89	22.16
Median:	211.77	60.07	874.10	4859.11	21.84
Variance:	231.69	23.49	24588.40	215602.00	1.77
Std.Dev.:	15.22	4.85	156.81	464.33	1.33
Std.Error:	2.83	0.90	29.12	86.234	0.25
Minimum:	189.15	47.81	431.72	4098.55	20.61
Maximum:	243.17	71.83	1013.99	5587.91	26.28
Range:	54.02	24.04	582.27	1489.36	5.68
Lower Quartile:	207.56	56.89	777.86	4325.71	21.22
Upper Quartile:	222.32	62.68	975.91	5129.07	22.49
Interquartile Range:	14.75	5.79	198.05	803.36	1.27
COV:	7.19%	8.07%	17.94%	9.56%	6.10%

methods have been used in the oil drilling industry to attempt the same end. Data for estimating the life expectancy of a particular bit are developed from collecting extensive field data. Laboratory tests using various bit designs and levels of rotary speed and weight on bit, establish ranges of penetration rates in different rock types. This data is combined with the field data enabling mathematical predictive models of bit life to be established (Lummus, 1970). However, the bit life predictions are not as accurate as the penetration rate estimates according to Estes (1971) due to other factors besides the weight to rotary speed operating conditions which affect bit life.

Trend analysis procedures fit a line through the time-series data in either a linear, quadratic, exponential power curve or S-curve manner. The linear trend is based on fitting a straight line having the equation Y = mx+b through the data. The quadratic curve is based on the function $Y = a+bX+cX^2$, which fits a curved line through the data. Both methods use least squares for estimating the coefficients. The exponential power curve is based on the function $Y = \exp(a+bX)$, which fits an exponential growth curve through the data. Coefficients are obtained by least squares after taking the natural logarithm of Y. This type of trend analysis is useful for data that decreases or increases at a nonconstant rate (Statgraphics Manual, 1987).

For the time period shown in Table 8.3, the net amount of time that the bit is actually in contact with the rock per day is about 8.2 hours. This is in terms of actual drilling time, based upon an average penetration rate of 215.15 ft/h for a total drilled footage, for the 8 day period between June 23 and July 2, of 14065 feet. This low value indicates how much time in the actual 12 hour shift that is taken up by other tasks. These include drill propelling, positioning and levelling, collaring each hole, cable handling, locating drill stakes, changing drill steel, reaming/cleaning the boreholes, lunch breaks and travel time to and from the drill to the dry.

This net drill time of 8.2 hours is therefore the spacing between the beginning and end of a typical monitoring period (ie. on a per day basis and represented by a group of boreholes) for this particular study. Assuming this approach is valid, the averaged drill data can be considered equally-spaced in time and thus suitable for treatment by trend analysis techniques.

It was already clear from the brief analysis of boreholes EXB45 and EXB45R above, that downpressure and torque were important indicators of bit performance. The general overall trend seen in that study was that downpressure and penetration rate were much higher and torque lower and consistent (within the same rock type) for a new bit, as compared to the lower downpressures and drill rates and higher, more variable torque observed at the end of a bit's life. The question is, does bit wear develop progressively, or is it a sudden (catastrophic) occurrence or both? If this process *is* progressive, then the change in response of the drilling parameters from those seen in EXB45R (new bit), to those recorded in EXB45 (old bit), should be also. If the speculated progressive changes (either decreasing or increasing) in the drill performance parameters do not occur at a constant rate, it may not be possible to fit a particular trend analysis equation to the data. Also, if the process is a sudden one, then the parameters may not show any deviations from their normal trends over time which could indicate bit wear, until just prior to failure. This possibility may again prevent fitting a trend analysis equation to the data. Possibly bit wear is a combination of factors, where normal wear of the inserts occurs as a progressive process, up until the point that the bearings also start to fail for any number of reasons with the rate of the process increasing through to complete failure.

This is apparently what occurred, based on the analysis of the data for bit #476472. Trend analysis of the recorded downpressure, W, for these boreholes gives the following quadratic trend equation,

$$W \text{ (psi)} = 657.73 + (51.37 \cdot X) - (1.964 \cdot X^2) \quad \ldots 8.1$$

where X is a time index used for the analysis. Here, X is based on the number of (equally-spaced) data points used in the analysis, with a maximum value equal to the total number of boreholes in the study, 29. Therefore, the first borehole drilled, EZ1163, has a X value equal to 1, while for the last hole EM 186, X is 29. Relating this to an actual time base, the range of X or actual hours drilled over the monitored life of the bit, is equal to 65.5 hours (total footage/average penetration rate), or 8.2 hours per day. Assuming that the 29 boreholes listed in Table 8.6 are equally-spaced in time, X then equals the time span between boreholes of 2.26 hours. The drilled footage between boreholes would therefore be equivalent to 486.2 feet and on a per day basis equal to 1764.2 feet.

For the purposes of equation 8.1, however, the values of X are related to a number between 1 and 29 rather than a specific time or footage base. However, utilizing the fact that X = 2.26 hours or 486.2 feet, the time drilled or cumulative footage of the bit at any point on the curve in Figure 8.14 can be determined.

Data conforming to equation 8.1 are plotted in Figure 8.14,

Table 8.6 - Averages of Drill Data for 29 Boreholes.

HOLE:	R(ft/h):	I(psi):	W(psi):	N(rpm):	T(ft-lb):	SE(T):	DH:	ENERGY:	DEPTH(ft):
EZ1163	243.17	22.15	784.81	53.26	4180.89	3622.08	0.55	34016.54	3299.00
EZ1164	210.08	22.27	777.86	58.62	4098.55	4428.73	0.61	37880.12	3299.00
EZ1255	208.42	21.00	850.16	59.74	4159.86	4613.25	0.62	41439.36	4714.00
EZ1132	239.44	21.96	720.56	71.84	4132.89	4658.02	0.61	45135.56	4714.00
EZ1250	240.39	21.92	874.10	69.05	4859.11	5270.76	0.63	49787.86	4714.00
EZ1284	195.14	21.52	862.44	47.80	4181.25	4123.55	0.59	32906.70	4714.00
EZ1346	199.61	21.15	929.61	57.69	4269.18	4865.18	0.63	43495.02	6711.00
EZ1348	215.61	21.77	926.71	58.57	4199.11	4504.10	0.62	43859.66	6711.00
EZ1377	207.57	21.77	938.22	54.02	4325.71	4429.18	0.61	40282.94	6711.00
EZ1339	232.11	21.15	889.77	60.24	4470.42	4567.81	0.60	44270.47	8611.00
EZ1432	210.94	20.71	969.88	64.13	5580.09	6306.60	0.65	50279.09	8611.00
EZ1458	216.23	21.21	982.87	56.14	4893.43	4956.91	0.62	43546.74	8611.00
EZ1460	235.07	21.22	975.91	59.88	5587.91	5555.37	0.62	46516.03	8611.00
EZ1461	201.67	21.46	989.59	55.96	5180.53	5483.25	0.64	43846.53	8611.00
EZ1462	209.81	21.69	971.08	62.68	4528.27	5181.18	0.65	48692.55	8611.00
EZ1434	189.15	21.71	993.07	56.89	5031.59	5799.17	0.66	44989.77	8611.00
EZ1435	195.52	21.84	984.38	56.65	5380.82	5907.46	0.65	44410.31	8611.00
EZ1497	205.36	20.61	1013.99	61.84	4511.18	5287.17	0.66	49722.66	10483.00
EZ1520	210.29	20.74	997.69	62.85	4822.54	5529.29	0.65	50028.63	10483.00
EZ1433	219.42	20.96	1009.95	63.92	4697.03	5278.77	0.65	51427.11	10483.00
EZ1546	211.77	22.32	724.70	62.16	4864.71	5419.47	0.61	38739.62	13272.00
EZ1577	229.47	22.54	853.75	61.98	5129.07	5244.45	0.61	43391.91	13272.00
EZ1611	222.32	23.33	828.14	62.50	5254.40	5559.47	0.61	43069.77	14712.00
EM119	241.95	23.18	700.03	62.68	4935.60	4907.32	0.58	37750.87	14712.00
EM127	213.09	23.02	863.84	62.15	4892.58	5376.45	0.63	44124.61	14712.00
EM122	218.12	22.49	588.93	52.54	4573.04	4210.15	0.54	27240.40	16573.00
EM188	207.76	24.17	714.46	60.07	5481.39	5911.80	0.60	36899.88	16573.00
EM187	192.10	25.51	431.72	58.42	4963.12	5532.14	0.56	25151.64	16573.00
EM186	217.89	26.28	469.51	62.88	5171.45	5560.30	0.56	29046.83	16573.00

where the average downpressures for each of the boreholes are plotted against an increasing time index, X. At the beginning of this plot, where the bit is still new, downpressures are below the level associated with drilling in these hard sandstone/siltstones. This is probably the result of the high excavating capabilities of the new bit when the inserts are at their maximum length and optimum shape. Here, maximum penetration rates are achieved for lower levels of both downpressure and applied torque. The curve shown at this point is positive and

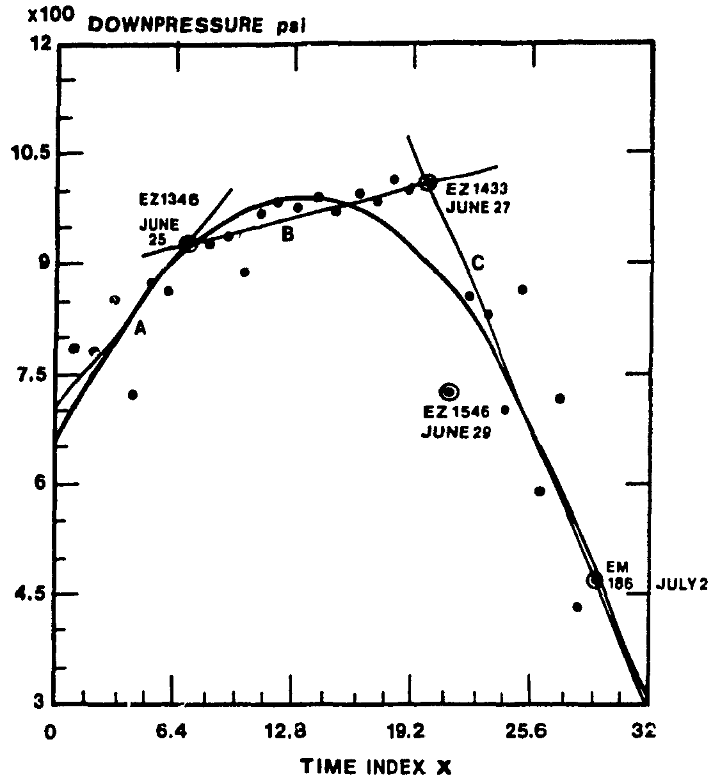

Figure 8.14 - Trend Analysis Plot for Downpressure (W).

increasing slightly, possibly reflecting the "breaking in" of the bit inserts as they wear to some equilibrium shape.

This process occurred over a period of 4 days (June 21 to June 24) or a total drilled footage of 6711 feet.

After this stage, the curve in Figure 8.14 levels off, and normal ranges of downpressure for sandstone and siltstone were seen to be maintained over the next 4 days (June 25 to June 28) for an additional 6561 feet of drilling. The total cumulative footage drilled up to this point in time with bit #476472 is 13272 feet.

However, something occurred to the bit on the night shift of June 27 or 28, based on a comparison of the monitored drill data for borehole EZ1433 on June 27 to that from borehole EZ1546 on

June 29.(Note that there was no drilling for the whole day shift on June 28; the drill was undergoing scheduled maintenance and had both rotary motors replaced. Drilling resumed on the night shift of June 28, but was not monitored). From Table 8.6, it can be seen that the average downpressure in EZ1433 is 285.3 psi higher than for EZ1576, as is the drill rate. However, the torque is higher in EZ1576 by 167 ft-lbs, indicative that a greater amount of work was required to be done to rotate the bit in this borehole in order to achieve the same penetration rate as for EZ1433. This is the first sign of decaying bit performance, and is shown in Figure 8.14 by the downward trend in both the data and the fitted curve, from this point onwards.

The straight lines following the trend of the fitted quadratic curve are proposed to outline several phases of bit wear defined by the results of the analysis. The first line (A) relates to the break-in period for the bit, where downpressures and torque are initially low, yet penetration rates are above the norm for the rocks being drilled. The rate of change in downpressure along this line is high and positive. The second line (B) is the normal range of downpressures for these sandstone/siltstones, for normal levels of torque and penetration rate. The last is the bit wear affected line (C), where the rate of change is negative and high, indicating a relatively rapid reduction in bit performance over time, to a point at which complete failure occurs.

Trend analysis also indicated that the monitored torque gradually increased as the bit wore. This parameter shows considerable variation, however, over the life of the bit, and thus the fitted curve from trend analysis does not appear to follow the data very closely.
The torque was demonstrated in an earlier section to be very sensitive to the changing nature of the rocks. However, as noted earlier in Table 8.5, the dispersion (COV) in the monitored

torque data in this study area (COV = 9.56%), was less than for the same parameter in nearly homogeneous sandstone/siltstones (COV = 10.6%), thus maintaining the initial assumption that the geology is constant for the study area. The observed dispersion in the data, therefore, could have resulted from the presence of softer materials, but overall appears to be a response to the condition of the bit and resulting effect on the downpressure.

The determined trend is shown in Figure 8.15, where a straight line fitted to the data indicates that as the drilled footage

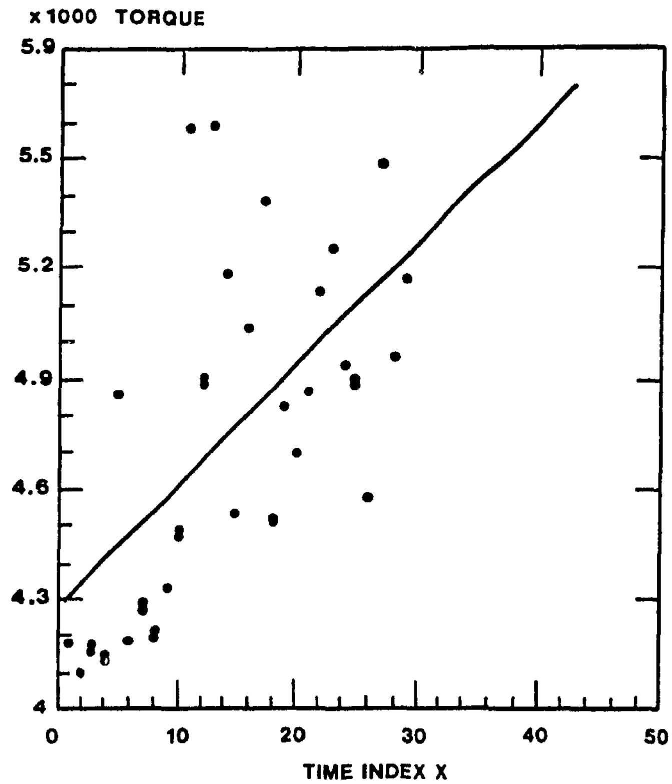

Figure 8.15 - Trend Analysis Plot for Torque (T).

(and bit wear) increases over time, so does the torque. This trend was expected, in that as the bit wears, higher applied torques are required to maintain acceptable rates of penetration, for the lower downpressures. As the wear continues, the torque increases for steadily decreasing downpressure, until total bit failure.

The linear equation thus determined to describe this fitted line is,

$$T\ (\text{ft-lbs}) = 32.98 \cdot X + 4276.19 \qquad ...8.2$$

where T is torque in ft-lbs, and X is the same time index as discussed above, equal to a number between 1 and 29.

To the drill operator, bit failure will be indicated by torque being in excess of the drill specifications (based on a gauge reading) for <u>any</u> combination of applied downpressure and rotary speed, in addition to very low rates of penetration. As well, high vibrations are usually generated in this situation.

A very interesting trend was apparent from the analysis of the monitored data for the bailing air pressure. In an individual borehole, this parameter shows very little variation, increasing only when a blockage of the bit or caving of the hole develops. This pressure cannot be adjusted by the operator, but is a set value based on the capacity of the drill air compressor and the bit type and diameter. However, using trend analysis in this case, it was clear that as bit wear progressed, there was a definite increase in the bailing air pressure. Figure 8.16 illustrates the nature of the quadratic curve which was fit to the data.

The equation for the curve in Figure 8.16 is given by,

$$I\ (\text{psi}) = X^2 \cdot (0.013395) - X \cdot (0.308275) + 22.832 \qquad ...8.3$$

where I is the bailing air pressure in psi, and X is the time index, a number between 1 and 29.

It can be seen from this plot that the trend of the air pressure is just the inverse of that for the downpressure, see Figure 8.14. The straight lines which bound the fitted curve are drawn

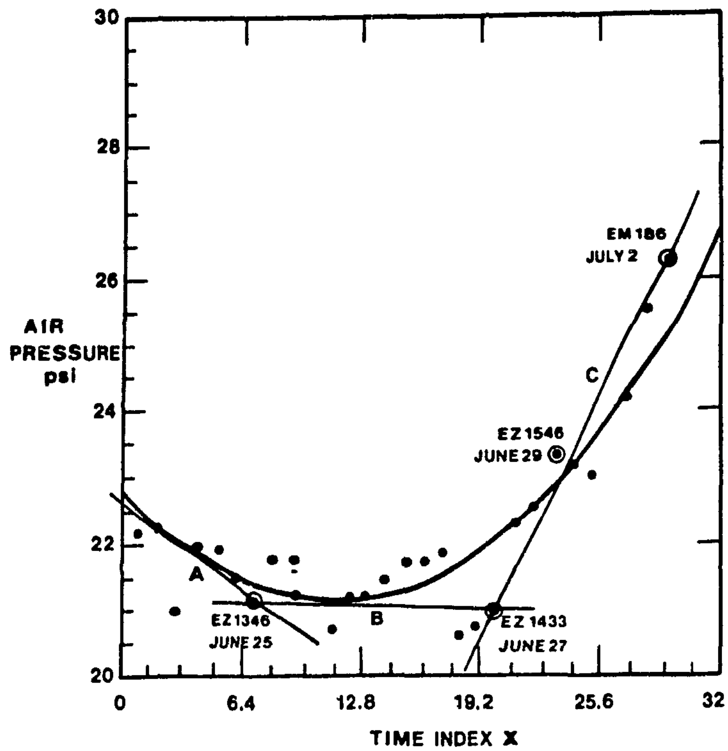

Figure 8.16 - Trend Analysis Plot for Bailing Air Pressure (I).

to represent similar processes as outlined for the downpressure trend. The first line (A) relates to the breaking-in period for the new bit, where as a result of its high excavation capability (at lower downpressures), greater volumes of material are created and thus required to be removed. This is reflected by the higher air pressures at first (> than 22 psi), which with time (and bit wear), settle to levels commonly observed in normal drilling (20 to 22 psi). This trend is shown by the second line (B), and continues for several days until borehole EZ1433 on June 27. After this borehole, the air pressure begins to rise (EZ1546, June 29) and continues to do so, as shown by the third line (C), right up until the failure of the bit. The rise in air pressure could be speculated to be a result of a combination of both inefficient cutting and cleaning of the bit. As the bit wears, the damage to inserts and cones reduces the effectiveness of the bit to break and clean the rock as designed. Therefore, larger more irregular shaped chips may be produced which the volume of air delivered to the bit may have difficulty in clearing. If this occurs, then the area beneath and around the bit could become clogged with this material resulting in a blockage in the returning air flow and subsequently a rise in pressure. In addition, if there has been damage to any of the cones, such that the free passage of air through them is restricted or prevented, the air pressure will also rise.

The trends indicated by this plot follow the identical ones determined earlier for the downpressure, including the actual boreholes and dates of sudden changes or breaks in the parameters. This plot, therefore, confirms the earlier statement that the condition of bit #476472 began to degrade rapidly after the night shift on June 27 or 28, as indicated by the sudden increase in air pressure between monitored holes EZ1433 to EZ1546.

The strong similarities between the trend plots for both downpressure and air pressure is also confirmed by the regression of these two parameters. A correlation coefficient of -0.863 was determined using a multiplicative model, with the equation,

$$I \text{ (psi)} = 102.79 \cdot W^{-0.228} \text{ (psi)} \quad \ldots 8.4$$

where I is the air pressure and W is the downpressure. This relationship is shown in Figure 8.17.

Analysis of the parameters of rotary speed and penetration rate indicated no significant trends in the data. It had been expected that a clear and gradual decrease in the penetration rate would be observed as the bit wore, but this was not readily apparent. Instead, it appeared that the steadily increasing torque balanced the effect of decreasing downpressures to maintain an essentially constant rate of penetration.

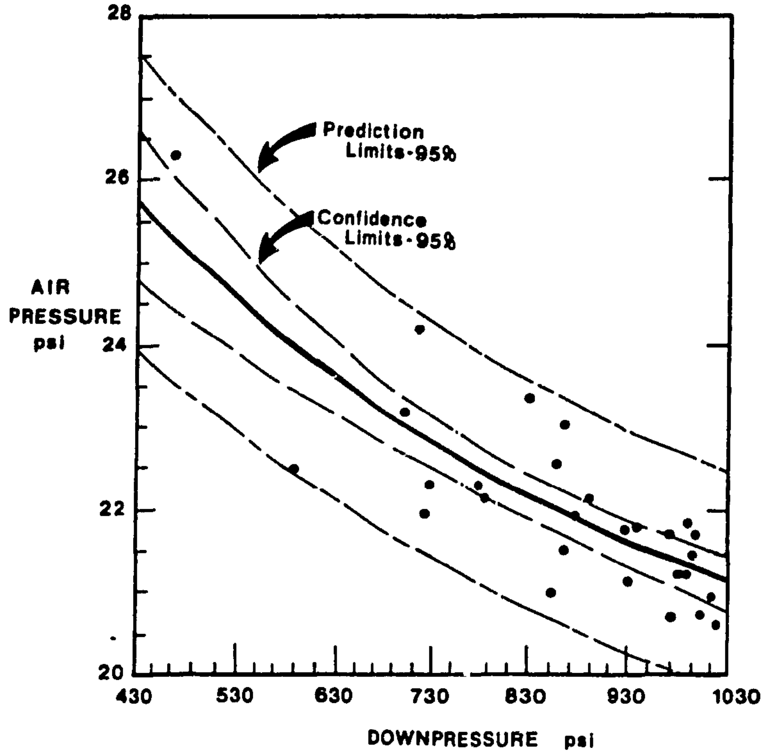

Figure 8.17 - Regression Curve for Bailing Air Pressure I versus Downpressure W.

Figure 8.18 shows star symbol plots for the parameters of downpressure, torque and bailing air pressure for the data presented previously in Table 8.6. The key to the star symbols is given in Figure 8.19.

The star symbols in Figure 8.18 represent the data for each of the boreholes in Table 8.6, beginning with EZ1163 when the bit is new and ending with EM186 just prior to bit failure. It is apparent that the changing shapes of the star symbols parallel the trends that were previously identified from Figures 8.14 to 8.16. As shown in Figure 8.18, characteristic shapes are obtained for the break-in, normal and failure periods during the life of the bit. As was demonstrated in sections 6.3.4 and 7.2 for the recognition of different rock types, this technique could be used in identifying particular drilling situations based on unique star symbol shapes. In this manner, the degree of wear could be

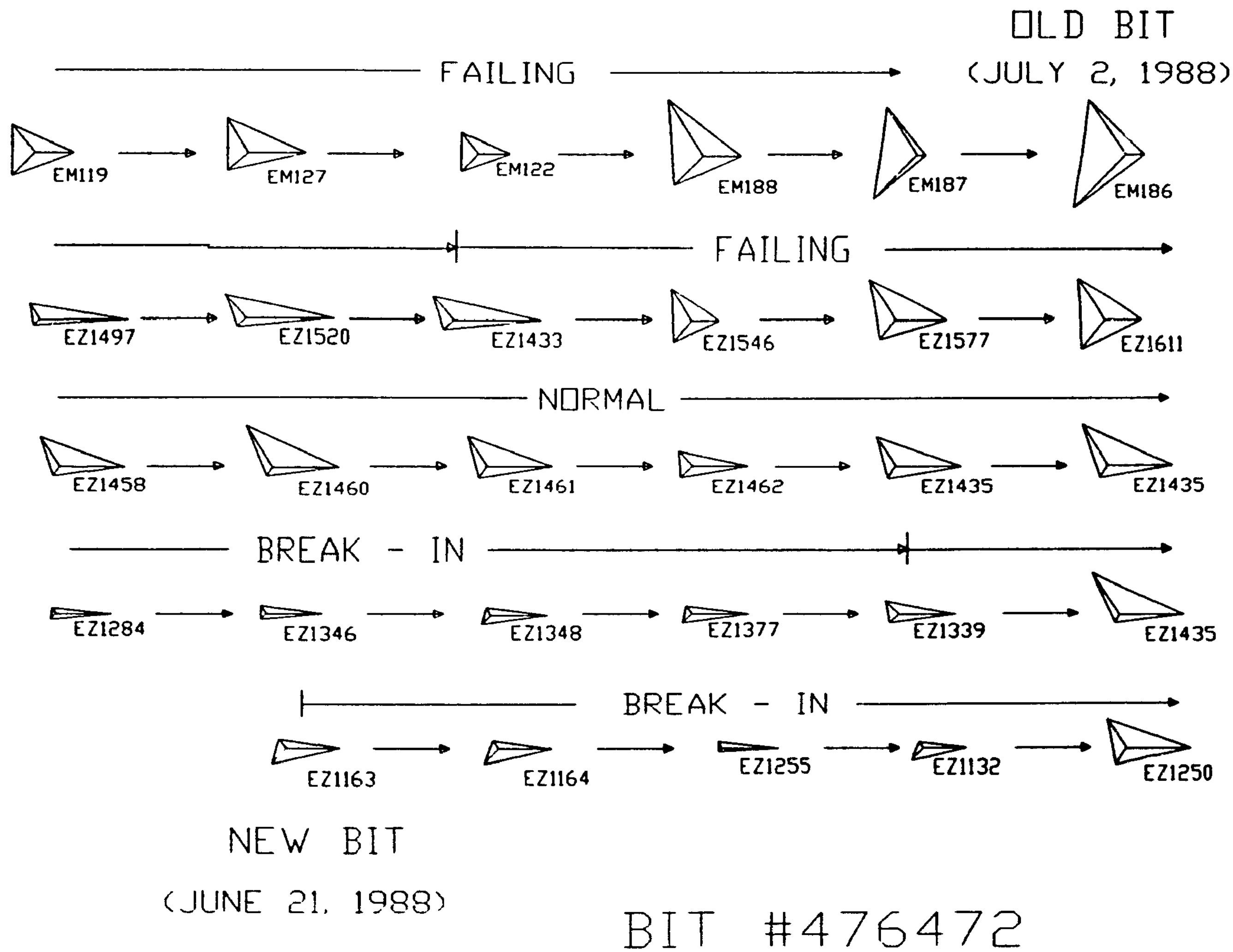

Figure 8.18 - Star Symbol Plots for Monitored Borehole Data Using Bit #476472.

readily assessed throughout the life of the bit based on a comparison of the star symbol shape at any point in time to that for a new bit.

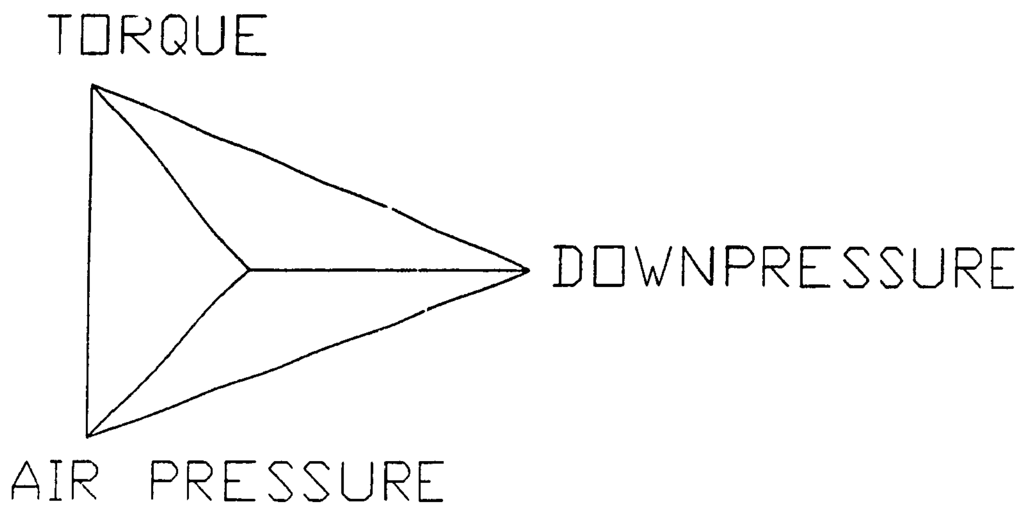

Figure 8.19 - Key to Star Symbol Plots in Figure 8.18.

Photographs of bit #476472 after it was changed, showed evidence for its failure. Figure 8.20 is a view of the bit looking at the shirttail area of cone #2. There is clear confirmation of wear at the gage of this cone, and also the complete removal of a few of the gage wear protection inserts. This cone was completely jammed, and it appears that the opening developed by the shirttail wear contributed to the failure of the bearings by entry of rock fragments.

Figure 8.20 - Bit #476472.

Another photograph of the same cone #2 from the front, Figure 8.21, shows that excessive wear of the cone shell also occurred in the area immediately in front of the "B" row inserts, where the "A" row inserts have been removed completely, exposing the end of the journal axis. Note as well in Figure 8.21, the deep gouging on the cone, possibly due to wear by an insert (s) broken off from itself or another cone.

Figure 8.22 is a view of cone #1, indicating similar cone wear as for cone #2. Again, the entire "A" row inserts and the tip of the cone shell have been worn off, exposing the thrust plug and the roller bearings. This cone, as for #2, was no longer able to rotate. No excessive wear at the shirttail was noticed for this cone, and so it would appear that the main cause of failure was bearing failure. This could have been the result of an internal

Figure 8.21 - Cone #2, Bit #476472.

failure due to actual roller bearing deterioration from overloading and/or the entrance of rock materials through the worn opening of the cone.

Apparently, cones #1 and 2 failed before #3, as witnessed by the excessive wear of their "C" and "D" row inserts shown in Figures 8.23 and 8.24. Some of the inserts of these cones have been worn nearly flat and others broken off, a result of continued rotation after failure. Cone #3 is shown in Figure 8.24, and looks to be relatively unworn. However, it no longer turned, and closer examination revealed that the cone shell was nearly worn through just behind the "B" row inserts. A hairline crack is visible on this cone in Figure 8.24.

The proposed sequence of events leading up to the failure of this bit are; (1) cone #2 failed first, due to roller bearing

Figure 8.22 - Cone #1, Bit #476472.

failure resulting from excessive gage wear, followed by wear of the cone, which may have also contributed to the jamming of the cone; (2) cone #1 failed next, due to wear of the cone shell with subsequent entry of material thus causing bearing failure - note the excessive wear of and number of broken inserts for both cones indicated that they jammed before cone #3; (3) the failure of cone #3 followed, possibly resulting from the unbalanced loading of its bearings from the failures of the other two cones.

Figure 8.23 - Bit #476472.

Figure 8.24 - Bit #476472, Cone #3.

To illustrate, as for the boreholes of EXB45 and EXB45R, the difference in drilling performance parameters between those recorded for a completely worn bit versus those for a new bit, the two boreholes EM186 and EM242 are discussed. Borehole EM186 was the last borehole monitored prior to failure of bit #476472. The failure occurred at the end of the night shift on July 3, after an additional 900 feet of drilling beyond EM186 was completed. This bit was changed for another of identical type and borehole EM242 was monitored on July 3, after only 50 feet of drilling with the new bit. EM242 was separated horizontally from EM186 by only 40 meters, and therefore the geology encountered in each hole can be considered the same.

Sample statistics for each borehole are given in Table 8.7, and the same values are also shown using Box and Whisker diagrams in Figures 8.25 to 8.29. Plots of the actual drill parameter logs for each borehole are illustrated in Figures 8.30 and 8.31

The statistics indicate several main differences between the recorded parameters in the boreholes. Although as in the previous study, no significant trend was seen between penetration rate decay with bit wear, it is clear from Table 8.7 that higher rates (average 37% improvement) are definitely achieved with the newer bit. It is also apparent that the increased penetration rates are attained in borehole EM242 for much higher downpressures (52% increase) at significantly lower torque (17.4% decrease). There is also less variation in the monitored penetration rates in EM242, giving a coefficient of variation (COV) of 13.1% as compared to 39.7% in hole EM186. This variation is probably the result of the operator continuously making adjustments to downpressure and rotary speed in an attempt to control the very high torque in EM186. The effect of operator influence is clear by a comparison of the COV's for rotary speed between the boreholes, in that the value for EM186 is 21.2% to 0.44% in EM242.

Table 8.7 - Summary Statistics for Boreholes EM186 and EM242.

EM 186:

	R (ft/h)	N (rpm)	W (psi)	T (ft-lb)	I (psi)
Sample Size:	209	209	209	209	209
Average:	152.41	59.23	434.56	4902.92	24.47
Median:	135.94	63.32	473.00	5085.81	26.28
Variance:	2915.69	179.56	15153.00	1.475E06	39.86
Std.Dev.:	53.99	13.39	123.09	1214.56	6.31
Std.Error:	3.37	0.92	8.52	84.01	0.44
Minimum:	86.48	14.78	35.00	737.60	2.60
Maximum:	326.05	74.18	571.00	7519.32	26.72
Range:	239.56	59.40	536.00	6781.72	24.12
Low Quart:	115.61	59.70	442.00	4486.53	26.12
Up Quart:	165.29	65.72	484.00	5704.36	26.40
Int.Range:	49.68	6.02	42.00	1217.83	0.28
COV:	39.72%	21.15%	26.02%	23.88%	24.01%

EM242:

	R (ft/h)	N (rpm)	W (psi)	T (ft-lb)	I (psi)
Sample Size:	231	231	231	231	231
Average:	241.09	57.69	907.67	4048.28	22.46
Median:	232.91	57.62	997.00	4215.22	22.36
Variance:	925.87	14.74	61217.60	791656.00	0.48
Std.Dev.:	30.43	3.84	247.42	889.75	0.69
Std.Error:	2.00	0.25	16.28	58.54	0.04
Minimum:	170.27	44.74	22.00	1156.29	22.12
Maximum:	343.91	68.50	1079.00	5741.95	29.16
Range:	173.64	23.76	1057.00	4585.66	7.04
Low.Quart:	223.10	56.04	889.00	3597.56	22.32
Up.Quart:	255.01	59.98	1042.00	4664.01	22.40
Int.Range:	31.92	3.94	153.00	1066.45	0.08
COV:	13.07%	0.44%	24.82%	21.11%	3.09%

The very low minimum value of downpressure reported in Table 8.7 for EM242 is associated with the procedure for collaring the borehole, where only the weight of the drill column with rotation is used for the first few meters of the hole, see Figure 8.31. This fact results in the higher than expected value of COV for the downpressure in EM242. A similar trend is seen in EM186 in Figure 8.30, also indicated by very high penetration rates in this soft, unconsolidated material.

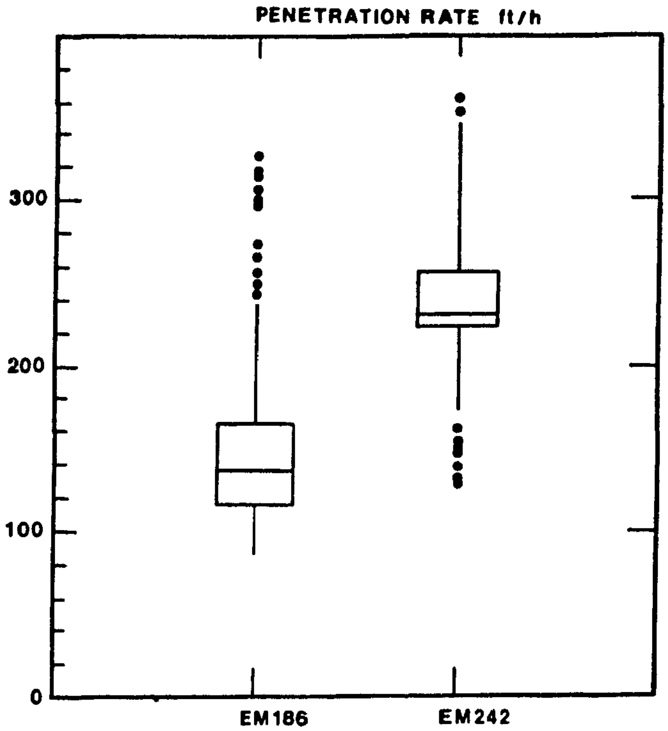

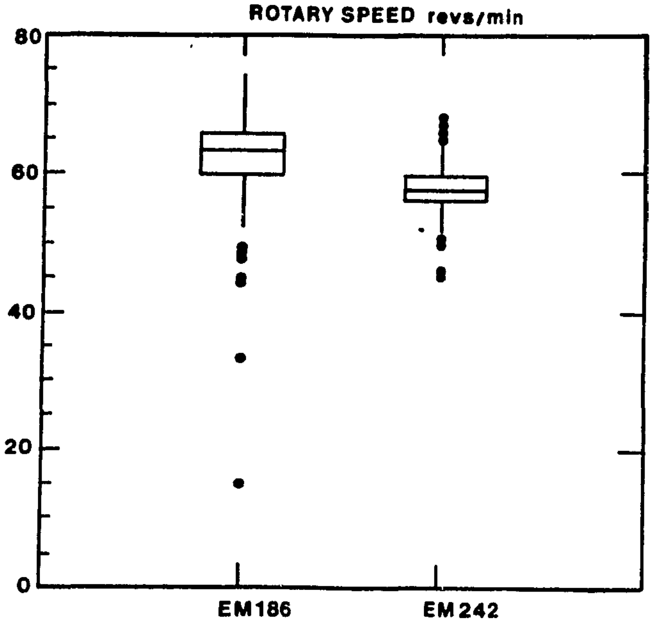

Figures 8.25 and 8.26 - Box and Whisker Plots for Boreholes EM 186 and EM 242.

The average air pressures listed in Table 8.7, indicate that this value is higher (by 8.2%) in EM186 for the worn bit. However, using the median values instead, the difference is significantly higher (15%), a fact also seen from examination of the upper and lower quartile values for each borehole illustrated in Figure 8.29. The coefficient of variation (COV) of the bailing air pressure is also much higher (24% versus 3.1%) in borehole EM186, indicating the greater dispersion of the data when using a worn bit.

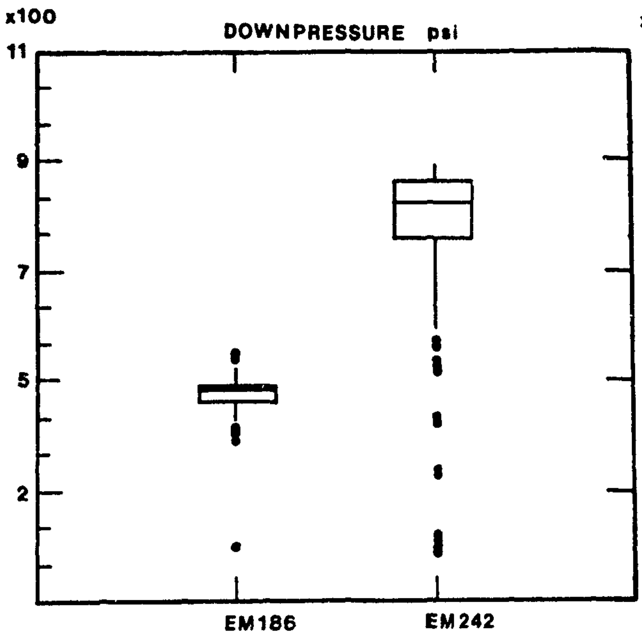

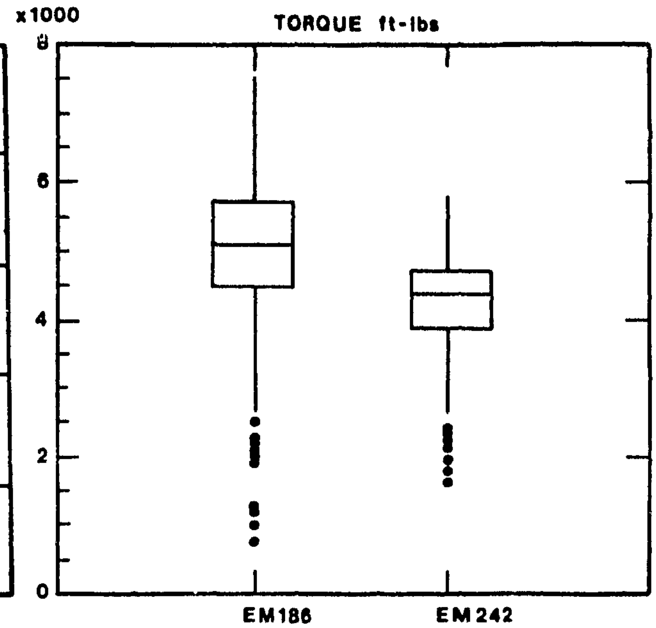

Figures 8.27 and 8.28 - Box and Whisker Plots for Boreholes EM186 and EM242.

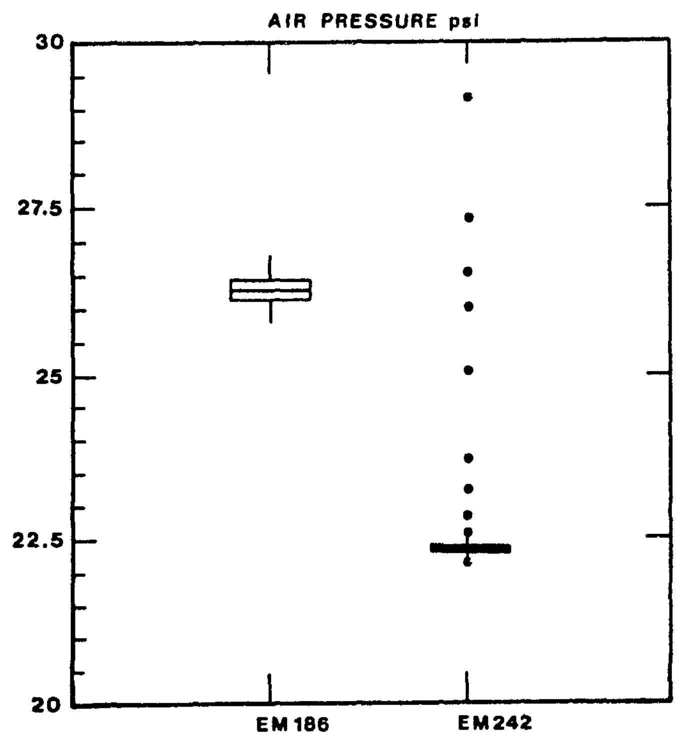

Figure 8.29 - Box and Whisker Plot for Boreholes EM186 and EM242.

Shown in Figures 8.30 and 8.31, but not discussed previously in relation to bit wear, is the calculated specific energy log. This data is based upon the recorded parameters and is determined using equation 2.10, discussed in section 2.3, 6.3, 6.4 and 6.5. It has been shown in another section of this work that this index shows very high correlation with both shear and compressive strength of the rock. It is interesting to note the significant differences in these log traces for each of the boreholes in these figures.

Since SE(T) is very dependent on torque, it is evident that the much higher and dispersed specific energies for EM186 (21.3% higher with COV = 39% versus 21.1% in EM242) result from the higher and more variable nature of the monitored torque.

It was expressed in section 6.4 that the parameter with the greatest amount of variation also had the greatest capability of identifying changing rock properties. This was assuming that the effects of bit wear were not influencing the drilling performance. The condition of the bit during that particular monitoring period was examined on a regular basis to ensure that this phenomenon was not a factor.

8.4 Conclusion:

It is concluded that some care must be taken when using calculated SE(T) to estimate the strength of rock, due to the effect bit wear can have on the monitored torque and downpressure. It will therefore be necessary to continuously evaluate the condition of the bit and establish the degree to which the particular level of wear is affecting the monitored drill performance parameters. Use of trend analysis techniques, could readily and rapidly evaluate the state of the bit on the basis of examining over time, the changing responses of certain key parameters which have already been shown to be reflective of its condition.

The trend analysis equations developed earlier, could provide the initial thresholds for the various parameters from which to develop a more detailed understanding of the causes and effects of bit wear and thus generate a more comprehensive classification of this phenomenon. The results further indicate the possibility of predicting the relative degree of wear on the basis of the variations in recorded drill performance parameters. By being able to forecast at any point in time, the relative condition of the bit, a correction factor could be applied to the calculated SE(T) indices for example, such that they would truly reflect the changing nature of the ground rather than that of the bit.

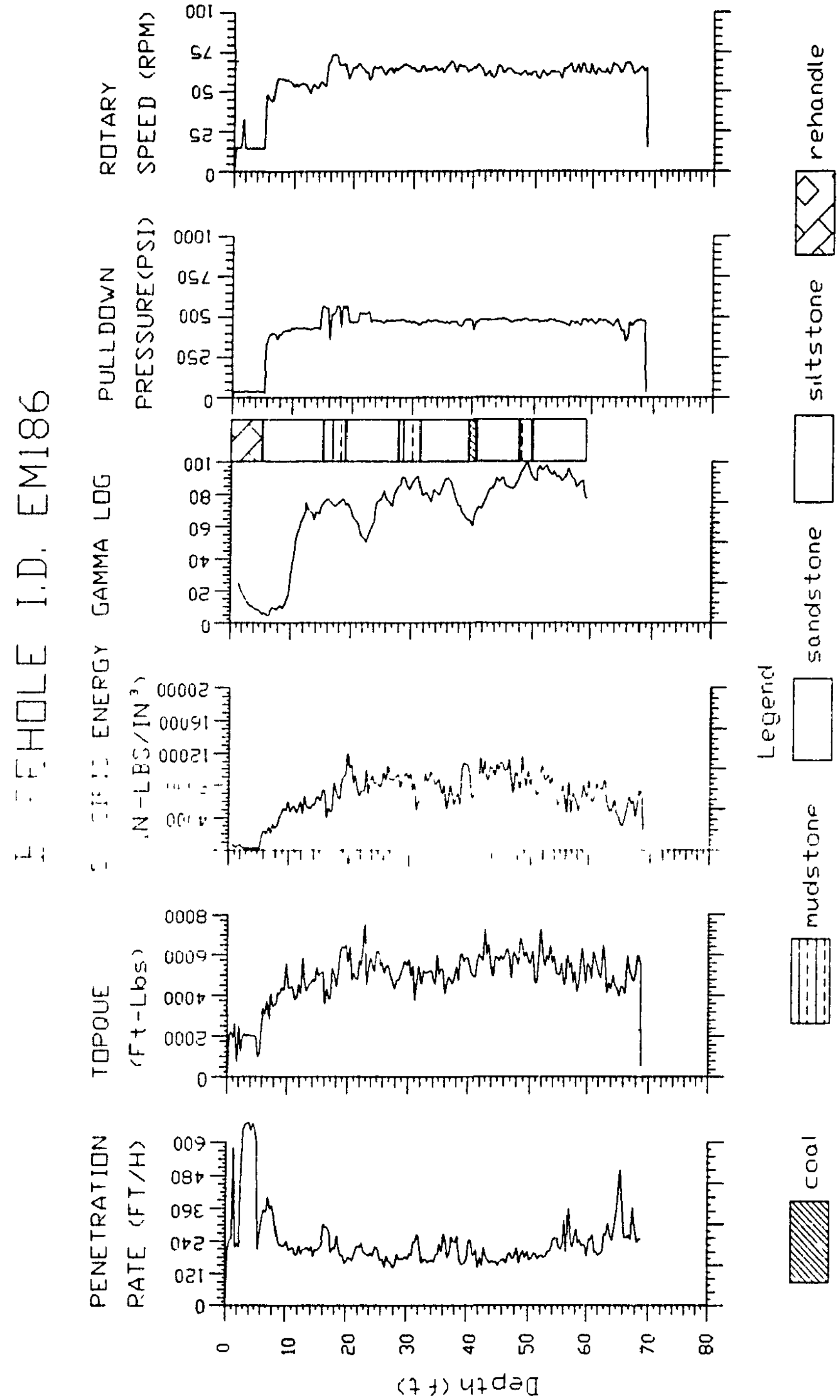

Figure 8.30 - Drill Performance Parameter Logs for Borehole EM186.

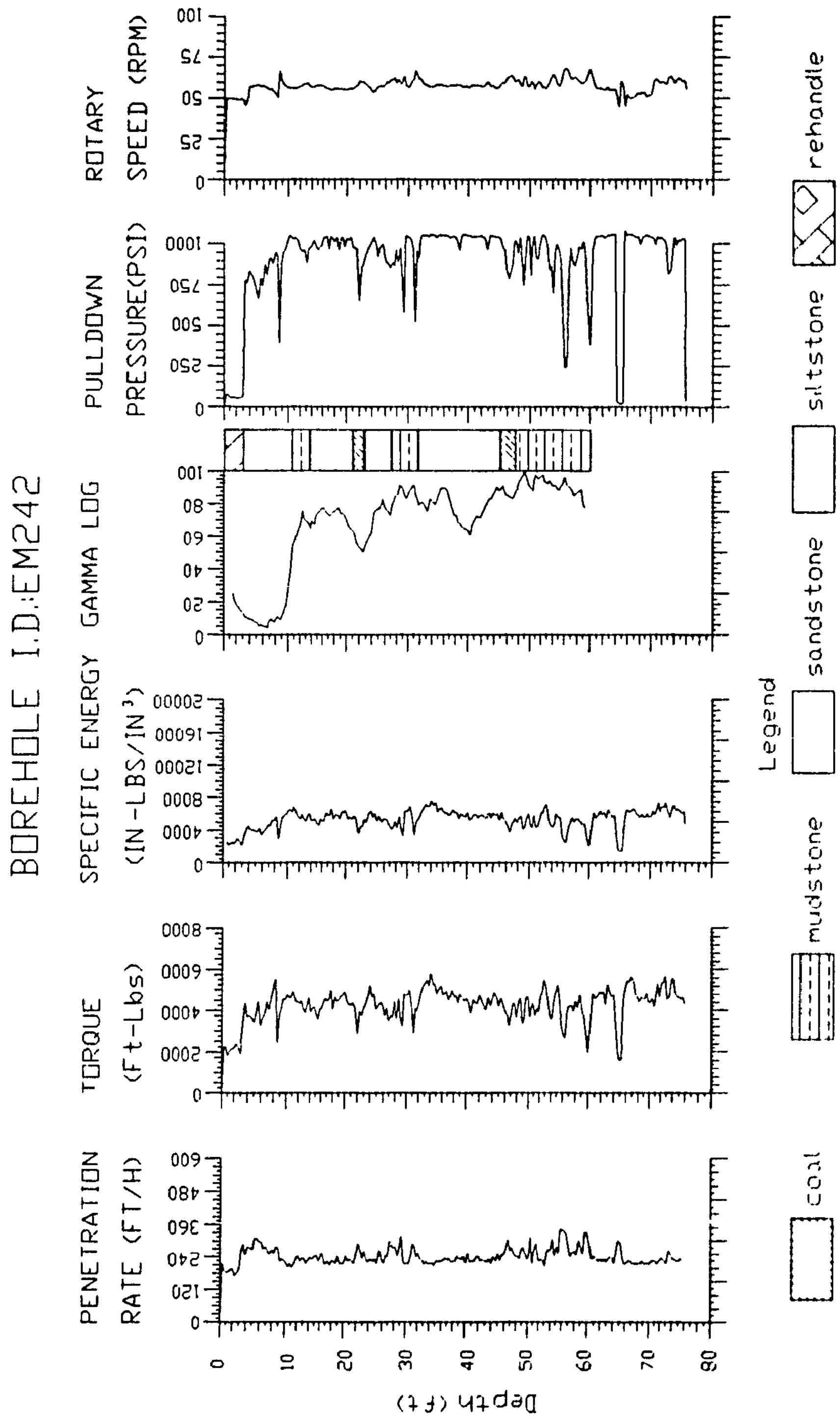

Figure 8.31 - Drill Performance Parameter Logs for Borehole EM242.

9.0 ROTARY BLASTHOLE DRILL AUTOMATION AND CONTROL:

9.1 Introduction:

Current and past research into drill automation is reviewed in the following section. Here the current research of the thesis will be related to blasthole drill automation. The concept of drilling intelligence is introduced as a necessary component to meet this end.

A basic control strategy for a rotary blasthole drill is subsequently outlined based upon the field monitoring and data analysis results discussed in earlier sections.

Drilling Intelligence is considered to include the capability for a drill to sense and understand:

- a - the operating parameters of the machine and the condition of its working parts;
- b - the location, orientation and size of the excavation produced;
- c - the location and orientation of the machine at the hole collar position;
- d - the nature of the medium which it is penetrating;

This capability is seen to be required in order for the machine itself to undertake decision-making for control in order to meet drilling objectives, which may be associated with the following monitoring and operational functions:

1 - performance, (e.g. drilling parameters of R, T, W, set-up times, overall productivity);
2 - maintenance, (e.g. bit wear, vibration levels);
3 - excavation, (e.g. hole deviation, size and spacing, collar position).

Performance monitoring and artificial intelligence techniques are considered to underlie the intelligence required for a drill to respond automatically to varying geological and operational conditions. This in order to achieve optimised productivity and precision. Safety and environmental benefits also are of potential from achieving drill autonomy, especially in more harsh underground or surface environments. In addition, such a capability enhances the drill's contribution to the characterization of the host rockmass for decision-making related to ground control and mine design.

This section considers aspects of the development of the logic base and strategies required for the automation and control of surface mining drilling equipment. Some past research has addressed the automation of drill rigs, primarily rotary types, in various surface and underground applications. The control systems thus developed relied at a basic level upon the monitoring of all of the primary drilling parameters, i.e. rate of penetration, rotary speed and torque, bit weight (pulldown) and bailing air/mud pressure and flow. Several other peripheral machine functions and effects (horizontal and vertical vibration etc.) were also monitored as part of more complex control schemes. The basis of rotary drill control logic has traditionally been to maintain bit torque within acceptable limits while maximizing the drill rate. This is obtained through the monitoring, feedback and control of rotary speed and bit weight, with both parameters being related to the drill rate and torque. The intelligence which is required as part of the strategy for controlling drilling operations, needs to be based upon a detailed understanding of the complex relationships that exist between drill performance paramet·rs and rock mechanical and structural properties. These area. were examined in detail in chapter 6.0.

9.2 Drilling Automation and Control - Past Studies:

Considerable work has been undertaken in the past to develop a strategy for the control of drilling rigs used in both the petroleum and mining industries. In petroleum drilling, for example, results obtained from both laboratory and oil field testing were used to evaluate the relationships between several drilling parameters and the rate of penetration (Young, 1969). The aim of this particular investigation was to devel'p drill optimization theories towards minimizing rotary tricone drilling costs. Minimum cost drilling theories were based upon a combination of historical data and empirical techniques for selecting optimum bit weights and rotary speeds. This approach required a quantitative evaluation of the variables involved, i.e. drilling rate, bit bearing and tooth wear and cost. The control strategy thus implemented assumed constant bit weight and rotary speed over the entire bit life. Rotary torque was also monitored at all times and maintained within preset maximum/minimum limits by continuously adjusting rotary speed and bit weight. The completed system was subsequently used by the Humble Oil Co. to control bit weight and rotary speed while respecting the concepts of minimum cost drilling.

A similar approach was followed in order to automate and control the performance of a diamond drill (Everell et.al.1973). The strategy developed sought to maintain the drill and bit system within normal operating conditions in the face of changing rock mass properties, while attempting to maximize penetration rate and minimize bit wear. Their objective was not to demonstrate that automatic control would eliminate the need for an operator, but rather to improve the economics of diamond drilling. This would be achieved through the automation of several drill functions, thereby assisting operators to improve overall performance through increased productivity and reduced drill and bit wear. The control theory involved maintaining acceptable target levels of torque through continuous variation of rotary speed and bit thrust. Rate of penetration, monitored within the system, was kept at the maximum permitted without the drill operating outside the lower and upper limit ranges set previously for the other parameters (primarily torque).

Research into tricone rock drilling control and optimization aimed to develop a unified model of the total drilling system

(Eronini et.al.,1981). This approach was based upon the concept that the greater the knowledge and understanding of a system then the better it can be controlled and optimised. They proposed a four component model:

1 - transmission line - consisting of surface structures, drill column, drill-string/borehole interaction and the flushing system,
2 - model of the rock bit,
3 - rock/bit interaction and rock fracture behaviour,
4 - drill performance criteria such as rate of penetration viz. specific energy.

Also included were considerations of bit-tooth wear and bottom hole cleaning. The use of the model for quantitative predictions required that the parameter thresholds be identified for the particular drilling rig, rock formation and operating conditions.

Similar control concepts and system designs have been associated with the control of pilot hole drilling in raise boring (Everell, 1972; Everell et.al.1975).

During a research program to automate a blasthole drill in the U.S.A., the drill operator was identified as the greatest single factor affecting its performance (Weston and Stoner,1970). It was also indicated, however, that optimising the performance of the drill did not imply eliminating the operator, but provided a means of *assisting* him. Upon examination of the various functions and motions performed by the blasthole rig, it became clear that the greatest demand for skill was during the actual drilling cycle. In this phase, the operator was seen to continually adjust pulldown pressure, rotary speed and bailing air pressure according to the changing nature of the material being drilled. In limited field trials, a blasthole drill was modified for automated control during the drilling cycle only. Here the automation mode began only after the drill had been positioned and levelled, and stopped when the bit reached its preset depth. Based on results from these trials it was concluded that:

1 - production footage using automation exceeded that from the past;

2 - bit costs per foot were significantly less than the best previous cost records in the same type of material;

3 - periods of severe vibration due to operator attempts to force progress through difficult ground were reduced.

It was indicated, however, that an overall increase in maintenance time occurred with the installed automation package. Further, longer term tests were seen to be necessary to refine the system, (hardware and logic), towards eventually reducing downtime and increasing machine availability.

This initial work formed the basis for the commercial development of an automated drilling control package by Bucyrus-Erie. This system was offered as an integral component on both 60R and 61R Series III drills as early as 1971. The original system was basically an electronic blackbox, incorporating electronic transducers and current-limit devices which fed back drill performance data to a central controller. The system would respond to the monitored signals when preset drilling and machine parameters were exceeded, through adjustments (individually or combined) to downfeed and water injection rate, rotary speed and air supply (Li,1974).

A PLC-based automation package, providing essentially the same capabilities as the older system, is currently being offered as a factory installed option on Bucyrus-Erie's new 49R drills. Several of these new drills with the automation system installed, have been sold in recent months (Matuszak,1988).

Similar systems were also developed by Gardner-Denver for their line of GD-120/130 rotary blasthole drills, and Marion for the M-4 and M-5 crawler rigs. The Gardner-Denver *programmed control package* offered several different hardware configurations depending upon the need of the customer. The basic system functions to limit, through feed back and control circuitry, W to a fixed maximum. In addition, a rotary motor current controller automatically decreases W if the rotary drive motor became overloaded (excessive T). Once the overloaded condition was rectified, normal levels of W were resumed. Additional hardware options offered were controllers for modifying N, vibration, main air pressure increases, feed rates and hydraulic pump motor overloads. An auto sequence controller was also available to reduce W over a preset initial depth during collaring. The basic automation system is still available, not as retrofit equipment, but only as a factory installed option on new drills (Kallio,1988).

The Marion control system was considered to be less complicated than competing automation packages due in part to the philosophy behind its development. It was considered that automation of only the primary drill functions was necessary to optimize drill performance, and that such a system should serve to enhance rather than substitute for the driller's skills. The Marion system thus controls only the parameters of W, I and T. Limits for each of these, are preset into the system, and are determined based upon ground conditions, projected rotary bit life and desired rate of production. The system was aimed at achieving maximum productivity in terms of increased drilling footage with lower downtime and maintenance costs, while reducing operator abuse of the equipment (Li,1974). An upgraded system, providing similar control functions to the original unit is available from Marion as an integral component on new drills. Due to the complexity of modifying older drills to accept the control system, the instrumentation is not offered as a retrofit option (Haas,1988).

The Furuholmen company in Finland had developed by 1980 a microprocessor-controlled drill jumbo prototype. This initial machine was capable of programming for automatic and precise drilling of complete rounds, according to predetermined drilling plans defined by fixed coordinates. The further development of this machine by Tampella was the Tamrock Datamatic computer-assisted, 3-boom drilling jumbo. Tamrock and Atlas Copco are both prominent in the development of computer-controlled, underground drifting and stope blasthole, as well as rock and cable bolting drills (Ulvelin and Puhakka,1988; Martin,1988; Schunnesson,1988). These machines variously control the collar location and orientation, hole length and rock/cable bolt installation. No attempt appears to have been made to remove the operator significantly from the drill, in fact, his presence tends to be regarded as necessary for overall control and *innovative planning* (Ulvelin and Puhakka,1988). These computer-controlled drills currently employ intelligence limited mainly to positioning and hole length control. Sensors have not yet been employed to monitor bit wear and condition, hole deviation and change in geology in order to place any decision-making capability onboard the drill. This is seen as where the development of drilling intelligence becomes a prerequisite.

At LKAB's Kirunavaara mine, an Atlas-Copco Simba 269 ITH drill was recently introduced. This particular drill features automated drilling through the use of an on-board microprocessor-based controller. The drill is remote-controlled, guided by a TV camera. The computer system enables the applied drilling forces to be controlled, primarily to maintain downfeed pressure constant over the length of hole, based on pre-programmed instructions. In addition, the system has the capability of monitoring and recording the important drilling parameters. Analysis of these and drill cuttings presently forms part of on-going research aimed to characterize the rock mass in terms of strength, structure and ore grade. Results to date have been successful in relating drill performance changes to iron content within 5 percent of actual grade (Schunnesson,1988).

In Canada, CANMET have sponsored a project with Vadeko Inc. to develop an onboard ITH blasthole drill system to accurately locate, in real time, the bit location in terms of collar and drill pattern coordinates (Pathak and Dias,1986). The primary objective of the work was to enable a GO-60 (CMS-CD-90) drill to drill holes with greater accuracy. The on-board computer provides control of the hole angle by maintaining the orientation of the drill head. Hole straightness is optimized by maintaining bit thrust constant over the entire length of hole, thereby compensating for the weight of steel at considerable depths. A second objective was to provide the maximum amount of operational automation such that the first objective could be achieved with minimal operator involvement (England and Kelly,1986). The hardware design incorporated two Sperry Accustar Inclinometers as vertical angle sensors in a down-hole assembly, together with power supply, processing electronics and microwave transmission equipment. An out-of-hole assembly unit served as the communication link with a controller subsystem, intended to control all drill functions (including rod handling), manual as well as automatic, whilst recording all events and data for future use (Pathak and Dias,1986).

In the investigations reviewed, complex control problems still appear to exist. Presently, experienced drill operators can identify by *feel* the changing nature of the ground being penetrated, and thus make adjustments to both the rotary speed and bit thrust in order to achieve optimum drill performance. However, if *full* automation is to be successfully implemented, then the skills of the operator must be emulated by the monitoring computer system, in order to control the drilling functions. This logic can only be developed through detailed analysis and understanding of the interactions between the bit and the material through which it is penetrating, as evidenced by the variation in performance parameters with changing rock mass properties.

The drill monitoring field investigations undertaken at the Fording River Mine by the author, have provided: (1) a more complete understanding of the relationships between primary rotary drilling parameters and, (2) how these are affected by changing rock mass characteristics.

Based on the defined parameter limits for each rock type, suitable pattern recognition techniques could be applied to permit an *automated* interpretation of the monitored data. This could be in terms of the micro- and macro-geological and geomechanical characteristics of the rock being drilled.

The work completed to data is seen as an essential phase in developing a functional control strategy for eventual *full* drill automation, where the logic of the operator is incorporated into the actual control system. In addition, the definition and classification of the *machine-rock* interactions in various drilling situations is fundamental to achieving optimal automation capabilities.

9.3 Rotary Blasthole Drill Performance Monitoring:

The automation and control of blasthole drill operations at the Fording River mine is a subject of continuing research by the author. This project is aimed towards improving drill productivity while also minimizing drilling costs, through reduced downtime and maintenance.

Programmable Logic Controller (PLC) systems are already in use at the mine on draglines, cable shovels, haul trucks, and drills for automated lubrication, systems (brakes, rotary drive units, electric motors) and maintenance monitoring, dust collection and remote propelling and operation. The automation project will in the near future, involve the development of a PLC-based control package for a 45R or 60R drill. The design of this system will include many of the innovations which formed part of the drill monitoring system used in the current thesis study. In addition, the experiences gained from the thesis project will greatly reduce the time required to get the system operational. Many of the problems associated with the design and implementation of an automation package were previously defined in terms of:

1 - the optimal sampling rates which should be used at the minesite based on the requirements of specific tasks,
2 - the identification of which are the crucial parameters for assessing overall drill performance. As well, the *thresholds* of each of these parameters was defined in terms of rock type and specific drilling situation eg. bit wear,
3 - the size of digital data files on a per borehole/shift/daily basis were established (based on point 1 above), enabling a determination of the memory requirements,
4 - definition of the best mode of data storage for the particular monitoring application and mining environment ie. portable memory modules or RF telemetry systems.
5 - identification of alternative and more suitable methods for the measurement of bit displacement, R, T and N, and,
6 - the development of a *technique* for the accurate acquisition, manipulation and interpretation of drilling performance parameter data. Through routine drill monitoring in the recent studies, a complete understanding of the variables exerting control over drilling performance was established, including operator- and rockmass-related factors.

It would seem very apparent that the automation and control of the blasthole drill, therefore, is a natural extension of the current investigation results.

Particular pattern recognition routines have been outlined to assist the automating of the interpretation of drill performance variation, permitting detailed assessments to be made regarding the geological and geomechanical nature of the rocks being drilled. The characteristic signal patterns and thresholds identified from the drill performance data are indicative of a particular circumstance i.e. rock type or machine situation (e.g. worn or plugged bit condition etc.) as outlined in chapter 6.0 and section 8.3. The star symbol plots introduced in sections 6.3.4 and 7.2 are a form of pattern recognition, and could be used towards an eventual automated process of recognizing their distinctive shapes in the different rock types. For example pattern recognition techniques would enable the extraction and identification of these distinctive and unique data features without manual intervention.

On the basis of the automated recognition of any one or group of circumstances from the data, drill performance could then be optimised through the implementation of appropriate control strategies to alter N and W as required.

The following summarized observations are based on the analysis of the drill performance monitoring data in the current study:

- Variations in R are due to the changing nature of the rock being drilled, but may also reflect changes in the operating tactics of the drill, i.e. increased/decreased W and/or N, and bit condition.

- Variations in T indicate very clearly the presence of strong/weak rock units. Variations may be due, however, to change in W which can be confirmed by examination of these logs. In general, at constant (set) W, T increases in stronger rocks, i.e. siltstones/sandstones (at maximum levels of W), whilst decreases in T occur in weaker rocks, i.e. mudstone and coal (with associated decreases in W).

- W, if maintained constant by the operator during drilling, will reflect variation in the rock nature by corresponding decreases in weak rock (coal and mudstone) and maintenance offset levels in stronger ground (siltstone/sandstone). W is generally decreased by the operator when the level of T begins to exceed the recommended panel gauge range, i.e. in the case of binding due to wet, hard or fractured ground. Additionally, W is set at approximately zero when collaring a blasthole in rehandle or other soft materials. In such situations, the weight of the drill steel assembly with low N is enough to initiate penetration, resulting in less damage to the bit and drill structure and reducing the chance of hole deviation. Standard collaring practice in weak materials, therefore, involves low W and N over a minimum depth of 10 feet, producing low T and fluctuating (mostly very high) values for R. After this depth, the drill parameters are brought up to levels associated with normal practice. W is also reduced and/or downfeed disengaged when I (bailing air pressure) increases above a recommended threshold of 40 psi. This situation indicates to the driller that the hole has possibly caved and/or the bit is plugged. Retracting the drill string several feet out of the hole serves to blow the bit clean and I should drop to operating levels. At this point, downfeed is engaged, and once the bit is resting on the hole bottom then normal levels of W with rotation can be set to resume drilling. It is important to note that, at certain applied W, a reduction in N is observed due to increased T (jamming the bit). This effect may in fact offset any increases in R which would be realistically achieved by the increased levels of W.

- N varies slightly throughout drilling, reacting mainly to the changing rock conditions or the driller responding to a particular situation. It is seen from the performance logs that when intersecting soft rock (coal) N increases slightly on its own due to reduced friction at the bit-rock interface. In hard ground N may or may not decrease, depending on whether W and/or the properties of the material vary. The value of N is decreased by the driller, generally in combination with slight decrease/increase in W, in order to reduce drill vibration in binding or hard ground. N is also maintained low by the operator when collaring the hole in rehandle or fractured ground.

- SE(T) is calculated from N, T, W and R (Teale 1965). Given the previously defined relationships between these parameters (see section 6.2), altering W will result in corresponding changes to R, T and N, and therefore SE(T). Section 6.5 demonstrated the good correlation between SE(T) and the rock compressive and shear strengths, making this parameter very useful to profile the changing nature of the rock mass.

9.4 Rotary Blasthole Drill Automation:

9.4.1. A Framework for Full Automation.

The recent field monitoring experience indicated that for surface electric rotary blasthole drills, the basic framework of an intelligent drill system providing *full* drill automation would require control of the following functions:

1 - positioning the rig at the hole collar: this is currently a manual task, yet the utilization of evolving satellite ground positioning or other survey technology may eventually enable setting-out to ± 1 foot of the blasthole pattern requirements. Recent installation of PLC-based, remote joystick controllers for propelling permit improved positioning of the drill by the operator exterior to the cabin.

2 - collaring: this task is considered to be within the capabilities of a control strategy, i.e. lower N and W for the first 5 to 10 feet of hole. After this stage, operating limits would be raised to those determined to be associated with normal drilling.

3 - drilling the hole according to design specifications: i.e. controlling the actual drilling cycle, by modification to N and W, in order to reduce hole deviation, caving and overall wear and tear. This stage would also be necessary to achieve more precise hole depths and end point locations in agreement with the blasthole pattern design. Experience in bench blasting in Coal Measures has indicated that at normal hole depths, c. 65 feet, the hole deviation is minimal (Scoble, personal communication). For deeper exploration holes, especially in steeply dipping strata, deviation may be acute and affect drilling performance, (i.e. increased torque and vibration due to increased friction developed between drill steel and borehole walls), as well as hole quality.

4 - drill pipe change: depending on the hole depth, the system should handle the functions of breaking and adding pipe

sections.

5 - minimizing maintenance while maximizing penetration rate: this requires drill performance monitoring and control of key parameters, such that for variable geology, suitable adjustments to W and N would be made, to maintain acceptable levels of T and vibration. Benefits would be in minimizing machinery (bit and drill) wear and failure , particularly electric motor overload due in part to excessive levels of T and vibration.

9.4.2. A Strategy for a Semi-Automated System.

An incremental approach to such blasthole drill automation is considered appropriate, based upon an initial control strategy confined only to the drilling cycle, in order to meet the immediate needs o the mine. The control logic is based mainly upon the drill response data acquired during the recent performance monitoring studies. This would allow the initial creation of a semi-automated system, in which strategy the operator performs collaring, pipe changing and rig positioning within the blasthole pattern. This approach is in line with that followed by the manufacturers of drill automation packages. They have identified that the primary sequence both requiring and being suitable for automation is from the time that the drill is levelled and ready to drill to when the bit reaches its preset depth (Li,1974). Those functions to be carried out automatically by a computer-based control system to enable this type of operation would include:

1 - Instantaneous changes to drill performance to be made as the bit faces changing rock mass characteristics. This is to maximize R while reducing the possibility of motor damage through maintenance of T within predefined motor limits. In addition, control would aim to minimize machine structural and bit wear due to excessive vertical and horizontal vibrations resulting from steel *slapping* and bit bouncing (Peck et.al.,1988).

2 - The characterisation of the bench geology, based on analysis of the digitally-monitored performance parameters. Drilling models would be used within the control logic to optimize drill performance, based upon an understanding of the relationships established between individual and groups of drilling parameters and changing rock mass properties, i.e. *drilling intelligence*. Such data also forms the basis for input into a mine's short range planning and reserve estimation systems.

3 - Monitoring of bit condition. This would allow bit changing prior to total failure, thus preventing or minimizing damage to the drill system, borehole deviation and caving resulting from excessive vibration of the drill string. Cost savings could result from early detection of bit failure, in terms of increased productivity resulting from higher levels of R, cleaner boreholes due to improved cutting and reduced vibration levels, and reduced downtime for jammed bits/steel or rotary motor damage. The monitoring of drill performance through known strata has been demonstrated to allow warning of impending bit failure. Bit wear could be predicted based upon a continuous comparison of levels of R, T, W, I and N data with time for consecutive boreholes over the life of the bit (trend analysis techniques - see section 8.3). Significant deviations between the drill performance signals for a *new* and *aging* bit appear to be detectable, primarily with regard to the levels of W, I and T during operation.

In addition, the monitoring of I would allow detection of caving ground conditions or a plugged bit. For such situations, appropriate measures would be taken, e.g. reduction in W and N and/or retraction of pipe.

4 - Accurate drilling of a hole of preset depth, unattended after manual rig positioning and set-up. While drilling proceeds the operator would be free to attend to other duties off the drill, e.g. cable maintenance.

5 - Monitoring and storage of production data enabling

detailed production statistics and reports to be generated; e.g. operating and/or downtime and delays on a per hour, shift, day or week basis.

6 - Flexibility to enable modifications of operating limits depending upon changing operator requirements. A change in pipe length and bit diameter for example would alter the thresholds of the primary drill parameters, pre-programmed within the control strategy framework. The thresholds or limits incorporated into the control strategy algorithms would be specific to the operating limits determined for a particular drill and bit type and size, operating over a known range of rock strengths. In light of these requirements, the semi-automation of a rotary blasthole drill should be accomplished by the monitoring and control of the following operating elements:

1 - Bailing air pressure, I, and air flow to detect:

- minimum levels of I and flow;
- maximum levels of I and flow;

These parameters would be monitored and a control output developed to coordinate with the valve for W. Maximum and minimum setpoints would be developed together with an acceptable deadband, with setpoints being adjustable. Airflow, along with I, would be monitored to maintain optimum bailing and sensing of caving holes or a plugged bit.

2 - Rotary speed, N, and armature voltage monitored for:

- maintenance of optimum bit speed for the ground conditions and bit life;

The bit rotary speed/armature voltage would be monitored and a control output developed to coordinate with the control valve for W. The bit setpoint would be adjustable for changing conditions and the setpoint deviation would be used to adjust the level of W.

3- Rotary torque, T, and armature current monitored for:

- maintenance of optimum T for maximum R and motor life;

The value of T and armature current would be monitored and a control output developed, coordinated with N signal to calculate rotary motor horsepower, for use as a drilling efficiency and motor limit indicator. Calculated SE(T) could be used in a similar manner within the control strategy.

4 - <u>Bit depth</u> for detection of:

- rotary head machinery upper and lower limits;
- hole depth limit;

5 - <u>Bit penetration rate</u>, R:

The value of R would be monitored and a control output developed to coordinate with N and T signals.

6 - Rotary machinery <u>pulldown hydraulic pressure</u>, W, to control:

- value of R,
- level of T.

7 - <u>Rotary speed</u>, N, field current:

- monitor for loss of power to drill,
- control for optimum N.

The monitored field current level when combined with other parameters should enable field adjustment to increase or decrease levels of T.

8 - Drill <u>machinery levelling</u>:

- monitor drill level in orthogonal directions,
- control the operation of levelling jacks

The drill level will be monitored with electronic clinometers and the output applied to levelling jack control valves. This ensures that the drill platform is level in order to avoid jammed steels and off-vertical blastholes. Monitoring of the hydraulic feed lines to the jacks would permit an early indication to be provided to the operator of line leaks, a common problem causing jammed steels and caved boreholes (Payton, 1987).

In addition to these, the vibration of the drill should be monitored. In a situation where the drill encounters hard or fractured ground, or voids, then uneven loading of the bit occurs, producing considerable horizontal and vertical vibration. The potential damage to bit, pipe and drill structures (mast) could be minimized or avoided if the threshold frequencies associated with any of these phenomena can be identified from vibration monitoring. Upon detection of such vibrations, the control strategy would respond immediately to reduce N and W. An interesting extension of vibration monitoring is the potential use of these signals to identify hard versus soft ground. Research undertaken in France, indicated that a portion of the energy developed by the bit at depth will propagate up the drillstem to surface. By monitoring the vibration at the drill head, it was seen that a portion of this energy was representative of the properties of the rocks being drilled. The exact range and amplitude of emitted frequencies due to rock drilling, were specific to the type of bit used and drilling conditions (Lutz et.al.,1972). This parameter could be useful when combined with other drill data, such as calculated SE(T) or T data, to improve the capability of performance monitoring to identify changing rock conditions, whilst optimizing the drill operation.

9.5 Conclusions:

Microprocessor-based instrumentation for monitoring the performance of drills has been successfully developed. Data from such systems forms the foundation for the development of a technique, through pattern recognition and artificial intelligence, aimed to characterize ground conditions and thence control drill operation. A strategy for the automation of rotary blasthole drills has evolved with this on-going research.

10.0 CONCLUSIONS:

This thesis has aimed to advance the following areas:

1 - the development and implementation of appropriate microprocessor-based instrumentation systems to monitor the performance of rotary blasthole drills,

2 - the analysis of drill performance parameters to determine their unique responses in different geological and geomechanical regimes,

3 - the understanding of machine-rock interaction using a tricone bit, based on an interpretation of the performance data,

4 - the applications of drill performance monitoring towards such areas as geological exploration, mine planning, bit selection and wear evaluation and drill automation and control.

A modified version of a monitoring system developed originally for use with small, crawler-type percussion drills, was successfully adapted to the Bucyrus-Erie blasthole drills at the Fording River Mine. Part of the modifications entailed the design and construction of an interface panel. This component enabled both torque and rotary speed to be monitored directly from the electrical motors of these machines. A suitable monitoring scheme was also created to permit the acquisition of a meaningful and complete performance parameter database during production drilling operations. Further work involved the development of software to assist in the processing, manipulation, analysis and presentation of the data.

Early phases of the studies were dedicated to an evaluation of the geology at the field site, and thence the physical, structural and geomechanical nature of the characteristic rock units. This was followed by an evaluation of the performance of the drill in response to these characteristic rock units: the hard sandstones and siltstones and soft mudstones and coals encountered at the mine. Through a detailed analysis of the monitored data, characteristic drill performance parameter ranges were identified for the particular and controlled geological conditions represented by these units. The expected range of variation in each monitored performance parameter when drilling in either sandstone/siltstones, mudstones or coals was confirmed through a statistical analysis. The extent of these ranges were illustrated using star symbol plots, which further demonstrated the reproducibility of the drill data in the identical rock units of neighbouring boreholes. Also identified was the relative importance of certain drill parameters to the rock breakage processes in the range of rock units at the mine. The prominent role of the applied torque in both soft and hard rock breakage was clearly demonstrated.

It has in the past been proposed that rock strength governs drilling performance. Prior work had indicated that rock breakage mechanisms were dependent upon the shear and compressive strengths of the rock being drilled. It was therefore important to know how these properties varied in the rocks of the study area. Through an understanding of the geological controls on rock strength, the effect which this had on drilling performance was shown to be reflected by characteristic variations in the parameters.

Several models were closely examined to establish whether combined drill parameter responses were more sensitive to changing rock properties than variations in the individual parameters. It was concluded that the calculated specific energy index, based on the work of Teale (1965), best reflected the observed variations in the different rock units. This index permitted the responses in all of the drilling parameters to be combined, thus increasing the overall sensitivity for the identification of changing ground conditions. This index is also primarily governed by the torque, the parameter which was observed in this research to be the most dominant in the hard rock breakage process. Downpressure was indicated to exert more control over rock breakage in the softer mudstones and coals, followed by the torque.

The capabilities of performance monitoring for geological exploration were examined, based on interpreted data acquired during production drilling. This is considered to be a very significant application area for a producing mine. The relationships established between the parameter responses in the rock units were used to identify the lateral and vertical variations in stratigraphy on mine benches. This data when combined with the mapping of exposed faces and geophysical log data, also permitted detailed cross-sections to be developed in order to validate the application of drill monitoring to mining engineering production planning and scheduling. The integration of interpreted drill data with Fording Coal Ltd. mainframe-based short and long term planning modules, is evident to permit the updating of mine models and bench plans on a hole-by-hole and timely basis. In addition, the benefits to blast design based on the precise identification of waste rock-coal boundaries should lead to substantial improvements in shovel productivity through optimized fragmentation. This application would also result in improved explosive use and reduced dilution.

The effect of tricone bit wear on drilling performance has been presented in detail. Based on the monitored results it was conclusively determined that tungsten-carbide bit wear, for the particular drill, bit and rock type at the study site, was a progressive phenomenon. Trend analysis techniques applied to the monitored data were demonstrated to be one effective approach to predicting the nature and degree of bit wear. The results indicated that trends in the downpressure and bailing air pressure best reflect the effect of bit wear. It was also concluded from this study, that a bit in an advanced state of wear severely reduces the ability to define changing geology on the basis of performance parameter variation. The responses in the drilling performance parameters to changing rock unit properties are therefore masked by their variations associated with cone bearing wear. However, degrading performance due to bearing wear, as observed, occurs at a late stage in the life of the bit.

Monitoring the performance of a particular drill was shown to offer the potential for a more scientific approach to bit selection. In the present study the types of failures were identified through an examination of the worn bits. A correlation of these observations to the trends witnessed in the performance parameters, as monitored over the life of the bit, indicated clearly the suitability of a bit according to ground conditions encountered. It can be concluded from these studies that tricone bits with improved gage wear protection and shorter inserts would reduce the types of failures observed. In addition, a more appropriate bit design would extend the overall life of the bit while also improving productivity through increased drill rates and drilled footage per bit.

It was apparent from this work that the continuous monitoring of drilling performance parameters can form an important foundation for the automation of drilling operations. Based on the defined thresholds of the individual parameters for different rock units and drilling situations, the control of the drill would initially involve the automated recognition of these setpoints. This could be accomplished using pattern recognition techniques. Upon identifying a particular condition of drilling, appropriate modifications would be instituted to adjust one or more of the performance parameters towards maintaining maximum productivity while minimizing machine damage and maintenance.

Isolation of the critical parameter responses as the bit wears, should also assist in the development of a more functional control strategy for drill automation. Based on these, the control strategy could compensate for the higher levels of torque developed through bit wear. By making adjustments to both rotary speed and downpressure, maximum drilling rates could be achieved for minimum levels of vibration.

The various applications of drill performance monitoring all indicate one important conclusion: that once the machine-rock interactions are properly qualified and/or quantified in relation to the rock, then the interpreted drill data can be used for a variety of mining engineering applications in exploration, planning and production phases.

11.0 RECOMMENDATIONS FOR FUTURE WORK:

This project has illustrated the wide array and extent of detailed information which can be extracted from machine performance data through effective capture and interpretation. In this respect, the proposed hypothesis has been answered, i.e. that monitored drill performance data can in fact be related to the geological environment. However, the results of this project were based upon a particular set of controlled field conditions, namely the drill and bit type and characterized rock units at the Fording River Mine.

This work also covered a wide range of related areas under field and production oriented conditions. Constraints prevented extensive examination of some further interesting aspects. Future work is recommended which would focus on further analysis of the relationships between the intact rock properties and the individual performance parameters using different bits (type and diameter) and drills.

The development of more detailed and appropriate methods of analyzing the degree of bit wear have been demonstrated through treatment of performance data using trend analysis techniques. Further work in this area would also be necessary to correlate the monitored changes in the drilling parameters with actual physical wear of the bit in terms of changes to insert shape/size, bearings and cone shell condition. The results would be useful for evaluating the effectiveness of a particular bit design for different rock types and operational conditions (levels of downpressure, torque, rotary speed). Using existing bit designs, an optimum bit type could therefore be selected or developed for a particular drill to improve overall productivity and minimize production costs. Based therefore on an improved understanding of how the machine and the rock interact, the bit and the drilling equipment could be more appropriately designed to match rock characteristics. Bit designs in general could be modified to better maintain overall drill performance as the bit wears, based on identified performance parameter trends. This could lead to the development of a bit which would still break rock effectively yet for lower levels of torque; this would greatly assist in preventing structural damage to the drill through vibration and motor overloading.

Applying pattern recognition techniques to the data acquired in this study should enable the development of the intelligence required as part of full drill automation. The particular drill parameter thresholds established in this study are clearly specific to the conditions of the particular mine site. The results of the thesis study form the basis of an on-going project into rotary drill automation between the author and the Fording River Mine.

Automation of drills, or simply monitoring their performance, in other mines would require an approach similar to these reported studies. Firstly, appropriate instrumentation would have to be developed and adapted to the particular drills. Secondly, the relationships between the drill and the rock types present would have to be clearly defined. Finally, an appreciation of the drilling procedures would be necessary in order to account for any operator-related influence on performance data.

12.0 ACKNOWLEDGEMENTS:

The author gratefully acknowledges the assistance of the many individuals with different aspects of the research both in Montreal and at the Fording River Mine.

Thanks are extended to C.Morency whose programming and assistance facilitated the data handling and manipulation. The assistance provided by Mr.C. Hendricks in the planning and organization of the field periods was important to the overall operation of the project. In addition, Mr. Hendricks provided valuable technical contributions during the actual drill monitoring phases.

The assistance of D.Corriveau and H. Casanova at the Fording River Mine, both during the equipment installation and monitoring phases was appreciated. Mr. Corriveau was also responsible along with M. Carter, for the preparation and testing of the core specimens at McGill University. The core thin sections were prepared by G. Pangiotidis of McGill and the analyses undertaken by P. Spahn of Heidelberg, W. Germany.

Thanks are also extended to the employees at the Fording River Mine and of Fording Coal Ltd., Calgary. The contributions of Mr.J.Gray in initially proposing the concept of a project with McGill is acknowledged. The author also recognizes the cooperation of Mr.D. Kennedy, Senior Mining Engineer at the Fording River Mine. In addition, M.Cole, D.Guglielmin, R.Dean, R.Gold, B.Dunn, K.Bergwall, B.Saul, K.Streeter, B.McEwen, and the many technical people involved in surveying, blasting and gamma logging as part of the Mine Engineering Group at the Fording River Mine also contributed to this work. The support and efforts of Mr.D.Stoakes and Mr.A.Brown are also acknowledged.

The Fording Geology department including K.Komenac, B.Musil, D.D'Andrea and J.Desjardins provided the author with much of the necessary geological data for the bench areas monitored. The contributions of Projects Engineering staff, ie. K.Muller, E.Bellerby, G.Donald, D.French and O. Baumgartner are also appreciated.

In the maintenance department of the mine, many people were involved with the drill monitoring equipment modifications and installation. D.Payton, E.Walters and B.Bekker, willingly provided, within already limited resources, the manpower to assist the author throughout the project. B.Daniels and M.Boyd were involved with the modifications to and calibration of the electrical interface panel during the initial installation period in May 1988. Their efforts and interest in the project made for the eventual successful implementation of the ADM system on #9 drill. The assistance of other individuals in departments such as the Machine and Radio Shops are also acknowledged for their contributions to the project.

The production group at the Fording River Mine were instrumental in allowing the research group to carry out their tasks in the field with a minimal amount of restriction. R.Campbell and R.LeGros permitted the team to have virtually unlimited access to the drills during both the instrumentation and monitoring phases. In addition, considerable flexibility was demonstrated by them in allowing occasional delays to production when necessary for equipment installation and testing. The cooperation and involvement of people at all levels in the field, primarily the Drill trainers A.Virch and R.Dortman, and the drillers on #9 drill, B.Brown, L.Golbeck, R.Hird and R.Dreyber and D.Bissonette was also instrumental in the success of the project.

Thanks are also due to Ms.P.Pinotti of Fording Coal Ltd. for her administrative assistance at the mine.

Very special thanks are extended to the author's thesis supervisor, Dr.M.J. Scoble for his guidance and support in all aspects of this project.

Mr. A. Bensoussan of Solroc Consultants, St. Laurent, Que. is also gratefully acknowledged for having provided an ADM drill monitoring unit for use by the author throughout the field studies at the Fording River Mine.

The strong moral support provided by the author's family was an important component throughout this work. In addition, the patience of his fiancee Alena, was admirable considering the two years consumed by the field studies.

Initial drill monitoring trials undertaken in June 1987 at the Fording River Mine were financed from a EMR Research Agreement grant. Additional financing for the two year project was awarded under the University-Industry granting scheme in August 1987 by the Natural Science and Engineering Research Council (NSERC) with field studies beginning officially in September 1987.

13.0 REFERENCES:

Al-Jassar, S. and Hawkins, A.R. 1977. Some geotechnical properties of the main Carboniferous limestone formation of the Clifton Gorge, Bristol. Proc. Conf. Rock Engng., Dept. of Mining Engineering, Univ. of Newcastle upon Tyne, April 4-7, 1977, pp.393.

Allen, J.H. 1973. Considerations for rock bit selection and operation. Europe and Oil, June 1973.

Allen, J.H. 1977. Determining parameters that affect the rate of penetration. Oil and Gas Jour., Oct. 3/10, 1977.

Allen, J.H. 1977. Contemporary methods for determining the parameters that affect the rate of penetration. Preprint of a paper presented at the 3rd Adriatic Symposium on Oil Well Drilling, Porec, Yugoslavia, May 1977.

Bauer, A. and Calder, P.N. 1971. Open pit drilling and blasting. Jour. South African Inst. Mining and Metallurgy, Vol. 71, no.6.

Bentson, H.G. 1956. Rock-bit design, selection and evaluation. Technical paper for Smith Tool Co., Calif.

Bingham, M.G. 1964. How rock properties are related to drilling. Oil and Gas Jour, December 14, 1964, pp.94-101.

Brady, B.H.G. and Brown, E.T. 1985. Rock mechanics for underground mining. Allen & Unwin Inc. Winchester, Mass. pp.527.

Brooks, W.B., Dean, J.T. and Gravely, W. 1963. Mobile electronic recording system and drill-off data illustrating its use. Jour. Pet. Tech. January 1963.

Brown, E.T., and Phillips, H.R. 1977. Recording drilling performance for tunnelling site investigation. Construction Industry, Research and Information Assoc., London, England, No.81.

Bucyrus-Erie 60R Series III Rotary Blasthole Drill - Operating Manual. 1978. Bucyrus-Erie Company, Milwaukee, Wi.

Bucyrus-Erie Co. 1979. Surface mining supervisory training program shovel/truck, Bucyrus-Erie Co., Milwaukee, Wi.

Campbell Scientific 21XL Micrologger Instruction Manual. 1986. Campbell Scientific Corp., Logan Utah.

Clark, G.B. 1987. Principles of rock fragmentation. John Wiley and Sons, Inc. New York, 610 p.

Cobbs, J.H. and Reader, L.R. 1973. Shaft drilling: state of the art. USBM Contract S0122047, March 1973.

Cunningham, R.A. 1960. How rotary speed shortens bit life, increases drilling costs. Oil and Gas Jour. Vol.58, no.28, July 11, 1960.

Cunningham, R.A. 1968. Analysis of downhole measurements of drill string forces and motions. Jour. of Engng. for Industry, Trans. ASME, May 1968.

Cunningham, R.A. 1978. An empirical approach for relating drilling parameters. Jour. Pet. Tech., July 1978, p.987-991.

Diely, F.H., Dareing, D.W., Paff, G.H., Ortloff, J.E. and Lynn, R.D. 1968. Downhole measurements of drill string forces and motions. Jour. of Engng. for Industry, Trans. ASME, May 1968.

Donald, R. 1984. Geology of the Mist Mountain Formation. Unpubl. MSc. thesis, Dept. of Geol. Sci., Univ. of Alberta, Edmonton.

Dresser Canada Inc., Security Division, Mining Operations, Tech. Brochure - Security "Super-Aire" blasthole bits. 1987.

Dresser-Security Inc. 1983. Strength test data. Letter to Fording Coal Ltd., Jan.3.

- 1979. Strength test data. Letter to Fording Coal Ltd., Aug.31.
- 1971. Strength test data. Letter to Fording Coal Ltd., May 19.

England, R. and J. Kelly, 1986. Development of the automatic GO-60 drill. 2nd. Conf. on Innovative Mining, Penn. State Univ.,pp. 31-35.

Eronini, I.E., Somerton, W.H. and Auslander, D.M. 1981. A dynamic model for rotary rock drilling. Trans. ASME, Vol.104, June 1981, p.108-120.

Estes, J.C. 1971. Selecting the proper rotary rock bit. Jour. Pet. Tech., November 1971.

Everell, M.D. 1972. Performance of raise borers as a function of geology and rock properties. 8th Canadian Rock Mech. Symposium, Toronto, November 1972.

Everell, M.D., Dessureault, M., Cauchon, A. and R.O. Tervo, 1973. A preliminary control strategy for the automatic control of an instrumented diamond drill. Proc. 6th. Conf. Drilling and Rock Mech., Soc. Pet. Eng. AIME, Austin, Texas, paper SPE 4235.

Everell, M.D., Tervo, R.O. and Turcotte, G. 1975. Instrumentation and data logging on a raise boring machine. CIM Bull., July 1975.

Fahy, M.P. and Guccione, M.J. 1979. Estimating strength of sandstone using petrographic thin section data. Bull. Assoc. Engng. Geol., Vol.16, No.4, pp.467-485.

Fish, B.G. 1961. The basic variables in rotary drilling. Mine and Quarry Engineering, Vol. 27, No. 2, February 1961.

Galle, E.M. and Woods, H.B. 1960. Best constant weight and rotary speed for lowest cost drilling. Oil and Gas Jour., November 1960.

Garner, C. 1971. Is there a better way of grading insert bits?. Smith Tool International, Irvine, Ca.

Garner, C.R. 1972. How to get more hole from carbide insert bits. Petroleum Engineer, September 1972.

Garner, C.R. 1977. Reading the dull bit appearance. Smith Int'l.Inc., Technical Services, Service Brochure.

Girard, H. 1985. Contributions to the exploitation of drill parameters for civil engineering (in French). Unpublished PhD thesis, University of Bordeaux, France.

Girard, H., Morlier, P., Puvilland, O., and Garzon, M. The digital Enpasol method-exploitation of drilling parameters in civil engineering. Geocontrol, St. Laurent, Quebec, Canada, 1985.

Gold, R.D., Kennedy, D.A. and Gray, J.H. A review of drilling and blasting practices at the Fording River Operations. 11th Canadian Institute of Mining and Metallurgy District 6 Meeting, Vancouver, Canada.

Golder Associates. 1977. Taylor Pit report. Report #1236.

Golder Associates. 1983. Strength test data. Letter to Fording Coal Ltd., Report #E/83/1236, Oct.14.

Haas, W., 1988. Personal communication. Marion Power Shovel Division, Dresser Industries, Marion, Ohio.

Hagan, T.N., and Reid, I.W. 1983. Performance monitoring of production blasthole drills - a means of increasing blasting efficiency. 2nd International Surface Mining and Quarrying Symposium, Institution of Mining and Metallurgy, Bristol, England, 245-254, October 4-6, 1983.

Hartmann, H.L. 1966. The effectiveness of indexing in percussion and rotary drilling. Int. J. Rock Mech. Min. Sci., Vol.3, pp.265-278.

Hoek, E. and Bieniawski, Z.T. 1965. Brittle fracture propagation in rock under compression. Intl. Jour. of Fracture Mechs., 1, pp.137-155.

Howarth, D.F. and Rowlands, J.C. 1987. Quantitative assessment of rock texture and correlation with drillability and strength properties. Rock Mechs and Rock Engng., 20, pp.57-85.

Howarth, D.F., Adamson, W.R. and Berndt, J.R. 1986. Correlation of model tunnel boring and drilling machine performances with rock properties. Int. J. Rock Mech. Min. Sci., 23, (2), pp.171-175.

Howie, W. 1988. Personal communication. U.S. Bureau of Mines, Spokane Research Center, Spokane, Washington.

Kallio, M., 1988. Personal communication. Gardner Denver Drills, Cooper Industries, Roanoke, Virginia.

Lane, et.al. 1947. Modified Wentworth scale. Trans. Am. Geophys. Union, Vol.28, pp. 936-938.

Lebel, J.R.G. An investigation to evaluate the relationship between Rock Quality Index (RQI) and powder factor for surface mining. Unpublished MSc. thesis, Univ. British Columbia, Vancouver, Canada, 1984.

Leighton, J.C.,Brawner, C.O., and Stewart, D. 1982. Development of a correlation between rotary drill performance and controlled blasting powder factors. CIM Bull. 75, No. 844, pp. 67-73.

Leighton, J.C. Correlating rotary drill performance to powder factors for improved blasting control. Proceedings of the International Symposium on Geotechnical Stability in Surface mining, Calgary, Canada, 121-132, November 1986.

Li, T.M., 1974. Rotary drilling with automated controls - new force in open-pit blast hole production. Coal Age Operating Handbook of Coal Surface Mining and Reclamation, vol. 2: Chironis, N,P, ed., McGraw-Hill Inc., New York, pp. 212-219.

Luisigna, R.W. and Felleman, J. 1983. Testing and demonstration of roof bolter instrumentation for detecting hazardous roof. U.S. Bureau of Mines Contract No. H0202008, April, pgs.165.

Lummus, J.L. 1970. Drilling optimization. Jour. Pet. Tech., Nov., pp.1379-1389.

Lutz, J., Raymond, M., Gstalder, S., Quichaud, C.,Raynal, J. and Muckleroy, J.A. 1972. Instantaneous logging based on a dynamic theory of drilling. Jour. Pet. Tech., June, pp. 750-758.

Macpherson, J.D., Nigh, E. and Muldowney, S. 1986. Borehole geoengineering system boosts data interpretation during drilling. GEOBYTE, Summer 1986. p.46-54.

Martin, D. 1988. At last a computer-controlled jumbo that really works. Tunnels and Tunnelling, May, pp. 33-35.

Matuszak, D.R. 1972. Stratigraphic correlation of subsurface geologic data by computer. Math. Geol. Vol.4, no.4, 1972.

Matuszak, R., 1988. Personal communication. Bucyrus-Erie Mining Systems Division, S.Milwaukee, Wisconsin.

Maurer, W.C. 1962. The "perfect cleaning" theory of rotary drilling. Jour. Pet. Tech., November 1962, p.1270-1274.

Mellor, M. 1972. The normalization of specific energy (Technical note). Int. Jour. Rock Mech. Min. Sci., 9, pp.661-663.

Miller, C.E. and Rollins, H.M. 1968. Evaluation of a vibration damping tool and of drill stem torque requirements from data recorded by an instrumented drill stem member. Jour. of Engng. for Industry, Trans. ASME, May 1968.

Mol, O., Danell, R. and Leung, L. Studies of rock fragmentation by drilling and blasting in open cut mines. 2nd International Symposium on Rock Fragmentation by Blasting. Keystone Colo.,381-392, 1987.

Morlan, E.A. 1962. Designing large diameter hole drilling programs. World Oil, April 1962.

Mottola, L. 1988. Micro-processor based equipment monitoring. Unpubl. term paper, Course 306-200A, Dept. of Mining Engng., McGill University, 55p.

Neilson, W.J. 1969. Shape of inserts gets added emphasis as carbide bits drill softer formations. Drilling Magazine, April 1969.

Nelmark, J.D. 1980. Large diameter blast hole drills. Mining Congress Journal, August 1980, p. 30-35.

Outmans, H.D. 1960. The effect of some drilling variables on the instantaneous rate of penetration. Trans. AIME, Vol.219, p.137.

Pathak, J. and Dias, M. 1986. Microprocessor controlled down-the-hole drill for enhancing productivity and accuracy in underground hardrock bulk mining methods. Proc. 8th W.V.U. Mining Electrotechnology Conf., W. Virginia University, pp. 86-92.

Paone, J., Madson, D. and Bruce, W.E. 1969. Drillability studies-laboratory percussive drilling. USBM RI 7300.

Payton, D. 1987. Automation on Rotary Blasthole Drills. Fording Coal Ltd. Internal Report.

Peck, J. Application of drill monitoring to rock mass characterization. Unpublished MEng Thesis, Department of Mining and Metallurgical Engineering, McGill University, Montreal, Canada, 1986.

Peck, J. , Scoble, M.J. and Hendricks, C. 1988. Monitoring while drilling production blastholes: applications in surface mining. Presented at the 14th Annual Meeting of the Society of Explosive Engineers, Los Angeles, Calif., Feb. 1 - 5, 1988.

Peck, J., Scoble, M.J. and Payton, D. 1989. Drilling intelligence and automation. Paper submitted for publication in the Jour. Mineral Resources, New York, April 1989.

Price, N.J. 1963. The influence of geological factors on the strength of Coal Measures rocks. Geological Magazine, Vol.100, No.5, pp.428-443.

Rabia, H. 1982. Technical note: Specific energy as a criterion for drill performance prediction. Int'l. Jour. Rock Mech. Min. Sci. Vol. 19, pp.39-42.

- 1985. Specific energy as a criterion for bit selection. Jour. of Pet. Tech., July, pp. 1225-1229.

- 1987. Bit performance and selection: a novel approach. Preprint of a paper presented at the 1987 SPE/IADC Drilling Conf., New Orleans, La., March 15-18, pp. 987-996.

Reed Mining Tools Inc. 1983. General Catalogue. Reed Mining Tools Inc., Grande Prairie, Tx.

Rowlands, N. 1977. An examination into the mineralogical and mechanical properties of Coal Measure strata. Unpubl. PhD. thesis, Dept. of Min. Exploitation, University College, Cardiff, England.

Sangha, C.M., Talbot, C.J. and Dhir, R.K. 1974. Microfracturing of a sandstone in uniaxial compression. Intl. Jour. Rock Mech. Min. Sci., Vol.11, pp.107-113.

Scheck, D.E., Mitchell, L.H. and Mack, G.W. 1982. Automated Blast Hole Logging and Design. U.S. Bureau of Mines, Grant No. G1115006, Final Report, December.

Schunnesson, H. 1988. Towards automated drilling in Sweden. Preprint 1st I.F.A.C. Workshop on Advances in Automation of Underground Hardrock Mining., L'Esterel, Quebec, Canada.

Schwaetzer, T. 1965. Geophysical Studies of the Continuity of Coal Seams. International Journal of Rock Mechanics and Mining Science, Vol. 2, pp. 167-196, 1965.

Sessoms, W. 1987. Personal Communication. Interactive Sciences Inc., Sanford, Florida, November.

Simon, R. 1959. A laboratory study of rock breakage by rotary drilling: a discussion. Trans. AIME, Vol.216, p.361.

Smart, B.G.D., Rowlands, N. and Isaacs, A.K. 1982. Progress towards establishing relationships between the mineralogy and physical properties of Coal Measure rocks. Intl. Jour. Rock Mech. Min. Sci., Vol.19, pp.81-89.

Smith-Gruner. 1987. General catalog 1986-1987. Smith Int'l. Inc., Okla.

Somerton, W.H. 1959. A laboratory study of rock breakage by rotary drilling. Trans. AIME, Vol. 216, p.92.

Statgraphics, Statistical Graphics System. 1986. Reference Guide to Ver.2.6., STSC Inc. Rockville, Md.

Teale, R., 1965. The concept of specific energy in rock drilling. Int. Jnl. Rock Mech. Min. Sci., vol. 2, pp. 57-73.

Ulvelin, K. and T. Puhakka, 1988. Computerized hardrock drilling. Proc. 3rd. Can. Symp. Mining Automation, Centre Recherche Minerales, Quebec City, pp. 9-14.

Vutukuri, V.S., Lama, R.D., and Saluja, S.S. 1974. Handbook on the mechanical properties of rocks, Vol.I, Trans Tech Publications, Clausthal, Germany, pps.280.

Warren, T.M. 1981. Drilling model for soft formation bits. Jour. Pet. Tech., Vol. 33, June 1981.

- 1984. Factors affecting torque for roller-cone bit. Jour. of Pet. Tech., Sept., pp.1500-1508.

Well logging and interpretation techniques. 1982. Dresser Atlas, Dresser Industries Inc., Dallas, Tx.

Weston, W.B. and T.A. Stoner, 1970. Automation of a blast hole drill. Ann. Meeting Soc. Min. Eng. of AIME, Denver, Colorado. Preprint 70-A0-60.

Young, F.S. 1969. Computerized drilling control. Jour. Pet. Tech., April 1969, p.483-496.

Appendix I - Petrographic Report:

Part 1: Introduction

A total of 13 thin sections were examined in order to define their composition, petrology and textures. They can be divided into 3 groups according to their mean grain size (Udden-Wentworth scale):

Group A: sandstones > 0.0625 mm

Group B: siltstones 0.0624 mm - 0.0039 mm

Group C: mudstones < 0.0038 mm

The results for each thin section are shown in Table I. The number of the samples correspond to the numbers of the compressive strength tests in Table 5.1.

Table I - Classification of Thin Sections.

Sample:	A	B	C	Grain Size:
1	x	-	-	0.350mm
6	-	x	-	0.028mm
7	-	x	-	0.034mm
12/13	-	x	-	0.048mm
24/25	x	-	-	0.175mm
25	-	x	-	0.059mm
26	x	-	-	0.088mm
29	-	x	-	0.023mm
45/46	x	-	-	0.200mm
61	x	-	-	0.126mm
67	x	-	-	0.075mm
79	-	-	x	0.004mm

In general, the siltstones and the mudstones show no remnant porosity, whereas some sandstones still exhibit a small percentage of porosity. It is not clear if this represents primary or secondary porosity. In most cases (e.g. sample # 1), carbonate rims the open vugs.

No micro- or macrofossils (fauna) have been observed in the sections. However, it should be kept in mind that organic debris represents paleoflora remains and thus strictly have to be considered as fossils.

Part 2: Petrographic Description

Sample # 1:

1. Composition:

quartz (detrital): 27.2%
microquartz (cement): 41.8%
calcite (cement): 3.8%
organic matter (detrital): 15.8%
muscovite (detrital): 1.2%
chlorite (cement): 10.1%
accessories:quartzitic rock fragments (RF), pyrite, hematite, kaolinite

2. Mean Grain Size: 0.35 mm (350 μm) - medium-grained sandstone

3. Petrography and Textures:

Although sample # 1 has a large mean grain size, the rock itself is not grain-supported. Many detrital quartz grains show early carbonate rims which have been sandwiched between the quartz grains and later syntaxial overgrowths.

Microquartz is clearly the most abundant cement type but calcite is also present in high percentages. It is not clear if all the carbonate represents diagenetic cement. Some of it could be detrital, some of it may also have been formed as a replacement of other detrital grains (feldspar ?).

Chlorite could only be detected in this and all other samples because some cements show a greenish colour. The grain size of the chlorite flakes are too small to be seen by means of an ordinary petrographic microscope. XRD (x-ray diffraction) may solve this uncertainty.

Kaolinite, occurs in minor amounts, showing a typical book-shaped crystallization pattern. Pyrite and hematite have been formed together with the microquartz cement.

No pronounced layering is visible at the scale of the microscopic.

Organic matter tends to occur in clusters but may also be oriented parallel to the bedding. This is generally the only hint to a "bedding" in this sample. Although some remnant porosity still exists, the rock can be determined as solid, due to the abundant quartz cement.

Sample #6:

1. Composition:

quartz (detrital): 29.7%
calcite (cement): 52.7%
organic matter (detrital): 15.1%
muscovite (detrital): 1.3%
feldspar (detrital): 0.6%
chlorite (cement): 0.6%
accessories: pyrite

2. Mean Grain Size: 0.028 mm - medium-grained siltstone

3. Petrography and Textures:

This medium-grained siltstone exhibits rhythmic sedimentation documented by well-developed layering. Organic matter occurs mainly parallel to the bedding. The subrounded quartz clasts show no pressure solution features. The siltstone is matrix-supported with calcite as the predominant cement type. Graded bedding can be inferred in some micro-beds. Framboidal pyrite occurs together with calcite in the matrix. Formation of framboidal pyrite is clearly enhanced by the presence of abundant organic matter.
In all thin sections the carbonate cement is usually very fine-grained and thus does not incorporate many grains, as it often does in other sedimentary rocks. The samples tend to become brittle because of the small-grained carbonate cement which may either break and/or may be diluted faster.

Sample # 7:

1. Composition:

quartz (detrital): 27.8%

calcite (cement): 58.7%

organic matter (detrital): 12.2%

muscovite (detrital): 0.8%

feldspar (detrital): 0.5%

accessories: zircon, microquartz cement, pyrite, illite, chlorite

2. Mean Grain Size: 0.034 mm (34 μm) - medium- to coarse-grained siltstone.

3. Petrography and Textures:

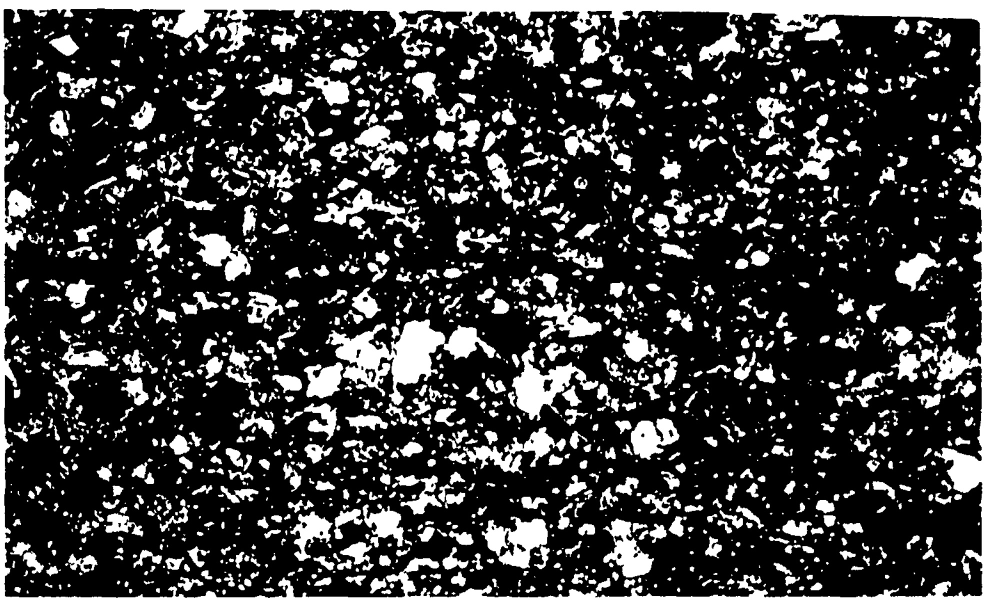

Figure 1 - Sample #7, Crossed Nicols, 100x.

The quartz clasts in this well-sorted siltstone are subrounded. The rock is matrix-supported and shows a relatively well developed layering see Figure 1. Organic matter mainly, is aligned parallel to the bedding (Fig.1). Organic matter tends to serve as gliding horizons when tectonic (or other) pressures are applied ie. zones of weakness. No pressure solution, such as concavo-convex or sutured quartz grain boundaries were seen.

Sample # 12/13:

1. Composition:

quartz (detrital): 55.5%
calcite (cement): 32.3%
organic matter (detrital): 9.0%
muscovite (detrital): 1.3%
chlorite (cement): 1.3%
zircon (detrital): 0.6%
accessories: pyrite, microquartz cement, quartzitic RF

2. Mean Grain Size: 0.048 mm - coarse-grained siltstone

3. Petrography and Textures:

This moderately well-sorted siltstone is generally grain-supported. The detrital quartz grains are subrounded and show minor pressure solution (concavo-convex grain boundaries). The rock is relatively well layered and several fining-upward cycles are apparent. Organic matter usually is concentrated at the bottom of the cycle together with the coarser grain fraction. No syntaxial overgrowth has been observed.

Sample # 24/25:

1. Composition:

quartz (detrital): 50.7%
micro quartz (cement): 25.3%
chlorite (cement): 3.9%
organic matter (detrital): 7.3%
calcite (cement): 12.3%
muscovite (detrital): 0.5%
accessories: quartzitic RF, fossil resin, feldspar, zircon, pyrite (framboidal, idiomorphic)

2. Mean Grain Size: 0.175mm - fine-grained sandstone

3. Petrography and Textures:

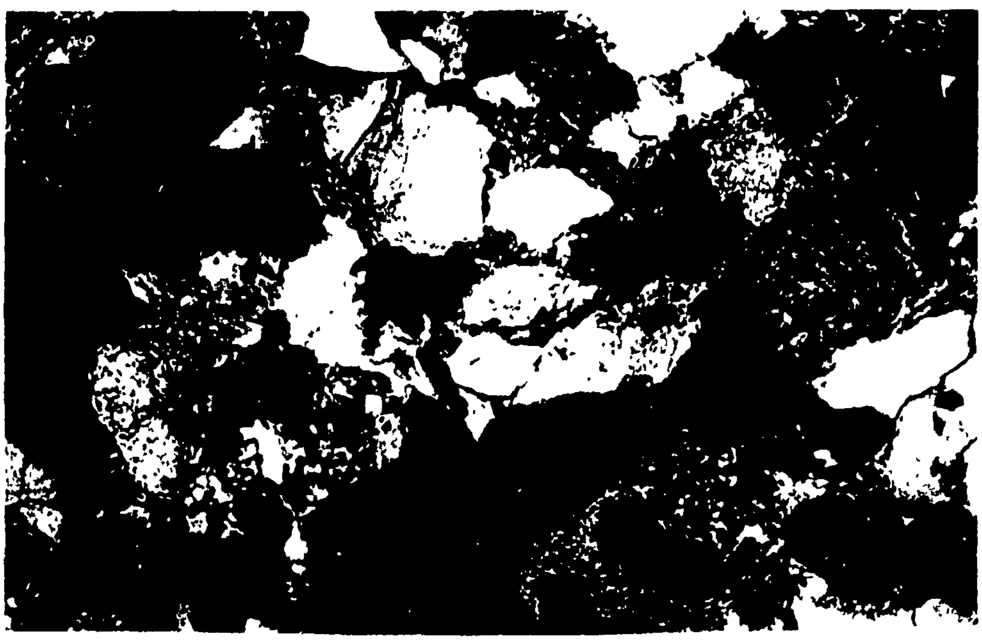

Figure 2 - Sample 24/25, Crossed Nicols, 100x.

This sandstone is grain-supported and exhibits only minor layering, see Figure 2. Quartz grains develop pressure solution and syntaxial overgrowth. Microquartz cement seems to be contemporaneous with framboidal pyrite formation, but postdates calcite cement crystallizaton. The relatively high silica content of this sample (total of 76%) may yield an increased rock strength. Organic matter and fossil resin, where present, tend be concentrated along certain layers.

Sample # 25:

1. Composition:

quartz (detrital): 35.6%
micro quartz (cement): 12.9%
chlorite (cement): 5.5%
organic matter (detrital): 9.2%
calcite (cement): 35.6%
muscovite (detrital): 0.6%
kaolinite (cement): 0.6%
accessories: fossil resin, zircon, pyrite

2. Mean Grain Size: 0.059mm - coarse siltstone

3. Petrography and Textures:

This moderately well-sorted siltstone is grain-supported. The detrital quartz clasts do not show syntaxial overgrowth but have developed minor pressure solution (concavo-convex grain boundaries). Organic matter is typically aligned parallel to the relatively well developed bedding.

Sample # 26:

1. Composition:

quartz (detrital): 34.5%

micro quartz (cement): 14.8%

chlorite (cement): 7.6%

organic matter (detrital): 16.0%

calcite (cement): 26.5%

muscovite (detrital): 0.6%

accessories: fossil resin, zircon

2. Mean Grain Size: 0.088mm - very fine-grained sandstone

3. Petrography and Textures:

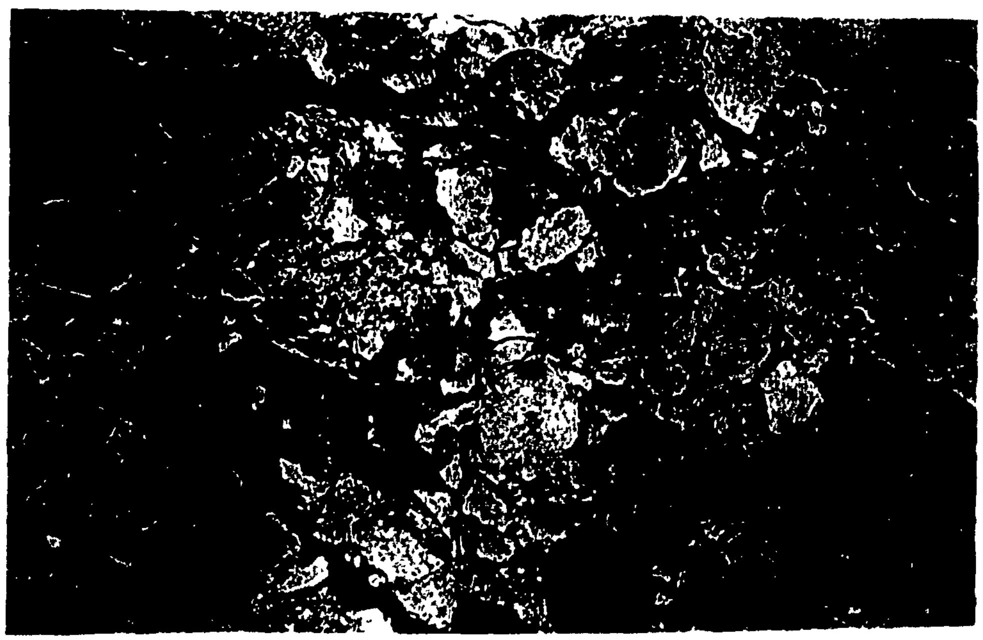

Figure 3 - Sample #26, Parallel Nicols, 100x.

This matrix-supported sandstone manifests macroscopically and microscopically a distinct bedding, see Figure 3. Planar foresets tend to be richer in organic matter (dark material in Figure 3), suggesting that the plant debris was actively transported in the water column. Some layers, being particularly rich in organic matter, will develop a reduced rock strength as a result of their pronounced lineation.

This sandstone is moderately well-sorted. Some quartz clasts, when occuring in larger percentages, exhibit a grain-supported texture. In those cases some syntaxial overgrowth is observed.

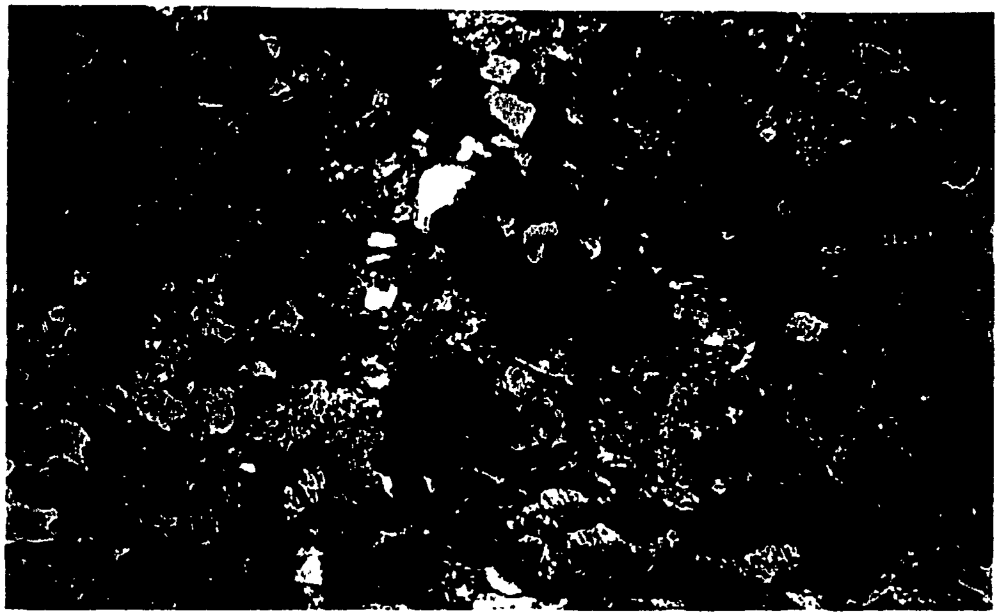

Figure 4 - Sample #26, Crossed Nicols, 100x.

Sample # 29:

1. Composition:

quartz (detrital): 28.0%
chlorite (cement): 16.1%
organic matter (detrital): 17.8%
calcite (cement): 35.6%
muscovite (detrital): 1.7%
zircon: 0.8%
accessories: fossil resin, pyrite

2. Mean Grain Size: 0.0225 mm - medium-grained siltstone

3. Petrography and Textures:

The quartz clasts in this matrix-supported siltstone are subrounded and moderately well sorted. They do not exhibit syntaxial overgrowth. Bedding is not easy to recognize under the microscope but is generally indicated by the presence of plant detritus and muscovite flakes, being oriented parallel to it. Framboidal pyrite has crystallized in close proximity to the organic matter, proving that this pattern of pyrite crystallization is clearly dependent on humic acids (low pH) and low oxigen fugacity (negative Eh).

Sample # 45/46:

1. Composition:

quartz (detrital): 45.7%
micro quartz (cement): 17.8%
composite quartz (RF): 0.7%
ore (pyrite, hematite): 13.6%
chlorite: 12.6%
illite: 5%
calcite: 3.5%
kaolinite: 1%
accessories: feldspar, zircon, organic matter

2. Mean Grain Size: 0.2 mm - fine-grained sandstone

3. Petrography and Textures:

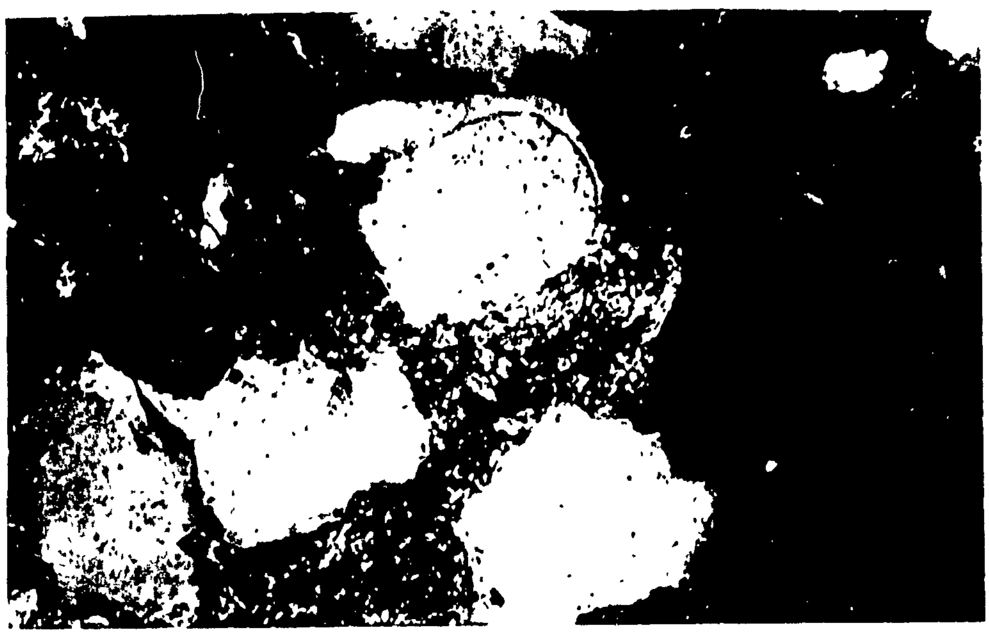

Figure 5 - Sample 45/46, Crossed Nicols, 200x.

Monocrystalline quartz represents by far the most abundant clast type in this fine-grained sandstone, being followed by composite quartz, feldspar, zircon and organic matter, see Figure 5. Some of the chlorite may be fragmental, but it usually occurs as a cement type. Other cements are, listed in order of abundance, microquartz, authigenic ore minerals (primary pyrite with hematite as a weathering product), chlorite, illite, calcite and kaolinite.

No lamination or preferred orientation of the mineral components is visible. The sandstone is generally grain-supported (Fig.5). Detrital quartz is subrounded to rounded with a mean grain-size of 0.2 mm. Detrital feldspar is rare and where occuring is subangular and with a mean grain-size of 0.55 mm. The sediment is both mineralogically and texturally submature, i.e. it is moderately well-sorted and only contains little detrital clay minerals and feldspar. Pressure solution is minor being expressed by concavo- convax quartz contacts. No real sutured grain boundaries were seen.

Organic matter usually does not occur in isolated layers. It has been introduced to the sediment being "glued" to detrital quartz. Later syntaxial overgrowth has enclosed and thus preserved most of it. Syngenetic framboidal pyrite and irregular pyrite/hematite grains often occur as coatings on the overgrowths but are also finely dispersed in the matrix. Illite and chlorite and microquartz probably crystallized at a later stage of diagenesis. Calcite filled the remaining vugs so that no remaining porosity has been observed.

The following suite of cement formation is envisaged:

	- ——— time ——— +
syntaxial quartz overgrowth	———
ore minerals	———
illite	———
chlorite	———
microquartz	———
kaolinite	———
calcite	———

Sample # 61:

1. Composition:

quartz (detrital): 51.9%
microquartz (cement): 16.0%
chlorite (cement): 3.1%
organic matter (detrital): 2.5%
calcite (cement): 25.3%
muscovite (detrital): 0.6%
kaolinite (cement): 0.6%
accessories: fossil resin, feldspar, zircon, tourmaline, biotite, composite quartz, ore (pyrite, hematite)

2. Mean Grain Size: 0.126 mm - fine-grained sandstone

3. Petrography and Textures:

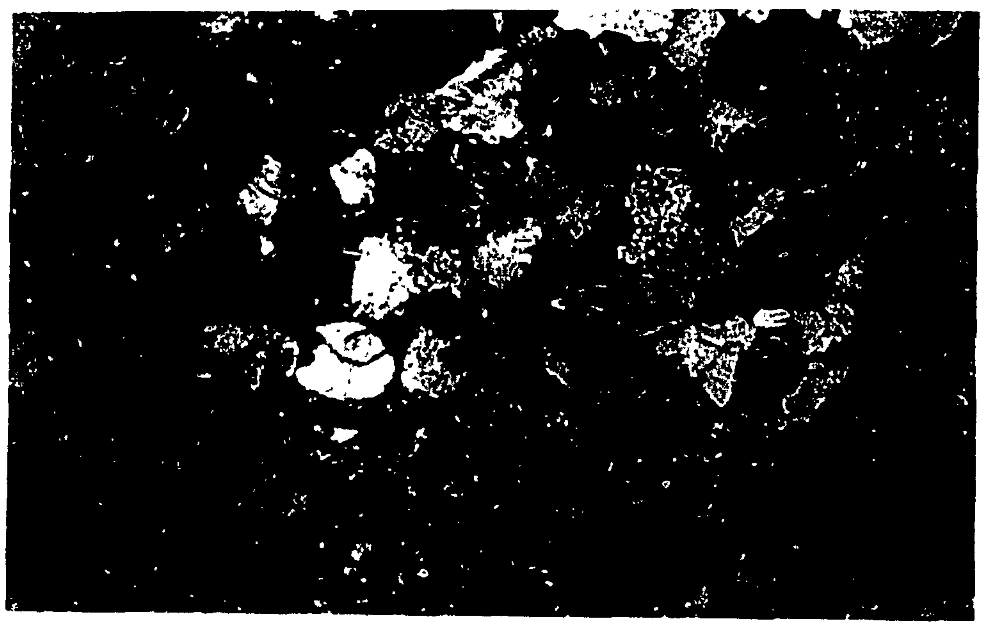

Figure 6 - Fining Down Sequence, Sample 61, Crossed Nicols, 100x.

Most of this thin section is occupied by a grain supported fine-grained sandstone. However, at the base of the section there is a sharp contact to a very fine-grained sandstone (Figure 6), and even lower a contact between the very fine-grained sandstone and a medium-grained siltstone (Figure 7). Figure 7 also demonstrates that the clay minerals appear to be concentrated in the siltstones. These photographs indicate the considerable amount of grain size variations present within these units.

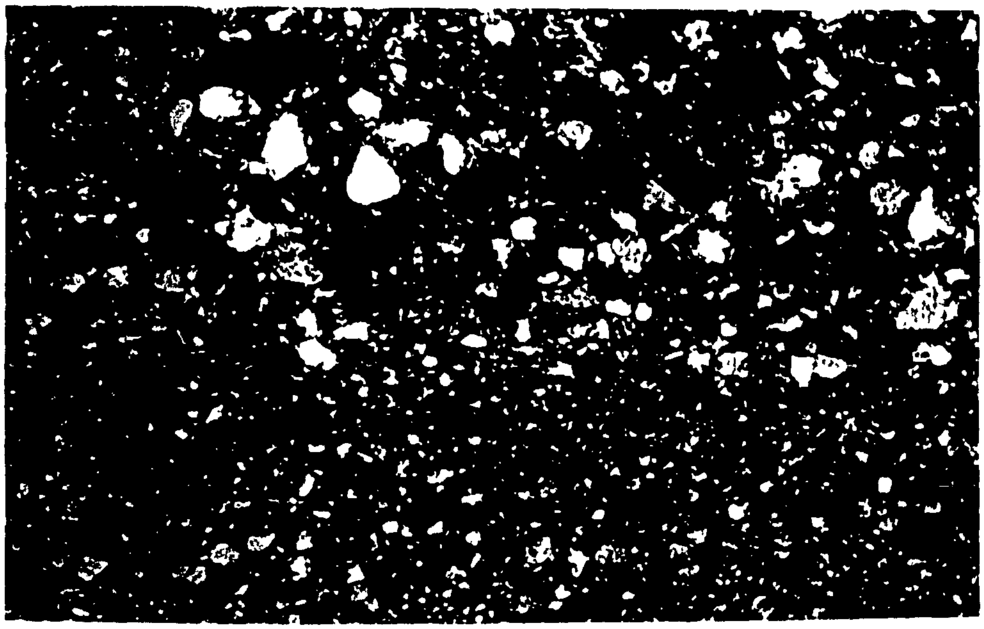

Figure 7 -- Fining Down Sequence, Sample 61, Crossed Nicols, 100x.

Detrital quartz in the mature and moderately well-sorted sandstone is subrounded (Fig. 6 and 7). The sandstone exhibits microscopically a poorly developed layering when organic matter is present. Macroscopically the rock is better layered. The quartz clasts have undergone intense pressure solution (concavo-convex and sutured grain boundaries).

Calcite is an early cement, coating detrital quartz. Later syntaxial overgrowth of the quartz has preserved the carbonate within the quartz. Rare detrital feldspar grains have been partially replaced by calcite. Some of the larger calcite crystals may also represent complete replacement of a precurser mineral (most likely feldspar). Microquartz is, together with kaolinite, pyrite and hematite, the final cement type. No remaining porosity has been observed. It is not clear if all chlorite is of diagenetic age. Some of it may also have a detrital origin.

Heavy minerals, like tourmaline and zircon, occur in larger concentrations at the base of the fine-grained sandstone. Minor erosional features are exhibited by the sharp contact to the underlying very fine-grained sandstone shown in Figure 6. The lower contact in Figure 7, between the very fine-grained sandstone and the medium-grained siltstone, is not as distinct as the latter one although it is clearly not gradational.

Sedimentation in this sample has thus occured in pulses with abruptly varying water energies.

Sample # 67:

1. Composition:

quartz (detrital): 46.3%
microquartz (cement): 9.9%
chlorite (cement): 3.7%
organic matter (detrital): 7.4%
calcite (cement): 31.5%
muscovite (detrital): 0.6%
biotite (detrital): 0.6%
accessories: fossil resin, zircon, tourmaline, feldspar, pyrite

2. Mean Grain Size: 0.075 mm - very fine-grained sandstone

3. Petrography and Textures:

This sandstone is generally matrix-supported. The detrital quartz grains are subrounded and well-sorted with minor syntaxial overgrowth.

This rock has been deposited under enhanced aquatic energetic conditions, as demonstrated by crossbedding. Organic matter is bound to specific layers and usually does not occur except as a finely dispersed component in the sediment.

Calcite is the predominant cement type, being followed by microquartz (together with pyrite formation) and chlorite. This rock is an interesting example for the tendency of calcite in this rock suite not to form large cement crystals. It usually occurs as fine crystals glueing the detrital clasts together.

Sample # 79:

1. Composition:

quartz (detrital): 55%

chlorite and illite (cement): 27%

organic matter (detrital): 15%

muscovite (detrital): 3%

accessories: fossil resin, pyrite

2. Mean Grain Size: 0.0037 mm (3.7 μm) - mudstone

3. Petrography and Textures:

Figure 8 - Sample #79, Crossed Nicols, 200x.

Sample# 79 represents the only mudstone sample examined. Its mean grain size has been calculated on the basis of the abundant very fined grained detrital quartz grains (Figure 8). The sheet silicates, with the exception of detrital muscovite, have grain sizes below 2 μm and are thus not able to be detected by an ordinary petrographic microscope.

Distinct coal micromeasures occur in the section, indicating a relatively well developed parallel bedding (Figure 8) and the heterogenous nature of these units. However, in some cases it appears that the bedding has been disturbed (Figure 9). Root fragments lead to the assumption that parts of the rock have been active as root horizons (irregular shape in Fig.8).

Figure 9 - Sample #79, Crossed Nicols, 100x.

The absence of pyrite also indicates that we are not dealing with a standard aquatic environment where organic matter has accumulated yielding favorable conditions for framboidal pyrite formation.

The coal measures generally do no longer show any remnant plant structures which would still be expected if coalification has not passed the high volatile bituminous coal stage (vitrinite reflection: 1.1%). Thus, it is assumed that the rocks lie in the stage of medium to low volatile bituminous coal.

Appendix II:

Table II - Table of Conversions Imperial to Metric.

Imperial:		Factor:		Metric:
ft	x	0.3048	=	m
ft/h	x	0.3048	=	m/h
psi	x	0.069	=	bar
lbs	x	0.4536	=	kgs
rpm	x	0.1047	=	rads/s
ft-lb	x	1.36	=	N•m
in-lbs/in^3	x	0.0069	=	MPa
psi	x	0.0069	=	MPa

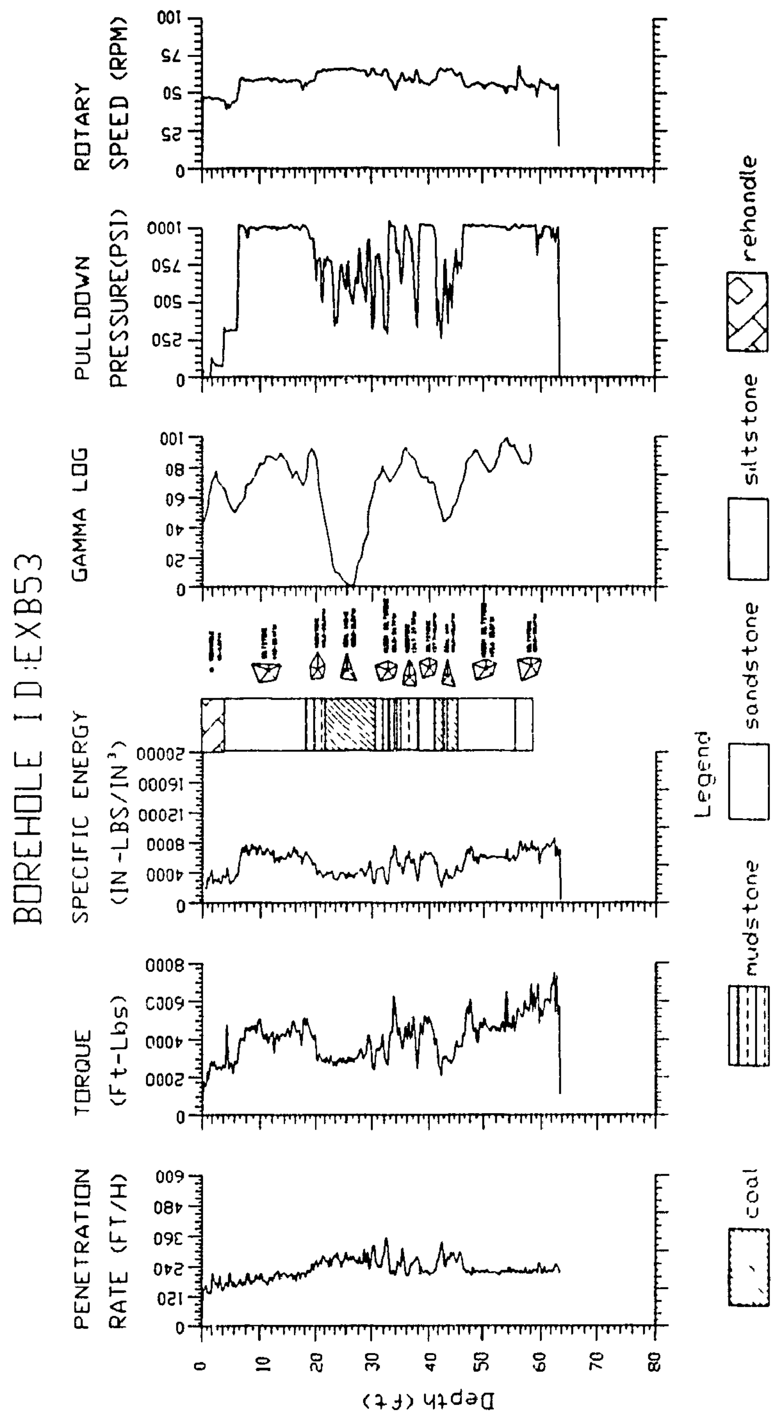

Figure 1 - Drill, Gamma, and Geologic Logs and Star Symbol Plots for Borehole EXB53.

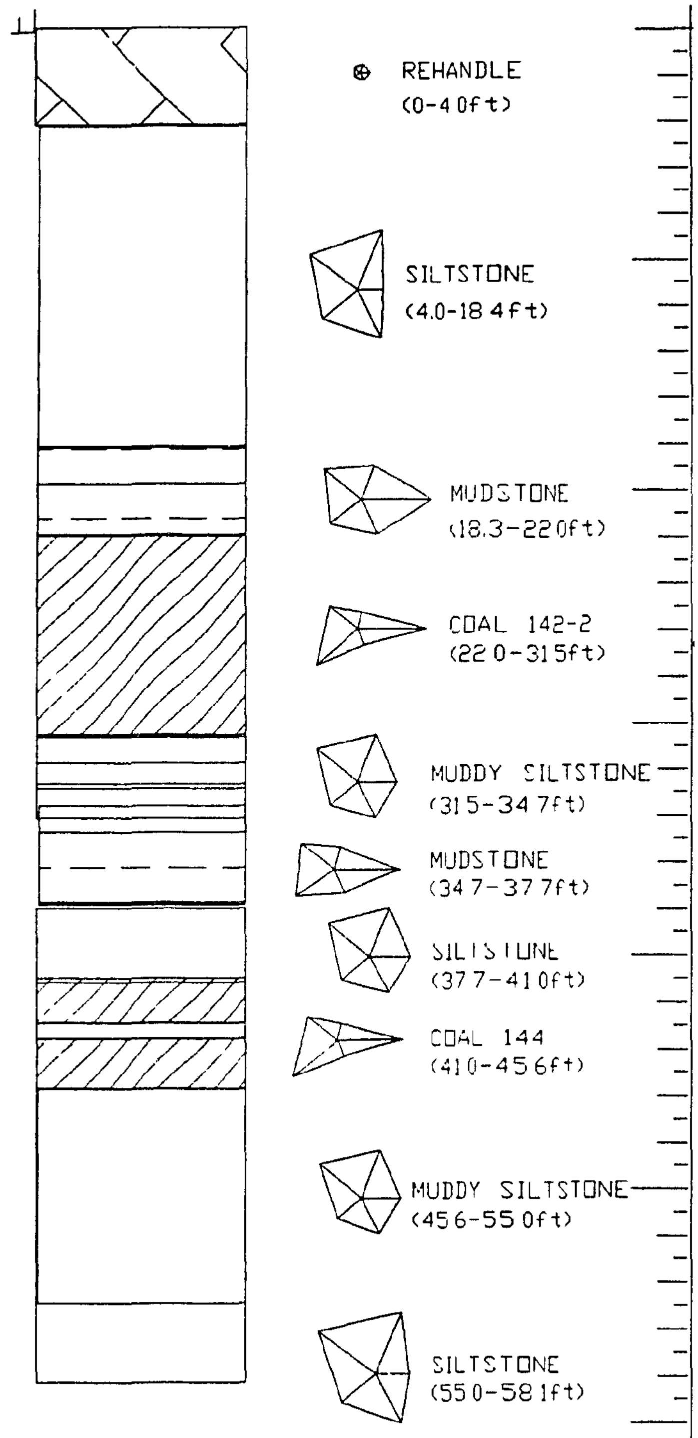

Figure 2 - Geological Log and Star Symbol Plots for Borehole EXB53.

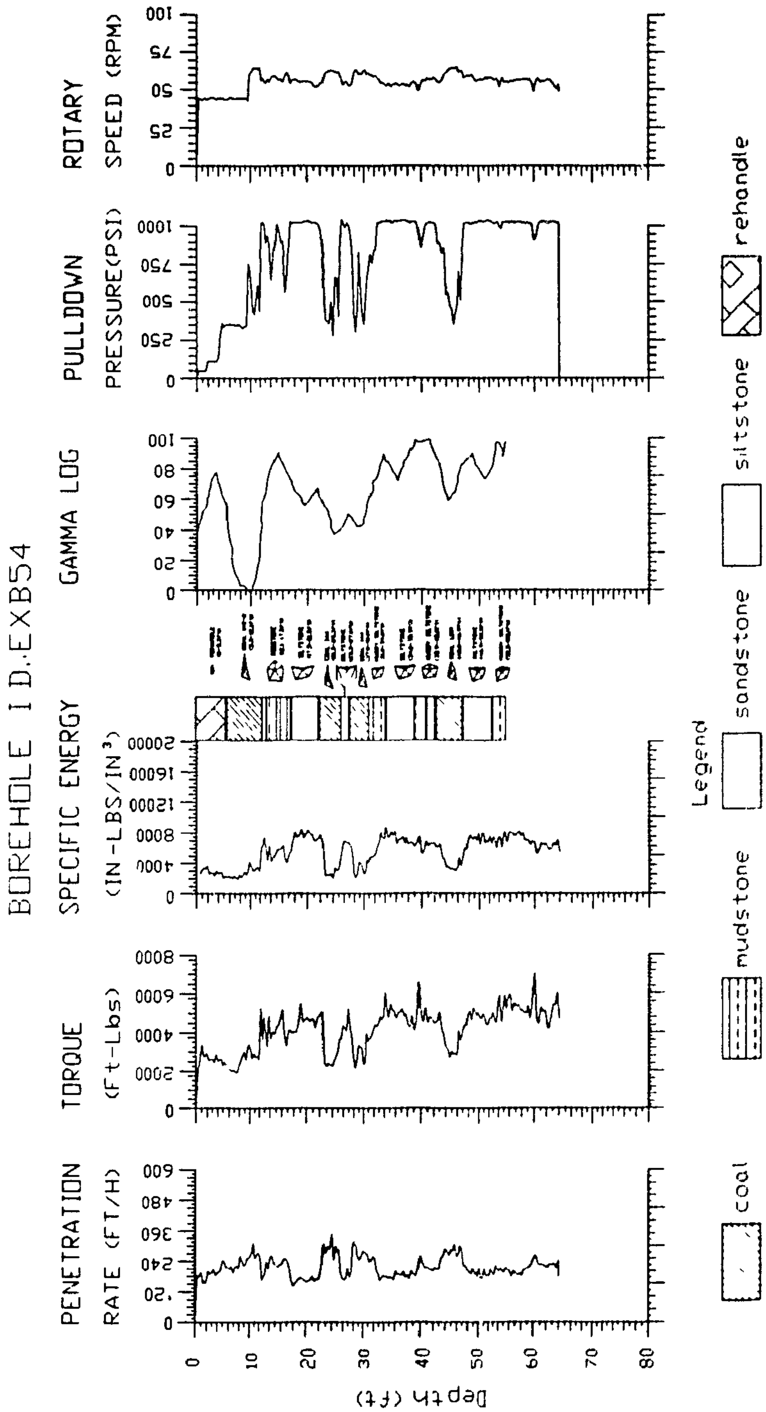

Figure 3 - Drill, Gamma and Geological Logs and Star Symbol Plots for Borehole EXB54.

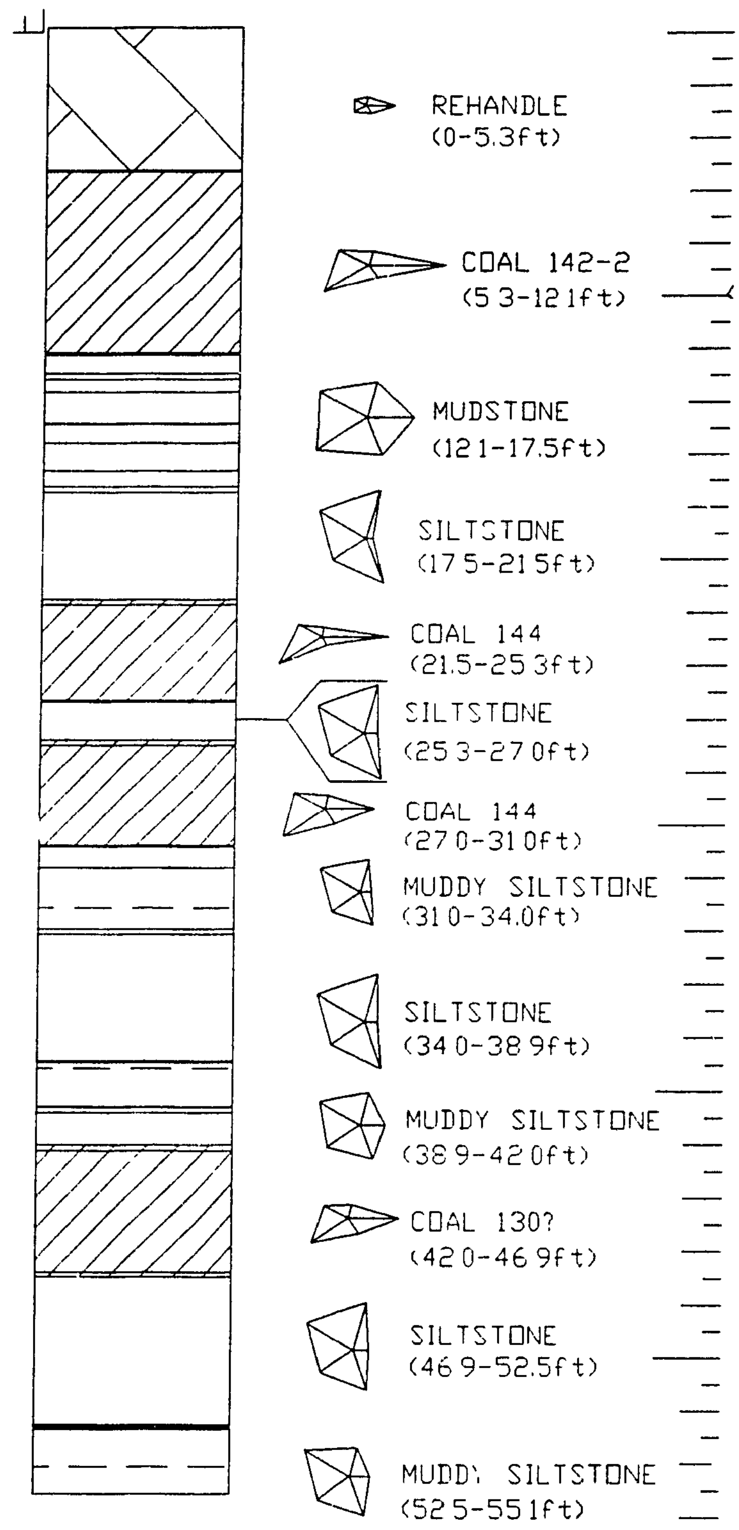

Figure 4 - Geological Log and Star Symbol Plots for Borehole EXB54.

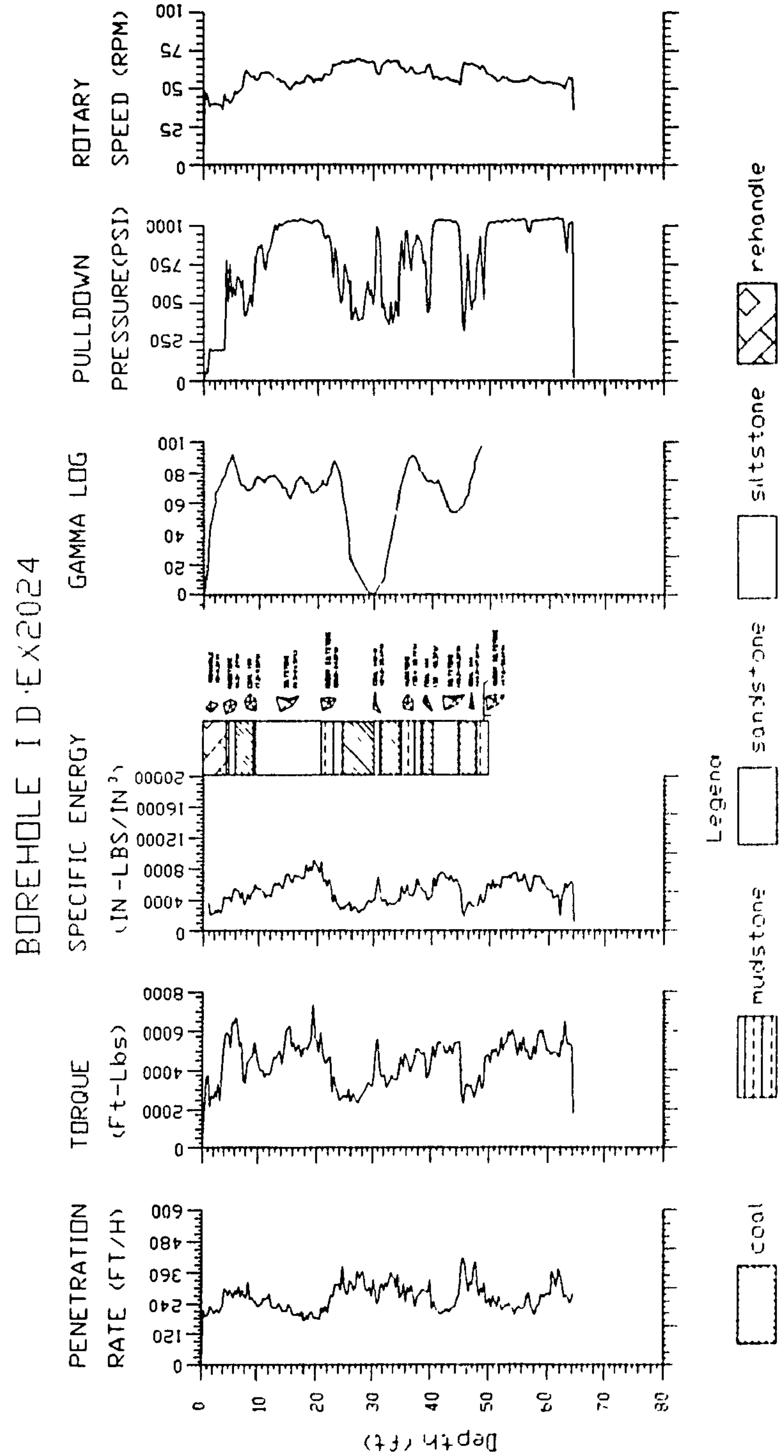

Figure 5 - Drill, Gamma, and Geologic Logs and Star Symbol Plots for Borehole EX2024.

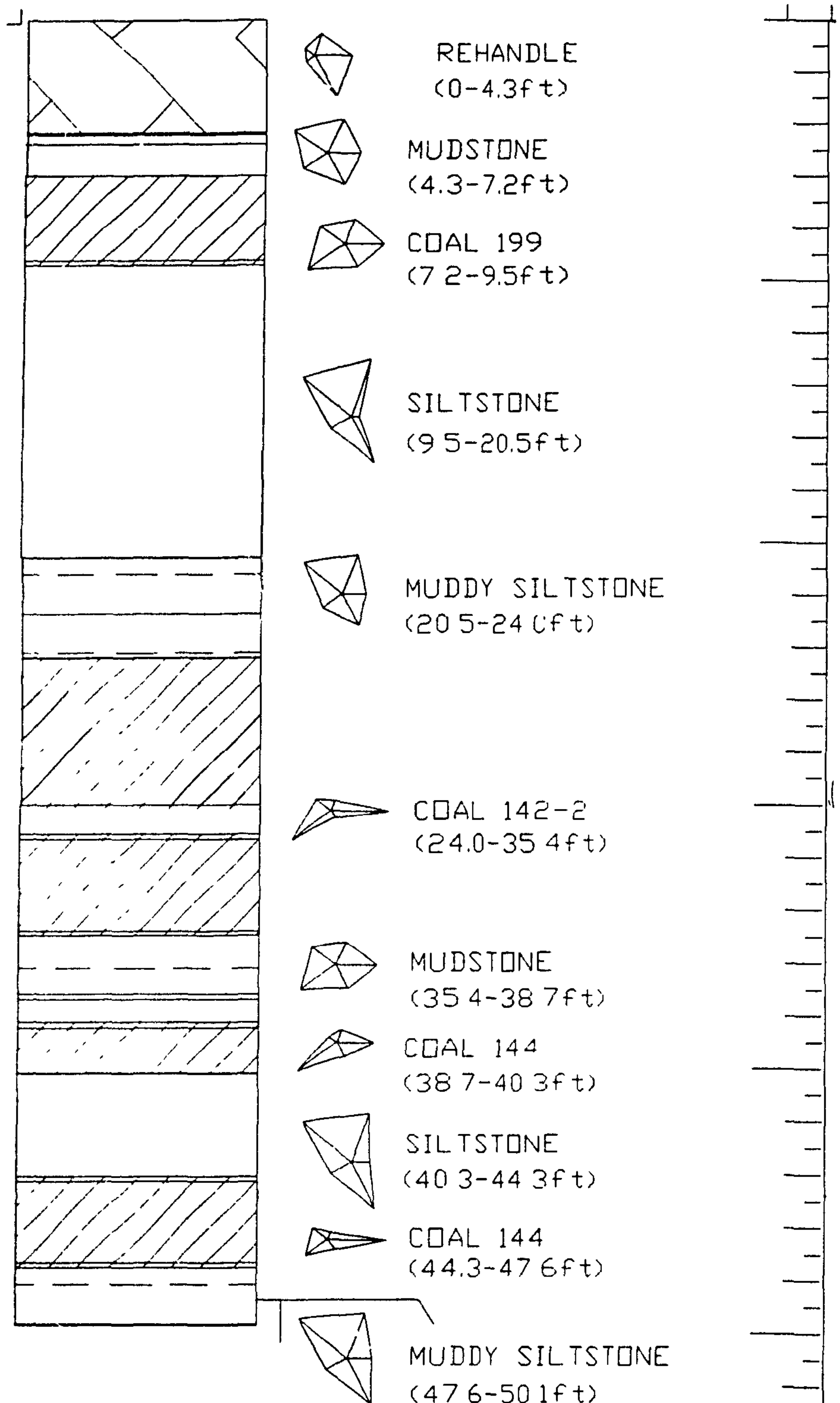

Figure 6 - Geological Log and Star Symbol Plots for Borehole EX2024.

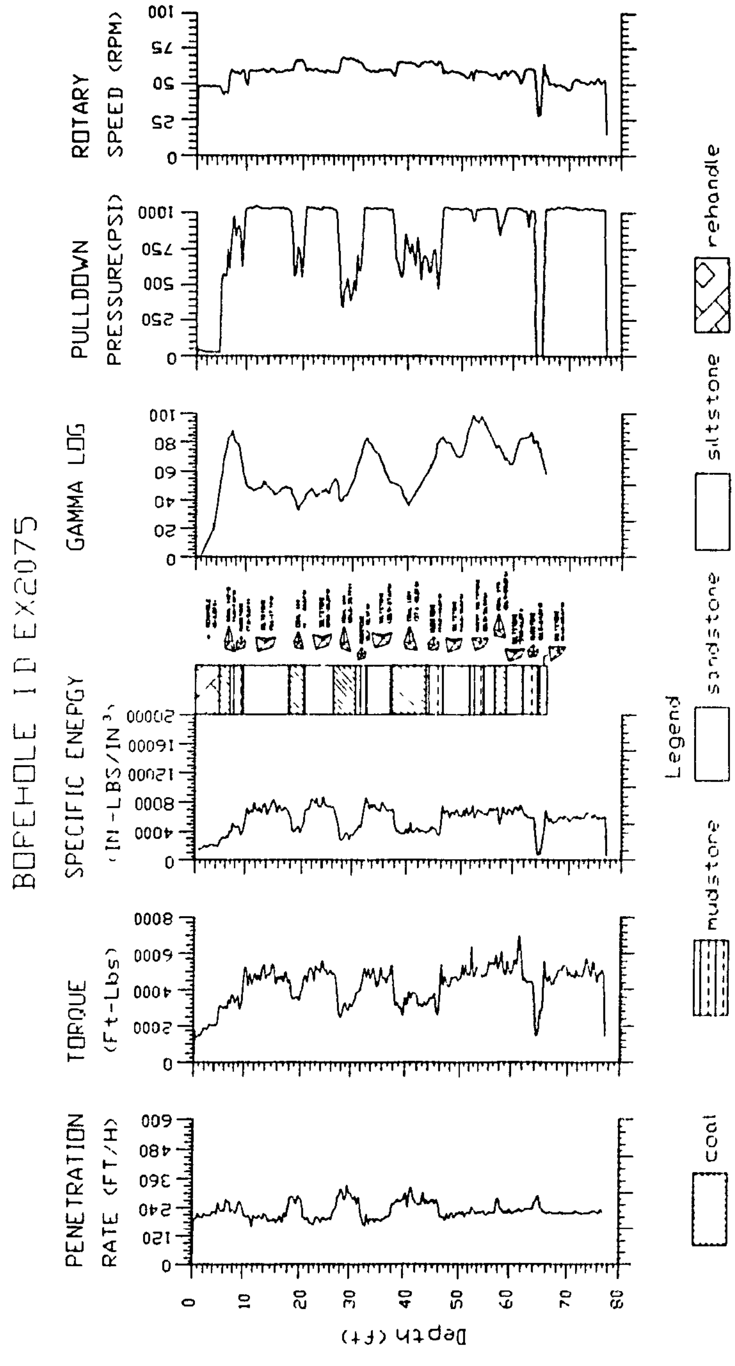

Figure 7 - Drill, Gamma and Geological Logs and Star Symbol Plots for Borehole EX2075.

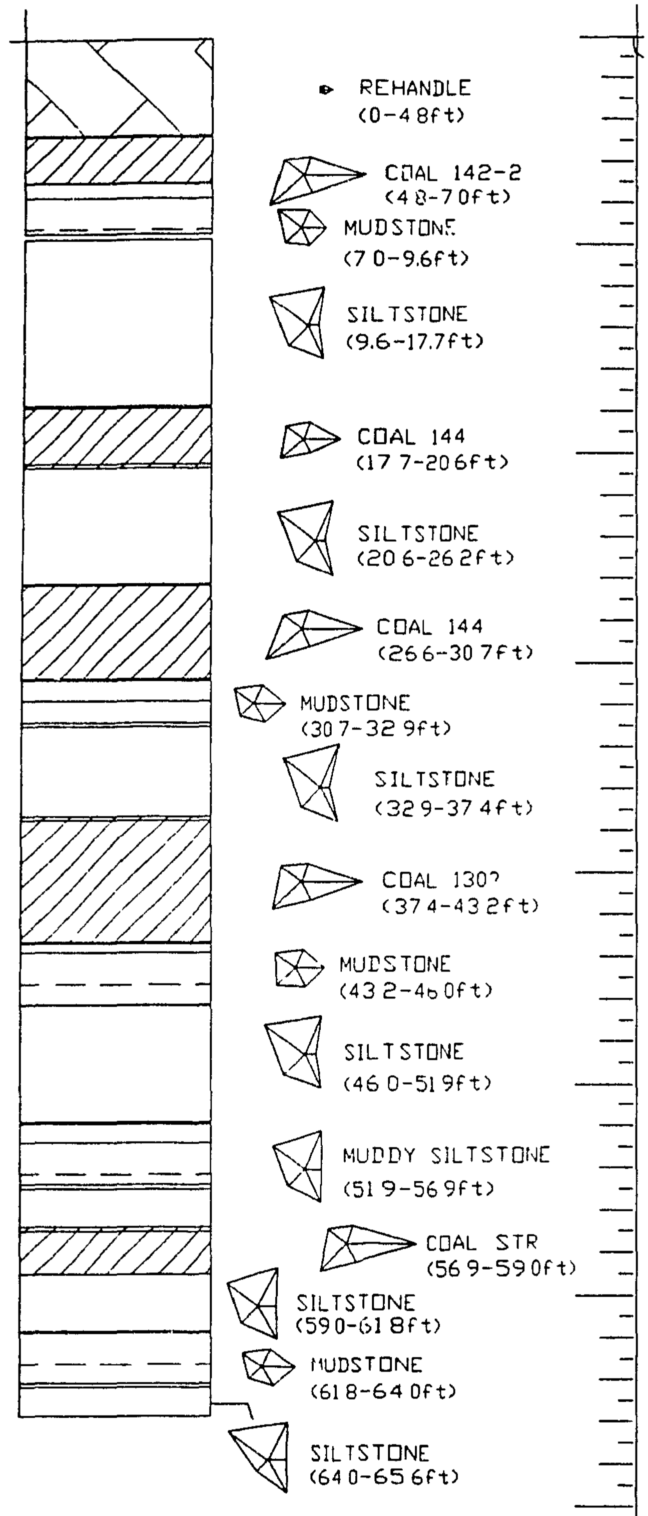

Figure 8 - Geological Log and Star Symbol Plots for Borehole EX2075.

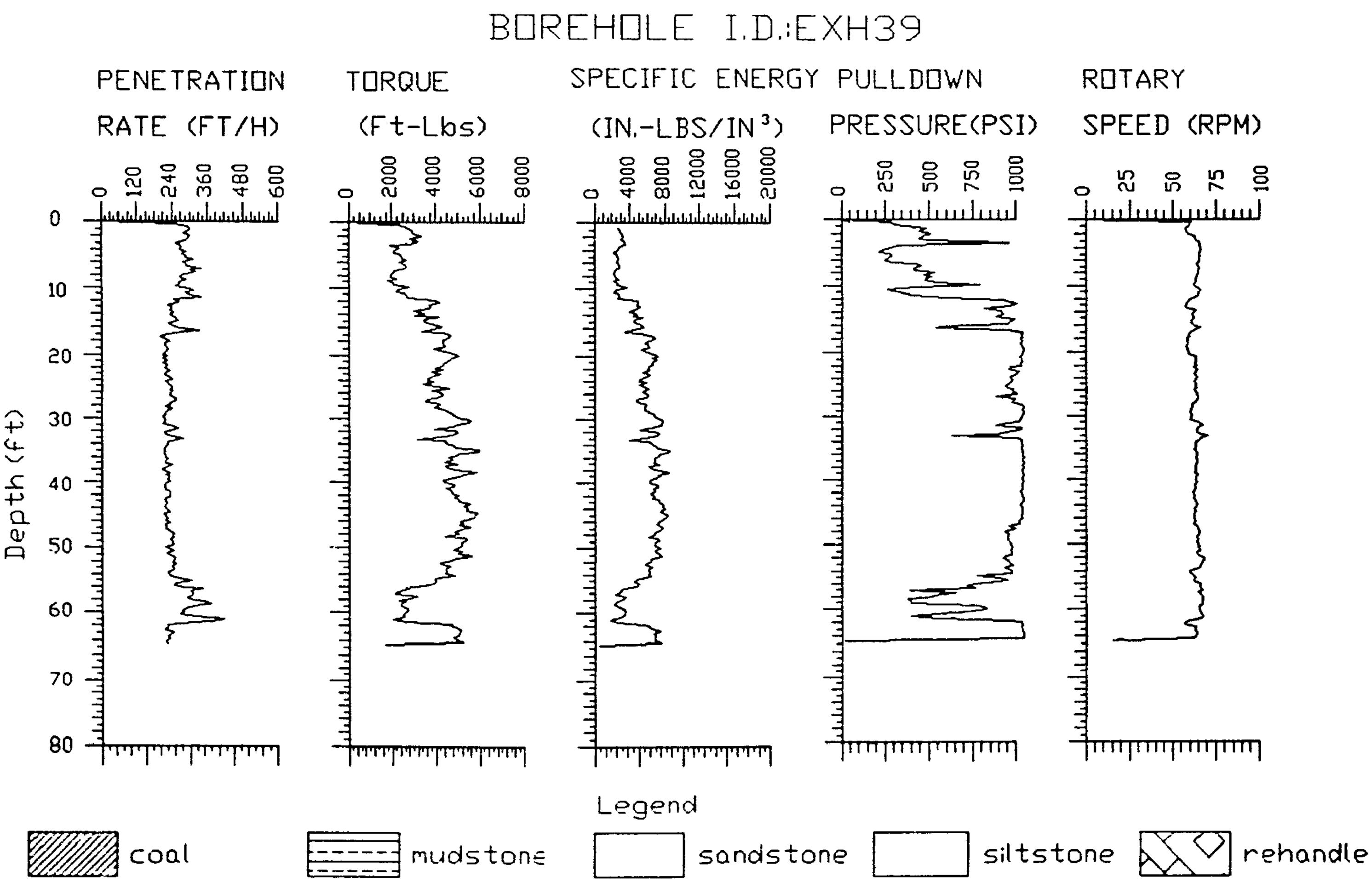

Figure 9 - Drill Logs for Borehole EXH39.

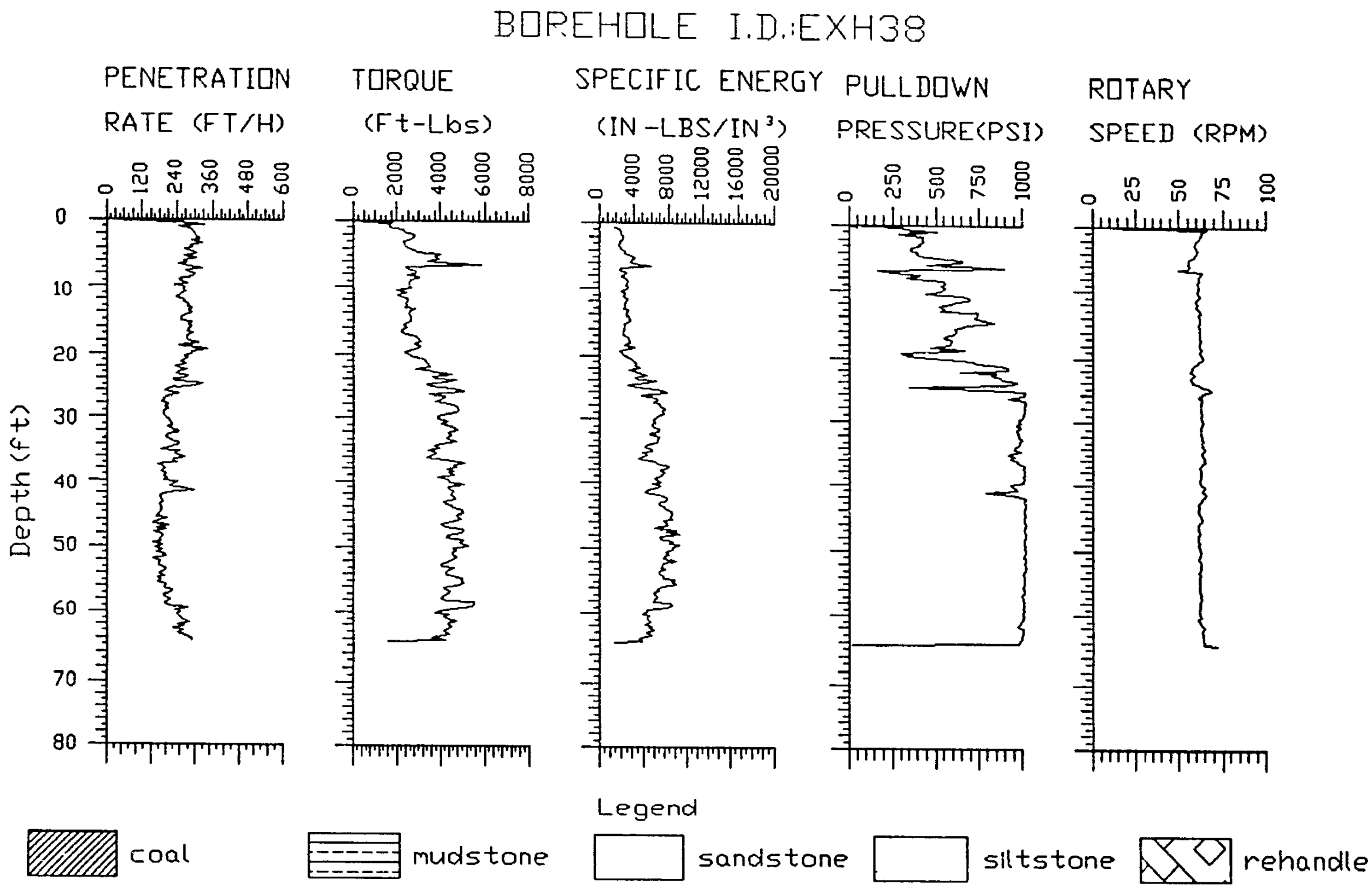

Figure 10 - Drill Logs for Borehole EXH38.

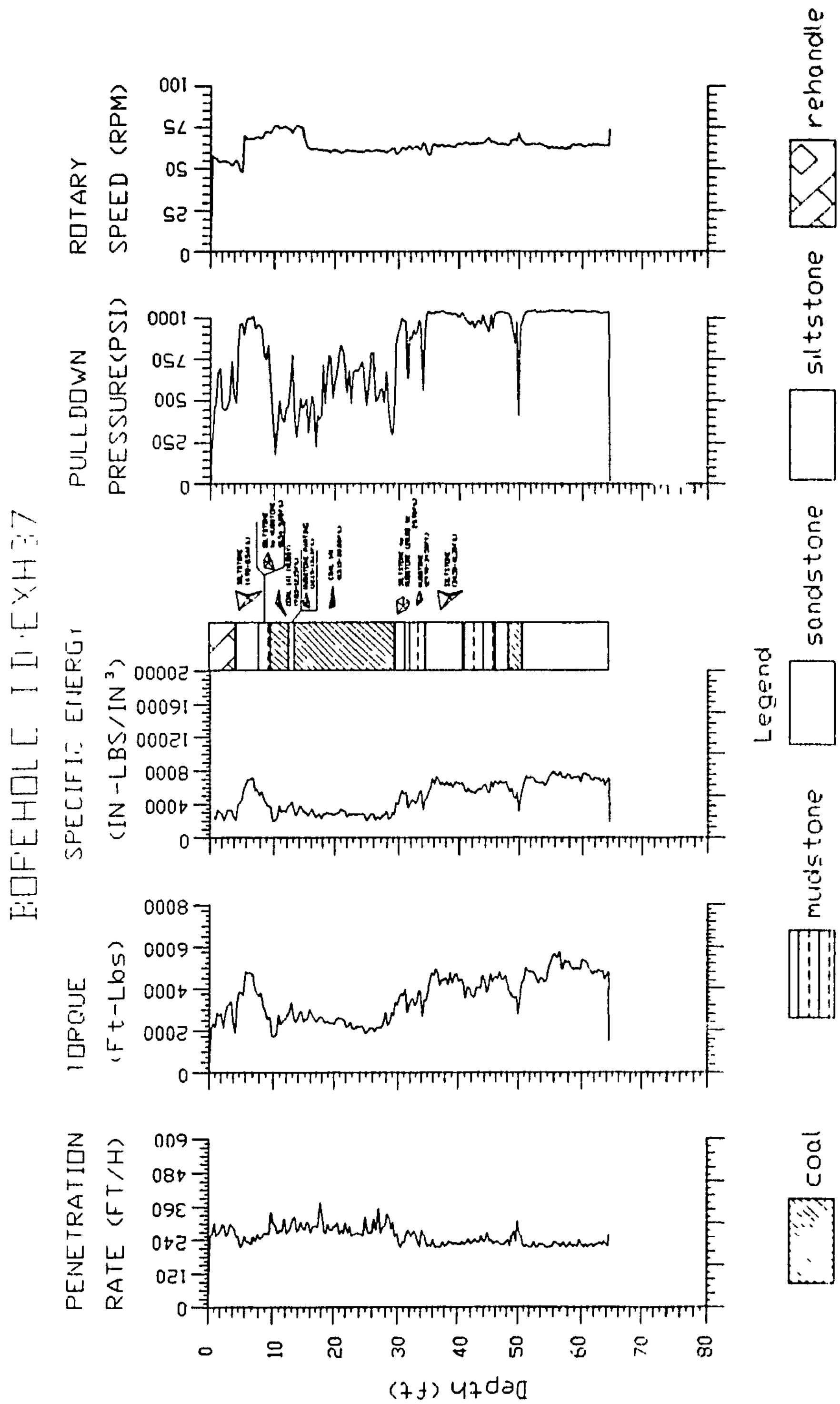

Figure 11 - Drill, Gamma and Geological Logs and Star Symbol Plots for Borehole EXH37.

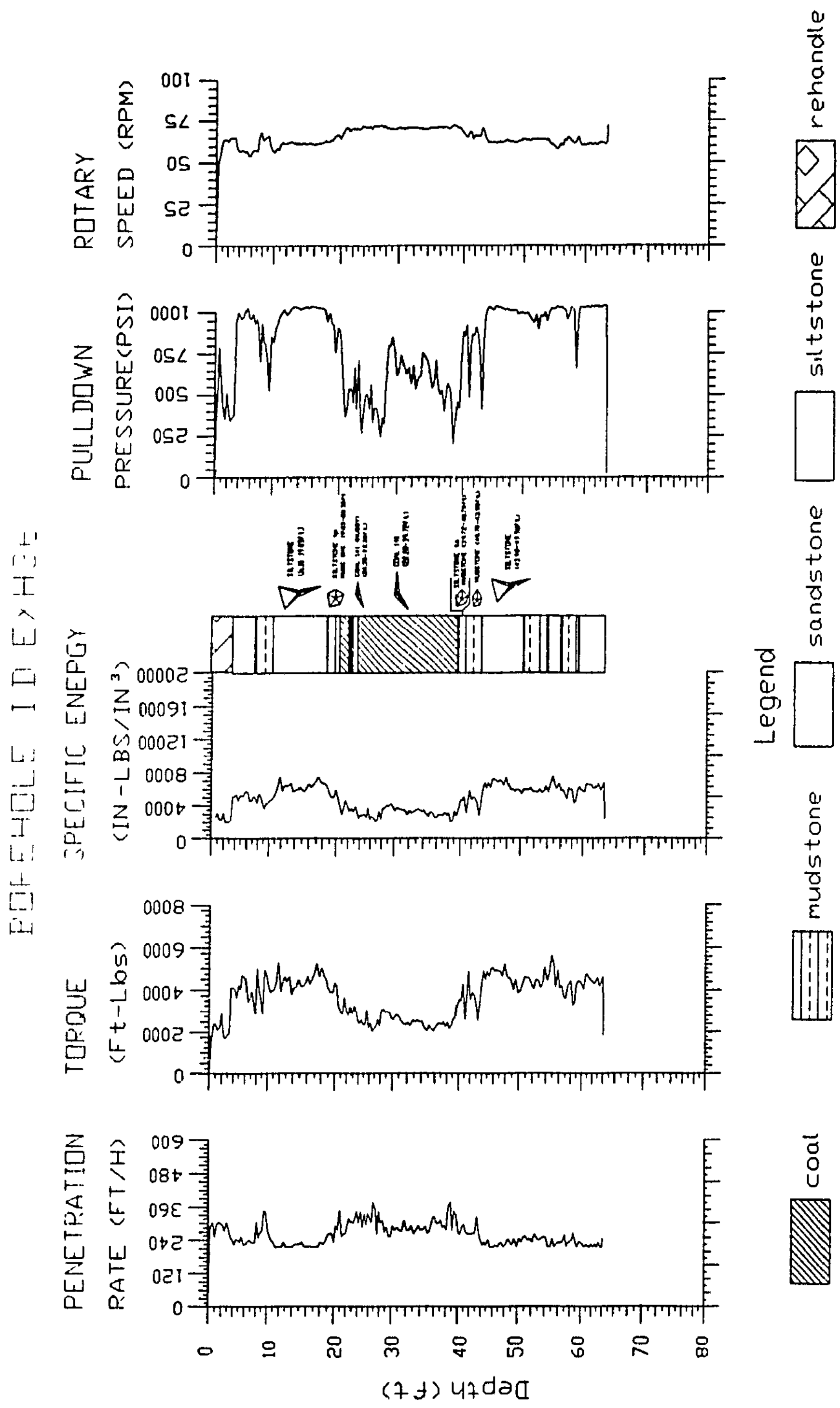

Figure 12 - Drill, Gamma and Geological Logs and Star Symbol Plots for Borehole EXH36.

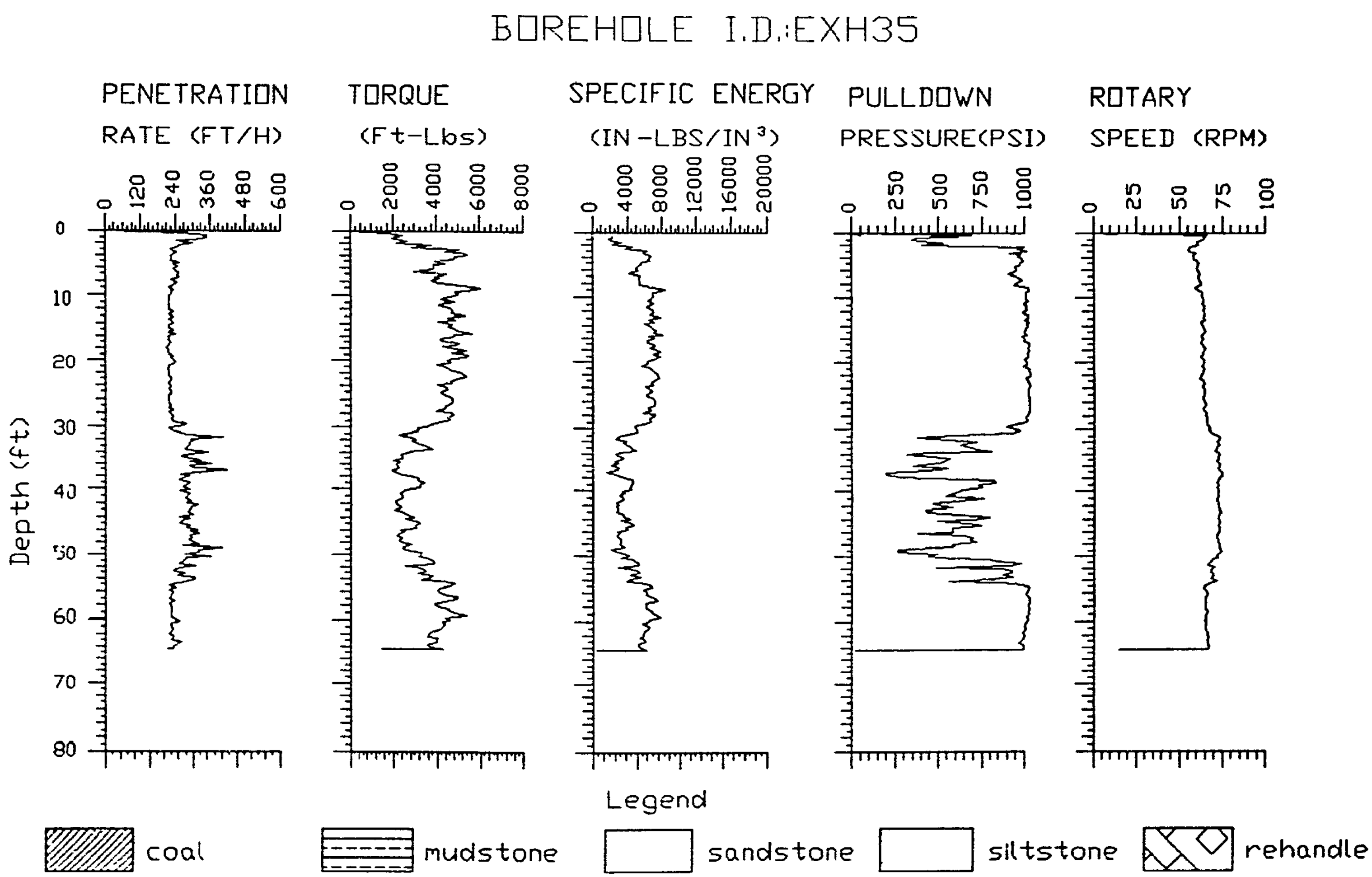

Figure 13 - Drill Logs for Borehole EXH35.

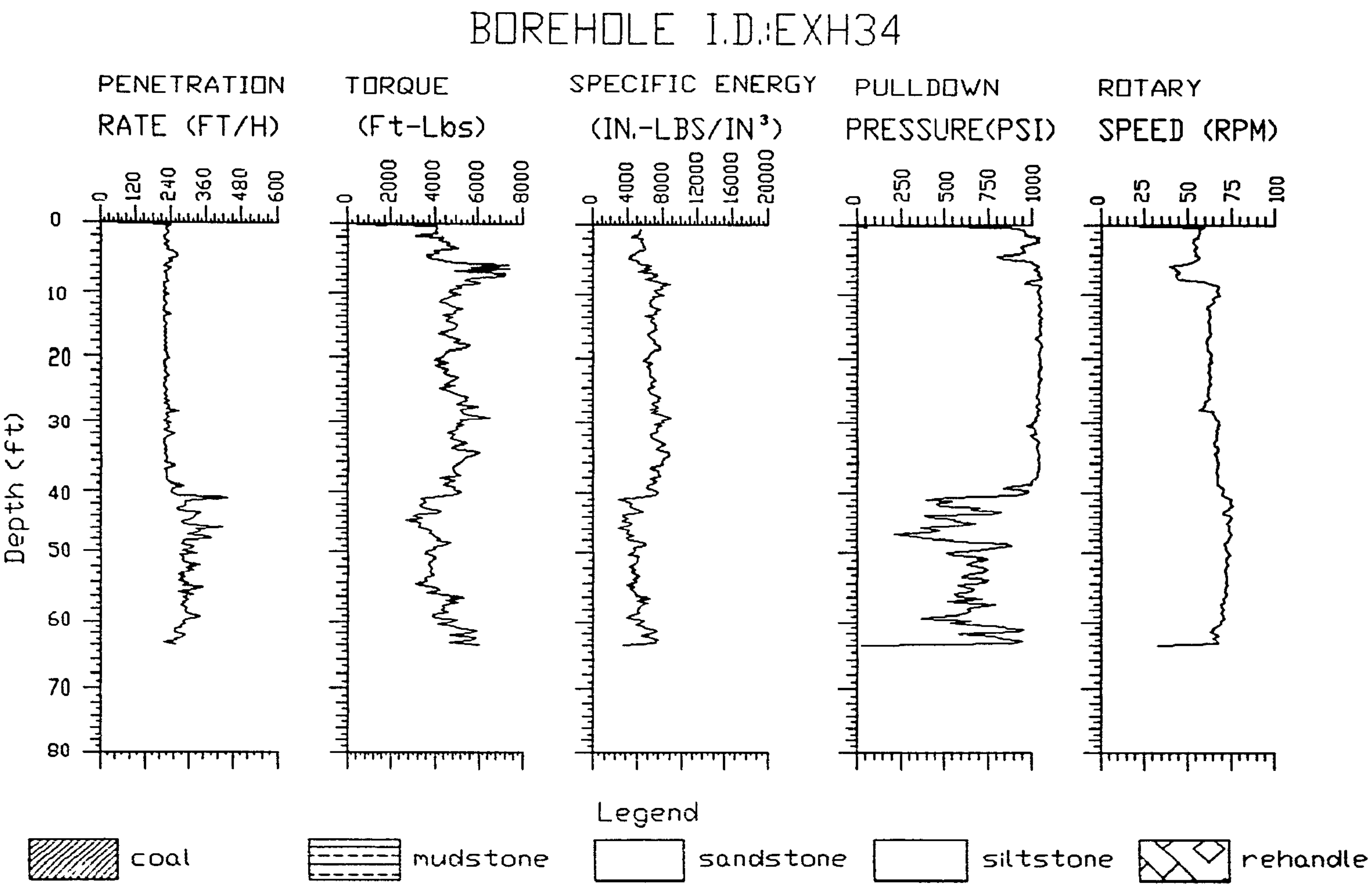

Figure 14 - Drill Logs for Borehole EXH34.

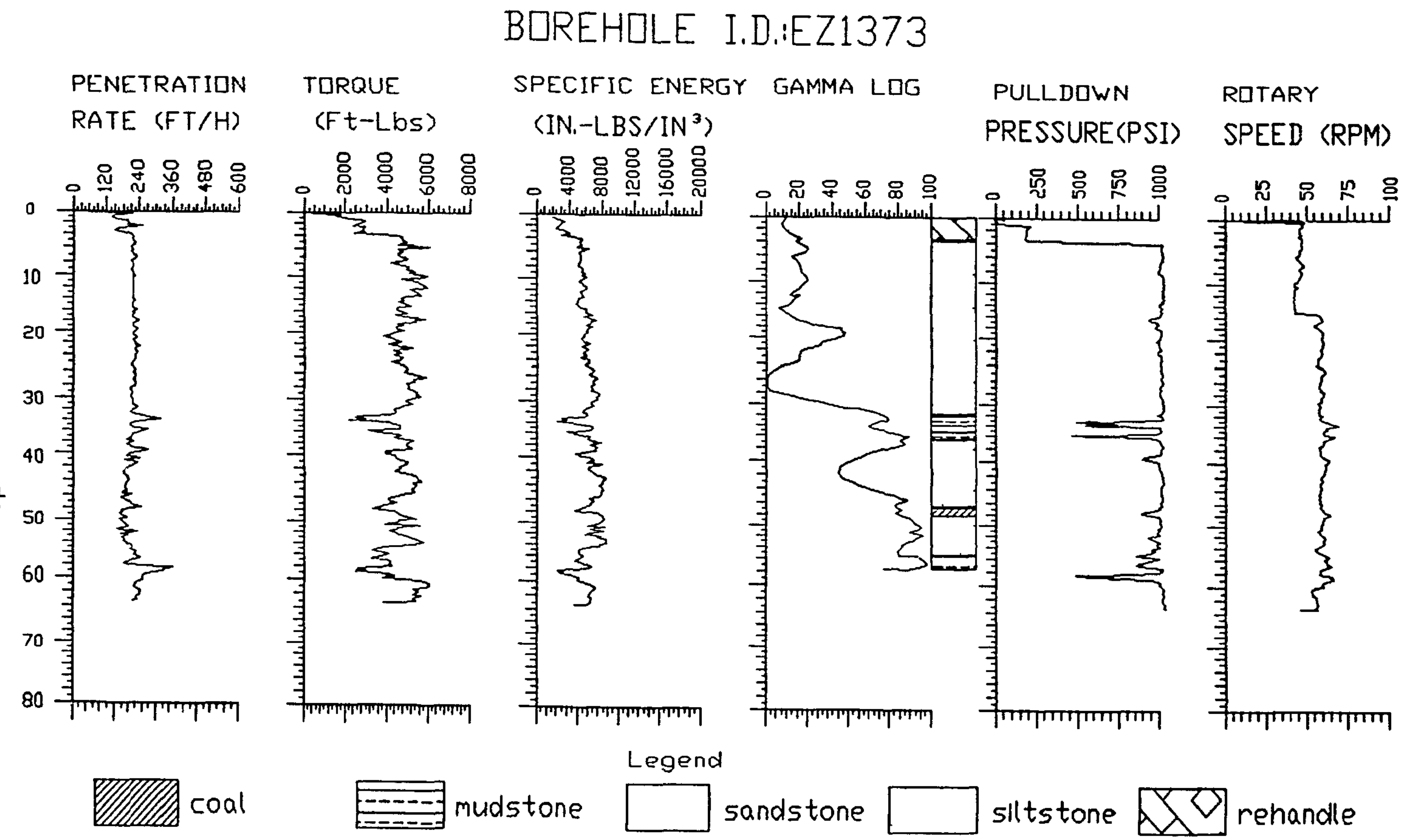

Figure 15 - Drill, Gamma and Geologic Logs for Borehole EZ1373.

Figure 16 - Drill, Gamma and Geological Logs for Borehole EZ1377.

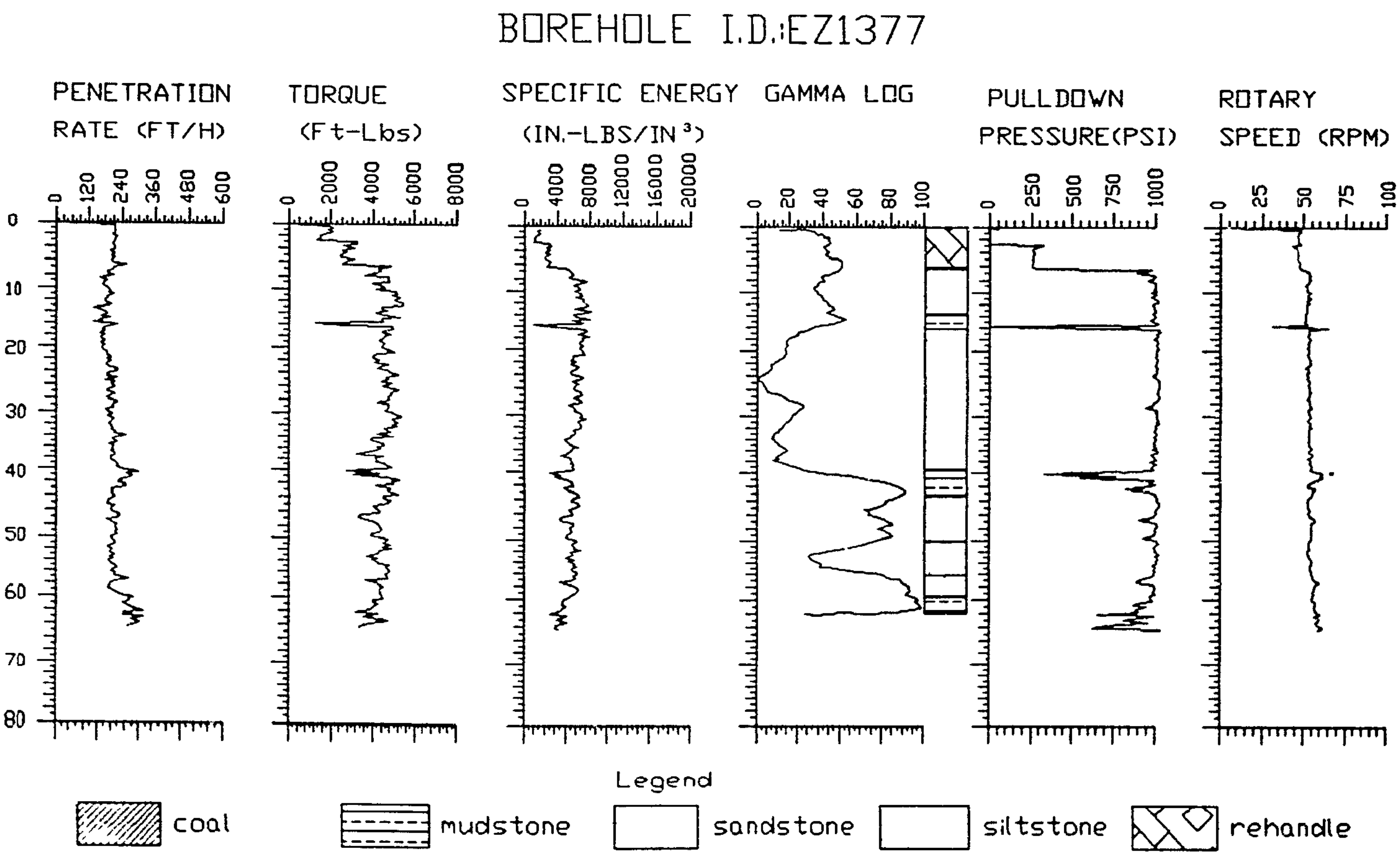

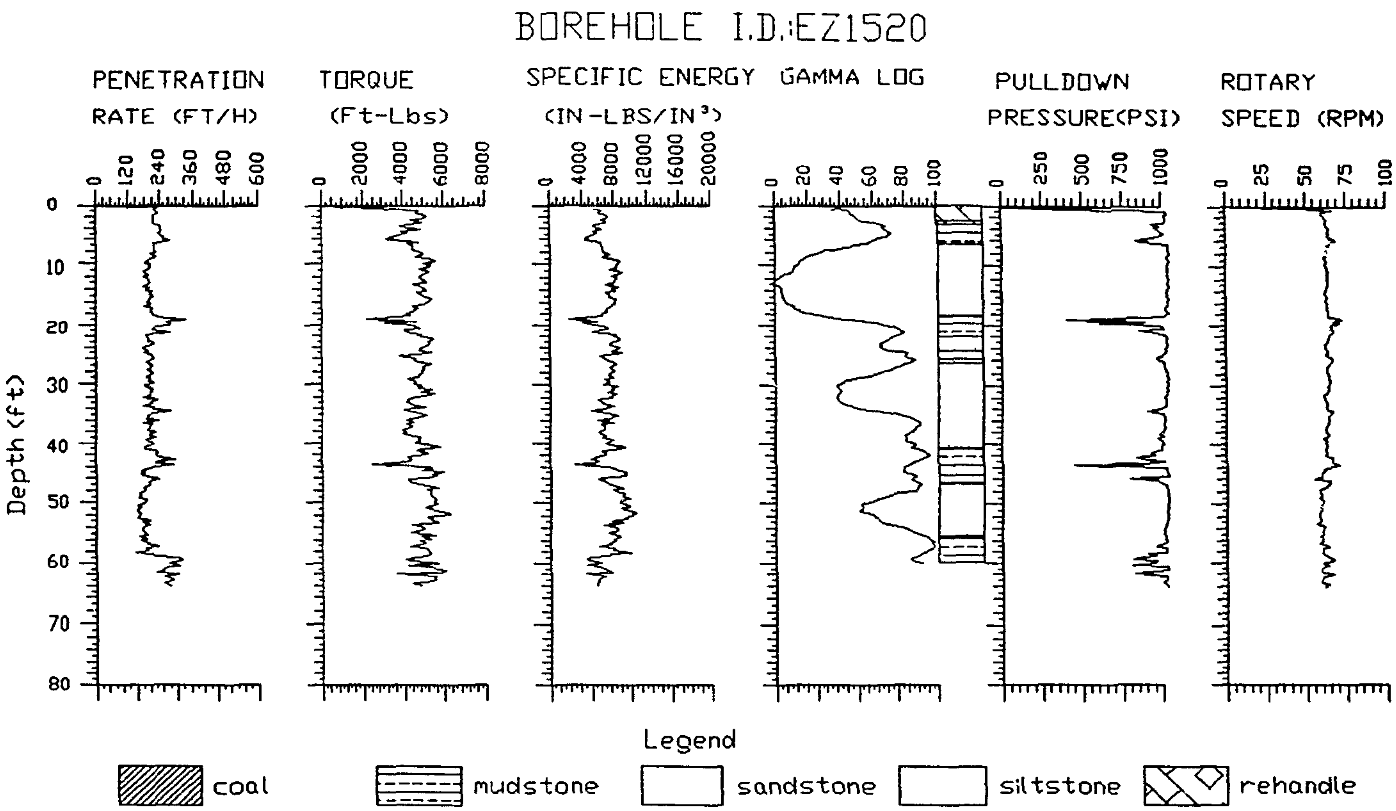

Figure 17 - Drill, Gamma and Geological Logs for Borehole EZ1520.

x1

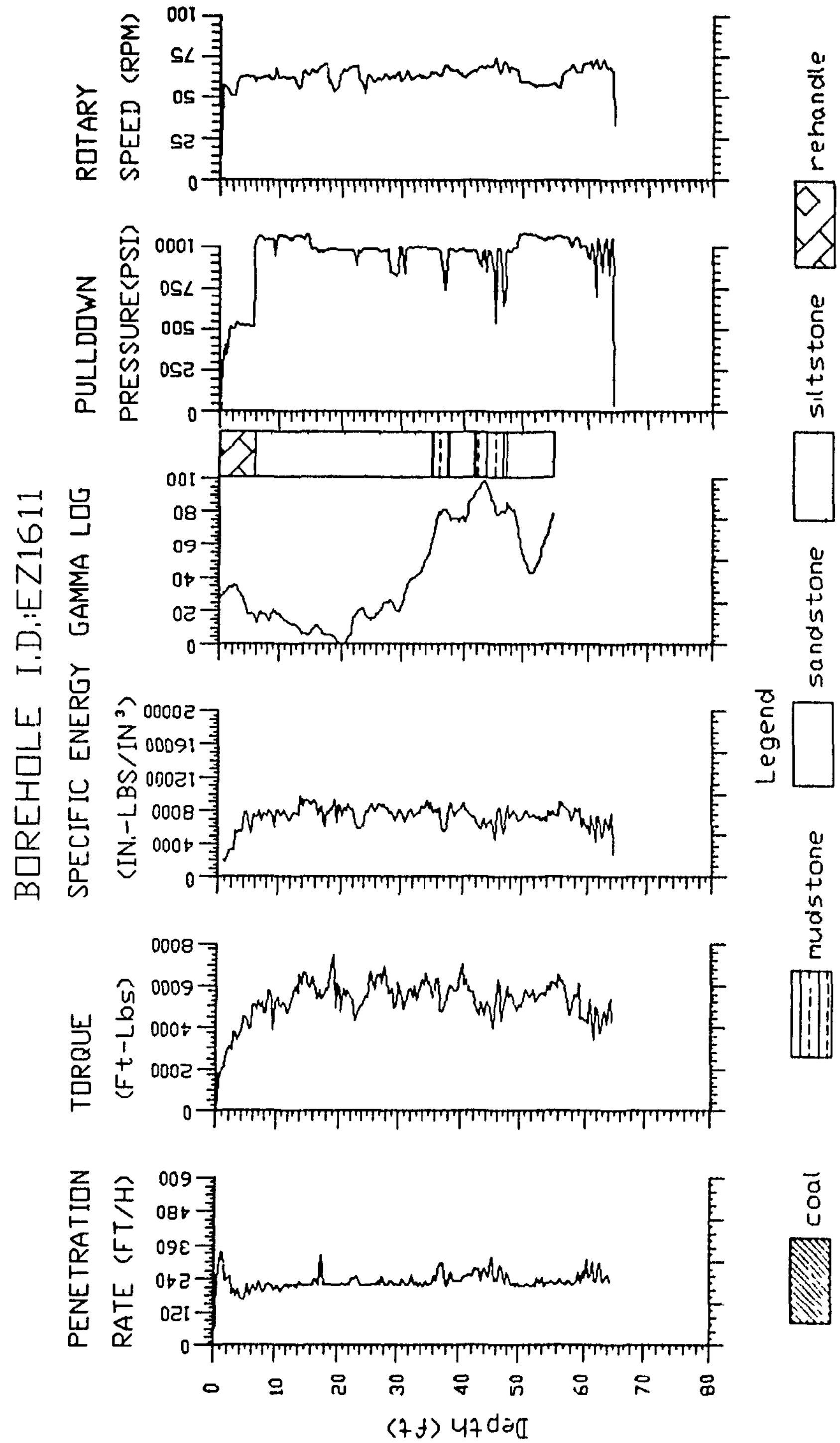

Figure 18 - Drill, Gamma and Geological Logs for Borehole EZ1611.

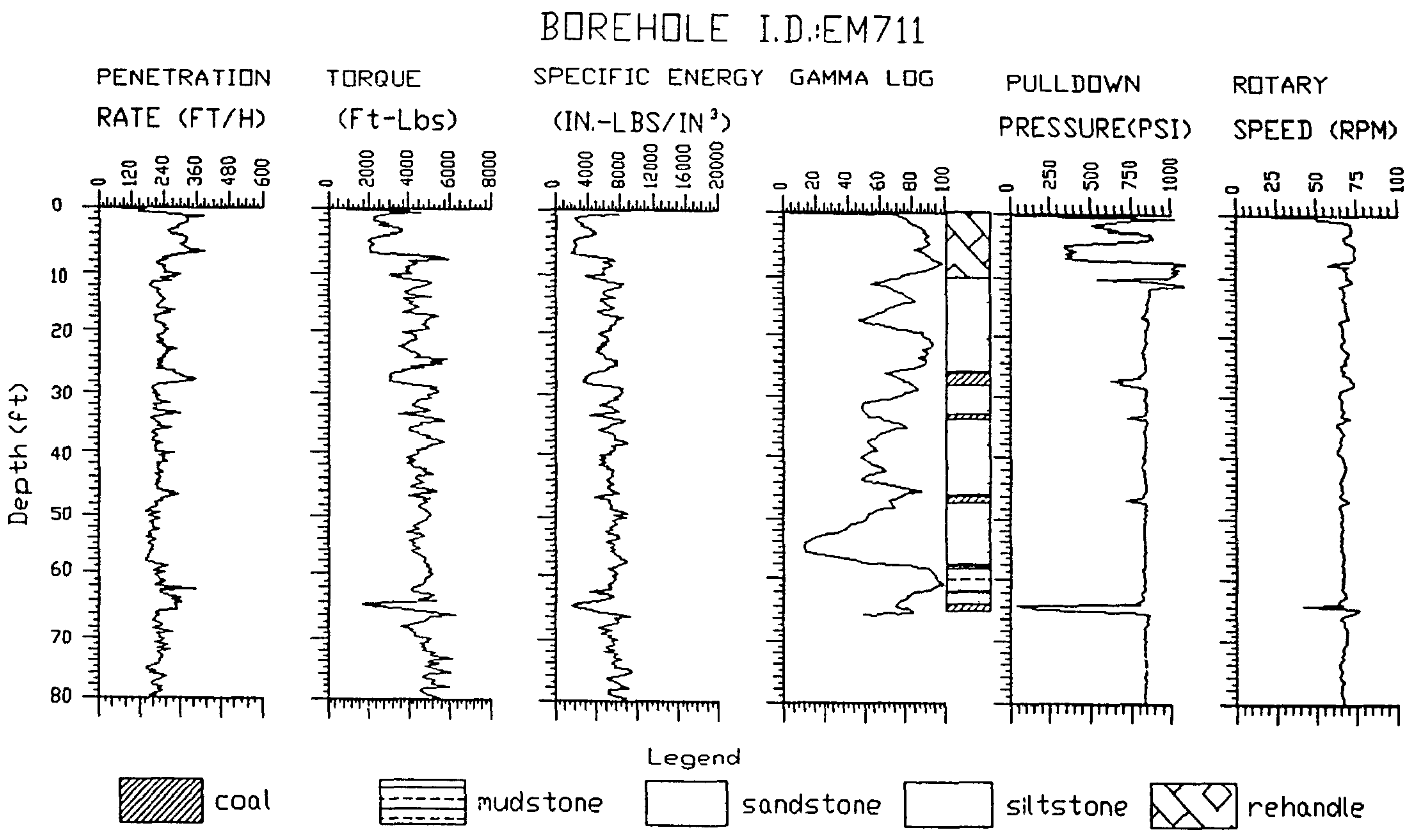

Figure 19 - Drill, Gamma and Geological Logs for Borehole EM711.

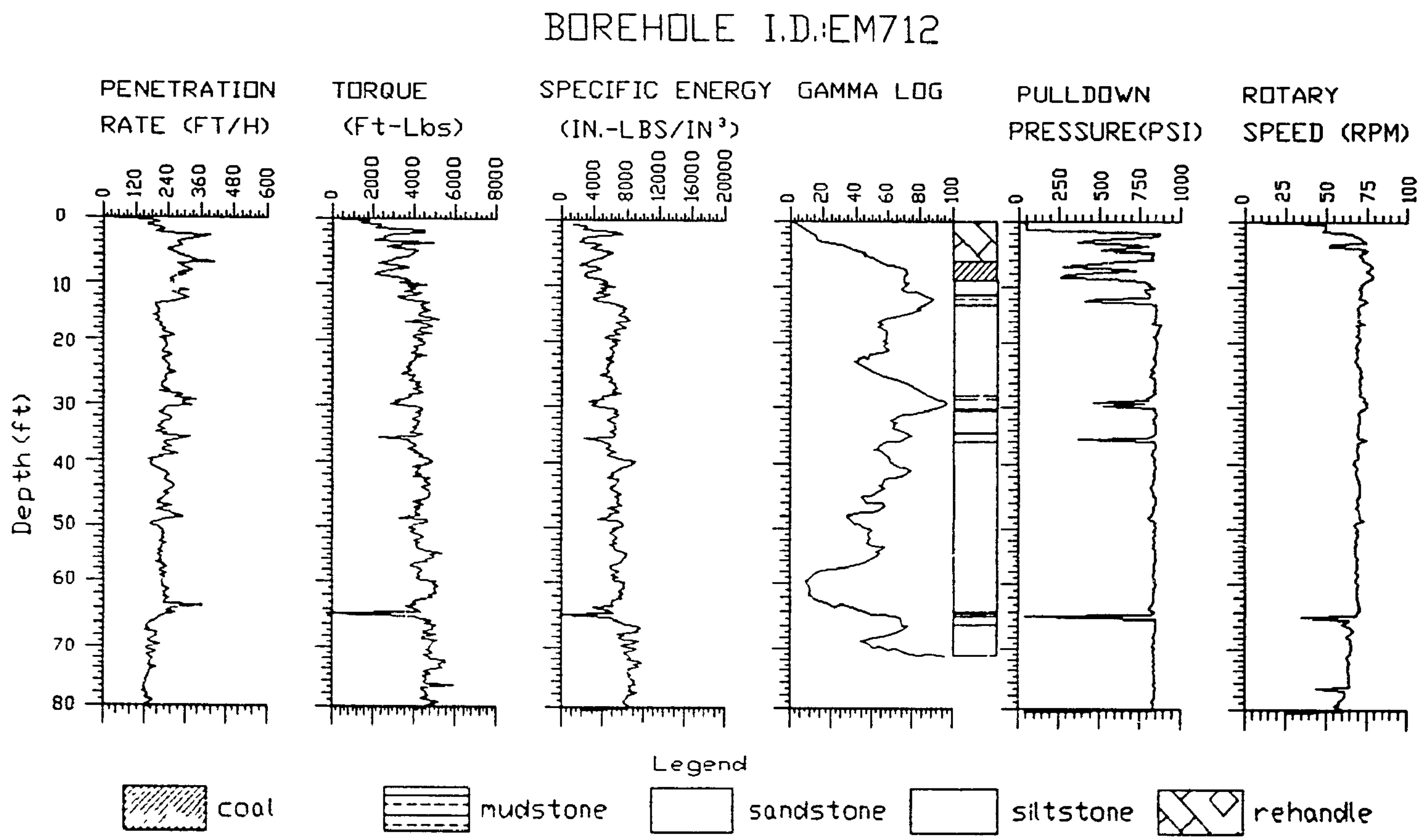

Figure 20 - Drill, Gamma and Geological Logs for Borehole EM712.

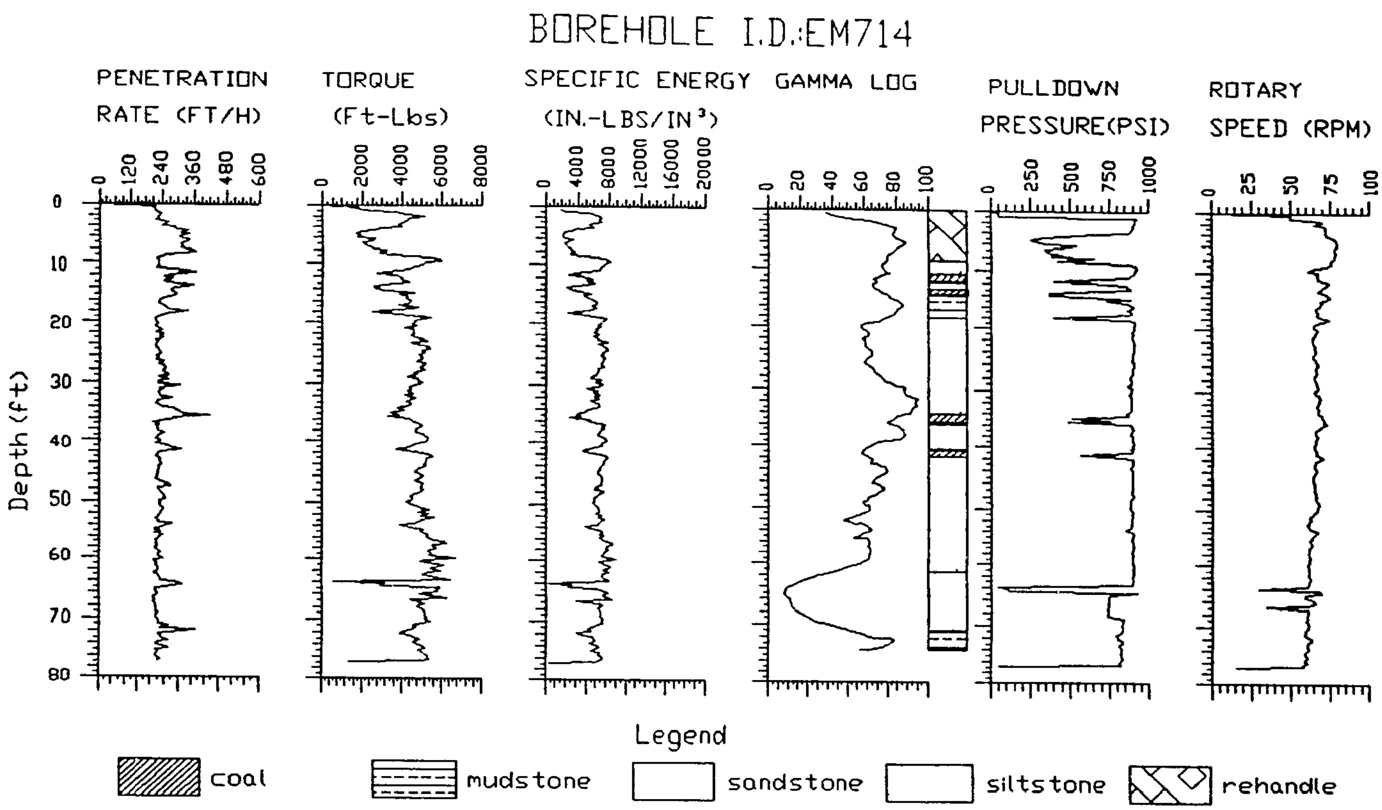

Figure 21 - Drill, Gamma and Geological Logs for Borehole EM714.

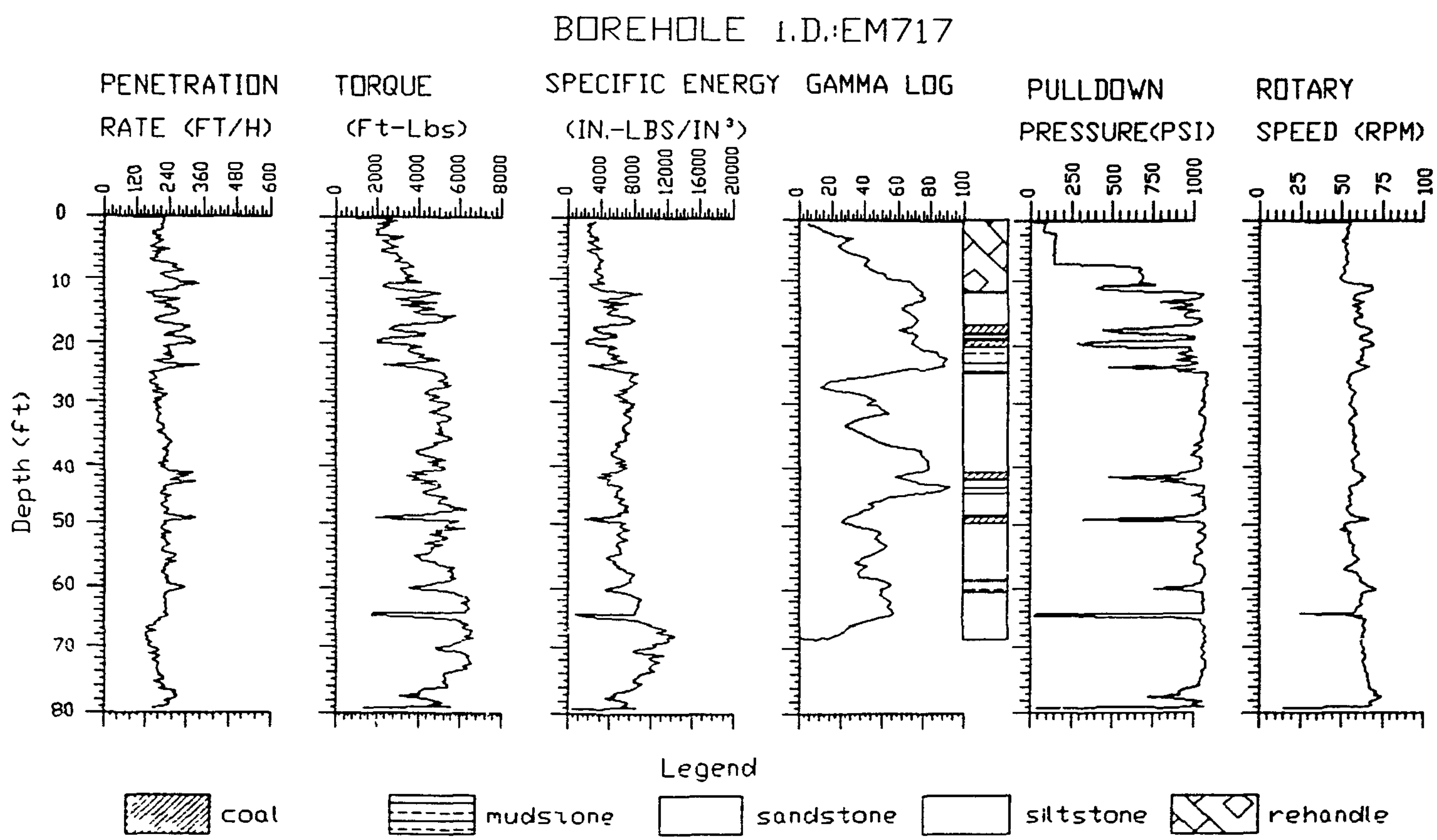

Figure 22 - Drill, Gamma and Geological Logs for Borehole EM717.

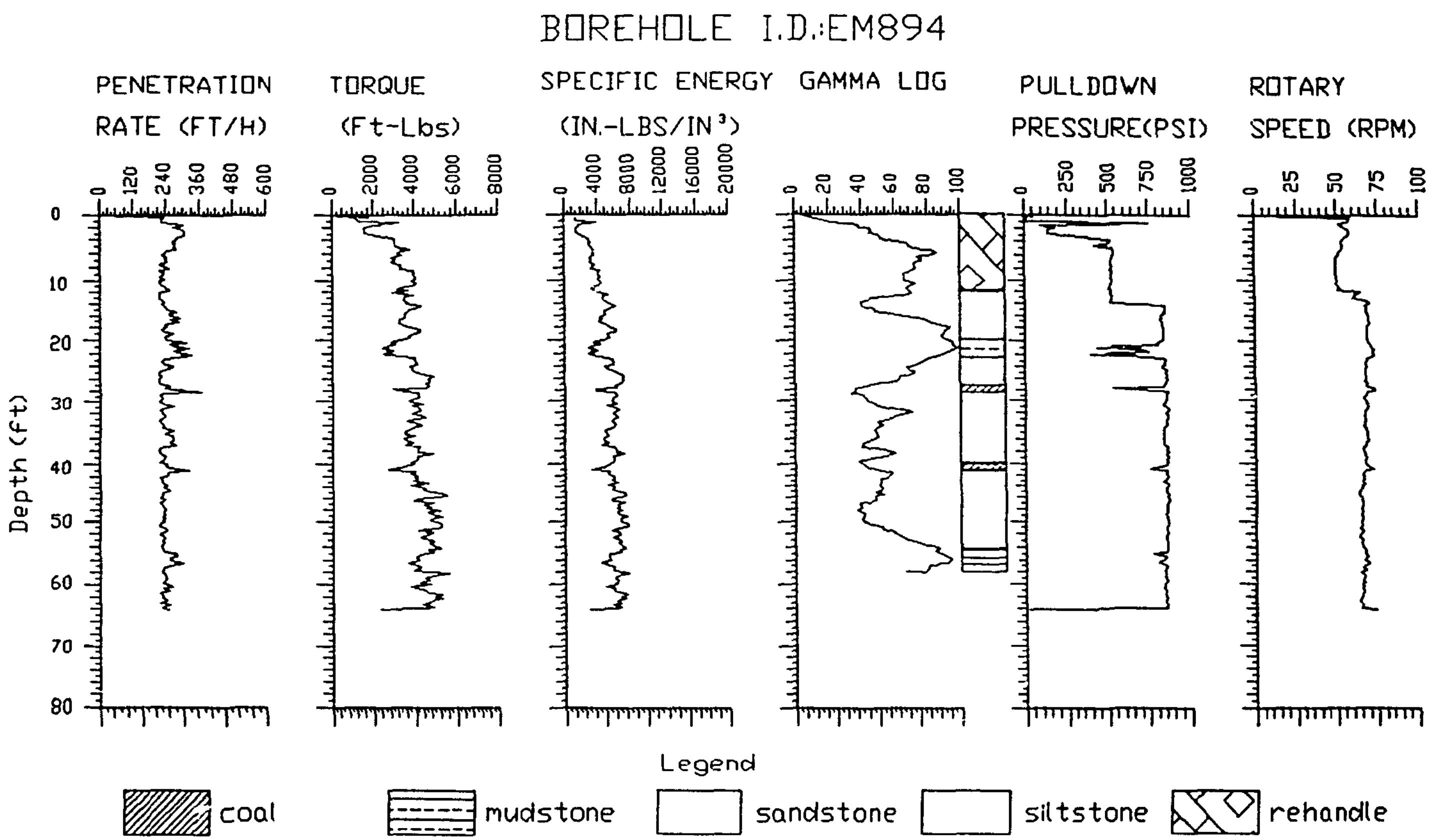

Figure 23 - Drill, Gamma and Geological Logs for Borehole EM894.

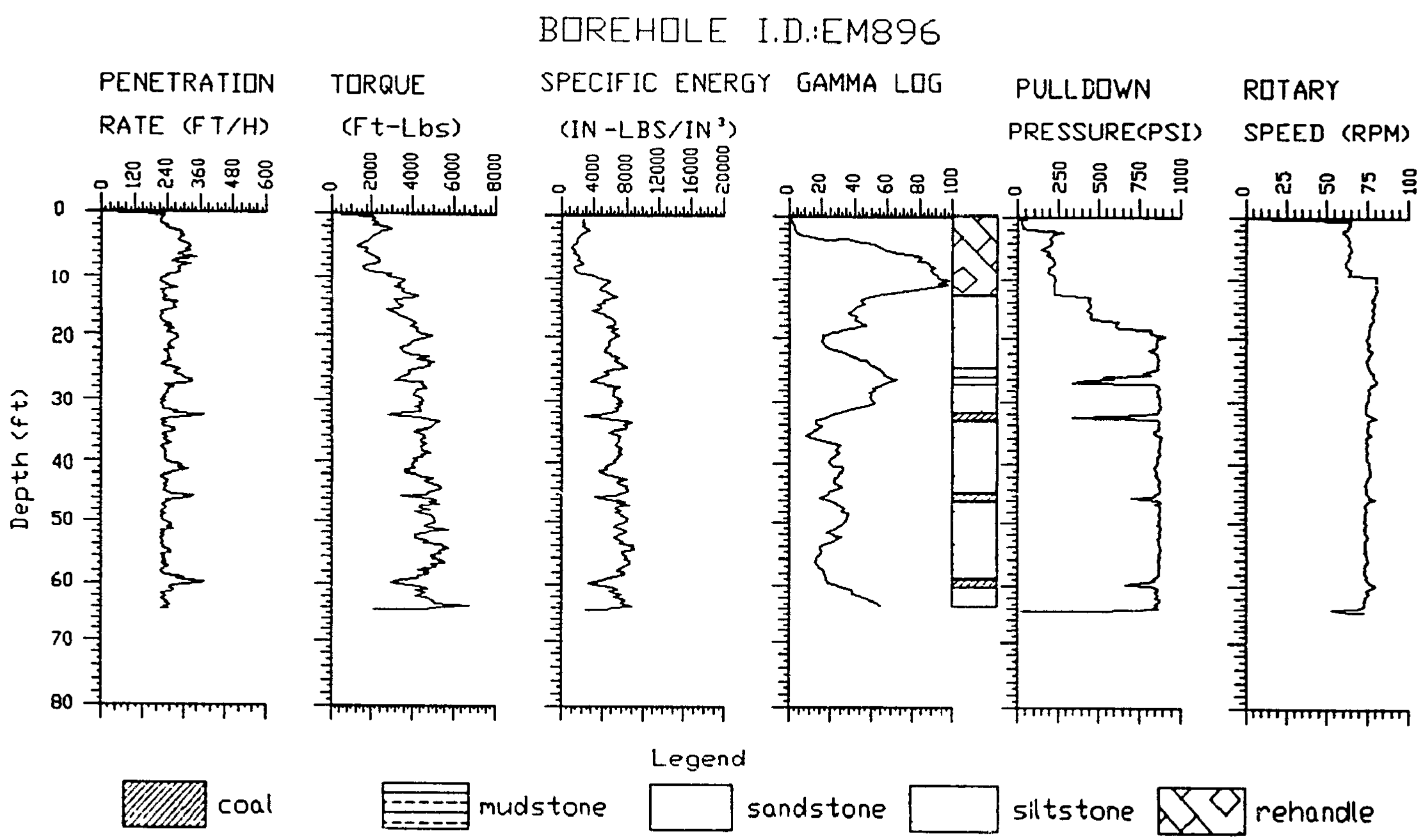

Figure 24 - Drill, Gamma and Geologic Logs for Borehole EM896.